Accelerated Life Testing of Electronic Circuit Boards

with Applications in Lead-Free Design

by

Joseph Moses Juarez

A Dissertation Presented in Partial Fulfillment
of the Requirements for the Degree
Doctor of Philosophy

Approved February 2012 by the
Graduate Supervisory Committee:

Douglas Montgomery, Co-Chair
Connie Borror, Co-Chair
Esma Gel
Marc Mignolet
Rong Pan

ARIZONA STATE UNIVERSITY

May 2012

ABSTRACT

This dissertation presents methods for addressing research problems that currently can only adequately be solved using Quality Reliability Engineering (QRE) approaches especially accelerated life testing (ALT) of electronic printed wiring boards with applications to avionics circuit boards. The methods presented in this research are generally applicable to circuit boards, but the data generated and their analysis is for high performance avionics. Avionics equipment typically requires 20 years expected life by aircraft equipment manufacturers and therefore ALT is the only practical way of performing life test estimates. Both thermal and vibration ALT induced failure are performed and analyzed to resolve industry questions relating to the introduction of lead-free solder product and processes into high reliability avionics. In chapter 2, thermal ALT using an industry standard failure machine implementing Interconnect Stress Test (IST) that simulates circuit board life data is compared to real production failure data by likelihood ratio tests to arrive at a mechanical theory. This mechanical theory results in a statistically equivalent energy bound such that failure distributions below a specific energy level are considered to be from the same distribution thus allowing testers to quantify parameter setting in IST prior to life testing. In chapter 3, vibration ALT comparing tin-lead and lead-free circuit board solder designs involves the use of the likelihood ratio (LR) test to assess both complete failure data and S-N curves to present methods for analyzing data. Failure data is analyzed using Regression and two-way analysis of variance (ANOVA) and reconciled with the LR test results that indicating that a costly aging pre-process

may be eliminated in certain cases. In chapter 4, vibration ALT for side-by-side tin-lead and lead-free solder black box designs are life tested. Commercial models from strain data do not exist at the low levels associated with life testing and need to be developed because testing performed and presented here indicate that both tin-lead and lead-free solders are similar. In addition, earlier failures due to vibration like connector failure modes will occur before solder interconnect failures.

DEDICATION

To my wife Debbie and son Eric who have patiently allowed me complete this long journey with love. One result has been my 16 year old son has become very motivated to pursue his PhD in Paleontology immediately after his undergraduate, but the most moving thing has been him telling me how much he loves me because we shared the same love for mathematics and science has made it all worth it. To my parents, Janie and Joe Juarez for teaching me that faith in God, love and a good education are the few things in life worth having. To my sister Margaret Juarez, M.D. who has always supported my educational goals and have always appreciated our sibling rivalry even though she always won. And to my youngest sister Cynthia who makes sure I don't take things too seriously. To my undergraduate teachers Dr. Raymond Buckwalter Landis and Leonard Spunt at California State University Northridge who encouraged me to attend graduate school and instilled a strong sense of deeper understanding. And to my graduate school mentor the late Professor Henry (Hank) Martyn Paynter at the Massachusetts Institute of Technology for telling me it was time to go back to graduate school after a score of year's hiatus and try a new field because if you aren't failing half the time you aren't learning and until now realized he was referring to mechanical failure!

ACKNOWLEDGMENTS

First and foremost, I want to acknowledge my co-chairs Professor Douglas Carter Montgomery and Professor Connie Margaret Borror for their deep insight and guidance; and always make me feel better about my progress on this dissertation after every meeting including the comedy in my errors. To Professor Marc Mignolet and Professor Rong Pan for their very helpful suggestions on making the dissertation better and Professor Esma Gel who reminds me to go beyond solving engineering problems to achieve broader synthesis for my work. Thank you Dr. Araxi Hovhannessian, Graduate Advisor for helping me maneuver through the university bureaucracy especially since I am the last of the students on a manual paper system. I am also very grateful to my work colleague Vicka White co-author on my first paper for performing extensive and long life tests. Thanks to the technicians Roger Bitinis and Peter Graziano who worked nights and weekends cheerfully to accomplish vibration life tests. I appreciate the efforts of Mike Robinson for performing the failure analysis on samples and countless others who helped me along the way. And finally to my mechanical engineering managers, Dan Robbins, Gerald Biehle, and especially Gary Schrank who lived through most of my years as a PhD student for allowing me the flexibility to attend courses, supported me in getting tuition reimbursement, and facilitated the funding of my research at Honeywell.

TABLE OF CONTENTS

Page

CHAPTER Page

LIST OF TABLES

Table Page

Table Page

Table Page

Table Page

Table Page

LIST OF FIGURES

Figure Page

Figure Page

Figure Page

Figure Page

Figure Page

Figure Page

Figure Page

PREFACE

This PhD journey began December 6, 1999 when I first met Dr. Montgomery and Dr. Borror my current co-chairs at an RSM short course for Honeywell. I had thought Dr. Montgomery was still at University of Washington, but to my good fortune he was at ASU. I then mentioned after class my desire to take all the courses he taught then he suggested that trading in my master's degree, taking a few more course in addition to his and then doing a PhD dissertation was a better option if I was going to take all his courses anyway. Five years later when time came to choose a PhD research topic, Dr. Montgomery suggested I find a problem of significance to Honeywell. This was a great strategy because it leads me to finding a research position in a sustainability area needing my background in mechanical and industrial engineering. This research uses accelerated test methods to assess the safety of flight in black boxes when eutectic tin-lead solder is replaced with more "green" technology. Tin-lead solder has been the industry baseline since electronics have been in existence and serves as our baseline for comparison to lead-free solders. Statistical comparisons for solders reach beyond any ever made for these technologies and the conclusions have tremendous cost savings ramifications. As the French writer Joseph Joubert (1754-1824) once wrote, "I love to see two truths at the same time. Every good comparison gives the mind this advantage." Even though this quote has been attributed to comparing great musical performances written by classical composers Dubal (2004); here powerful statistical methodologies are applied to two metallurgies competing for the longest life.

Chapter 1

INTRODUCTION

This dissertation presents methods for addressing accelerated life testing (ALT) of electronic printed wiring boards with applications to avionics circuit boards. The methods presented in this research are generally applicable to circuit boards, but the data generated and their analysis is for high performance avionics. Avionics equipment typically requires 20 years expected life by aircraft equipment manufacturers and therefore ALT is the only practical way of performing life test estimates. In recent years, the main motivation for ALT of avionics circuit boards has been a worldwide industry shift away from using lead in solder and components to new metallurgies that replace lead to promote more Sustainable technologies. This shift to new metallurgies has also prompted concerns about their performance in high reliability avionics. This issue will be discussed next in further detail and provides the motivation for why this dissertation develops the methodologies for solving problems of engineering significance.

1.1 Background on transition to lead-free

This transition to lead free solders in the world marketplace has prompted several actions by the US government as it pertains to the reliability of commercial, military, and space applications. The chronology of these actions and their test reports discussed here will demonstrate the direction that research has taken and the problems addressed in this dissertation.

In May 2001, the Department of Defense sponsored a consortium under the auspices of the Joint Group on Pollution Prevention (JG-PP) presently managed jointly by the Joint Council on Aging Aircraft (JCAA) and tasked with a project now called the JCAA/JG-PP Lead-Free Solder Project with membership from all Armed Forces, NASA, Industry, Sandia National Labs, National Center for Manufacturing Sciences (NCMS), among others to address for the first time the issue of lead free design impacts on highly reliable electronics in a very concerted manner (Woodrow, 2006). The JG-PP lead-free solder project was established because military and space applications are typically more severe than traditional commercial electronic applications.

The purpose of the JG-PP lead-free solder project is to characterize, demonstrate and validate the performance of lead-free solders as potential replacements for conventional tin-lead solders used on circuit card assemblies. The consortium wrote a test plan called the joint test protocol to describe the testing to be performed (JG-PP, 2004). In the introduction to the their report the impetus for funding tests states that with the "U.S. EPA citing that lead and lead compounds are on top 17 chemicals imposing greatest threats to human health enacted legislation in 2001, lowering the Toxic Release Inventory (TRI) reporting threshold to 100 pounds annually. Previously, facilities were not required to report amounts less than 10,000 pounds a year; this legislation also applied to federal facilities" too. This began a strong drive in the U.S. for the electronic industry to seek lead-free alloys although the electronics industry had begun transition to using lead-free solders in the 1990's.

In addition, the European's Union recently enacted "Restriction of Hazardous Substances (RoHS)" directive and furthermore a pact between the U.S., Europe's Soldertec at Tin Technology Ltd. and the Japan Electronics and Information Technology Industries Association (JEITA) are partnerships and agreements for example impacting the electronic industry toward further lead-free designs. Globalization in electronics manufacturing and therefore global commercial grade electronics manufacturers are initiating their own efforts in lead-free to retain their worldwide markets is leading to major concerns that these components are finding their way into the inventory of aerospace or military assembly processes under government acquisition reform initiatives like commercial off-the-shelf (COTS). "This situation results in increased risks associated with manufacturing and subsequent repair of military electronic systems. If the military electronics industry does not proactively participate in determining the impact of lead-free solders, it is possible that parts with lead or Sn-Pb finishes may become impossible to procure or acquisition costs for 'military lead containing components' will become prohibitive."

What we have established here again is that, similar to the transition from metals to composites and plastics with applications in household goods to stealth technologies, is another major technology trend with far reaching implications from cell phones to satellites. This new technology trend should have us asking how reliable is air travel which is already in our minds as more structural elements are made of composite materials and are being used in modern aircraft.

The Joint Test Protocol project plan goes on to state the project's focus is on lead-free solders used on plated through holes (PTH), surface mount technology (SMT), and mixed technology circuit card assembly applications. These are the most important technologies related to the transition to lead-free and the test plan in Table 4 of Chapter 2 Engineering and Testing Requirements include performance requirements using accelerated testing with *MIL-STD-810F* ("Method 514.5: Vibration", 2000) and specifies validation tests for vibration, mechanical shock, thermal shock, thermal cycling, and combined environments test with acceptance criteria better than or equal to the tin lead controls (JG-PP, 2004). Table 5 lists extended performance requirements that will not be further discussed because they relate to environmental tests that are not subject to modeling analysis, but are test based like salt, fog, and humidity tests. Additional tables discuss testing levels and methodology discussed later. In the section on Quality Assurance (JG-PP, 2004, p. 10), the testers were told, "Statistical distributions of failures will be represented by a Weibull distribution."

On 20 April 2004 the Project's Joint Test Protocol meets NASA core testing needs with buy-in from key NASA stakeholders and in 2006 project results are published as part of the NASA DoD TEERM Project 1 and reside on the NASA TEERM website (Kessel, 2010). Eight (8) test reports with discussions make up chapter 4 and modeling based on these test results are in Chapter 10. These results, Woodrow (2006), Starr (2006), CALCE (2006), Woodrow (2007), formed the basis in 2006 for identifying the research in this Dissertation focused on thermal accelerated testing for PTH the subject of section

2 and vibration accelerated testing issues discussed in sections 3 and 4. Coincidently Europe passed legislation banning the use of lead (and other materials) in new electronics starting July 1, 2006.

Let it be known that aerospace and military electronics are currently exempt from European legislation, but it will become increasingly difficult for programs to procure electronics made with tin lead solder.

In response to the global transition to lead-free solder the aerospace industry formed the AIA-GEIA-AMC Lead-free Electronics in Aerospace Project Working group (LEAP) to develop standards for addressing problems that are unique to and within the control of the aerospace industry. The performance testing standard GEIA-STD-0005-3 published by the LEAP Working Group is jointly sponsored by the Aerospace Industries Association (AIA), the Avionics Maintenance Conference (AMC), and the Government Engineering and Information Technology Association (GEIA) and has borrowed from the NASA/DoD Joint Test Protocol (GEIA-STD-0005-3, 2007).

In addition, the Office of Naval Research (ONR) and the Joint Defense Manufacturing Technology Panel sponsored the Lead free (Pb-free) Electronics Manhattan Project to produce reliable hardware given the current climate within the electronics industry to avoid issues associated with this transition to lead-free electronics for future Navy and Military war-fighting programs (ONR, 2009) in its Phase I of the Manhattan project published lead free electronic best practices that form the current baseline which future improvement can be measured and assembled by nationally recognized subject matter experts. Their report also

identifies known issues with the current baseline practices and discusses technical gaps. These gaps are further addressed in concert with this dissertation. One such finding is that testing must now go beyond qualification tests to develop life models and therefore existing highly reliable products and their designs will need to address transition to avoid obsolescence methods for cost effectively qualifying the same products sharing the same fit, form, and function, but with lead-free solder.

To this end, qualification by similarity is being pursued by taking products containing tin-lead solder and lead-free solder, performing life-testing on both, and comparing the results. Moreover, qualification testing or "elephant tests" as Nelson (1990, pp. 37-39) calls them has typically only provided qualitative go/no-go information and testing is on few specimens if not one. In addition, qualification testing is not life testing and only provides customers with a qualitative satisfaction for tin-lead based solder designs that have withstood the test of time. The reason for life-testing is that the industry needs to go beyond qualification tests and understand design margins associated with the lead-free metallurgies based on statistical data from testing and establish models that predict life for these lead-free products. Typical failure modes associated with avionics end of life are caused by thermal, vibration, and shock induced failure. This dissertation will focus on the first two failure mechanisms and recommends augmenting standard practices to develop comparisons between tin-lead solder and lead-free solder.

1.2 Approaches

In chapter 2 we demonstrate that accelerated thermal testing parameters applicable to both tin-lead and lead-free solders in circuit boards are established using a single energy value as a test of statistical significance.

A standard practice using ALT based thermally induced failure or low-cycle fatigue (Dieter, 1976) is to subject a circuit board coupon to a prescribed number of specific thermal cycles that represents in-service use of the product and then use an acceptance test which is industry dependent. For avionics, the standard practice employs interconnect stress test (IST) per IPC-TM-650 (2001, "2.6.26) with all coupons in a lot passing 350 thermal cycles as the acceptance test criteria. In addition, the avionics industry is beginning to assess appropriate ALT using IST to simulate the soldering process or preconditioning on the boards including re-work cycles which is representative of a more realistic product life cycle. This problem addressed in chapter 2 for both tin-lead and lead-free coupon testing appears in a co-authored paper by this author, Juarez and White (2009). Extensions to this paper included here explains IST further, describes the use environment, shows simplifications to the energy equation and more data is included to prove the theory.

Other low cycle fatigue testing and analysis approaches used in circuit board design involve solder joint stresses due to the thermal coefficient of expansion mismatches between components and the circuit board material induced by thermal variations seen in flight operations. This dissertation will not address these thermal ALT methods; computer codes exist to perform these

analyses for solder joint component failure like those of Clech (2008) and CALCE (2011), and the books by Lau (1994) and Steinberg (1991) show how to predict solder joint failures. Work on lead-free ALT for low cycle fatigue of solder joint failure is gaining momentum and the recent case study by Monroe and Pan (2008) address ALT for lead-free solder joint low cycle fatigue.

The second failure mechanism studied for avionics is due to vibration fatigue failures (Dieter, 1976) caused by the dynamic loading of solder joints between the components and circuit boards in bending. Chapter 3 and Chapter 4 provide examples of accelerated testing to resolve differences between tin-lead and lead-free solder applications. Fatigue failure is also referred to as high-cycle fatigue because the stress inducing cycles are on the order of 100 hertz.

In chapter 3 we use vibration accelerated testing to understand similarity between Tin-Lead and Lead-free S-N curves are similar in failure life for the same shared strain levels. Finally, chapter 4 examines direct comparisons of tin-lead and lead-free avionics system level black boxes using partially accelerated life testing (PALT) and investigates finding a single accelerated test value needed to reduce qualification test times, but is not accelerated so high that unwanted failure modes are induced.

Chapter 2

VALIDATING CIRCUIT BOARD INTERCONNECT STRESS TEST (IST) PRECONDITIONING PROCESSES USING STATISTICAL MODEL COMPARISONS OF ACCELERATED TEST DATA

2.1 Problem statement

This chapter assesses the preconditioning process as part of ALT using Interconnect Stress Test (IST) technology as documented in IPC-TM-650 (2001, "2.6.26"). Statistical methods are used to assess Interconnect Stress Testing (IST) accelerated life test (ALT) parameters for preconditioning that result in simulating the life of coupons that have been subjected to actual re-flow oven heating as a baseline process at temperature excursions and ramp rates not yet attempted by analytical models (George, Das, Osterman, and Pecht 2011).

When circuit boards are fabricated, coupons are also made on the same printed circuit board for quality acceptance. Prior to subjecting the coupons to ALT using IST that simulates the in-use life process of the circuit board, additional life is removed from the board by an accelerated IST preconditioning process simulating the soldering of components on the board. The preconditioning process using IST is accelerated using a five minute cycle time versus using the actual process for soldering components with a re-flow oven (RFO) twelve minute cycle time.

The goal is to find what IST settings of ramp time to cycle time, maximum preconditioning temperature, and number of preconditioning cycles lead to equivalent failure times had the preconditioning been done on a reflow oven with the same manufacturing reflow profile. The result is testing cycle time is reduced;

the reflow oven does not have to be tied up in testing coupons or holding up production; and all testing can be done on the IST machine. The IST parameters are no longer requiring several iterations of life testing to confirm the parameter settings, but calculated prior to testing thus saving weeks of effort.

2.2 Methodology

Accelerated life test data is generated on an IST Machine (Figure 2.1) for coupons fabricated by three suppliers, but preconditioning is performed both by using IST and a re-flow oven Figure 2.4 on the supplier coupons to create different data sets for comparison. The preconditioning of coupons in this dissertation represents two modes of heat transfer into the coupons: IST is resistive heat transfer and the re-flow oven is convection heat transfer. While IST is used to accept lots of circuit boards for Avionics applications after all the test coupons survive a predetermined number of ALT cycles determined to represent the life of an aircraft, this project forced the test coupons to be driven beyond the normal test limits of 350 cycles (Cluff and Osterman, 2002) and (Slough, 2005) to precipitate failures and study differences in preconditioning processes. The failure mode of the data presented in this dissertation is thermally induced fatigue due to the expansion and contraction of the via barrels (a via is the mechanism by which different circuit layers are connected); the arrows in Figure 2.2 show the fractures in the barrels. Failure is determined when coupon resistance is at greater than 10% resistance change from the original resistance at the initial cycle at the highest point of the test temperature after preconditioning. The resistance increases because when a crack forms less material is left to conduct current. The ALT IST is resistive heating with coupons fabricated so that current flows through these barrels to heat them up in ramping cycles with five minute cycle times then repeated until failure occurs. The coupon (Figure 2.3) is made of 14

layers of circuitry with an electrical circuit daisy chain to each via; the coupon dimensions are 5 inches long by .7 inches wide by .1 inches thick. A common practice is to use five preconditioning cycles (PCCs) completed on an IST machine to simulate assembly and six preconditioning cycles when a re-flow oven is used, but are preconditioning cycles equivalent? The study analyzes three supplier data sets as follows to resolve this question:

1. For supplier 1 coupons, five IST PCCs data set and six IST PCCs data set are compared to a six re-flow oven PCCs data set,
2. For supplier 2 coupons, five IST PCCs are compared to six re-flow oven PCCs; and
3. For supplier 3 coupons, five IST PCCs are compared to six IST PCCs.

What will be shown in the data analysis results section is that the distribution of failures is Weibull and that six IST PCCs are similar to six re-flow oven PCCs using likelihood-ratio tests regardless of whether a supplier's coupons would be passed or rejected after in use life IST. These supplier data set comparisons are made by applying the likelihood-ratio (LR) test, furthermore; Tobias and Trindade (1995, p. 174) write that, "in the case of censored life test data… (likelihood-ratio test) is usually the only method that can be used." The distribution parameters are maximum likelihood estimates (MLE) computed in Minitab version 16 and the resulting likelihoods for each of the comparison groups are then evaluated in the (LR) test equation (Meeker and Escobar, 1998, p. 185), (Nelson, 1990, 470-485), and (Tobias and Trindade, 1995, p. 175).

The statistical hypothesis is stated formally as the null hypothesis, H_0: The assumed distribution is an adequate fit to the data sets; and the alternative hypothesis, H_1: The assumed distribution is not an adequate fit to the data sets. The null hypothesis is rejected if

$$\text{LR} = -2Log\left[\frac{L(\hat{\mu}_0,\hat{\sigma}_0)}{L(\hat{\mu}_1,\hat{\sigma}_1)+L(\hat{\mu}_2,\hat{\sigma}_2)}\right] > \chi^2_{(\alpha;df)}. \quad (1)$$

The numerator is computed by forcing both data sets to have the same distribution parameters and maximizing the likelihood of the observed data. The denominator is the maximized likelihood of all the data with each data set allowed to have its own distribution parameters $(\hat{\mu}_1,\hat{\sigma}_1),(\hat{\mu}_2,\hat{\sigma}_2)$. This is a two parameter Weibull model where $(\hat{\mu}_0,\hat{\sigma}_0)$ and $(\hat{\mu}_1,\hat{\sigma}_1),(\hat{\mu}_2,\hat{\sigma}_2)$ are the maximum likelihood estimates. In this analysis, the Chi-squared distribution with $\alpha = 0.05$ and 2 degrees-of-freedom (df) results in 5.99 (Montgomery and Runger, 2003, p. 655). The 2 df result from the four parameters estimated for each of the two Weibull distribution parameters in the paired data sets minus the two parameters estimated for the combined data sets (Tobias and Trindade, 1995) and (Meeker and Escobar, 1998).

The left hand side of equation (1) can be rewritten as

$$T = -2\begin{bmatrix} \log likelihood(\hat{\mu}_0, \hat{\sigma}_0) \\ -\{\log likelihood(\hat{\mu}_1, \hat{\sigma}_1) + \log likelihood(\hat{\mu}_2, \hat{\sigma}_2)\} \end{bmatrix}. \quad (2)$$

Equation (2) will be used throughout the subsequent sections for comparing Weibull data sets. Additional data sets are introduced and compared using the LR test that explains how accepting the null hypothesis is bounded by an energy equation. Each data set has an associated preconditioning energy; the difference in energies between these data sets in joule equivalent (JE) units has an upper bound at delta 123 JE where the null hypothesis is accepted when they are compared by an LR test.

Figure 2.1 IST machine capable of performing both preconditioning and accelerated testing of six coupons at a time.

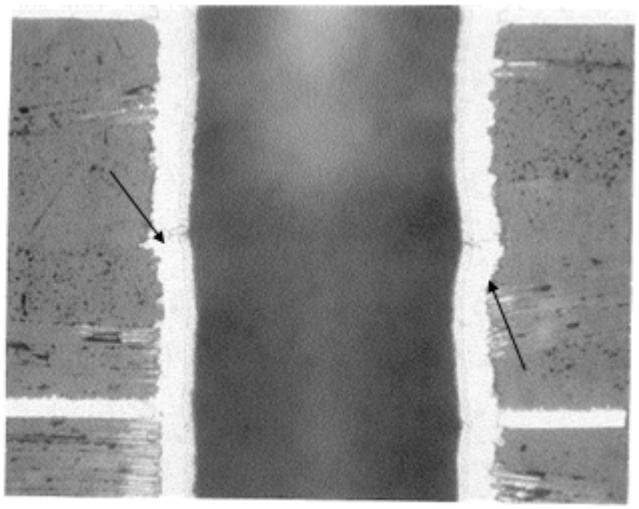

Figure 2.2 Failure mode is a cracked via barrel at arrow points due to thermally induced fatigue.

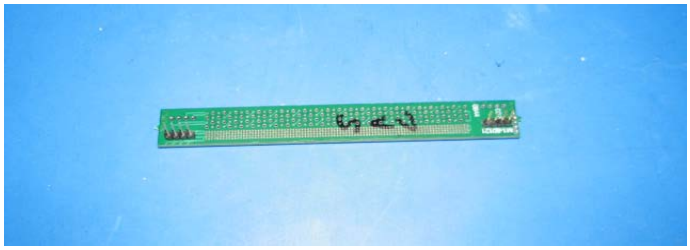

Figure 2.3 A typical IST coupon used in this study.

2.3 Background on IST and re-flow ovens

The IST is quite different from the traditional thermal chamber (or re-flow oven) test and this section describes the difference and why the IST is a good advantageous alternative to the traditional thermal chamber.

As discussed in Section 2.1 IST is used both for pre-condition thermal cycling and for in-use Accelerated Life Testing (ALT) thermal cycling of coupons to produce test data. That section only refers the reader to reference IPC-TM-650 (2001, "2.6.26") to learn about IST and more needs to be explained here. In reference IPC-TM-650 (2001, "2.6.26") the IPC Industry Standard test method for direct

current induced thermal cycling specifies that testing be performed on an Interconnect Stress Test system shown in Figure 2.1. An excerpted description of IST from literature by PWB Interconnect Solutions Incorporated, maker of the IST equipment, says, “The I.S.T. system automatically passes a predetermined constant direct current through a specifically designed printed wiring board interconnect coupon, the current elevates the temperature of the metallization and adjacent materials. IST utilizes the interconnect circuitry to heat the internal environment of the coupon. Heat generation is created throughout the daisy chain of copper conductors, pads and vias. The temperature to which the coupon is heated is directly proportional to the measured resistance and the amount of current that is passed through the conductors, pads and holes. There is a physical principle that can be described mathematically defining the relationship of the interconnect temperature to the amount of current being passed through the daisy chain. This is further influenced by the amount of metallization and its resistivity (a value that describes how hard it is for electrons to flow through the entire interconnect). The IST system uses this principle to raise the resistance/temperature of the circuit to a predetermined value, (an algorithm considered proprietary at this time. Once that resistance/temperature has been achieved the system turns off the current). After the 3 minute heating stage the coupons are forced air cooled for 2 minutes to return the coupons back to ambient, this constitutes a single thermal cycle. During each thermal excursion, the system continuously monitors the minute resistance changes in the plated through holes and inner layer to barrel post interconnects. As the temperature of

the interconnect changes, the resistance value of the interconnect changes proportionally. The IST system is designed to quantify the ability of the total interconnect to withstand these thermal/mechanical strains from the as manufactured state until the products reach the point of interconnect failure." The alternative to IST is a re-flow oven conveyer system for pre-conditioning of the coupons and a dual chamber thermal shock test for in-use ALT thermal cycling; this latter equipment was not used in the study since IST is more cost effective for in-use ALT thermal cycling. Dual chambers are large (3m by 3m by 2m); require liquid nitrogen for ramping temperatures and external equipment to detect failures of the daisy chained coupons. The pre-condition re-flow oven conveyer system in Figure 2.4 below with arrows in the direction of coupon heating also shows oven indicators numbered 1 through 8 with temperature below these numbers and the associated graph step-points and their timed temperature set-points. For example point 2 on the re-flow oven shows 100C below it and the associated graph at point 2 is at 100C after 4 minutes. One pass through the convection heating oven represents one pre-condition cycle. The coupons are air heated and the resulting heat transfer stresses the daisy chained circuitry which in turn thermally stresses the via barrels. Additional pre-condition cycles require taking the coupons out of the oven conveyer and then placing them into the oven at the left again, this process takes 20 minutes in the oven. These re-flow machines are typically 4 meters long and bolt to the factory floor. This method was described in Section 2.1 to produce what is called re-flow oven pre-conditioned coupons. Recall that a pre-conditioning cycle takes the place of the

operation that solders components to a circuit board. The goal of the dissertation was to compare IST and re-flow oven pre-conditioning.

The IST advantage: coupons are placed in the machine (see Figure 2.1) and pre-condition cycles are programmed to the desired number of cycles for a cycle time of five minutes each and then programming in-use ALT thermal cycling means that all the work is done using one set-up and machine versus having to use two large pieces of equipment namely the re-flow oven then moving the coupons to a Dual Chamber.

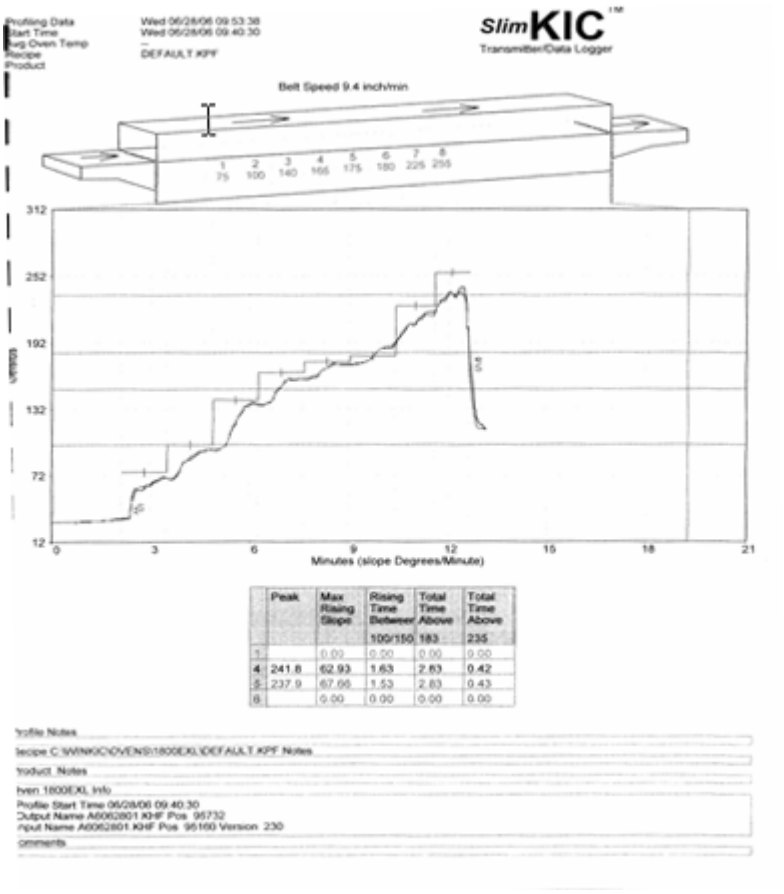

Figure 2.4 Reflow oven (RFO) preconditioning conveyer

2.4 Description of test data

The fundamental test response is cycles to failure for data analysis purposes, Table 2.1. Due to the basic physics of failure for the three suppliers, no cross supplier data can be analyzed, but within supplier data the coupon part numbers are the same and combinations of preconditioning cycles and processes are compared. Supplier data failure Weibull models vary widely, but what is shown here is that appropriate Weibull comparisons produce consistent results regardless of supplier quality. The data sets shown in Table 2.1 are explained as follows by column:

1. Column 1, labeled S1_IST5PCC, contains supplier 1 coupons subjected to five IST PCCs for each of the 17 coupon results in the data set with three censored coupons at 1000+ cycles; not included is an 18^{th} outlier coupon deemed a premature failure;
2. Column 2, labeled S1_IST6PCC, contains supplier 1 coupons subjected to six IST PCCs for each of the six coupons and one censored coupon at 851+ cycles;
3. Column 3, labeled S1_RFO6PCC, contains supplier 1 coupons with six Re-Flow Oven PCCs for each of the six coupons;
4. Column 4, labeled S2_IST5PCC, contains supplier 2 coupons with five IST PCCs for each of the six coupons;
5. Column 5, labeled S2_RFO6PCC, contains supplier 2 coupons with six re-flow oven PCCs for each of the six coupons;

6. Column 6, labeled S3_IST5PCC, contains suppler 3 coupons with five IST PCCs for each of the 18 coupons with 12 censored coupons at 1500+ cycles;
7. Column 7, labeled S3_IST6PCC, contains supplier 3 coupons with six IST PCCs for each of the 18 coupons with one coupon censored at 1151+ cycles and six censored coupons at 1500+ cycles.

Table 2.1 Cycles to failure data sets using either IST or re-flow oven preconditioning processes with five or six preconditioning cycles for coupons made by three suppliers.

S1_IST5 PCC	S1_IST6 PCC	S1_RFO 6PCC	S2_IST5 PCC	S2_RFO 6PCC	S3_IST5 PCC	S3_IST6 PCC
539	578	616	8	103	1500	556
449	491	798	23	84	1500	1108
918	754	668	75	86	1500	990
321	520	764	121	190	1500	956
819	578	637	11	81	1500	1151
1000	851	747	73	92	1500	805
483					607	662
769					608	945
1000					649	936
623					827	933
611					1065	1048
387					803	851
618					1500	1500
340					1500	1500
869					1500	1500
1000					1500	1500
665					1500	1500
					1500	1500

2.5 How test data was collected

The data was generated between May 10, 2006 and July 12, 2006 for supplier 1 and supplier 2. The supplier 3 data was generated between August 18, 2007 and October 15, 2007 to further corroborate the results. Each data set was preconditioned first, then regular ALT IST is performed simulating the thermal stress environment seen by avionics electronics throughout the life of the products. The regular ALT IST cycles typically consist of 350 accelerated ramped thermal cycles developed from aircraft thermal probability spectral density flight data. Regular ALT IST performed with lots consisting of six samples or coupons is tested continuously for six days then terminated at 1500 cycles. Therefore the test data is time censored or Type I censored data; both complete data (3 data sets) and right censored data (4 data sets) are represented in Table 2.1.

Preconditioning is completed on an IST machine (6 coupons per lot are tested at a time) with a cycle that starts at room temperature, 25C then ramps to a temperature of 230C after three minutes, samples then cool to room temperature again after two minutes. Once preconditioning cycles are complete, regular IST cycling starts at room temperature and ramps to 150C after three minutes then cools to room temperature after two minutes. Referring to Table 2.1 for samples made by supplier 1 five IST PCCs were performed for 18 samples (3 lots) and six PCCs were also performed at for six additional samples (1 lot). While five PCCs are typically used in this process, six PCCs were serendipitously performed once

we discoursed the origin of the data taken from the IST machine and would be a major comparison factor when comparing both processes. Referring to Table 2.1 for samples made by Supplier 2 only six samples (1 lot) were preconditioned for five cycles. Referring again to Table 2.1 for samples made by supplier 3, 18 samples (3 lots) were preconditioned for five cycles and another 18 samples were preconditioned for six cycles.

A re-flow oven preconditioning temperature profile used on printed circuit boards cycles six times from room temperature ramped for 12 minutes to 250C then cooled to room temperature in eight minutes. Referring to Table 2.1 columns three and five, one lot each of supplier 1 and supplier 2 were subjected to six re-flow oven PCCs. After re-flow oven preconditioning, samples are subjected to regular IST cycling from room temperature ramped to 150C after three minutes then cooled to room temperature after two minutes before starting the cycle again.

2.6 Data analysis results

In Table 2.2, the Weibull distribution likelihoods, shape, scale, mean or mean time to failure (MTTF), median and standard deviation are calculated using Minitab version 16, but only the likelihood is used for the LR test. Prior to the selection of the Weibull distribution as the appropriate failure distribution for the data, all the data sets used in the comparisons are Anderson-Darling adjusted AD* ranked by lowest values from 1 to 5 (in parenthesis) based on the Minitab version 16 goodness-of-fit calculations for Weibull, normal, logistic, lognormal and log logistic distributions respectively. The last row in Table 2.3 shows the lowest is

better AD* goodness of fit totals for the Weibull (28) and lognormal (27) distributions. Both Weibull and lognormal distributions have the best goodness-of-fit based on the Minitab version 15 software notes explanations for (AD*) rankings that are calculated and tabulated in Table 2.3. Anderson-Darling goodness-of-fit is chosen as an appropriate method over chi-squared goodness-of-fit for its superior performance when applied to small data samples like in the supplier data sets. The Weibull distribution is chosen over the lognormal distribution because at the highest cycles to failure, the Weibull distribution is a better fit when the individual plots (not shown) are examined for each of the data set fits.

Comparisons are now made on individual supplier data between IST or re-flow oven preconditioning factor levels and preconditioning cycle factor level combinations.

Three basic factors at two levels are studied:

1. Factor one is supplier quality with one level being supplier 1 and supplier 3 because they are high performing circuit board manufacturers, and exceed 350 cycles to failure, the second level is supplier 2 coupons which never exceed 190 cycles to failure;
2. Factor two is preconditioning method of either using an accelerated five minute cycle time IST or a re-flow oven twelve minute cycle time, but with both maximum temperatures remaining constant; and
3. Factor three is the number of preconditioning cycles either five or six.

For supplier 1 there are three pairs of data set comparisons between combinations of IST or re-flow and number of preconditioning cycles as follows. Referring to Table 2.2 the first data set comparison pair is five IST PCCs (row S1_IST5PCC) compared to six re-flow oven PCCs (row S1_RFO6PCC) and represents the current operating procedure. Using the LR test equation (2) and the respective log-likelihood values for data sets in rows S1_IST5PCC, S1_RFO6PCC and S1_IST5;RFO6 in Table 2.2,

$$T = -2[-140.209 + 101.083 + 33.854] = 10.544 > \chi^2_{.05,2} = 5.99,$$

where row S1_IST5, RFO6 contains the log-likelihood associated with the combined distribution parameters from rows S1_IST5PCC and S1_RFO6PCC. Since LR is greater than chi-squared the null hypothesis is rejected and coupons with five IST PCCs are not similar to coupons with six re-flow oven PCCs, Figure 2.5. The second data set comparison pair for Supplier 1 is six IST PCCs (row S1_IST6PCC) compared to six re-flow oven PCCs (row S1_RFO6PCC) using the log-likelihoods in rows S1_IST6PCC, S1_RFO6PCC and row S1_IST6; RFO6, Table 2.2 and the LR test equation (2):

$$T = -2[-69.790 + 33.698 + 33.854] = 4.476 < \chi^2_{.05,2} = 5.99.$$

The null hypothesis, H_0 is not rejected and coupons with six IST PCCs are similar to coupons with six re-flow oven PCCs, Figure 2.6. The third data set

comparison pair for supplier 1 is five IST PCCs (S1_IST5PCC) compared to six IST PCCs (S1_IST6PCC) using the log-likelihoods in rows S1_IST5PCC, S1_IST6PCC and S1_IST5;IST6 in Table 2.2 and the LR test equation (2):

$$T = -2[-135.535 + 101.083 + 33.698] = 1.508 < \chi^2_{.05,2} = 5.99.$$

The null hypothesis, H_0 is not rejected and coupons with five IST PCCs are similar to coupons with six IST PCCs, Figure 2.7. What these three data set comparisons for supplier 1 resolve is an energy ranking of the processes: five IST PCCs of energy are less than six IST PCCs of energy are less than six re-flow oven PCCs of energy. Furthermore, since IST cycles are identical the amount of energy in joules absorbed by the coupons is less for five cycles than in six cycles and in turn less than six re-flow oven cycles. The mode of heat transfer is conduction for IST due to the heat generation of the daisy chain conductors into the coupon and is proportional to a coupon conduction coefficient times the temperature difference in time during ramp cycling. The mode of heat transfer for the re-flow oven is convection of heat into the coupons proportional to a convection coefficient times the temperature difference in time during its ramp cycling. The remaining data set comparisons for supplier 2 and supplier 3 will corroborate this energy relation.

The supplier 2 data set comparison pair is five IST PCCs (row S2_IST5PCC) to six re-flow oven PCCs (row S2_RFO6PCC) in Table 2.2. Using the LR test equation (2) and the log-likelihood values for data sets in rows

S2_IST5PCC, S2_RFO6PCC and S2_IST5;RFO6 in Table 2.2, where row S2_IST5;RFO6 contains the log-likelihood associated with the combined distribution parameters from rows S2_IST5PCC and S2_RFO6PCC:

$$T = -2[-63.008 + 29.580 + 30.263] = 6.33 > \chi^2_{.05,2} = 5.99.$$

So the null hypothesis, H_0 is rejected and coupons with five IST PCCs are not similar to coupons with six re-flow oven PCCs, Figure 2.8. This result corroborates the Supplier 1 LR test for five IST PCCs and six RFO PCCs.

The supplier 3 data set comparison pair is five IST PCCs (row S3_IST5PCC) to six IST PCCs (row S3_IST6PCC) in Table 2.2. Using the LR test equation (2) and the log-likelihood values for data sets in rows S3_IST5PCC, S3_IST6PCC and S3_IST5; IST6 in Table 2.2, where row S3_IST5; IST6 contains the log-likelihood associated with the combined distribution parameters from rows S3_IST5PCC and S3_IST6PCC:

$$T = -2[-145.656 + 54.694 + 88.827] = 4.27 < \chi^2_{.05,2} = 5.99.$$

So the null hypothesis, H_0 is not rejected and coupons with five IST PCCs are similar to coupons with six IST PCCs, Figure 2.9. This result corroborates the supplier 1 LR test for five IST PCCs and six IST PCCs.

Table 2.2 Summary of Weibull statistics for the Comparison Set data used in likelihood-ratio tests

Comparison Set Label	Log-Likelihood	Shape(95% CI)	Scale(95%CI)	Mean (MTTF)	Median	Std. Dev.
S1_IST5PCC	-101.083	2.72609 (1.76602, 4.20811)	786.969 (648.740, 954.652)	700.072	687.968	277.225
S1_IST6PCC	-33.698	4.25147 (2.13140, 8.48034)	701.833 (570.002, 864.153)	638.370	643.863	169.472
S1_RFO6PCC	-33.854	12.0173 (6.30736, 22.8962)	736.106 (686.084, 789.776)	705.438	713.995	71.3043
S1_IST5;RFO6	-140.209	3.32724 (2.32386, 4.76385)	773.055 (676.506, 883.382)	693.729	692.421	229.762
S1_IST6;RFO6	-69.790	6.22788 (3.87727, 10.0035)	719.708 (652.884, 793.371)	669.057	678.575	125.264
S1_IST5;IST6	-135.535	2.93824 (2.03673, 4.23877)	767.449 (657.907, 895.229)	684.701	677.448	253.536
S2_IST5PCC	-29.580	1.17394 (.610317, 2.25807)	54.7767 (26.6814, 112.456)	51.8279	40.0872	44.2969
S2_RFO6PCC	-30.263	2.81817 (1.60957, 4.93429)	119.011 (87.8910, 161.149)	105.999	104.497	40.7450
S2_IST5;RFO6	-63.008	1.5595 (.974301, 2.49619)	87.0597 (59.5969, 127.178)	78.2509	68.8255	51.2632
S3_IST5PCC	-54.694	1.63707 (.775889, 3.45409)	2518.76 (1292.10, 4909.94)	2253.74	2013.52	1412.31
S3_IST6PCC	-88.827	2.63211 (1.58641, 4.36707)	1416.41 (1124.91, 1783.43)	1258.54	1232.29	514.277
S3_IST5;IST6	-145.656	2.10116 (1.36992, 3.22272)	1763.64 (1364.60, 2279.38)	1562.04	1481.34	781.085

Table 2.3 Distribution Identification rankings using adjusted Anderson-Darling goodness-of-fit in Minitab 16

Distribution Fit	Weibull	Normal	Logistic	Lognormal	Loglogistic
S1_IST5PCC	15.721 (2)	15.742(4)	15.783(5)	15.706(1)	15.724(3)
S1_IST6PCC	9.031(3)	9.029(2)	9.096(5)	9.008(1)	9.074(4)
S1_RFO6PCC	2.224(3)	2.254(4)	2.200(2)	2.256(5)	2.194(1)
S1_IST5,RFO6	12.314(2)	12.296(1)	12.321(3)	12.401(5)	12.347(4)
S1_IST6,RFO6	5.219(1)	5.236(5)	5.285(4)	5.24(2)	5.26(3)
S1_IST5,IST6	16.424(3)	16.445(4)	16.482(5)	16.316(1)	16.344(2)
S2_IST5PCC	2.271(2)	2.308(4)	2.316(5)	2.297(3)	2.207(1)
S2_RFO6PCC	2.699(2)	2.855(3)	3.091(5)	2.681(1)	2.863(4)
S2_IST5,RFO6	1.749(3)	1.533(2)	1.497(1)	2.083(5)	1.760(4)
S3_IST5PCC	74.509(2)	74.522(4)	74.520(3)	74.503(1)	74.503(1)
S3_IST6PCC	49.246(3)	49.256(4)	49.238(2)	49.148(1)	49.148(1)
S3_IST5,IST6	128.369(2)	128.427(4)	128.412(3)	128.292(1)	128.295(2)
AD Fit Totals	28	41	43	27	30

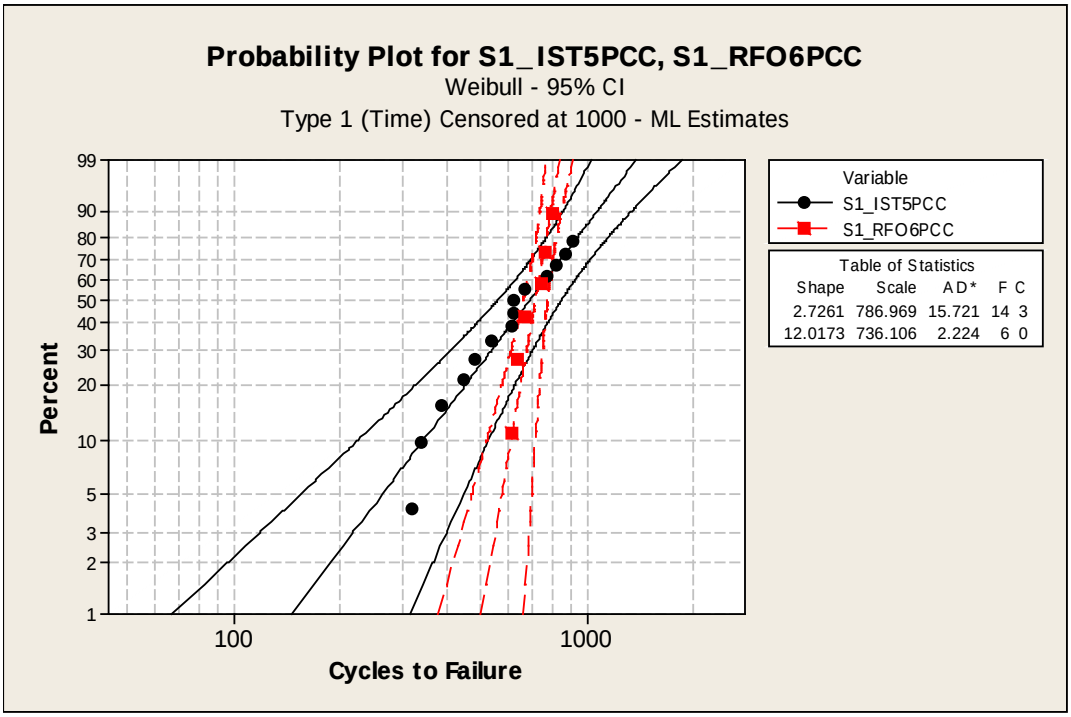

Figure 2.5 Five IST PCCs are significantly different from six re-flow oven PCCs for supplier 1

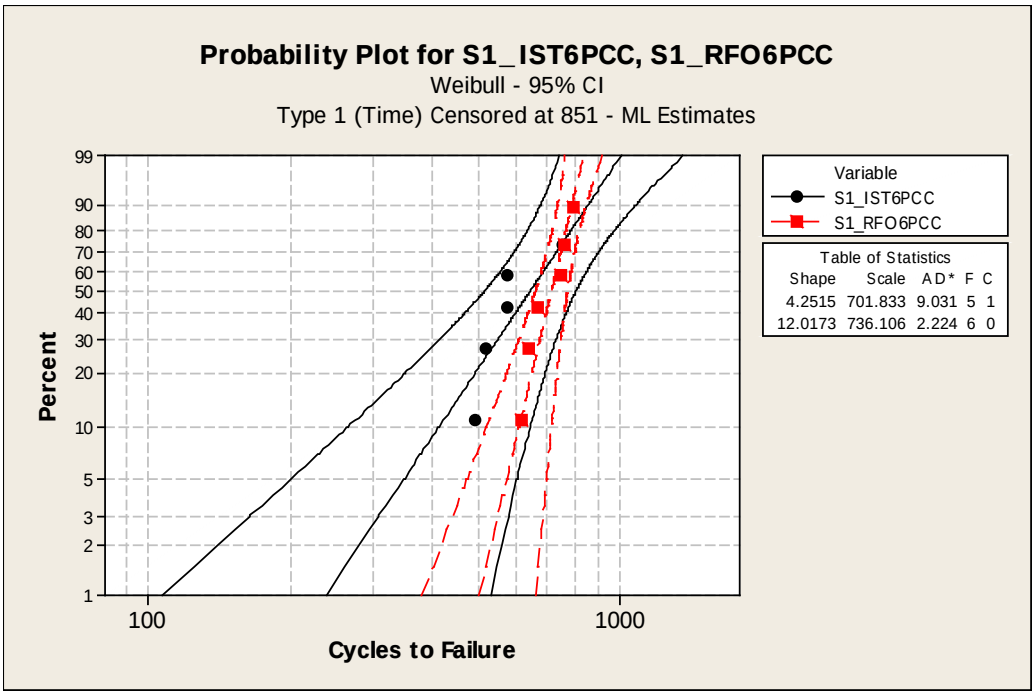

Figure 2.6 Six IST PCCs are similar to six re-flow oven PCCs for supplier 1

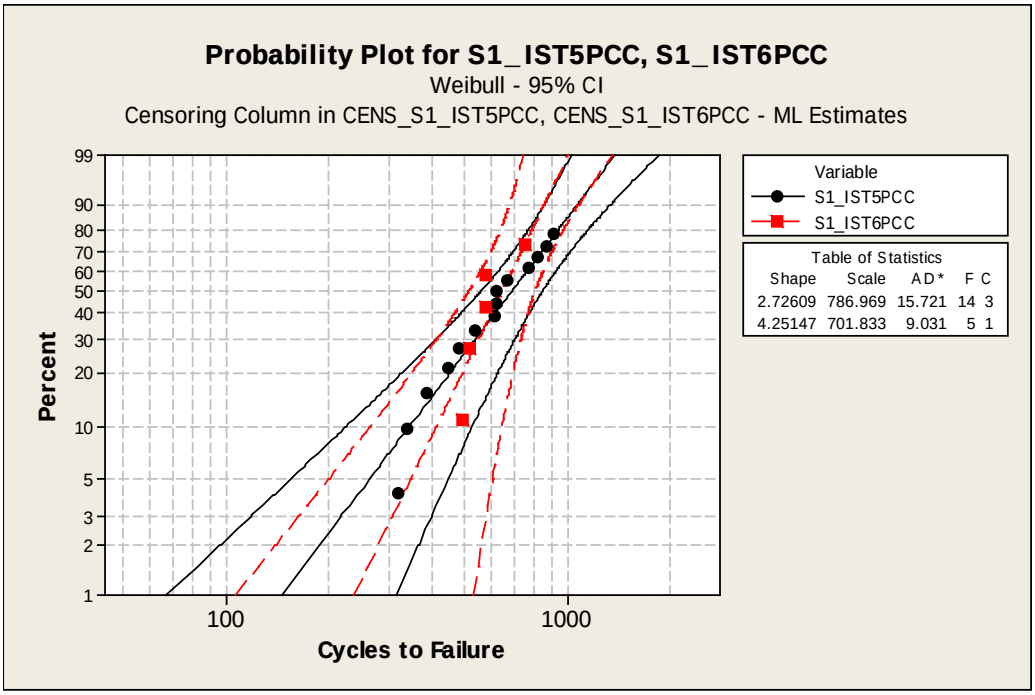

Figure 2.7 Five IST PCCs are similar to six IST PCCs for supplier 1

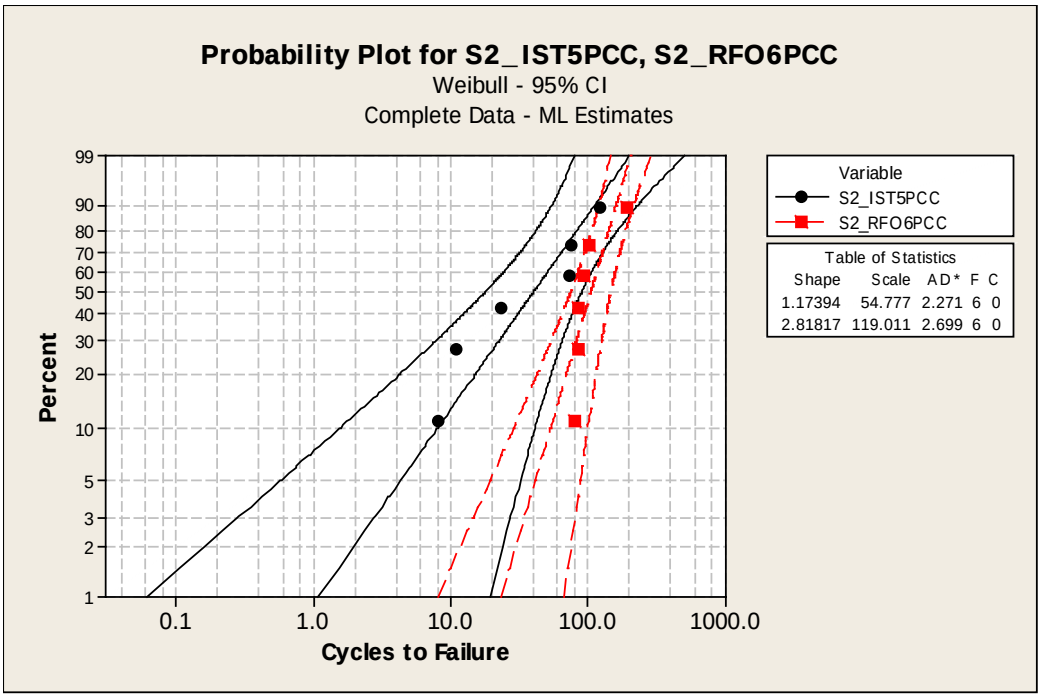

Figure 2.8 Five IST PCCs are significantly different from six re-flow oven PCCs for supplier 2

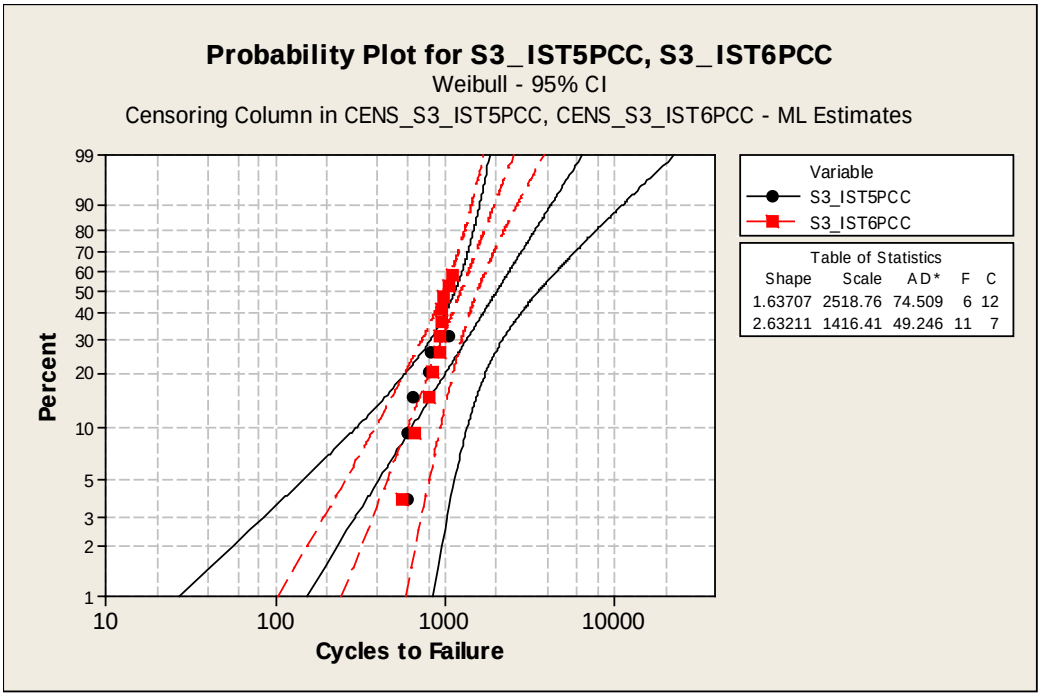

Figure 2.9 Five IST PCCs are similar to six IST PCCs for supplier 3

2.7 Validation by root mean square power calculations

The statistical analysis infers that the energy inputs to the coupons are

5 IST PCC are less than 6 IST PCC and less than 6 RFO PCC;

therefore, by computing the root mean square (RMS) power heat transfer input to both an IST preconditioning cycle and a re-flow oven preconditioning cycle and showing they are close validates why 6 IST PCC are similar to 6 RFO PCC. The following calculation is first order and represents heat transfer to a coupon by resistive heating for IST and convection for a re-flow oven for a single cycle. The heat transfer constants of proportionality are different between conductive and convective modes of energy transfer, but the assumption is that transients due to these heat transfer coefficients are short compared to the time heat is absorbed as calculated by Blattau (1999). By the energy theorem (Feynman, Leighton and Sands, 1963, pp. 50-7, 50-8), the energy in one period of a waveform is proportional to

$$\int_0^T f^2(t)dt$$

where $f(t)$ is the temperature ramp as a function of time. The RMS power of the waveform in Scott (1965, pp. 294-296) is

$$P_{rms} = \sqrt{\frac{1}{T}\int_0^T f^2(t)dt}\,. \qquad (3)$$

We obtain the RMS power of the waveforms represented in Table 2.4 as follows.

For the IST cycle $f_{IST} = \begin{cases} K[(230^O C - 25^O C)/3]t; 0 < t < 3, \\ 0 \qquad\qquad\qquad\qquad ; 3 < t < 5. \end{cases}$

Where K = 1 is a heat transfer coefficient with units Joules/sec-sec-^{o}C appropriate for scaling to RMS power and the value 1 is associated with joule heating of the IST coupon circuit calibrated to the IST machine power limits for one coupon. The period is T=5 minutes and the RMS value is

$$P_{rms}^{IST} = \sqrt{\frac{1}{5}\int_0^3 [(205/3)t]^2\, dt} = 41\sqrt{5} = 91.7 watts\,.$$

For the RFO cycle

$$f_{RFO} = \begin{cases} K[(250^{O}C - 25^{O}C)/12)]t; 0 < t < 12, \\ 0 \qquad\qquad\qquad\qquad ; 12 < t < 20. \end{cases}$$

Here K = 1 is a heat transfer coefficient with units Joules/sec-sec-^{o}C and associated with joule heating of the IST coupon circuit through convection from the reflow oven.

The period is T=20 minutes and the RMS value is

$$P_{rms}^{RFO} = \sqrt{\frac{1}{20}\int_0^{12} [(225/12)t]^2\, dt} = 45\sqrt{5} = 100.6 watts.$$

Comparing both RMS powers, (100.6 watts – 91.7 watts)/100.6 watts = 8.8% error. This result is consistent with the inequality based on the statistics that cycle per cycle there is less heat transfer to the coupons yet close enough to be from the same distribution, but that one less IST cycle is sufficient to be close to 6 IST PCC and does not contain enough power to be close to 6 RFO PCC.

Table 2.4 Ramping waveforms for an IST and RFO preconditioning cycle

Preconditioning Cycle Method	Room Temp., ^{O}C	Max. Ramp Temp., ^{O}C	Ramp Time, min.	Cycle Time, min.	RMS Power, watts
IST	25	230	3	5	91.7
RFO	25	250	12	20	100.6
Modified IST	25	250	3	5	100.6

Furthermore, this power gap can be brought to parity by matching the maximum ramp temperature and obtaining the RMS power of the Modified IST waveform in Table 2.4 (the last row entry), as follows:

For the Modified IST cycle

$$f_{MIST} = \begin{cases} [K(250^{O}C - 25^{O}C)/3]t; 0 < t < 3, \\ 0 \qquad\qquad\qquad\qquad ; 3 < t < 5. \end{cases}$$

The period is T=5 minutes, K = 1 is a heat transfer coefficient with units Joules/sec-sec-^{o}C, and the RMS value is

$$P_{rms}^{MIST} = \sqrt{\frac{1}{5}\int_{0}^{3}[(225/3)t]^{2}\,dt} = 100.6 watts \,.$$

Therefore with the Modified IST maximum ramp temperature equivalent to the RFO maximum ramp temperature results in equivalent RMS power values. RMS power values of ramping cycles are equivalent provided that the ratios of the ramp time to cycle time remain the same, also the integrals result in the same power whether units of seconds or minutes are used since watts are in units of

joules/second. In conclusion, the Minitab version 15 Weibull distribution calculations used in LR tests indicate that the current processes should be reconsidered so they are comparable to a re-flow oven preconditioning process. This means that only one more IST preconditioning cycle is needed and the cost is only an additional 5 minutes on the IST machine. In addition, the maximum ramp temperatures should also be the same based on a simple physical model constructed to explain the statistical results. What would be useful to the industry is that once re-flow oven temperatures are set then IST only needs to be matched in cycle time and temperature.

2.8 Total energy approach and the theory of a statistically equivalent energy bound

In the last section, we calibrate the hypothetical Modified IST condition to RFO by equating the RMS power which happens when the maximum ramp temperatures are the same for IST and reflow on a cycle-by-cycle basis assuming that the ramp time to cycle time are also equivalent. This assumption leads to a simple energy relationship of three factors. Number of preconditioning cycles, PCCs is a multiplicative time factor of power applied to the coupons. And the power factors: difference between room temperature and maximum ramp temperature, ΔT and ramp time to cycle time, (RT: CT);

$$\text{Energy} = \text{PCC}*\Delta T*(\text{RT: CT}). \qquad (4)$$

A more precise total energy relation is the heat transfer equation in units of power multiplied by the PCC time factor,

$$\text{Energy} = mC\Delta T*(\text{RT: CT})*(\text{PCC}).$$

Setting the m term equal one incorporates the material, geometry and coupon constants like board thickness = 0.1 inches, PTH barrel aspect ratio = 8 which is board thickness to PTH hole diameter because these parameters are equated on all coupons tested for comparison. In addition, the constant C equals one because Blattau (1999) shows that the assumption: coupons reach steady state temperatures so fast that the coupons are always at the readout temperatures is valid. Although IST coupons are joule heated and RFO coupons are convectively heated and have different heat transfer coefficients and units, the mC term equal one normalizes the power units. Therefore equation (4) will be the basis for establishing energy bounds on data sets when in the null hypothesis of equality of mean cycles-to-failure for two samples is not rejected.

Statistical equivalent data sets are those that upon comparison result in T < 5.99 using the LR test equation (2). Similarly, if using equation (4) to calculate a joule equivalent for each data set and then taking the JE difference between these data sets results in less than 123 JE then the data sets are statistically equivalent and the null hypothesis of equality of mean cycles-to-failure for two samples is not rejected. This value of 123 JE is the statistically equivalent energy bound. For example based on the IST data in Table 2.4, applying equation (4):

(IST6PCC)*(205)*(.6) = 738 JE minus

(IST5PCC)*(205)*(.6) = 615 JE is a difference of 123 JE and is the highest energy bound with statistically significant equivalence meaning the null hypothesis of equality of mean cycles-to-failure for two samples is not rejected.

In subsequent data sets JE difference calculations show that 123 JE is the energy bound that consistently results in the null hypothesis of equality of mean cycles-to-failure for two samples is not rejected.

First proving that the Modified IST is indeed having the same effect as RFO, ALT testing is performed with failure data shown in Table 2.5 columns one and two. Note the IST ALT parameters are set to the same RFO conditions using equation (4) with six (6) preconditioning cycles; maximum ramp temperatures equal to 240C. The ratio of ramp time to cycle time is 0.6 for IST, but 0.606 for RFO. Using the respective likelihood data in Table 2.6 and applying the LR test equation (2) shows that null hypothesis is not rejected.

$T=-2[\log \text{likelihood}(\mu_0, \sigma_0) - \{\log \text{likelihood}(\mu_1, \sigma_1) + \log \text{likelihood}\ (\mu_2, \sigma_2)\}]$

$T = -2(-223.032 - \{-66.459 - 155.008\})$

$T = 3.13 < 5.99.$

Also in Table 2.6, the joule equivalent values result in a difference of 8 JE, well below the 123 JE energy bound.

Beyond the Modified IST condition to RFO, other tests using equation (4) are presented that validate the generality of the energy relation by using the LR test. This includes testing to show that fewer IST PCCs, but higher maximum ramp temperatures lead to accepting the null hypothesis when the RFO PCCs are higher with a lower maximum ramp temperature and RT: CT kept constant. The failure data for these test cases are in Table 2.5, note that the "S" before values are suspensions. Therefore a test is constructed where the preconditioned maximum ramp temperature is higher (245C) during 5 IST PCC than the maximum ramp

temperature (240C) during 6 RFO PCC. The actual ratio of ramp time to cycle time is 0.6 for IST, but 0.606 for RFO. Failure data for these conditions are in Table 2.5 columns two and three. Using the respective likelihood data in Table 2.7 and applying the LR test equation (2) shows that null hypothesis is not rejected.

$T=-2[\log likelihood(\mu_0, \sigma_0) - \{\log likelihood(\mu_1, \sigma_1) + \log likelihood(\mu_2, \sigma_2)\}]$

$T = -2(-227.234 - \{-70.858 - 155.008\})$

$T = 2.736 < 5.99.$

Also in Table 2.7, the joule equivalent values result in a difference of 122 JE just below the 123 JE energy bound.

Also included in this section is a re-analysis of test data, Table 2.8 from a research report in Slough (2005) with 54 coupons subjected to 6 IST PCC with a maximum ramp temperature of 230C and a RT: CT ratio of (0.6) and 58 coupons subjected to 6 RFO PCC with a maximum ramp temperature of 230C, but an RT: CT of (0.5). Failure data for these conditions are in Table 2.8 and again note that the "S" before values are suspensions. Using the respective likelihood data in Table 2.9 and applying the LR test equation (2) shows that null hypothesis is not accepted.

$T=-2[\log likelihood(\mu_0, \sigma_0) - \{\log likelihood(\mu_1, \sigma_1) + \log likelihood\ (\mu_2, \sigma_2)\}]$

$T = -2(-725.261 - \{-314.293 – 377.433\})$

$T = 67.07 > 5.99.$

Also in Table 2.9, the joule equivalent values result in a difference of 123 JE and are at the 123 JE energy bound. This example shows that the ramp time to cycle

time ratio significantly affects IST parameter settings even though the maximum temperature is the same for the same number of preconditioning cycles. Sough (2005), acknowledges that "IST was more severe than by the traditional reflow oven...reflow profile reaches the peak temperature around 5.25 versus IST preconditioning reaching peak temperature at 3 minutes where the difference can be attributed to the reflow profile having a lengthy soak zone before reaching peak temperature." This "difference" can be quantified using equation (3) and the calculated power for the Slough (2005) reflow oven is 83.7 watts per cycle and the one for IST is 91.7 watts per cycle taken from Table 2.4 since it is the same condition as Slough (2005) for IST.

Table 2.5 ALT failure data for Modified IST (column 1) to calibrate RFO (column 2) and data for a lower PCC count, but higher temperature (column 3) relative to RFO (column 2)

IST 6PCC X 240C	RFO 6PCC X 240C	IST 5PCC X 245C
1934	1971	S1800
1880	1491	1567
2424	1559	1744
2464	1622	S1800
1179	2437	1728
1512	1889	1713
S1800	2045	S1800
2149	1802	S1800
1903	1765	S1800
2185	S1800	S1800
	S1800	S2821
	S1800	S2821
	S1800	S2821
	1706	2610
	1616	S2821
	1196	1056
	S1800	1473
	S1800	1809
	2733	
	2176	
	S2800	
	S2800	
	1674	
	2120	
	2076	
	S2800	
	1195	
	1055	
	S1800	

Table 2.6 Comparison between IST 6PCC X 240C and RFO 6PCC X 240C

Comparison Set Label	Ramp Time-to-Cycle Time	Log-Likelihood	Shape (beta) 95% CI	Scale (eta) 95% CI	Mean (MTTF)	Median	Std. Dev.	Joule Equivalent
IST_6PCCX240C	0.6	-66.459	6.44356 (Lower: 3.81520, Upper: 10.8827)	2131.19 (Lower: 1919.76, Upper: 2365.89)	1984.86	2013.35	360.107	774
RFO_6PCCX240C	0.606	-155.008	3.86187 (Lower: 2.73174; Upper: 5.45955)	2290.01 (Lower: 2038.181; Upper: 2572.95)	2071.55	2082.67	599.916	782
IST_6PCC:RFO6PCCs		-223.032	4.29485 (Lower: 3.23496; Upper: 5.701997)	2233.66 (Lower: 2048.83; Upper: 2435.17)	2032.88	2050.95	534.734	

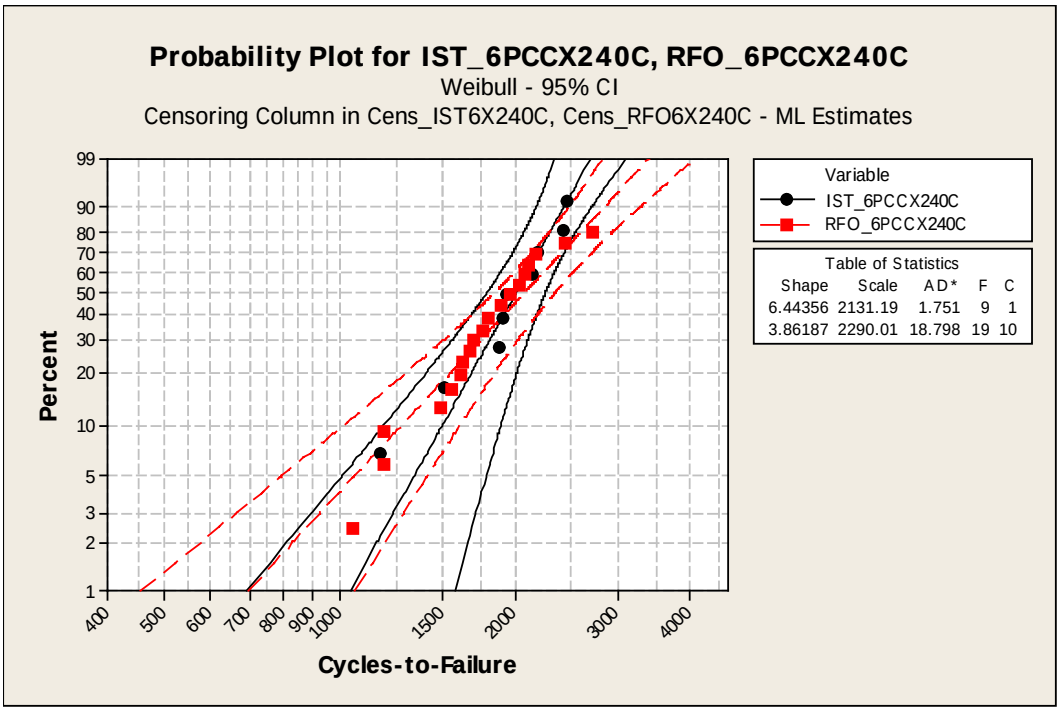

Figure 2.10 Distribution for six IST PCCs at 240C is similar to six RFO PCCs at 240C

Table 2.7 Comparison between IST 5PCC X 245C and RFO 6PCC X 240C

Comparison Set Label	Ramp Time-to-Cycle Time	Log-Likelihood	Shape (beta) 95% CI	Scale (eta) 95% CI	Mean (MTTF)	Median	Std. Dev.	Joule Equivalent
IST_5PCCX245C	0.6	-70.858	2.98436 (Lower: 1.69447, Upper: 5.25617)	2784.32 (Lower: 2161.52, Upper: 3586.57)	2485.77	2462.54	907.687	660
RFO_6PCCX240C	0.606	-155.008	3.86187 (Lower: 2.73174; Upper: 5.45955)	2290.01 (Lower: 2038.181; Upper: 2572.95)	2071.55	2082.67	599.916	782
IST_5PCC:RFO6PCCs		-227.234	3.48560 (Lower: 2.59027; Upper: 4.69041)	2440.39 (Lower: 2186.79; Upper: 2723.40)	2195.26	2196.81	697.29	

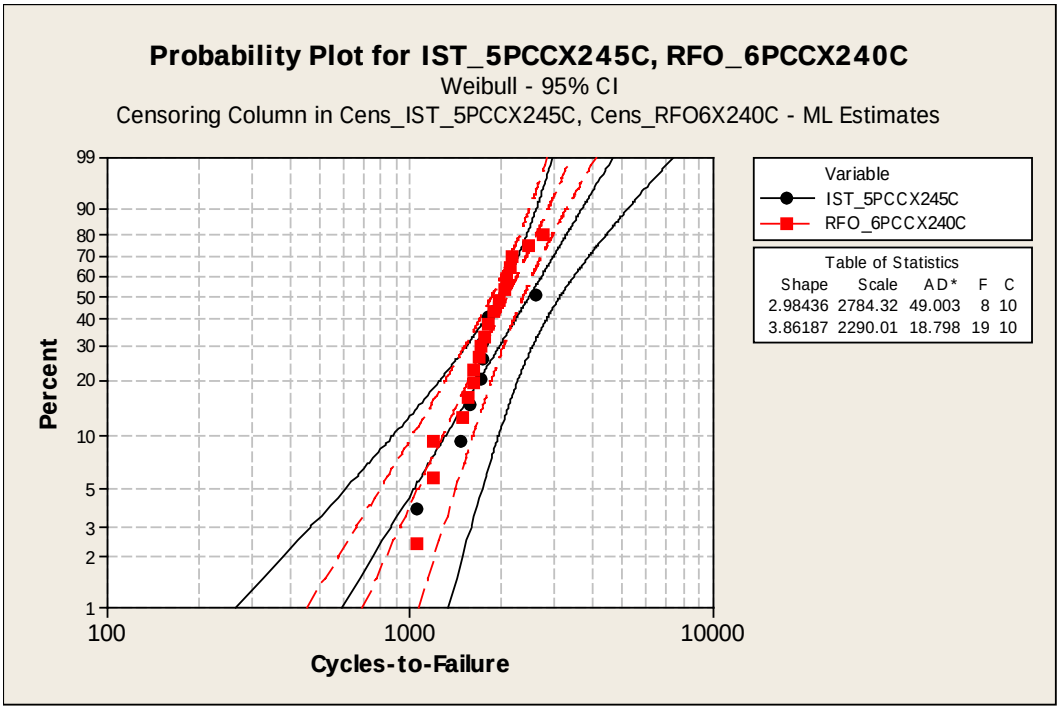

Figure 2.11 Distribution for five IST PCCs at 245C is similar to six RFO PCCs at 240C

Table 2.8 Multek failure data set with different ramp time to cycle times

54 Coupons with 6 IST PCCX230C ramp time to cycle time = 0.6	58 Coupons with 6 RFO PCCX230C ramp time to cycle time = 0.5
235	352
287	292
331	454
135	256
317	278
349	684
302	348
198	352
216	323
179	676
441	465
137	578
115	665
225	388
166	290
181	183
418	329
208	472
239	319
145	330
240	740
344	265
247	254
149	416
163	424
202	248
210	294
144	604
208	551
167	393
183	S1000
145	246
124	270
229	292
296	221
204	268
264	402
270	361
147	267
220	389
401	477
243	853
318	442
196	672
142	446
211	537
254	340
310	407
279	513
485	796
295	732
218	S1000
198	963
248	395
	568
	617
	453
	579

Table 2.9 Multek data comparison between IST 6PCC X 230C and RFO 6PCC X 230C for different ramp time to cycle time ratios

Comparison Set Label	Ramp Time to Cycle Time	Log-Likelihood	Shape (beta) 95% CI	Scale (eta) 95% CI	Mean (MTTF)	Median	Std. Dev.	Joule Equivalent
IST_6PCCX230C	0.6	-314.293	3.00175 (Lower: 2.47309, Upper: 3.64342)	264.938 (Lower: 241.091, Upper: 291.143)	236.59	234.486	85.94	738
RFO_6PCCX230C	0.5	-377.433	2.35779 (Lower: 1.94118; Upper: 2.86382)	525.045 (Lower: 567.375; Upper: 589.831)	465.302	449.455	209.8	615
IST_6PCC:RFO6PCC		-725.261	1.94533 (Lower: 1.69850; Upper: 2.22803)	402.007 (Lower: 363.283; Upper: 444.859)	356.485	332.973	191.0	

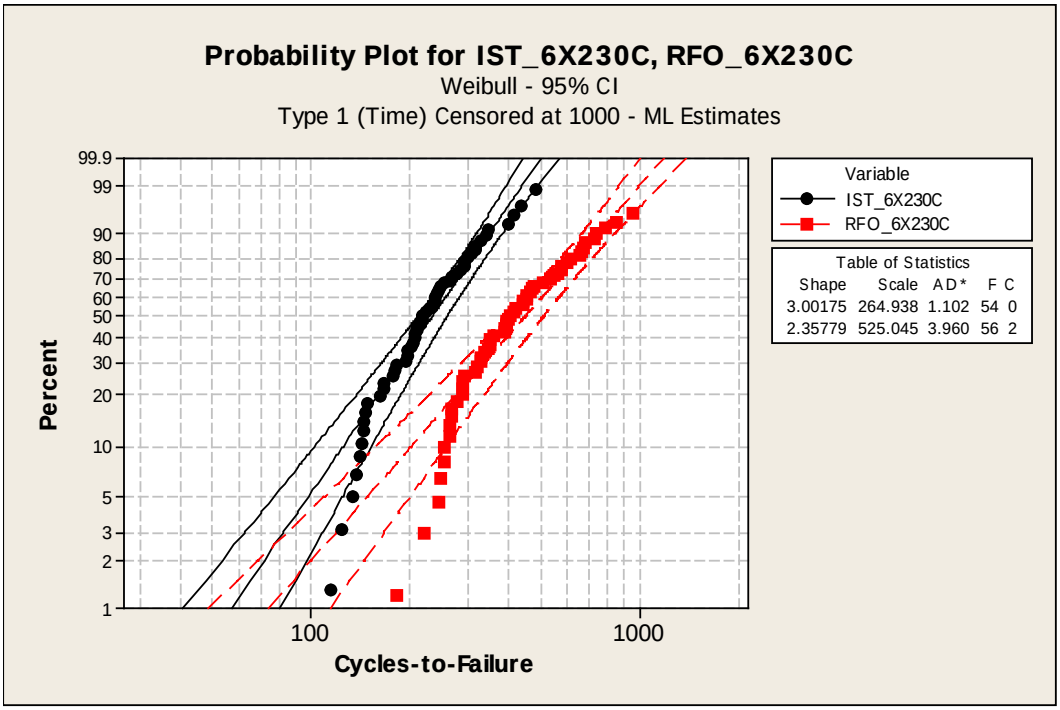

Figure 2.12 Six IST PCCs are significantly different from six re-flow oven PCCs both at 230C when the ramp time-to-cycle time ratios are different by 20%

2.9 Applications in lead-free solder IST preconditioning

Lead-free IST thermal cycled coupons will accommodate 96.5%Sn 3.0%Ag 0.5%Cu (SAC305) solder alloys that re-flow between 230C to 250C and appropriate temperatures are still in the experimental stage versus current technology solders melting at 183C (361F) for eutectic tin lead solders see Van Vlack (1975, p. 302). Recall RFO represents the actual process seen by the circuit boards and research is continuing on what the appropriate temperature and ramp rates to use. The current study included re-flowed coupons at 250C (523K) or 10C higher than nominal re-flow temperatures proposed for lead-free and therefore this work is applicable to lead-free designs.

Chapter 3

DISCRIMINATING BETWEEN TIN-LEAD AND LEAD-FREE SOLDER INTERCONNECT FAILURE DATA IN HIGH CYCLE FATIGUE

3.1 Statement of the problem

In this chapter of the Dissertation, accelerated testing of circuit boards subjected to harmonic vibration testing specifically addresses methods for finding the most significant factors that lead to predictive failure modeling of tin-lead and lead-free solder interconnects. Steinberg (2000, pp. 172-173) presents a harmonic vibration failure relationship that uses component type, component length, printed wiring board assembly (PBA) length along the longest dimension of the component, board thickness, and component location on the PBA as important predictive factors. The Steinberg relation though is for tin-lead solder only. What is needed is a model that takes into account factors like lead-free metallurgies; thermal preconditioning before vibration; and for ball grid array (BGA) type components examines the relationship between solder ball size, ball count, ball spacing, ball distributions like full grid arrays or peripheral grid arrangements, and number of balls. Some of these factors may not be important relative to the tin-lead solder baseline model; regardless, the problem is multivariable in nature since tin-lead and lead-free solder must always be a factor along with others and at various vibration loading levels for test matrices addressing aspects of this problem.

Here testing produced data using factors involving both tin-lead as a baseline and 96.5%Sn 3.0%Ag 0.5%Cu (SAC305); thermal preconditioning; and various vibration levels. A lot of factors are fixed like room temperature testing; only one full grid array type 1156 I/O BGA is used; and only a single geometry PBA, but the PBA is fully populated with 20 BGAs so location matters on the board for vibration and the BGA is large and susceptible to early failures compared to longer life for smaller components.

All the data is analyzed to demonstrate how predictive modeling might use likelihood-ratio (LR) tests to examine differences of the failure distributions for the two solders. The additional factors like surface finish and vibration use regression analysis and two-way analysis of variance (ANOVA) to identify significance in the factors. Finally S-N curve development techniques take vibration qualitative factor levels from the lead-free part of the previous analysis and quantity these factors for further analysis using the LR test.

In the previous chapter of this Dissertation, the likelihood ratio test was used to compare preconditioning due to both a re-flow oven and IST as it applied to a thermally induced mode of failure. In this chapter the analysis begins by also applying the likelihood ratio test to discriminate between failure times for vibration induced bending strain for tin-lead and lead-free solder interconnects given two other factors: preconditioning or aging before vibration and surface chemical finishes. Both these factors have high processing cost implications. Aging can take 120 cycles with temperature excursions between -40C and 85C. Different finishes lead to material properties that have not been resolved in the

literature and thermal preconditioning has not been included in most test matrices like Woodrow (2006), Woodrow (2010) and Zhou, Al-Bassyiouni, and Dasgupta (2010). Woodrow (2006) reports that thermal aging promotes Krikendall voids that lead to lower reliability for shock, but is this reason enough not to subject aged circuit boards to vibration?

The LR test is not enough and therefore the data is subjected to multivariable regression analysis to show that preconditioning may not be important. Two-way ANOVA provides more insight into differences between tin-lead and lead-free for increasing vibration levels, but these levels are discretized into four vibration levels. Further resolution on the data can be accomplished by using S-N curves to take discrete vibration levels and convert the vibration level to a more quantitative variable.

3.2 Literature search

Here we review how data is analyzed to reach conclusion about important factors necessary for predicting solder joint life and how specifically tin-lead and lead-free performance are compared when harmonic loading is applied. How multiple regression or ANOVA are applied to vibration test data in general is also reviewed. In addition, S-N curve development and how it is incorporated into analysis for predicting life is presented using Steinberg (2000) equations.

The reason for starting with the LR test is that because failure times have always been reported as Weibull, (Woodrow, 2006). The LR test is the logical way to begin comparisons, but researchers have resorted to comparisons by averaging the failure times then looking for the larger average on a bar chart

(Zhou and Dasgupta, 2006) and (Zhou, Al-Bassyiouni, and Dasgupta, 2010) or discussing Weibull curve comparisons using least squares generated characteristic life (Arnold, 2008) for vibration tests. Thermal tests are also reported as Weibull and statistical comparisons resort to Kruskal-Wallis one-way analysis of variance (George, Das, Osterman, and Pecht 2011) because only one parameter is compared at a time.

Additional rationale for testing to failure and selecting multiple factors can be found in the baseline finding of the ONR (2009, Chapter 7) on Reliability Issues/Gaps/Misconceptions for vibration (high mechanical cycling) begins with, "Tests to failure of assemblies are expected to help identify reliability issues, but MIL-STD-810 (2000) and other tests do not require tests to failure. Passing a qualification is insufficient to determine life expectancy." These qualification tests are accelerated tests, but not life tests so testing to failure is essential for building predictive failure models. Furthermore, ONR (2009, Chapter 7) states, "The level of testing and data available for model development and validation for vibration fatigue is extremely limited. Isothermal aging of solder has been demonstrated to reduce vibration fatigue life of both Sn-Pb and mainstream Pb-free solders. However, Pb-free solder exhibits a stronger aging dependence which makes it difficult to properly evaluate the effect during vibration testing." The analysis in this dissertation shows that for thermal cycle aging no significant difference in failure time exists between tin-lead and lead-free solders after vibration.

In addition, the ONR (2009, Chapter 7) goes on to say, “majority of reported vibration test data has been either from step stress tests showing SAC soldered interconnects failing prior to Sn-Pb joints, or from time terminated tests with no failures for mainstream Pb-free solders. The latter results do not allow for the development of fatigue models, and the use of step stress tests requires the assumption of damage accumulation models unlikely to be even roughly valid…” The conclusions and recommendations of this reliability section provide insight into future research directions, “…the lack of test to failure under single load levels ... micro-structural aging, does not allow confidence in model estimates. Further research should be sponsored to establish vibration fatigue models based on package types and mainstream Pb-free solders used in CCA.”

3.3 Methodology

Based on these major baseline finding and recommendations experimental factors are chosen so that the package type is the largest in current use because it is more susceptible to bending fatigue, single load levels using narrow band harmonic vibration to failure because it makes developing S-N curves less complicated in this level of development, and aging of both tin lead and lead free solder prior to vibration testing. The likelihood ratio test is first applied to examine differences between tin-lead and lead-free data sets for all experimental runs. Next the data was split in half along surface finish and both a regression analysis and ANOVA are investigated. After the data is analyzed using LR tests, because several modes of failure are detected in the data only half the failures for each data set are analyzed further after finding good Weibull fits. The data sets with Electro-less Nickel Immersion Gold (ENIG) are analyzed using regression and the data sets using Organic Solder Preservative (OSP) are applied ANOVA. The goal is to assess whether thermal aging matters and its relative importance to differences in tin lead and lead free solders.

Another approach is to directly compare tin-lead and lead-free S-N curve data; this dissertation will look only at a tin-lead circuit board at two different vibration levels to generate the S-N curves. The basic method of presenting engineering fatigue data is by means of the S-N curve, where stress (S) is presented as a function of the number of cycles to failure (N). “The basic method of presenting engineering fatigue data is by means of the S-N curve, a plot of

stress S against the number of cycles to failure N," as described by Dieter (1976). This strain data is measured using strain gauges and with a laser vibrometer off-line. The associated cycles to failure are performed with two different coupons using an event detector and controlling the vibration by monitoring the displacement of the boards with an accelerometer in the center of the board. The two control levels are 220 mils and 260 mils peak-to-peak. The strain data was recorded at 9 locations and Bezier smoothing was used to extrapolate to the nine circuit components.

Bezier smoothing is used to interpolate strains to the 20 BGA locations from the nine measured strains. The matrix form of the Bezier parametric (Faux and Pratt 1979, pp. 136-137) surface is

$$\mathbf{r} = \mathbf{r}(u,v) = [1\ u\ u^2\ u^3]\ \mathbf{MBM}^{\mathbf{T}}\ [1\ v\ v^2\ v^3]^T \qquad (5)$$

where **M** and **B** are represented respectively by

$$\mathbf{M} = \begin{bmatrix} 1 & 0 & 0 & 0 \\ -3 & 3 & 0 & 0 \\ 3 & -6 & 3 & 0 \\ -1 & 3 & -3 & 1 \end{bmatrix} \text{ and } \mathbf{B} = \begin{bmatrix} \mathbf{r00} & \mathbf{r01} & \mathbf{r02} & \mathbf{r03} \\ \mathbf{r10} & \mathbf{r11} & \mathbf{r12} & \mathbf{r13} \\ \mathbf{r20} & \mathbf{r21} & \mathbf{r22} & \mathbf{r23} \\ \mathbf{r30} & \mathbf{r31} & \mathbf{r32} & \mathbf{r33} \end{bmatrix}$$

The strain gauge values at the corners of the coupon are associated with the Bezier surface: **r**00 = strain gauge 1, **r**03 = strain gauge 3, **r**30 = strain gauge 7, and **r**33 = strain gauge 9, see Figure 3.27. The remaining **r** vectors control the shape of the surface. The strain observations $S_{ij} = r(u_i, v_j) + \epsilon_{ij,}$ i = 1, 2, 3, j = 1, 2, 3, where $u_i, v_j \in [0,1]$ and $\epsilon_{ij} \sim N(0, \sigma^2)$, and the objective is to estimate r(u, v) by minimizing $\frac{1}{9}\sum_{i=1}^{3}\sum_{j=1}^{3} 1\,(S_{ij} - r(u_i, v_j)^2$ + roughness constant (Gu, 2000, pp. 330-331) usually a second derivative functional which is kept constant,

but increasing. This first term penalizes lack of fit and the second term is the roughness of the estimate.

Laser vibrometer data measures displacement on the opposite card side of where the 20 components are located then converted to strain as discussed next. Calculate strain from displacement using fundamental relation between curvature of an elastic curve and the linear strain by

$$K = -\varepsilon/w \tag{6}$$

(Popov 1968, Intro to Mechanics of Solids, pp. 380-382), where K is the curvature, ε is strain, and w is the distance from the neutral surface to the strained fibers. The maximum strain occurs at $w = t/2$ where t is the thickness of the circuit board. Rearranging equation (6) the strain equation becomes:

$$\varepsilon = -Kt/2 \tag{7}$$

The curvature $K \approx d^2Z/dx^2$, the distance x locates the point on the elastic curve of length L and Z gives the deflection of the same point from its initial position. Assuming a simply supported beam, the mode shape for mode 1 from Blevins (1979) is $Z = Z_0 Sin(\pi x/L)$.

Solving for K by substitution and double differentiation of Z,

$$dZ/dx = Z_0(\pi/L)Cos(\pi x/L)$$

$$d^2Z/dx^2 = -Z_0(\pi^2/L^2)\,Sin(\pi x/L)$$

$$K = -(\pi^2/L^2)Z.$$

Substituting this curvature into equation (7) leads to the strain equation,

$$\varepsilon = (t/2)(\pi/L)^2 Z_0 Sin(\pi x/L). \tag{8}$$

Conversely, solving for displacement, Z_0 given the strain is accomplished by rearranging equation (8) to become,

$$Z_0 = \varepsilon(2/t)/[\ (\pi\ /\ L)^2\ \ Sin(\pi x/L)]. \tag{9}$$

Calculate life in cycles to failure using displacements, Z_0 for linear systems applying Steinberg (2000, p. 168)

$$N_0 = N_S(Z_S/Z_0)^b, \tag{10}$$

where N_0 = number of cycles to failure, N_S = 10,000,000 cycles and

$$Z_S = (0.00022B)/(Chr\sqrt{l})\ , \tag{11}$$

developed by Steinberg (2000, p. 172); and b=4 is the slope of the solder (63/37 tin/lead), Steinberg (2000, p. 44). Now Z_S is the maximum desired PCB displacement for components to achieve 10 million stress reversals in a sinusoidal vibration environment, and the parameters are defined in Steinberg (2000, pp. 173 and 217) including the values used in this chapter for the test vehicle, Figure 3.27:

B = length of PCB edge parallel to component (in.), B = 13 inches

l = length of electronic component (in.), l = 1.38 inches for a BGA

h = thickness of PCB (in.), h = 0.090 inches thick for circuit board in test vehicle

C = constant for different types of electronic components, C = 1.75 for a BGA

r = relative position factor for component on PCB,

= 1.0 when component is at the center of PCB at x = L/2 in equation (11)

= sin (3π/8) when component is at x = 3L/8 in equation (11)

= sin (π/4) when component is at x = L/4 in equation (11).

3.4 Analysis of test vehicles failure data

This analysis is based on test vehicle failure data focused on large ball grid arrays (BGA) data includes test time-to-failure for SAC305 and SnPb with and without pre-conditioning under high cycle fatigue for twenty (20) 1156 I/O BGA on a single test vehicle (see Figure 3.27). The test vehicles were subjected to narrow band harmonic vibration sine dwells at 45 hertz just off the fundamental frequency at 61 hertz. In the first set of tests G levels were controlled so that two different mid-board displacements are maintained at 220 mils and 260 mils thus four test vehicles total are tested with no preconditioning and ENIG finish, the results for the complete failure times are in Table 3.1.

Four more test vehicles are preconditioned with thermal cycling -40-85C for 120 cycle, the finish is ENIG, and the two different mid-board displacements are maintained at 250 mils and 400 mils the complete failure times are shown in Table 3.2.

Eight additional Test Vehicles with OSP finish and preconditioned at 125C for 100 hours then subjected to four different vibration levels (210 mils, 220 mils, 250 miles, 270 mils) have their complete failure times represented in Tables 3.3 for Tin Lead solder, and in Table 3.4 for Lead free solder. Note that in Tables 3.1, 3.2, 3.3, and 3.5, the S before a failure time designates a censored data point.

First complete failure data using Table 3.1 is analyzed using least squares and exhibited several modes of failure; not surprising since some areas of the

coupon saw much higher board deflections than others. A subsequent attempt is made to deal with the several modes by truncating data sets at 12 points and using least squares analysis to show a better fit for a two parameter Weibull. Using Minitab 16, the analysis shown on the right side of Figure 3.1 reproduces identically the preliminary results for the 12 truncated data points which use Reliasoft analysis in least squares mode. On the left side of Figure 3.1 is a maximum likelihood estimate (MLE) fit that shows poor Weibull fit and exhibits several modes of failure even though the least squares truncated results looked appeared to fit well. The reason why the least squares analysis is not adequate for censored data is that, unlike MLE, least squares cannot handle censored points in its analysis and the complete data sets show a lot of censoring, MLE also has desirable attributes like lack of bias, minimum variance, Sufficiency, and Consistency, (Tobias and Trindade, 1995, p. 95).

So the approach was to start with the complete failure data sets shown in Tables 3.1, 3.2, 3.3, and 3.4 that represent a total of 320 1156 I/O BGAs and perform LR tests using MLE to perform data comparisons as described in the next section 3.5.

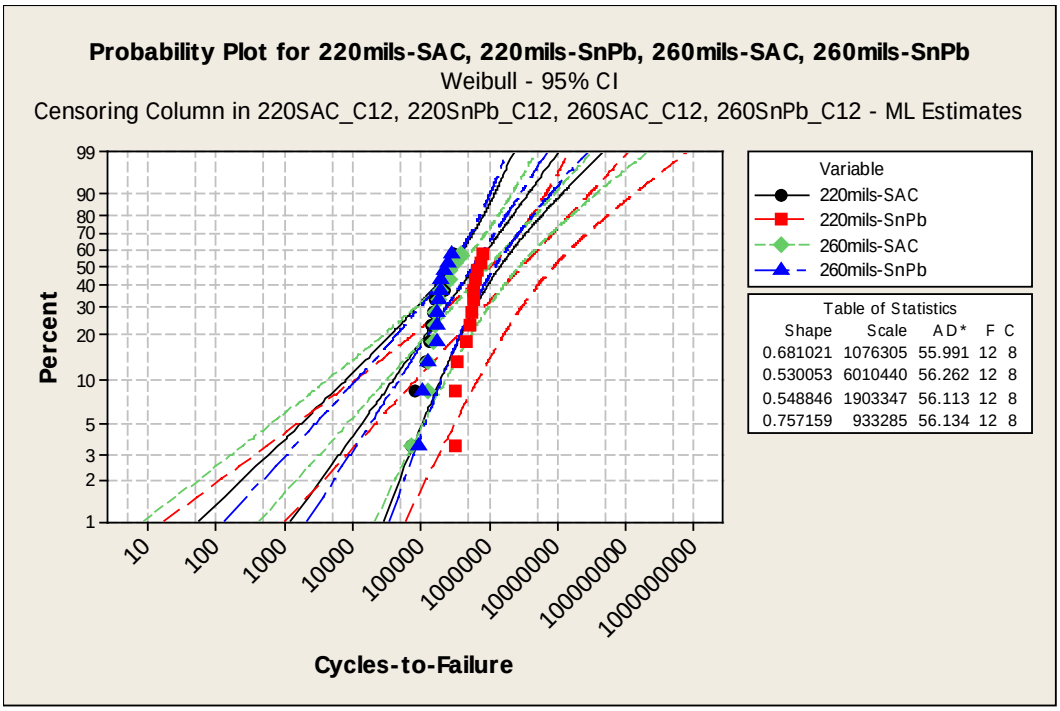

Figure 3.1a First 12 failures using Weibull MLE for SnPb & SAC305

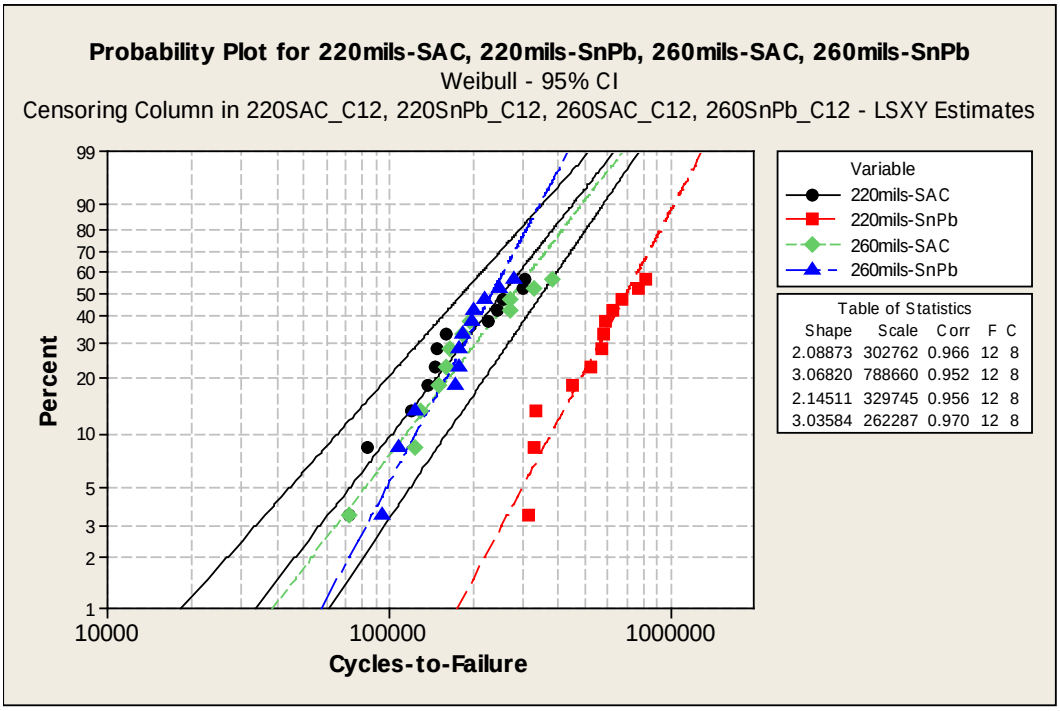

Figure 3.1b First 12 failures using least squares for SnPb & SAC305

Table 3.1 Complete failure data: four test vehicles plated with ENIG and not preconditioned

220mils-SAC	220mils-SnPb	260mils-SAC	260mils-SnPb
72900	315900	72900	94500
83700	329400	124200	108000
121500	334800	129600	124200
137700	453600	151200	172800
145800	526500	159300	178200
148500	575100	164700	178200
159300	583200	183600	183600
226800	588600	194400	197100
245700	623700	270000	199800
253800	677700	272700	218700
302400	769500	329400	248400
305100	826200	383400	280800
558900	4158000	596700	407700
693900	6666300	1795500	718200
815400	7219800	1873800	718200
1217700	S7638300	2143800	880200
1236600	S7638300	S2870100	1277100
1236600	S7638300	S2870100	1287900
1244700	S7638300	S2870100	1428300
2705400	S7638300	S2870100	1582200

Table 3.2 Complete failure data: four test vehicles plated with ENIG and pre-conditioned with -40C to 85C temperature excursions per thermal cycle for 120 cycles

250mils_SnPb	250mils_SAC	400mils_SnPb	400mils_SAC
121500	43200	59400	59400
135000	56700	59400	59400
275400	67500	59400	59400
275400	78300	59400	59400
361800	110700	59400	59400
364500	113400	75600	59400
386100	113400	91800	59400
491400	129600	97200	59400
499500	132300	S248400	59400
504900	137700	S248400	59400
513000	153900	S248400	91800
634500	172800	S248400	99900
1679400	588600	S248400	102600
1690200	756000	S248400	102600
2573100	815400	S248400	S102600
2853900	S866700	S248400	S102600
3115800	S866700	S248400	S102600
S3118500	S866700	S248400	S102600
S3118500	S866700	S248400	S102600
S3118500	S866700	S248400	S102600

Table 3.3 Complete failure data: four test vehicles plated with OSP at different vibration levels each using Sn-Pb solder and pre-conditioned at 125C for 100 hours.

210mils_SnPb	220mils_Sn-Pb	250mils_Sn-Pb	270mils_Sn-Pb
81000	1	1	1
310500	251100	1	91800
791100	507600	618300	102600
1428300	656100	796500	116100
1657800	842400	874800	145800
10492200	6822900	904500	151200
13335300	13451400	1188000	307800
14742000	15417000	1201500	378000
25479900	24818400	1223100	383400
26306100	25995600	1271700	499500
27267300	27072900	1274400	561600
28479600	29778300	1552500	591300
S39833100	30253500	1976400	642600
S39833100	S35000000	S2970000	648000
S39833100	S35000000	S2970000	S982800
S39833100	S35000000	S2970000	S982800
S39833100	S35000000	S2970000	S982800
S39833100	S35000000	S2970000	S982800
S39833100	S35000000	S2970000	S982800
S39833100	S35000000	S2970000	S982800

Table 3.4 Complete failure data: four test vehicles plated with OSP at different vibration levels each using SAC solder and pre-conditioned at 125C for 100 hours

210mils_SAC	220mils_SAC	250mils_SAC	270mils_SAC
37800	129600	40500	10800
86400	864000	43200	10800
286200	947700	45900	13500
1279800	1282500	59400	40500
1547100	1998000	62100	40500
2322000	2154600	67500	62100
3072600	2154600	75600	67500
3080700	2160000	75600	70200
4284900	2160000	110700	78300
4476600	2160000	116100	78300
6447600	2160000	132300	105300
7198200	2160000	132300	129600
11545200	2192400	245700	143100
24721200	2214000	272700	202500
S39833100	4239000	315900	S796500
S39833100	S26419500	S704700	S796500
S39833100	S26419500	S704700	S796500
S39833100	S26419500	S704700	S796500
S39833100	S26419500	S704700	S796500
S39833100	S26419500	S704700	S796500

3.5 LR comparisons of test vehicle

In this subsection, 16 test vehicles comprising all 320 failures of the same type of device an 1156 I/O BGA associated with the complete failure data in Tables 3.1, 3.2, 3.3, and 3.4 and are compared using the LR test. Applying the LR test equation (2) also used in the last chapter reproduced here for convenience:

$$T = -2\begin{bmatrix} \log likelihood(\hat{\mu}_0, \hat{\sigma}_0) \\ -\{\log likelihood(\hat{\mu}_1, \hat{\sigma}_1) + \log likelihood(\hat{\mu}_2, \hat{\sigma}_2)\} \end{bmatrix},$$

the LR test analysis uses Minitab 16 for calculating the rows in summary Table 3.5 showing comparisons between Sn-Pb and SAC305 using a Weibull distribution for an LR test containing two independent parameters, characteristic life and shape. Two parameter Weibull distributions are chosen based on MLE calculations from distribution identification plots in Appendix A using the adjusted Anderson-Darling criteria.

The following discussion shows how the LR test results in first two rows of Table 3.5 are achieved. The log-likelihoods for the first row in Table 3.5 that compares 220 mils vibration levels and no preconditioning between Sn-Pb and SAC305 uses the log-likelihoods found in Table 3.8 for the first term in equation (2), then Table 3.6 for the second term, and Table 3.7 for the third term. Figure 3.2 is the Weibull probability plot for the Sn-Pb and SAC305 distributions for 220 mils taken separately. Figure 3.3 represents the Weibull distributions for Sn-Pb and SAC305 taken as one distribution. The log-likelihoods for the second row in

Table 3.5 that compares 260 mils vibration levels and no preconditioning between Sn-Pb and SAC305 uses the log-likelihoods found in Table 3.11 for the first term in equation (2), then Table 3.9 for the second term, and Table 3.10 for the third term. Figures 3.4 and 3.5 are graphical representations of the Weibull distributions represented in the LR test equation (2). These example calculations for the 220 mils and 260 mils using both Sn-Pb and SAC305 with the distribution analysis in this section show $T = 21 > 5.99$ is the chi-squared .95 for 220 mils and $T = 8.76 > 5.99$ the chi-squared .95, 2 for 260 mils, Table 3.5. The significance is that tin-lead and SAC305 are significantly different given that the finish is ENIG, no-preconditioning is performed, and the level of vibration is at 220 mils or 260 mils.

The calculations for the next six rows in Table 3.5 are found the same way using data in Appendix A and Appendix B. Other observations from Table 3.5 include test vehicles with an ENIG finish perform similar to each other at lower vibration levels than at higher vibration levels for preconditioned samples. Understanding the role preconditioning has on ENIG finishes will be reconciled in the next section.

The test vehicles with an OSP finish all have the same preconditioning and indicate that Sn-Pb and SAC305 behave similarly, with cycle time affected more by increasing vibration level; although at the 250 mils vibration level Sn-Pb and SAC305 are not similar. This anomaly will be examined in the next section for OSP finishes.

Table 3.5 LR-test between Sn-Pb and SAC Test Vehicle with ENIG/OSP board finish with either no-preconditioning, -40-85C for 120 cycles of pre-conditioning, or 125C for 100 hours of pre-conditioning at various vibration levels with accompanying characteristic life

Board Finish	Vibration Level (mils)	Sn-Pb	SAC305	LR-Test	Sn-Pb Characteristic Life c, CDF, F(c) = 63.2% Cycles-to-fail/Shape parameter	SAC Characteristic Life c, CDF, F(c) = 63.2% Cycles-to-fail/Shape parameter
ENIG	220	No-precondition	No-precondition	21>5.99	3.91 x 10^6/ 0.645386	0.597 x 10^6/ 1.00314
ENIG	260	No-precondition	No-precondition	8.76>5.99	0.55 x 10^6/ 1.12781	1.15 x 10^6/ .679601
ENIG	250	-40-85C for 120 cycles	-40-85C for 120 cycles	5.412<5.99	1.48 x 10^6/ 0.894312	0.512 x 10^6/ 0.802960
ENIG	400	-40-85C for 120 cycles	-40-85C for 120 cycles	26.05>5.99	0.469 x 10^6/ 0.932113	0.096 x 10^6/ 3.23712
OSP	210	125C for 100 hours	125C for 100 hours	1.53<5.99	48.6 x 10^6/ 0.549409	21.3 x 10^6/ 0.463898
OSP	220	125C for 100 hours	125C for 100 hours	4.332<5.99	44.3 x 10^6/ 0.393733	9.28 x 10^6/ 0.564618
OSP	250	125C for 100 hours	125C for 100 hours	12.476>5.99	4.05 x 10^6/ 0.381309	0.346 x 10^6/ 0.772265
OSP	270	125C for 100 hours	125C for 100 hours	1.428<5.99	0.833 x 10^6/ 0.611171	0.399 x 10^6/ 0.548023

Table 3.6 Weibull Distribution Analysis: for 220mils-SAC no preconditioning

Censoring Information Count
Uncensored value 20
Type 1 (Time) Censored at 7638300
Estimation Method: Maximum Likelihood

Parameter Estimates

Parameter	Estimate	Standard Error	95.0% Normal CI Lower	Upper
Shape	1.00314	0.168247	0.722100	1.39356
Scale	596503	141125	375171	948409

Log-Likelihood = -285.947

Goodness-of-Fit
Anderson-Darling (adjusted) = 1.308

Characteristics of Distribution

	Estimate	Standard Error	95.0% Normal CI Lower	Upper
Mean(MTTF)	595715	132896	384723	922422
Standard Deviation	593851	162473	347373	1015218
Median	413939	109083	246958	693824
First Quartile(Q1)	172274	62684.3	84430.0	351513
Third Quartile(Q3)	826083	185264	532263	1282098
Interquartile Range(IQR)	653809	148628	418746	1020825

Table of Percentiles

Percent	Percentile	Standard Error	95.0% Normal CI Lower	Upper
1	6082.01	5335.16	1089.86	33941.0
2	12199.1	9330.74	2724.37	54624.6
3	18368.7	12848.8	4663.03	72358.1
4	24595.5	16067.5	6835.80	88495.5
5	30882.4	19070.6	9206.07	103597
6	37231.8	21906.7	11751.1	117964
7	43645.5	24607.7	14455.3	131781
8	50125.7	27196.1	17307.5	145173
9	56673.9	29688.7	20299.2	158229
10	63292.1	32098.6	23424.1	171016
20	133732	53263.8	61265.2	291916
30	213445	71755.7	110441	412517
40	305350	89752.1	171634	543242
50	413939	109083	246958	693824
60	546719	132239	340312	878317
70	717756	163698	459033	1122300
80	958605	213680	619300	1483810
90	1369917	316290	871297	2153882
91	1432400	333669	907365	2261240
92	1502240	353607	947061	2382873
93	1581406	376839	991305	2522781
94	1672781	404454	1041433	2686872
95	1780835	438161	1099492	2884399
96	1913054	480871	1168870	3131035
97	2083472	538140	1255830	3456563
98	2323588	622716	1374166	3928975
99	2733894	776552	1566756	4770481

Table 3.7 Weibull Distribution Analysis for 220mils-SnPb no preconditioning

Censoring Information	Count
Uncensored value	15
Right censored value	5

Type 1 (Time) Censored at 7638300
Estimation Method: Maximum Likelihood

Parameter Estimates

Parameter	Estimate	Standard Error	95.0% Normal CI Lower	Upper
Shape	0.645386	0.136805	0.425977	0.977806
Scale	3906350	1562947	1783207	8557374

Log-Likelihood = -241.132

Goodness-of-Fit
Anderson-Darling (adjusted) = 30.144

Characteristics of Distribution

	Estimate	Standard Error	95.0% Normal CI Lower	Upper
Mean(MTTF)	5379846	2492094	2170050	13337365
Standard Deviation	8652802	5453669	2515726	29761182
Median	2213791	928354	973162	5036028
First Quartile(Q1)	566732	326493	183233	1752883
Third Quartile(Q3)	6479934	2675296	2884993	14554469
Interquartile Range(IQR)	5913201	2529561	2556783	13675758

Table of Percentiles

Percent	Percentile	Standard Error	95.0% Normal CI Lower	Upper
1	3134.94	4915.94	145.028	67765.4
2	9248.49	12463.7	659.101	129774
3	17472.4	21308.2	1600.61	190731
4	27504.7	31056.0	3008.17	251485
5	39179.7	41503.7	4913.25	312431
6	52393.4	52526.7	7343.59	373804
7	67075.8	64041.1	10324.6	435770
8	83178.8	75987.5	13880.4	498451
9	100669	88322.1	18033.8	561953
10	119522	101012	22807.2	626364
20	382321	244215	109322	1337055
30	790743	417178	281165	2223870
40	1379594	633871	560605	3395047
50	2213791	928354	973162	5036028
60	3411483	1369757	1553010	7493975
70	5208150	2103682	2359746	11494811
80	8165912	3491842	3531999	18879423
90	14223615	6854118	5531342	36575435
91	15244653	7473331	5832249	39847309
92	16415471	8198794	6167601	43690849
93	17779566	9063406	6546485	48287438
94	19401713	10116783	6982189	53912387
95	21384231	11438398	7495265	61009895
96	23902245	13166418	8120057	70358783
97	27292458	15571350	8920741	83499600
98	32335055	19294052	10040814	104130585
99	41633604	26539565	11935511	145226881

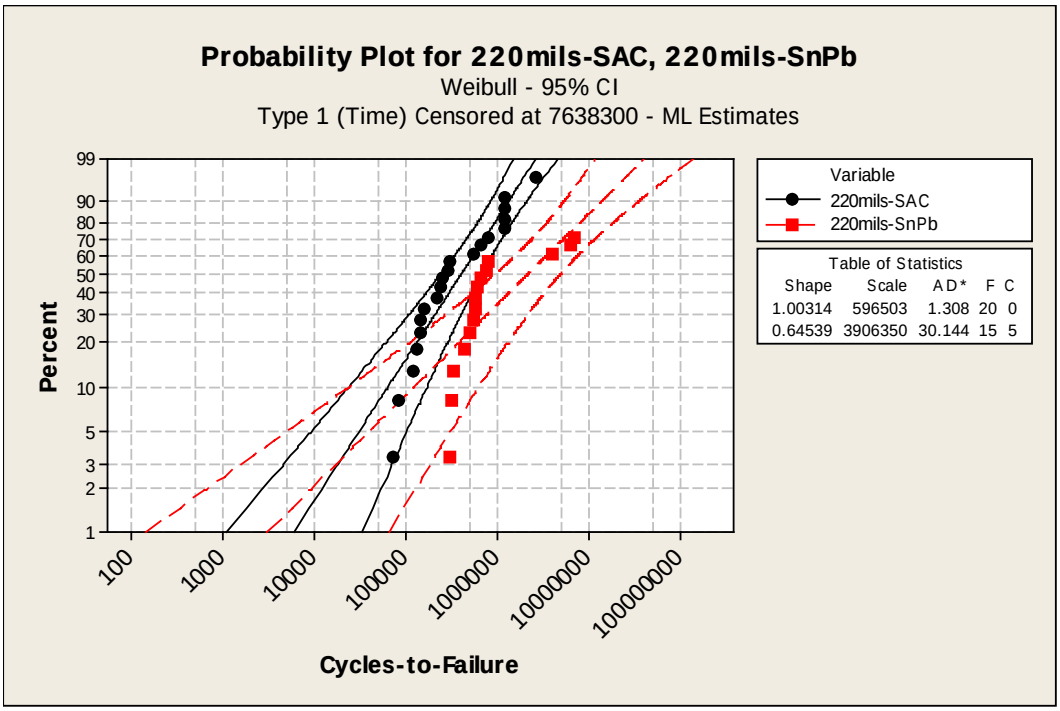

Figure 3.2 Probability Plot for 220mils-SAC, 220mils-SnPb

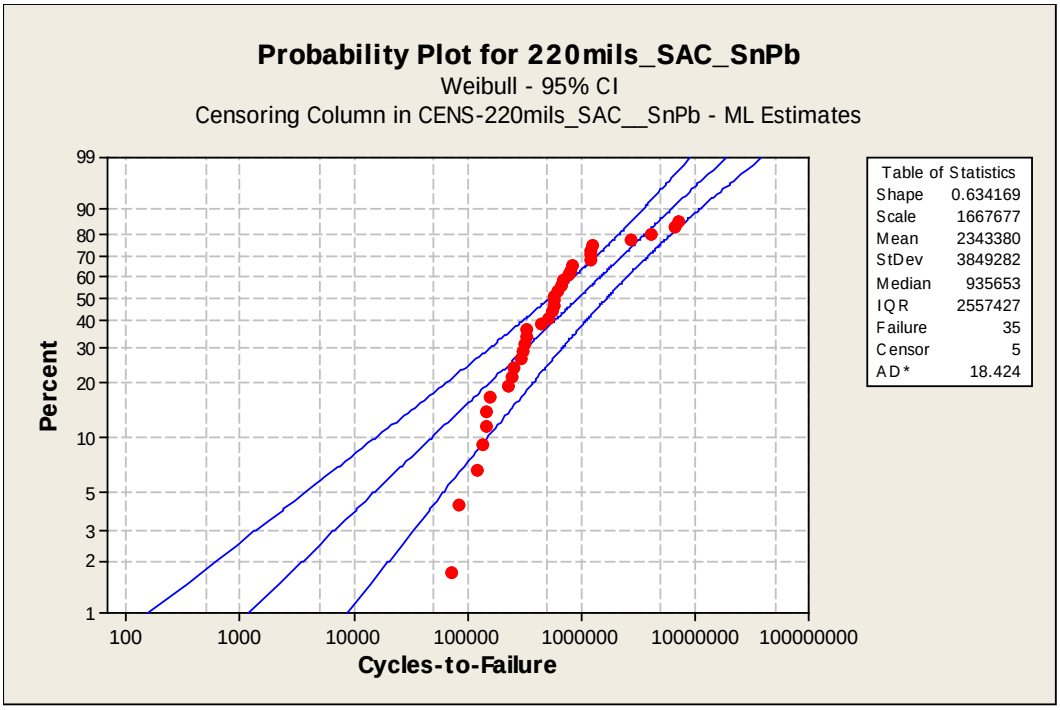

Figure 3.3 Probability Plot for 220mils_SAC_SnPb as a single distribution

Table 3.8 Weibull Distribution Analysis: 220mils_SAC_SnPb as a single distribution

Censoring Information	Count
Uncensored value	35
Right censored value	5

Estimation Method: Maximum Likelihood

Parameter Estimates

		Standard	95.0% Normal CI	
Parameter	Estimate	Error	Lower	Upper
Shape	0.634169	0.0824240	0.491556	0.818158
Scale	1667677	452933	979331	2839843

Log-Likelihood = -537.332

Goodness-of-Fit
Anderson-Darling (adjusted) = 18.424

Characteristics of Distribution

		Standard	95.0% Normal CI	
	Estimate	Error	Lower	Upper
Mean(MTTF)	2343380	666730	1341719	4092830
Standard Deviation	3849282	1423800	1864366	7947459
Median	935653	276363	524440	1669298
First Quartile(Q1)	233824	95153.6	105317	519137
Third Quartile(Q3)	2791251	745120	1654139	4710054
Interquartile Range(IQR)	2557427	690982	1505983	4342966

Table of Percentiles

		Standard	95.0% Normal CI	
Percent	Percentile	Error	Lower	Upper
1	1179.83	1215.26	156.693	8883.56
2	3547.89	3166.78	616.882	20405.0
3	6778.59	5508.72	1378.47	33333.5
4	10756.7	8134.47	2443.31	47356.3
5	15418.8	10987.8	3814.74	62321.0
6	20725.1	14033.5	5497.04	78138.8
7	26649.2	17247.7	7495.08	94753.2
8	33173.0	20613.3	9814.25	112127
9	40283.9	24117.3	12460.4	130236
10	47974.0	27750.1	15439.6	149065
20	156645	70112.5	65152.1	376621
30	328175	122989	157436	684080
40	578225	189213	304480	1098084
50	935653	276363	524440	1669298
60	1452926	400424	846553	2493635
70	2234774	596490	1324454	3770770
80	3531908	954931	2079064	5999996
90	6212659	1812875	3506662	11006800
91	6666802	1971069	3734703	11900878
92	7188227	2156608	3992498	12941924
93	7796555	2378033	4288221	14175174
94	8521035	2648246	4633915	15668832
95	9407913	2987947	5048382	17532115
96	10536429	3433194	5563366	19954886
97	12059138	4054744	6238924	23308957
98	14330110	5020699	7211448	28475843
99	18533673	6911708	8923298	38494402

Table 3.9 Weibull Distribution Analysis: 260mils-SAC no preconditioning

Censoring Information	Count
Uncensored value	16
Right censored value	4

Type 1 (Time) Censored at 2870100
Estimation Method: Maximum Likelihood

Parameter Estimates

Parameter	Estimate	Standard Error	95.0% Normal CI Lower	Upper
Shape	0.679601	0.137230	0.457481	1.00957
Scale	1147800	423794	556651	2366732

Log-Likelihood = -238.694

Goodness-of-Fit
Anderson-Darling (adjusted) = 21.753

Characteristics of Distribution

	Estimate	Standard Error	95.0% Normal CI Lower	Upper
Mean(MTTF)	1495792	608105	674249	3318347
Standard Deviation	2263538	1243753	771037	6645078
Median	669343	263589	309345	1448287
First Quartile(Q1)	183520	99981.8	63088.1	533849
Third Quartile(Q3)	1856091	693490	892413	3860405
Interquartile Range(IQR)	1672572	645473	785041	3563505

Table of Percentiles

Percent	Percentile	Standard Error	95.0% Normal CI Lower	Upper
1	1318.78	1907.04	77.4970	22442.0
2	3684.34	4592.70	320.109	42405.5
3	6741.13	7621.26	735.187	61811.3
4	10372.1	10876.9	1328.12	81001.8
5	14513.9	14302.3	2103.73	100133
6	19126.9	17863.6	3066.63	119296
7	24184.2	21538.6	4221.32	138553
8	29667.0	25311.9	5572.24	157950
9	35561.7	29172.4	7123.87	177521
10	41858.6	33112.0	8880.69	197298
20	126282	76101.9	38759.2	411439
30	251801	125788	94588.3	670313
40	427173	185611	182283	1001060
50	669343	263589	309345	1448287
60	1009253	375796	486468	2093850
70	1508306	555980	732363	3106366
80	2311942	887511	1089474	4906108
90	3916053	1670846	1696954	9037059
91	4182542	1813349	1788135	9783188
92	4487022	1979789	1889672	10654427
93	4840393	2177494	2004287	11689644
94	5258846	2417493	2135959	12947562
95	5767887	2717398	2290836	14522434
96	6411029	3107737	2479186	16578548
97	7271627	3648060	2720178	19438640
98	8541920	4478807	3056629	23870868
99	10859238	6080135	3624164	32537998

Table 3.10 Weibull Distribution Analysis: 260mils-SnPb no preconditioning

Censoring Information	Count
Uncensored value	20

Type 1 (Time) Censored at 2870100
Estimation Method: Maximum Likelihood

Parameter Estimates

Parameter	Estimate	Standard Error	95.0% Normal CI Lower	Upper
Shape	1.12781	0.192196	0.807566	1.57505
Scale	550177	115847	364141	831255

Log-Likelihood = -283.157

Goodness-of-Fit
Anderson-Darling (adjusted) = 1.712

Characteristics of Distribution

	Estimate	Standard Error	95.0% Normal CI Lower	Upper
Mean(MTTF)	526668	104873	356485	778095
Standard Deviation	467888	115390	288549	758689
Median	397527	93446.6	250769	630171
First Quartile(Q1)	182278	59478.5	96157.2	345531
Third Quartile(Q3)	734990	146582	497191	1086526
Interquartile Range(IQR)	552712	113994	368929	828048

Table of Percentiles

Percent	Percentile	Standard Error	95.0% Normal CI Lower	Upper
1	9312.97	7368.84	1975.06	43913.4
2	17296.3	11927.8	4476.63	66827.6
3	24891.7	15693.0	7234.63	85643.5
4	32271.5	18995.3	10181.0	102293
5	39513.6	21979.3	13282.2	117550
6	46663.0	24725.0	16517.9	131823
7	53748.8	27283.0	19874.6	145358
8	60791.6	29687.8	23343.0	158318
9	67806.6	31964.4	26916.0	170818
10	74806.0	34131.8	30588.4	182943
20	145515	52029.9	72203.3	293266
30	220554	66420.9	122228	397977
40	303274	79682.8	181213	507553
50	397527	93446.6	250769	630171
60	509141	109655	333821	776538
70	648609	131567	435833	965262
80	838986	166345	568837	1237432
90	1152575	237183	770024	1725179
91	1199218	249076	798188	1801737
92	1251088	262680	829027	1888022
93	1309563	278479	863214	1986710
94	1376656	297185	901722	2101735
95	1455475	319914	946042	2239233
96	1551208	348557	998631	2409546
97	1673531	386701	1064015	2632207
98	1844034	442531	1152120	2951483
99	2131006	542730	1293595	3510516

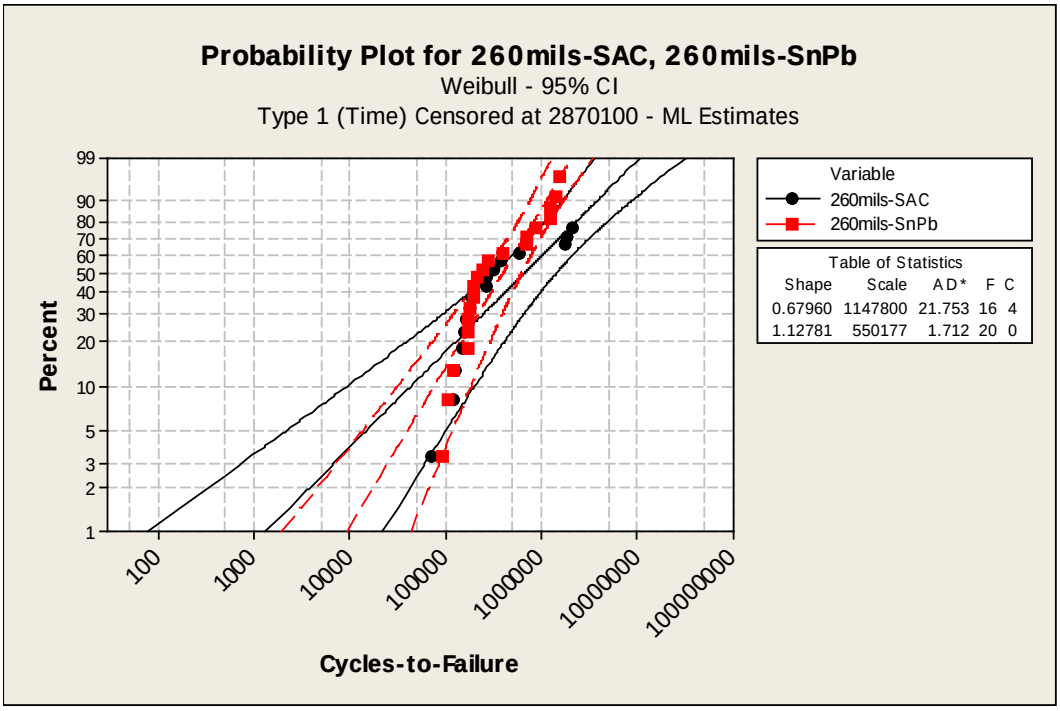

Figure 3.4 Probability Plot for 260mils-SAC, 260mils-SnPb

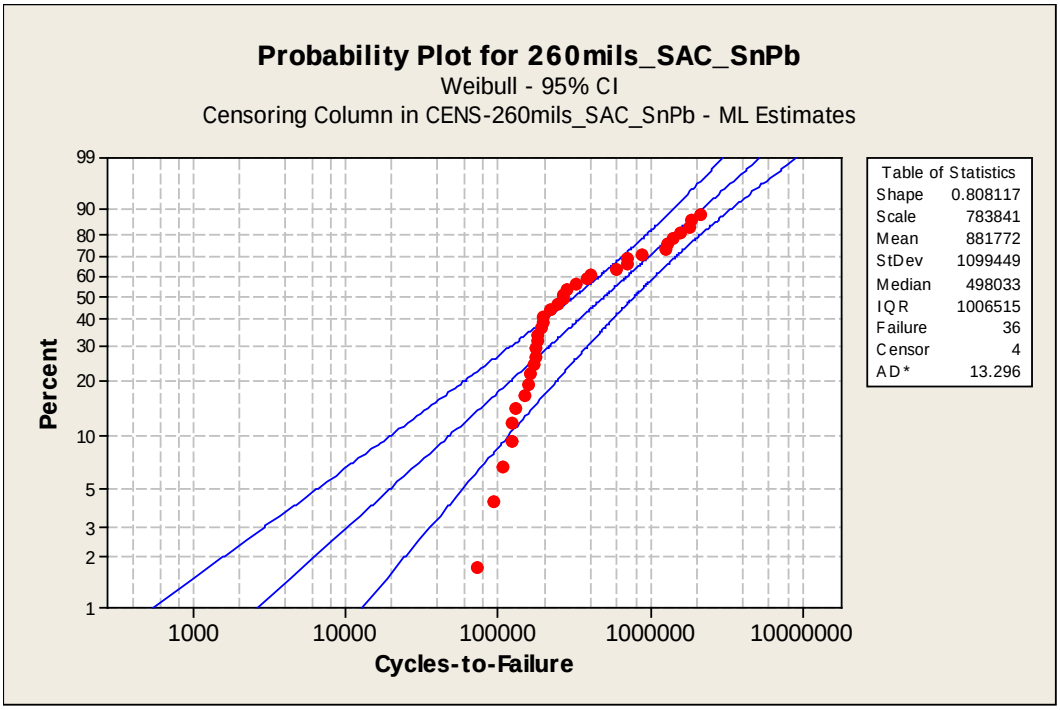

Figure 3.5 Probability Plot for 260mils_SAC_SnPb as a single distribution

Table 3.11 Weibull Distribution Analysis: 260mils_SAC_SnPb as a single distribution

Censoring Information	Count
Uncensored value	36
Right censored value	4

Estimation Method: Maximum Likelihood

Parameter Estimates

Parameter	Estimate	Standard Error	95.0% Normal CI Lower	Upper
Shape	0.808117	0.104014	0.627935	1.04000
Scale	783841	165792	517832	1186498

Log-Likelihood = -526.231

Goodness-of-Fit
Anderson-Darling (adjusted) = 13.296

Characteristics of Distribution

	Estimate	Standard Error	95.0% Normal CI Lower	Upper
Mean(MTTF)	881772	185795	583449	1332629
Standard Deviation	1099449	302183	641538	1884201
Median	498033	115328	316335	784096
First Quartile(Q1)	167750	53768.8	89501.1	314411
Third Quartile(Q3)	1174265	242255	783719	1759431
Interquartile Range(IQR)	1006515	212871	664962	1523505

Table of Percentiles

Percent	Percentile	Standard Error	95.0% Normal CI Lower	Upper
1	2642.64	2131.10	544.010	12837.2
2	6269.99	4385.84	1591.68	24699.0
3	10421.1	6641.40	2988.42	36340.2
4	14972.3	8883.99	4679.67	47902.6
5	19861.0	11110.3	6634.89	59452.0
6	25049.5	13320.1	8834.31	71027.3
7	30512.9	15514.0	11264.2	82654.7
8	36233.7	17693.1	13914.5	94353.6
9	42199.2	19858.8	16777.7	106139
10	48400.1	22012.4	19848.1	118025
20	122500	43177.1	61393.0	244431
30	218872	64598.5	122734	390316
40	341375	87849.9	206150	565303
50	498033	115328	316335	784096
60	703471	151267	461544	1072211
70	986249	204124	657375	1479653
80	1412459	294147	939100	2124418
90	2200137	491555	1419954	3408985
91	2325383	526132	1492468	3623130
92	2466943	566135	1573324	3868121
93	2629334	613171	1664724	4152879
94	2819220	669637	1769892	4490671
95	3047010	739333	1893810	4902429
96	3330302	828781	2044810	5423931
97	3702438	950563	2238467	6123856
98	4239276	1133945	2509617	7161034
99	5187493	1477066	2968860	9064111

3.6 Regression and ANOVA

In the last section, the LR test was used to compare between Sn-Pb and SAC305 data set which also contained other combinations of factors.

Four of the tests vehicle data set combinations have an ENIG finish at four different vibration levels and are either preconditioned or not. For this data, the LR test indicated that the role of preconditioning on failure time may not be important; the structure of the data lends to regression analysis because the vibration levels are not at the same levels as the preconditioning.

The other four test vehicle data sets have an OSP finish at four different, but increasing vibration levels and are all preconditioned test vehicles. For this data, the LR test indicated that Sn-Pb and SAC305 behaved similarly and that failure time is more vibration level dependent.

The data in Table 3.5 was split in two all the data with ENIG plating uses regression analysis on Table 3.12; and the OSP data with the same preconditioning uses two-way ANOVA on Table 3.20 with data analyzed in Minitab 16.

Examination of the complete failure data in Tables 3.1 through 3.4 and the distribution plots in Appendix A indicate several modes of failure in the data. Therefore the data in Tables 3.12 and 3.20 is reanalyzed with only the first ten failures for each of the 16 combination shown in Table 3.5 indicated. First identification distribution analysis is calculated to show Weibull is adequately

modeled in the reduced data sets, Appendix C. Truncated data analysis is performed so that the vibration levels of the regression factor apply only to those failed components that actually have strains at the corresponding displacement levels in column two of Table 3.5.

Regression

This regression analysis begins with looking at the main effects plot Figure 3.6 based on the data in Table 3.12 and proceeds with the three qualitative factors: vibration level, solder type Sn-Pb or SAC305, and preconditioning or not. The results in Table 3.13 show the preconditioning factor with P-value of 0.939 is not an important factor. The variance inflation factors (VIF) are very close to one and therefore give confidence in the regression coefficients, but the adjusted R-squared is 47.8% and the predicted R-squared is 44.7% and the residual plots Figure 3.7 show an open funnel pattern.

The next step is to take out the preconditioning factor first and the results in Table 3.14 an improvement in the model, the adjusted R-squared is 48.5% and the predicted R-squared is 46.2% and the residual plots Figure 3.8 still show an open funnel pattern that is due to the non-normality of the Weibull distribution.

Due to the open funnel, a Box-Cox transformation was applied in Minitab 16 general regression without the preconditioning factor (Montgomery, Peck, and Vining 2001, pp. 142, 186). In Table 3.15, the results show further improvement

in the model, the adjusted R-squared is 66.5% and the predicted R-squared is 65.1% and the residual plots Figure 3.9 have become more normalized.

Using the Box-Cox transformation with the preconditioning factor included this time Table 3.16 model results did not change and the P-value of 0.182 for the preconditioning factor again showed that it had no significance in our model. Residual plots in Figure 3.10 again did showed more normality than without transforming the data. The interaction plot in Figure 3.11 indicates an interaction between solder and vibration level and a subsequent Box-Cox transformation with the interaction, but leaving out the preconditioning further improved the model Table 3.17 to an adjusted R-squared of 67.9% and the predicted R-squared is 67.9%.

One more transformation of the data to logarithmic cycles to failure in Table 3.18 using the three factors: vibration level, solder, and preconditioning also showed improved model capability over simple multi-regression with an adjusted R-squared of 62.8% and the predicted R-squared is 60.4% and the residual plots Figure 3.12 showed reasonable normality, but the Durbin-Watson statistic = 0.785 indicated autocorrelation due to the increasing failures of each subsequent combination of runs, but the VIF are close to one and the model coefficients are not contributing to the variance. The major finding is that again preconditioning is not a significant factor with P-value of 0.406.

The next logarithmic transformation run Table 3.19 dropped the preconditioning factor and the model with vibration level and solder as factors

showed further improvement with an adjusted R-squared of 63.0% and the predicted R-squared is 61.4% and the residual plots Figure 3.13 showed reasonable normality, but the Durbin-Watson is statistic = 0.792, and the VIF are close to one and the model coefficients are not contributing to the variance.

The variety of analysis on this data whether transformed or not indicated that cycles to failure are a function of vibration level and the solder alloy, but not preconditioning so that this step may be avoided in the processing of circuit cards.

Two-way ANOVA

In Table 3.20, the data for two-way ANOVA of two solder levels and four vibration levels is analyzed using Minitab 16 and show in Table 3.21 that the two factors and the interaction are significant, but adjusted R-squared is 34.8%. The vibration levels have been transformed to micro strain using equation (8) and therefore represent a quantitative factor with the assumption that the failures are all at those strain levels. Reviewing Figure 3.14 the individual value plot and the Box plot in Figure 3.16 show that both alloys perform poorly at the upper strain levels and that Sn-Pb out performs on average SAC305 at the lower strain levels. Figure 3.15 residual plots show a large open funnel due to the dispersion in the Sn-Pb at the lower strain level. The main effects Figure 3.17 and interaction plots Figure 3.18 are consistent with the individual and Box plots and therefore in the next run Table 3.22 the interaction between solder and micro-strain are included, with no difference in adjusted R-squared and Residual plots, Figure 3.19.

Next a Box-Cox transformation is performed Table 3.23 in Minitab 16 using the same factors as the previous run and the adjusted R-squared improved to 62.3% and the P-value of 0.073 for the solder factor lost its significance which corroborated the LR test results of the last section when the full set of failures are run. The residual plots Figure 3.20 are better behaved.

Table 3.12 Regression data, response is cycles-to-failure and regression factors are vibration levels (4), solder type (2), and preconditioning (yes/no)

Observation Number	Cycles-to-Failure, y	Vibration Level mils, x1	Solder Type, x2	Preconditioning, x3
1	315900	220	0	0
2	329400	220	0	0
3	334800	220	0	0
4	453600	220	0	0
5	526500	220	0	0
6	575100	220	0	0
7	583200	220	0	0
8	588600	220	0	0
9	623700	220	0	0
10	677700	220	0	0
11	72900	220	1	0
12	83700	220	1	0
13	121500	220	1	0
14	137700	220	1	0
15	145800	220	1	0
16	148500	220	1	0
17	159300	220	1	0
18	226800	220	1	0
19	245700	220	1	0
20	253800	220	1	0
21	94500	260	0	0
22	108000	260	0	0
23	124200	260	0	0
24	172800	260	0	0
25	178200	260	0	0
26	178200	260	0	0
27	183600	260	0	0
28	197100	260	0	0
29	199800	260	0	0
30	218700	260	0	0
31	72900	260	1	0
32	124200	260	1	0
33	129600	260	1	0
34	151200	260	1	0
35	159300	260	1	0
36	164700	260	1	0

37	183600	260	1	0
38	194400	260	1	0
39	270000	260	1	0
40	272700	260	1	0
41	121500	250	0	1
42	135000	250	0	1
43	275400	250	0	1
44	275400	250	0	1
45	361800	250	0	1
46	364500	250	0	1
47	386100	250	0	1
48	491400	250	0	1
49	499500	250	0	1
50	504900	250	0	1
51	43200	250	1	1
52	56700	250	1	1
53	67500	250	1	1
54	78300	250	1	1
55	110700	250	1	1
56	113400	250	1	1
57	113400	250	1	1
58	129600	250	1	1
59	132300	250	1	1
60	137700	250	1	1
61	59400	400	0	1
62	59400	400	0	1
63	59400	400	0	1
64	59400	400	0	1
65	59400	400	0	1
66	75600	400	0	1
67	91800	400	0	1
68	97200	400	0	1
69	59400	400	1	1
70	59400	400	1	1
71	59400	400	1	1
72	59400	400	1	1
73	59400	400	1	1
74	59400	400	1	1
75	59400	400	1	1
76	59400	400	1	1
77	59400	400	1	1
78	59400	400	1	1

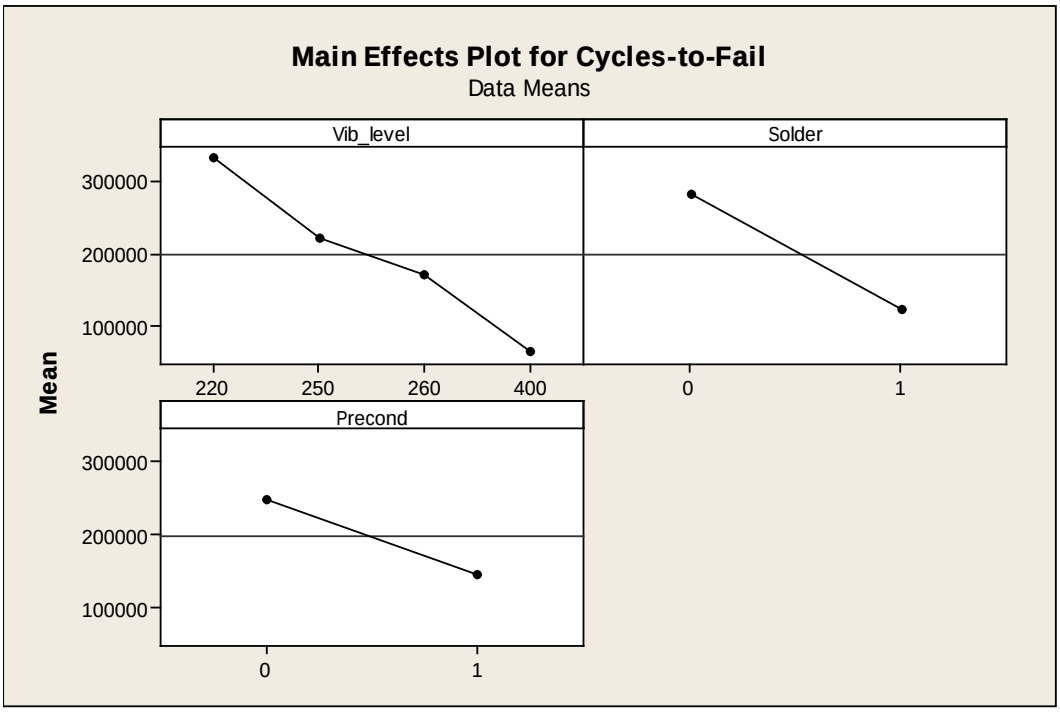

Figure 3.6 Main Effects Plot: Cycles-to-Fail versus Vib_level, Solder, and Preconditioning

Table 3.13 Regression Analysis: Cycles-to-Fail versus Vib_level, Solder, and Preconditioning

The regression equation is
Cycles-to-Fail = 611552 - 1195 Vib_level - 150181 Solder - 2544 Precond

Predictor	Coef	SE Coef	T	P	VIF
Constant	611552	62416	9.80	0.000	
Vib_level	-1195.5	244.3	-4.89	0.000	1.561
Solder	-150181	26498	-5.67	0.000	1.002
Precond	-2544	33047	-0.08	0.939	1.559

S = 116852 R-Sq = 49.8% R-Sq(adj) = 47.8%
PRESS = 1.112930E+12 R-Sq(pred) = 44.73%

Analysis of Variance

Source	DF	SS	MS	F	P
Regression	3	1.00338E+12	3.34462E+11	24.49	0.000
Residual Error	74	1.01042E+12	13654303076		
Lack of Fit	4	5.73908E+11	1.43477E+11	23.01	0.000
Pure Error	70	4.36511E+11	6235866000		
Total	77	2.01380E+12			

Source	DF	Seq SS
Vib_level	1	5.64716E+11
Solder	1	4.38587E+11
Precond	1	80890569

Unusual Observations

Obs	Vib_level	Cycles-to-Fail	Fit	SE Fit	Residual	St Resid
7	220	583200	348547	23150	234653	2.05R
8	220	588600	348547	23150	240053	2.10R
9	220	623700	348547	23150	275153	2.40R
10	220	677700	348547	23150	329153	2.87R

R denotes an observation with a large standardized residual.

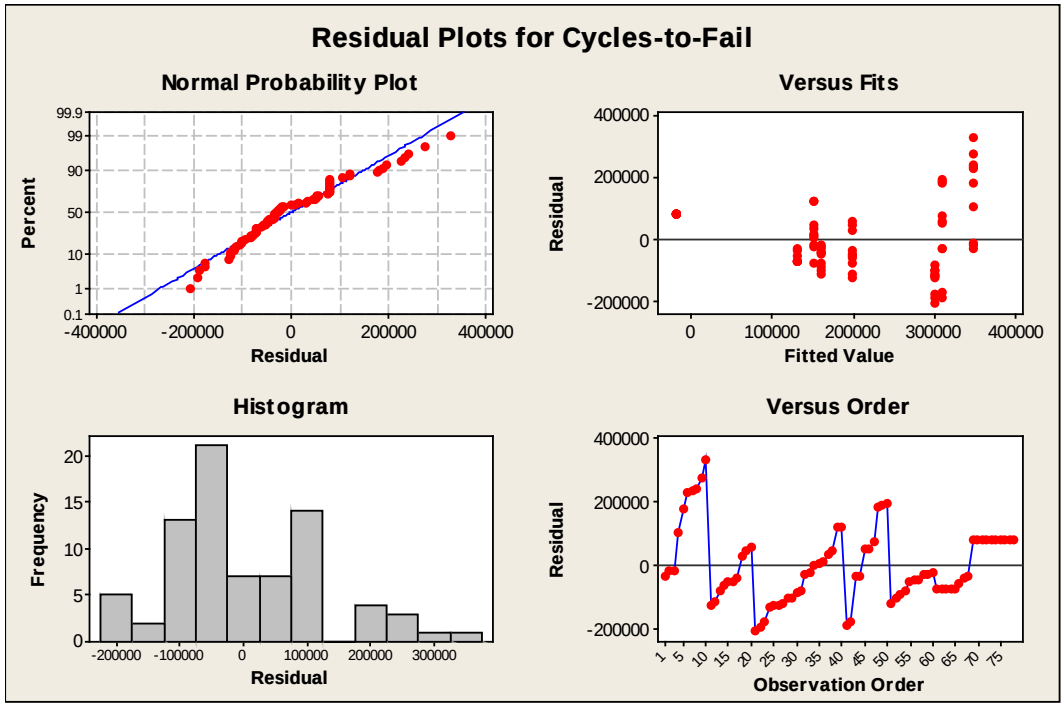

Figure 3.7 Residual Plots for Cycles-to-Failure

Table 3.14 General Regression Analysis: Cycles-to-Fail versus Vib_level, Solder

Regression Equation
Cycles-to-Fail = 613456 - 1206.73 Vib_level - 150178 Solder

Coefficients

Term	Coef	SE Coef	T	P
Constant	613456	56926.5	10.7763	0.000
Vib_level	-1207	194.4	-6.2067	0.000
Solder	-150178	26321.9	-5.7055	0.000

Summary of Model
S = 116075 R-Sq = 49.82% R-Sq(adj) = 48.48%
PRESS = 1.084376E+12 R-Sq(pred) = 46.15%

Analysis of Variance

Source	DF	Seq SS	Adj SS	Adj MS	F	P
Regression	2	1.00330E+12	1.00330E+12	5.01652E+11	37.2330	0.0000000
Vib_level	1	5.64716E+11	5.19034E+11	5.19034E+11	38.5231	0.0000000
Solder	1	4.38587E+11	4.38587E+11	4.38587E+11	32.5523	0.0000002
Error	75	1.01050E+12	1.01050E+12	1.34733E+10		
Lack-of-Fit	5	5.73989E+11	5.73989E+11	1.14798E+11	18.4093	0.0000000
Pure Error	70	4.36511E+11	4.36511E+11	6.23587E+09		
Total	77	2.01380E+12				

Fits and Diagnostics for Unusual Observations

Obs	Cycles-to-Fail	Fit	SE Fit	Residual	St Resid	
7	583200	347976	21781.7	235224	2.06314	R
8	588600	347976	21781.7	240624	2.11050	R
9	623700	347976	21781.7	275724	2.41836	R
10	677700	347976	21781.7	329724	2.89199	R

R denotes an observation with a large standardized residual.

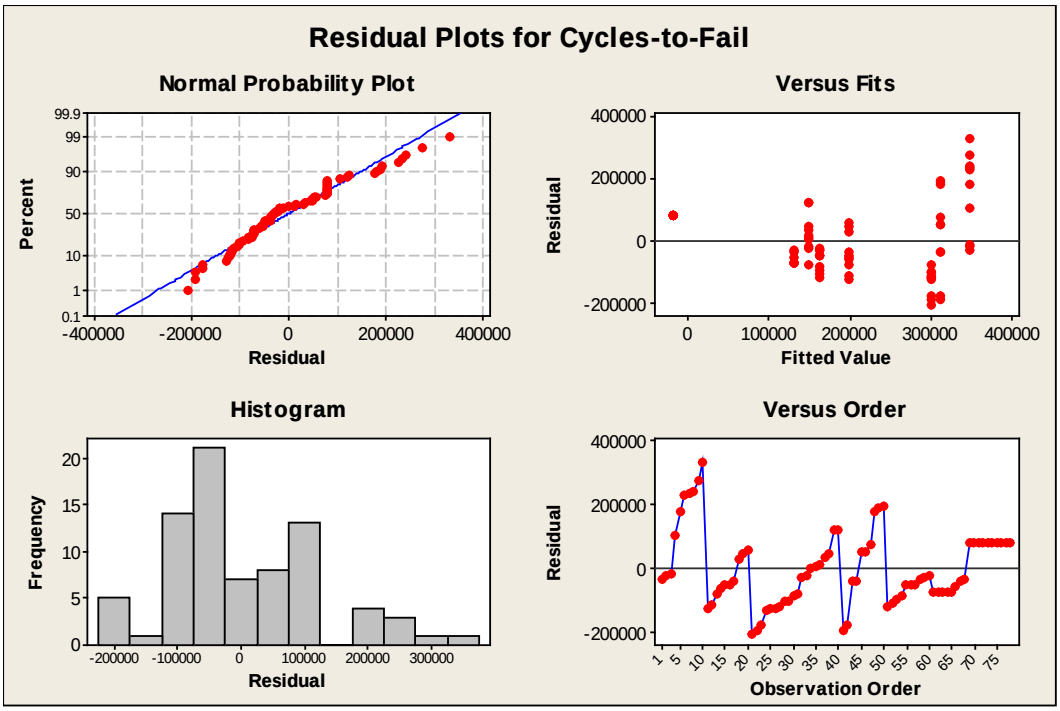

Figure 3.8 Residual Plots for Cycles-To-Failure

Table 3.15 General Regression Analysis: Cycles-to-Fail versus Vib_level, Solder

Box-Cox transformation of the response with rounded lambda = -0.5
The 95% CI for lambda is (*, -1.995)

Regression Equation
Cycles-to-Fail^-0.5 = 0.000428608 - 1.00276e-005 Vib_level - 0.000757755 Solder

Coefficients

Term	Coef	SE Coef	T	P
Constant	0.0004286	0.0002756	1.5550	0.124
Vib_level	-0.0000100	0.0000009	-10.6518	0.000
Solder	-0.0007578	0.0001275	-5.9454	0.000

Summary of Model
S = 0.000562037 R-Sq = 67.38% R-Sq(adj) = 66.51%
PRESS = 0.0000253341 R-Sq(pred) = 65.12%

Analysis of Variance

Source	DF	Seq SS	Adj SS	Adj MS	F	P
Regression	2	0.0000489	0.0000489	0.0000245	77.459	0.0000000
Vib_level	1	0.0000378	0.0000358	0.0000358	113.460	0.0000000
Solder	1	0.0000112	0.0000112	0.0000112	35.348	0.0000001
Error	75	0.0000237	0.0000237	0.0000003		
Lack-of-Fit	5	0.0000083	0.0000083	0.0000017	7.598	0.0000095
Pure Error	70	0.0000154	0.0000154	0.0000002		
Total	77	0.0000726				

Fits and Diagnostics for Unusual Observations for Transformed Response

Obs	Cycles-to-Fail^-0.5	Fit	SE Fit	Residual	St Resid	
11	-0.0037037	-0.0025352	0.0001066	-0.0011685	-2.11743	R
51	-0.0048113	-0.0028360	0.0000940	-0.0019752	-3.56456	R
52	-0.0041996	-0.0028360	0.0000940	-0.0013636	-2.46075	R

Fits for Unusual Observations for Original Response

Obs	Cycles-to-Fail	Fit	
11	72900	155585	R
51	43200	124329	R
52	56700	124329	R

R denotes an observation with a large standardized residual.

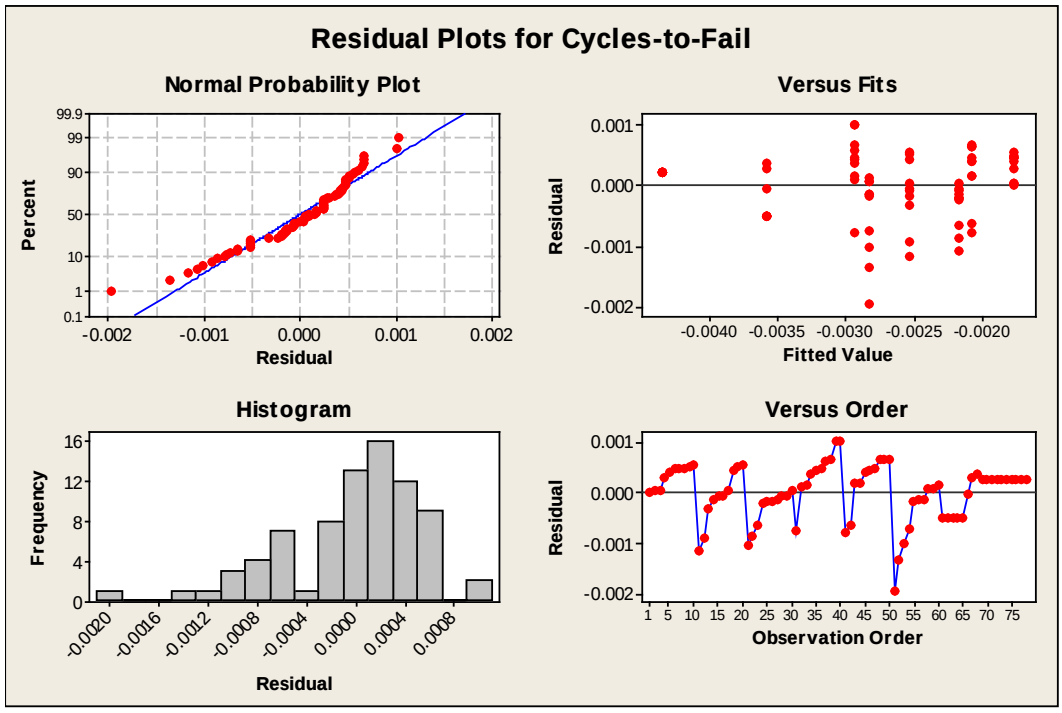

Figure 3.9 Residual Plots for Cycles-To-Failure

Table 3.16 General Regression Analysis: Cycles-to-Fail versus Vib_level, Solder, Preconditioning

Box-Cox transformation of the response with rounded lambda = -0.5
The 95% CI for lambda is (*, -1.995)

Regression Equation
Cycles-to-Fail^-0.5 = 0.000269114 - 9.085e-006 Vib_level - 0.000757975 Solder
- 0.000213139 Precond

Coefficients

Term	Coef	SE Coef	T	P
Constant	0.0002691	0.0002986	0.90129	0.370
Vib_level	-0.0000091	0.0000012	-7.77460	0.000
Solder	-0.0007580	0.0001268	-5.97950	0.000
Precond	-0.0002131	0.0001581	-1.34819	0.182

Summary of Model
S = 0.000558999 R-Sq = 68.16% R-Sq(adj) = 66.87%
PRESS = 0.0000257158 R-Sq(pred) = 64.59%

Analysis of Variance

Source	DF	Seq SS	Adj SS	Adj MS	F	P
Regression	3	0.0000495	0.0000495	0.0000165	52.8079	0.000000
Vib_level	1	0.0000378	0.0000189	0.0000189	60.4445	0.000000
Solder	1	0.0000112	0.0000112	0.0000112	35.7544	0.000000
Precond	1	0.0000006	0.0000006	0.0000006	1.8176	0.181711
Error	74	0.0000231	0.0000231	0.0000003		
Lack-of-Fit	4	0.0000078	0.0000078	0.0000019	8.8500	0.000008
Pure Error	70	0.0000154	0.0000154	0.0000002		
Total	77	0.0000726				

Fits and Diagnostics for Unusual Observations for Transformed Response

Obs	Cycles-to-Fail^-0.5	Fit	SE Fit	Residual	St Resid	
11	-0.0037037	-0.0024876	0.0001117	-0.0012161	-2.22038	R
21	-0.0032530	-0.0020930	0.0001117	-0.0011600	-2.11791	R
51	-0.0048113	-0.0029733	0.0001382	-0.0018380	-3.39334	R
52	-0.0041996	-0.0029733	0.0001382	-0.0012264	-2.26411	R

Fits for Unusual Observations for Original Response

Obs	Cycles-to-Fail	Fit	
11	72900	161604	R
21	94500	228279	R
51	43200	113119	R
52	56700	113119	R

R denotes an observation with a large standardized residual.

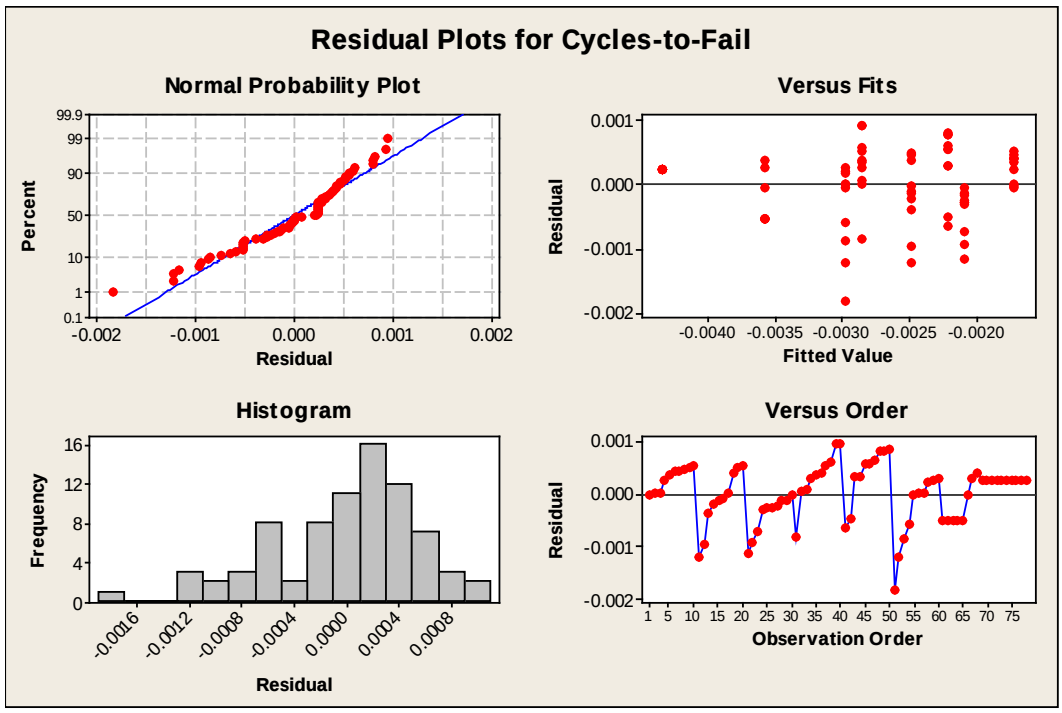

Figure 3.10 Residual Plots for Cycles-To-Failure

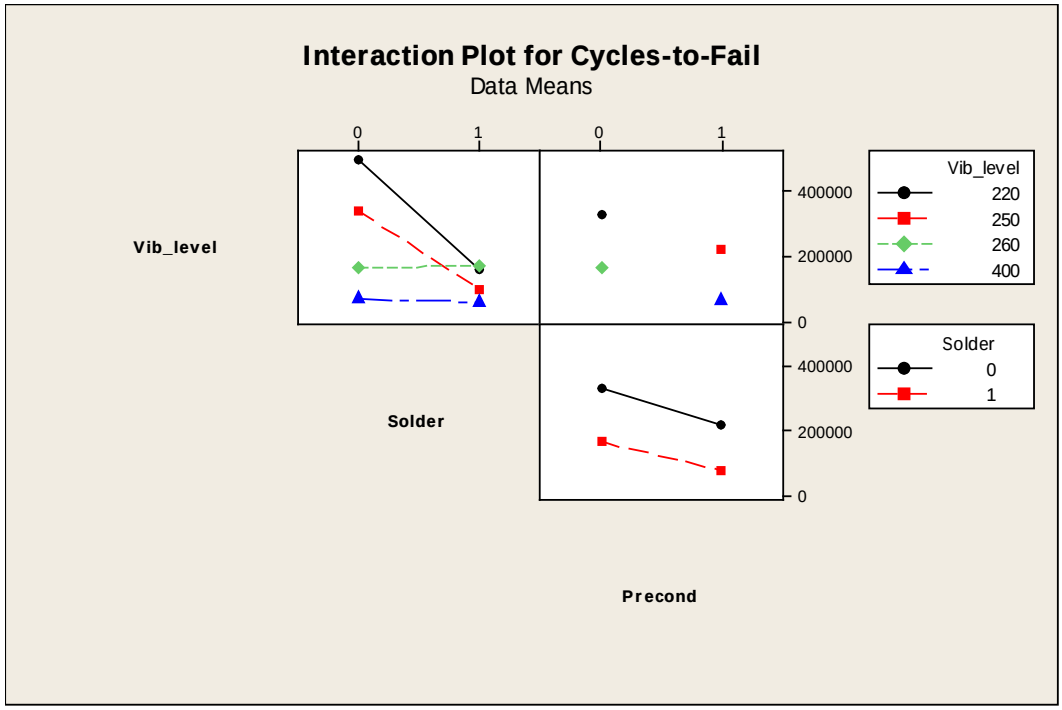

Figure 3.11 Interaction Plots for Cycles-To-Failure

Table 3.17 General Regression Analysis: Cycles-to-Fail versus Vib_level, Solder

Box-Cox transformation of the response with rounded lambda = -0.5
The 95% CI for lambda is (*, -1.995)

Regression Equation
Cycles-to-Fail^-0.5 = 0.00115808 - 1.26676e-005 Vib_level - 0.00212055 Solder
+ 4.88186e-006 Vib_level*Solder

Coefficients

Term	Coef	SE Coef	T	P
Constant	0.0011581	0.0003791	3.05484	0.003
Vib_level	-0.0000127	0.0000013	-9.49004	0.000
Solder	-0.0021206	0.0005213	-4.06779	0.000
Vib_level*Solder	0.0000049	0.0000018	2.68948	0.009

Summary of Model
S = 0.000540044 R-Sq = 70.28% R-Sq(adj) = 69.08%
PRESS = 0.0000232975 R-Sq(pred) = 67.92%

Analysis of Variance

Source	DF	Seq SS	Adj SS	Adj MS	F	P
Regression	3	0.0000510	0.0000510	0.0000170	58.3419	0.0000000
Vib_level	1	0.0000378	0.0000263	0.0000263	90.0609	0.0000000
Solder	1	0.0000112	0.0000048	0.0000048	16.5469	0.0001174
Vib_level*Solder	1	0.0000021	0.0000021	0.0000021	7.2333	0.0088387
Error	74	0.0000216	0.0000216	0.0000003		
Lack-of-Fit	4	0.0000062	0.0000062	0.0000016	7.0933	0.0000746
Pure Error	70	0.0000154	0.0000154	0.0000002		
Total	77	0.0000726				

Fits and Diagnostics for Unusual Observations for Transformed Response

Obs	Cycles-to-Fail^-0.5	Fit	SE Fit	Residual	St Resid	
21	-0.0032530	-0.0021355	0.0000903	-0.0011175	-2.09882	R
40	-0.0019149	-0.0029868	0.0000898	0.0010718	2.01268	R
51	-0.0048113	-0.0029089	0.0000943	-0.0019023	-3.57752	R
52	-0.0041996	-0.0029089	0.0000943	-0.0012907	-2.42726	R

Fits for Unusual Observations for Original Response

Obs	Cycles-to-Fail	Fit	
21	94500	219282	R
40	272700	112098	R
51	43200	118179	R
52	56700	118179	R

R denotes an observation with a large standardized residual.

Table 3.18 Regression Analysis: Log(cycles-to-failure) versus Vibration level, SnPb_SAC305, pre-conditioning

The regression equation is
Log(cycles-to-fail) = 14.2 - 0.00673 Vibration level - 0.645 SnPb_SAC305
- 0.108 Pre-Condition

Predictor	Coef	SE Coef	T	P	VIF
Constant	14.1792	0.2446	57.97	0.000	
Vibration level	-0.0067281	0.0009572	-7.03	0.000	1.561
SnPb_SAC305	-0.6447	0.1038	-6.21	0.000	1.002
Pre-Condition	-0.1082	0.1295	-0.84	0.406	1.559

S = 0.457907 R-Sq = 64.3% R-Sq(adj) = 62.8%
PRESS = 17.1906 R-Sq(pred) = 60.42%

Analysis of Variance

Source	DF	SS	MS	F	P
Regression	3	27.9112	9.3037	44.37	0.000
Residual Error	74	15.5162	0.2097		
Lack of Fit	4	6.9206	1.7302	14.09	0.000
Pure Error	70	8.5956	0.1228		
Total	77	43.4274			

Source	DF	Seq SS
Vibration level	1	19.6860
SnPb_SAC305	1	8.0789
Pre-Condition	1	0.1463

Unusual Observations

Obs	Vibration level	Log(cycles-to-fail)	Fit	SE Fit	Residual	St Resid
21	260	11.4564	12.4299	0.0915	-0.9735	-2.17R
51	250	10.6736	11.7443	0.1132	-1.0707	-2.41R

R denotes an observation with a large standardized residual.

Durbin-Watson statistic = 0.785018

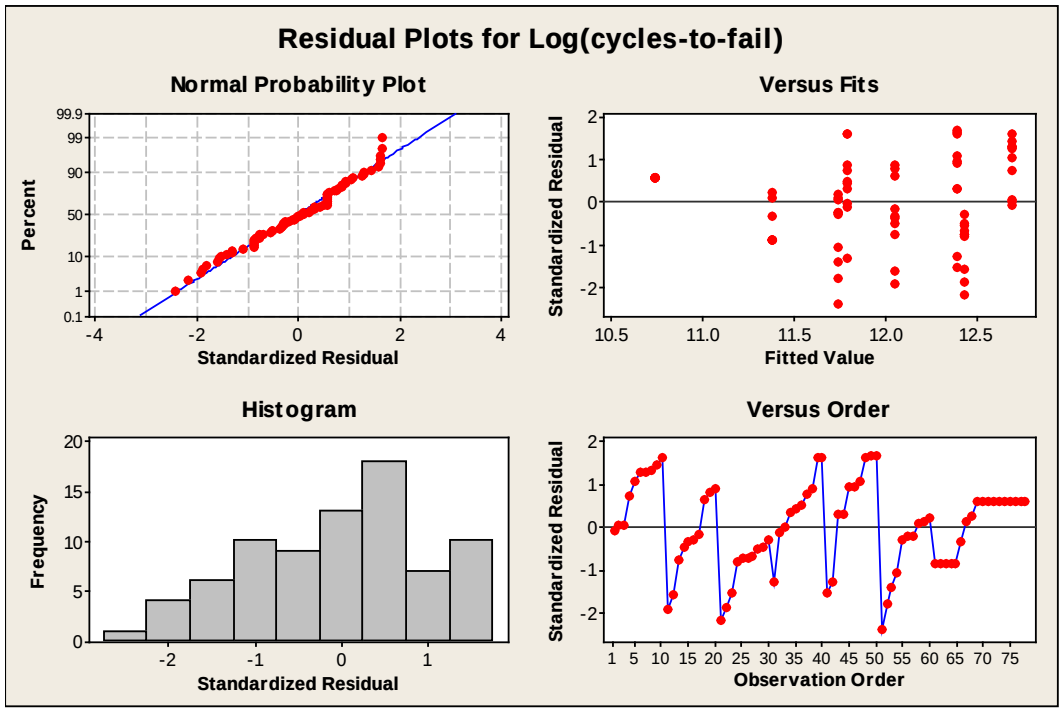

Figure 3.12 Residual Plots for Log(Cycles-To-Failure)

Table 3.19 Regression Analysis: Log(cycles-to-failure) versus Vibration level and SnPb_SAC305

The regression equation is
Log(cycles-to-fail) = 14.3 - 0.00721 Vibration level - 0.645 SnPb_SAC305

Predictor	Coef	SE Coef	T	P	VIF
Constant	14.2602	0.2241	63.63	0.000	
Vibration level	-0.0072065	0.0007654	-9.41	0.000	1.002
SnPb_SAC305	-0.6445	0.1036	-6.22	0.000	1.002

S = 0.456983 R-Sq = 63.9% R-Sq(adj) = 63.0%
PRESS = 16.7676 R-Sq(pred) = 61.39%

Analysis of Variance

Source	DF	SS	MS	F	P
Regression	2	27.765	13.882	66.48	0.000
Residual Error	75	15.663	0.209		
Lack of Fit	5	7.067	1.413	11.51	0.000
Pure Error	70	8.596	0.123		
Total	77	43.427			

Source	DF	Seq SS
Vibration level	1	19.686
SnPb_SAC305	1	8.079

Unusual Observations

Obs	Vibration level	Log(cycles-to-fail)	Fit	SE Fit	Residual	St Resid
21	260	11.4564	12.3865	0.0752	-0.9301	-2.06R
51	250	10.6736	11.8140	0.0764	-1.1404	-2.53R

R denotes an observation with a large standardized residual.

Durbin-Watson statistic = 0.791533

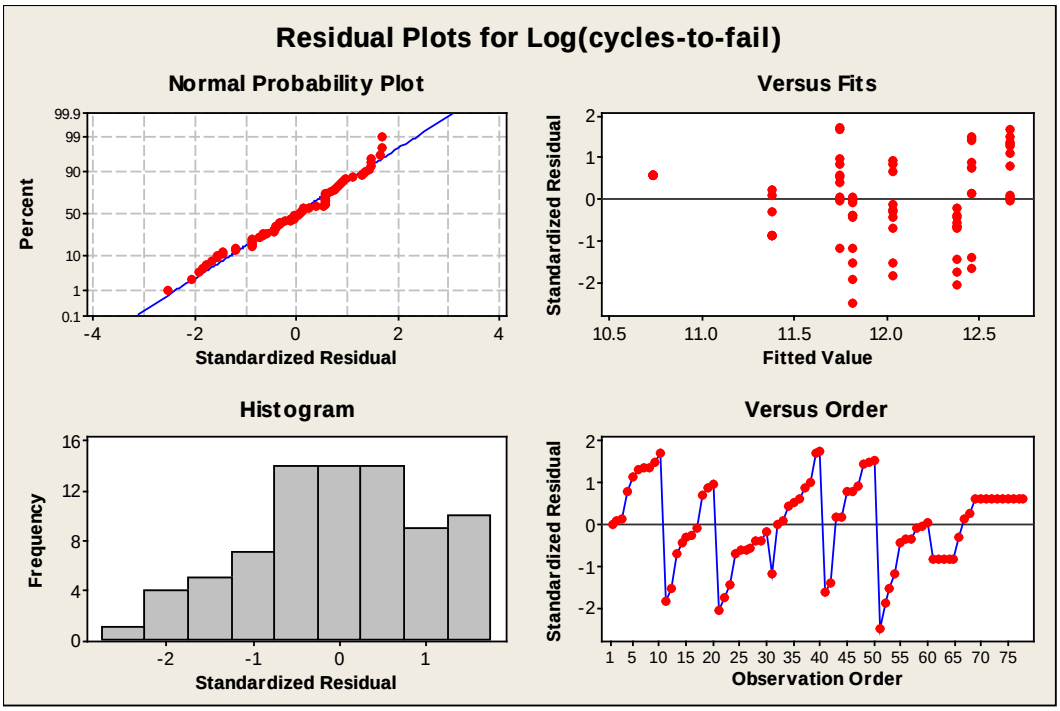

Figure 3.13 Residual Plots for Log(Cycles-To-Failure)

Table 3.20 Two-way analysis-of-variance data, two solder levels vs four vibration levels

Solder Type	210 mils	220 mils	250 mils	270 mils
0	81000	251100	618300	91800
0	310500	507600	796500	102600
0	791100	656100	874800	116100
0	1428300	842400	904500	145800
0	1657800	6822900	1188000	151200
0	10492200	13451400	1201500	307800
0	13335300	15417000	1223100	378000
0	14742000	24818400	1271700	383400
0	25479900	25995600	1274400	499500
0	26306100	27072900	1552500	561600
1	37800	129600	40500	10800
1	86400	864000	43200	10800
1	286200	947700	45900	13500
1	1279800	1282500	59400	40500
1	1547100	1998000	62100	40500
1	2322000	2154600	67500	62100
1	3072600	2154600	75600	67500
1	3080700	2160000	75600	70200
1	4284900	2160000	110700	78300
1	4476600	2160000	116100	78300

Table 3.21 Two-way ANOVA: Cycles-To-Failure versus SnPb_SAC305, microStrain

Source	DF	SS	MS	F	P
SnPb_SAC305	1	4.34538E+14	4.34538E+14	14.64	0.000
microStrain	3	6.82342E+14	2.27447E+14	7.66	0.000
Interaction	3	3.44087E+14	1.14696E+14	3.86	0.013
Error	72	2.13701E+15	2.96807E+13		
Total	79	3.59798E+15			

S = 5448002 R-Sq = 40.61% R-Sq(adj) = 34.83%

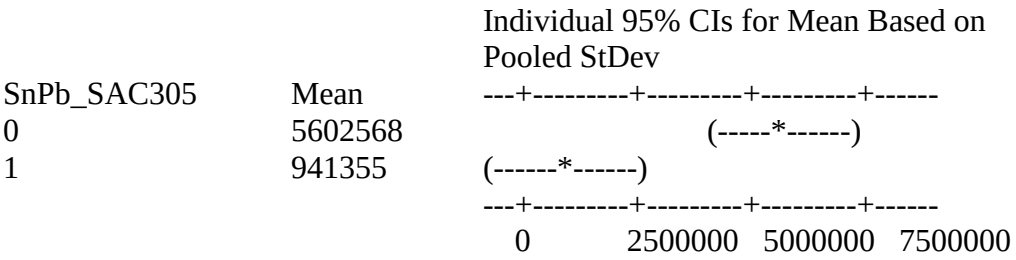

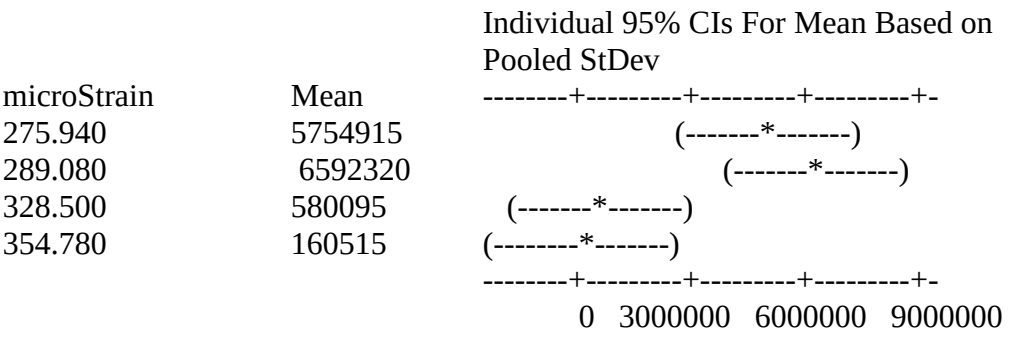

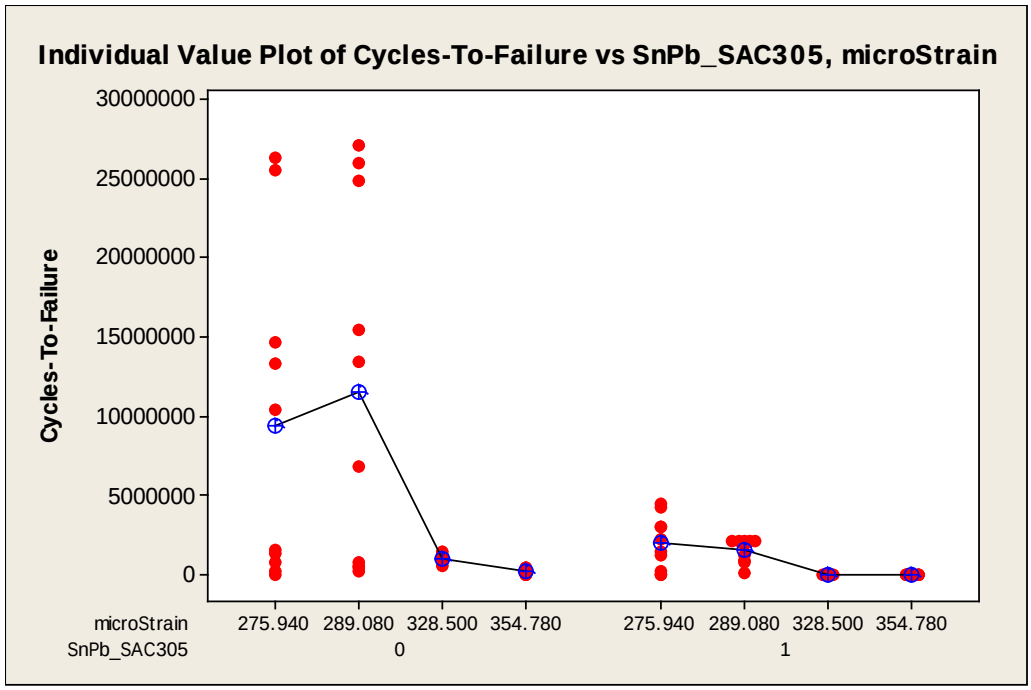

Figure 3.14 Individual Value Plot of Cycles-to-Failure

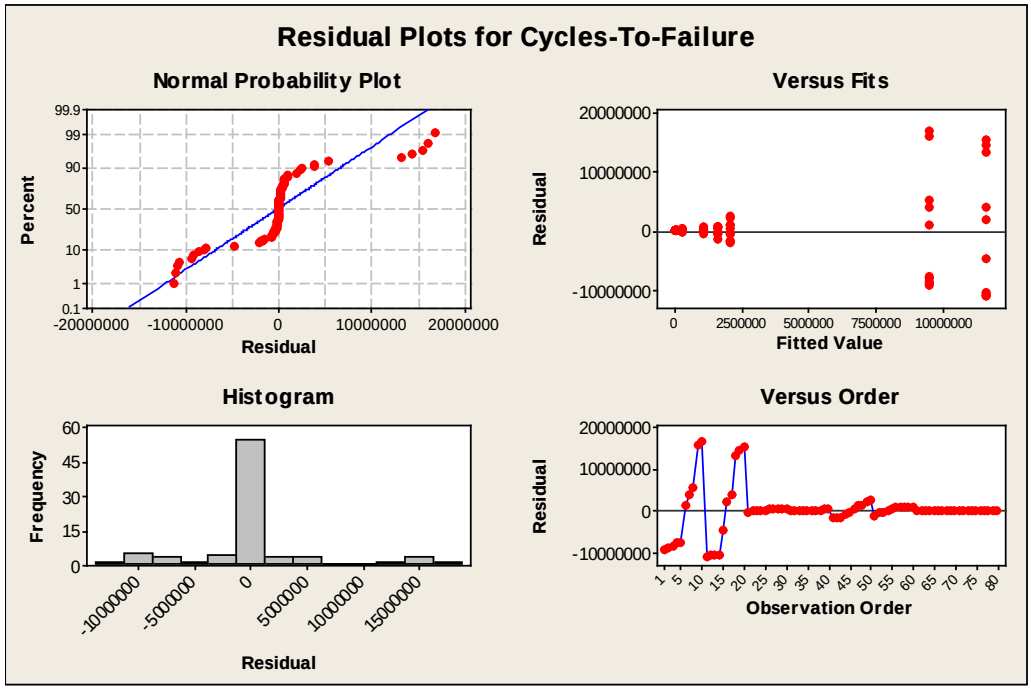

Figure 3.15 Residual Plots for Cycles-To-Failure

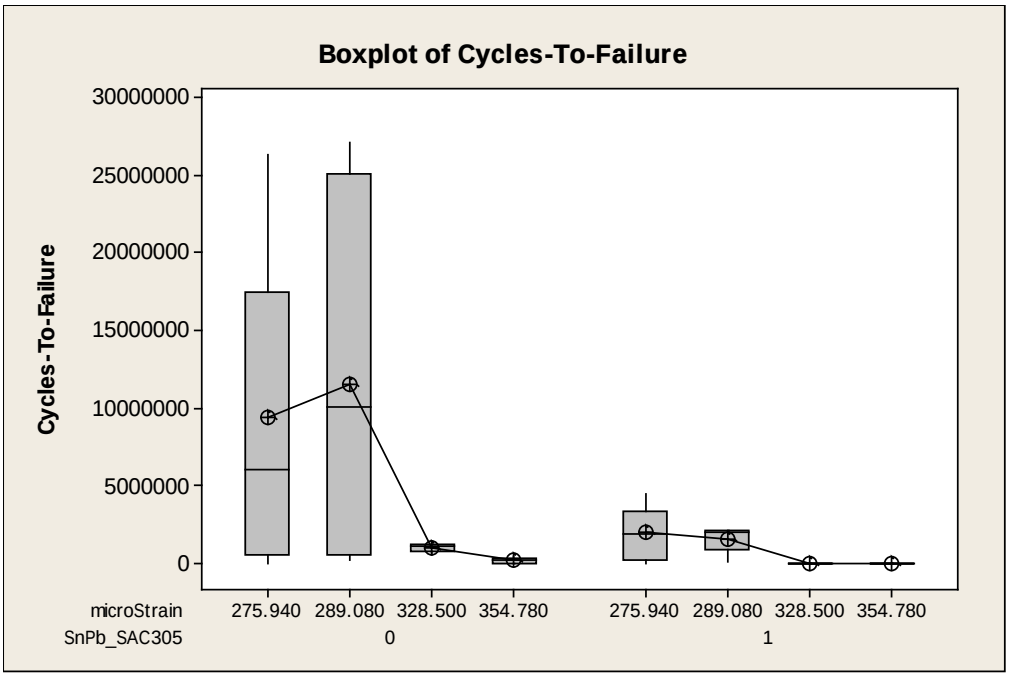

Figure 3.16 Boxplot of Cycles-to-Failure

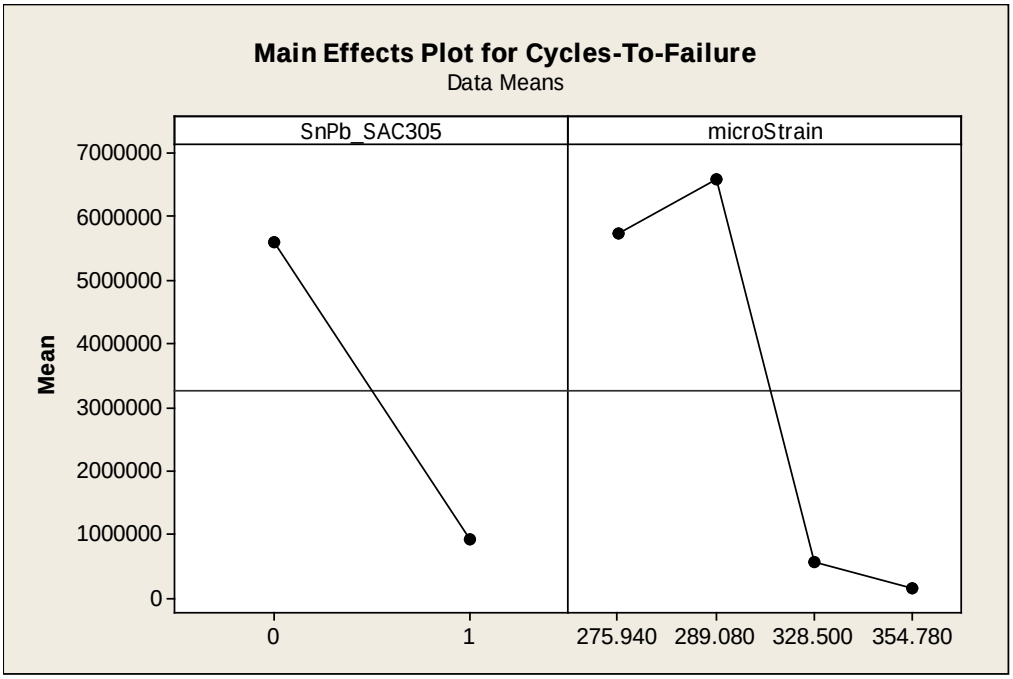

Figure 3.17 Main Effects Plot for Cycles-to-Fail

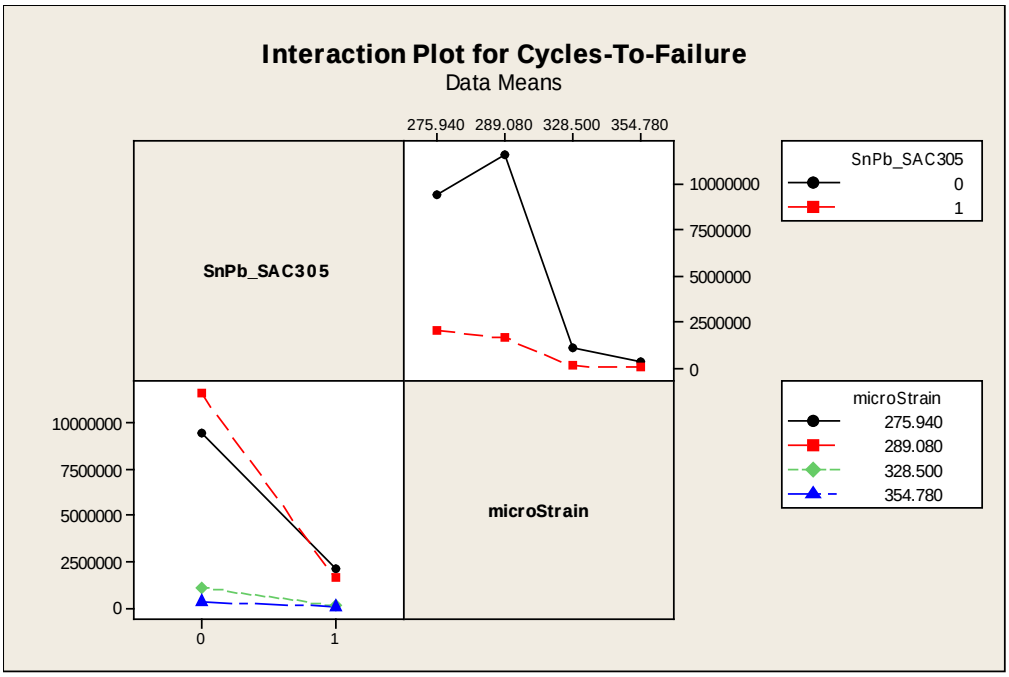

Figure 3.18 Interaction Plot for Cycles-to-Fail

Table 3.22 General Regression Analysis: Cycles-To-Failure versus SnPb_SAC305, microStrain

Regression Equation

Cycles-To-Failure = 5.15783e+007 - 4.20852e+007 SnPb_SAC305 - 147323 microStrain + 119920 SnPb_SAC305*microStrain

Coefficients

Term	Coef	SE Coef	T	P
Constant	51578290	8670547	5.94868	0.000
SnPb_SAC305	-42085197	12262006	-3.43216	0.001
microStrain	-147323	27645	-5.32918	0.000
SnPb_SAC305*microStrain	119920	39095	3.06738	0.003

Summary of Model

S = 5478921 R-Sq = 36.59% R-Sq(adj) = 34.09%

PRESS = 2.513756E+15 R-Sq(pred) = 30.13%

Analysis of Variance

Source	DF	Seq SS	Adj SS	Adj MS	F
Regression	3	1.31657E+15	1.31657E+15	4.38856E+14	14.6195
SnPb_SAC305	1	4.34538E+14	3.53611E+14	3.53611E+14	11.7797
microStrain	1	5.99590E+14	8.52533E+14	8.52533E+14	28.4002
SnPb_SAC305*microStrain	1	2.82439E+14	2.82439E+14	2.82439E+14	9.4088
Error	76	2.28141E+15	2.28141E+15	3.00186E+13	
Lack-of-Fit	4	1.44399E+14	1.44399E+14	3.60998E+13	1.2163
Pure Error	72	2.13701E+15	2.13701E+15	2.96807E+13	
Total	79	3.59798E+15			

Source	P
Regression	0.000000
SnPb_SAC305	0.000972
microStrain	0.000001
SnPb_SAC305*microStrain	0.002991
Error	
Lack-of-Fit	0.311463
Pure Error	
Total	

Fits and Diagnostics for Unusual Observations

Obs	Cycles-To-Failure	Fit	SE Fit	Residual	St Resid	
1	81000	10926072	1322246	-10845072	-2.03971	R
9	25479900	10926072	1322246	14553828	2.73724	R
10	26306100	10926072	1322246	15380028	2.89263	R
18	24818400	8990252	1074505	15828148	2.94613	R
19	25995600	8990252	1074505	17005348	3.16524	R
20	27072900	8990252	1074505	18082648	3.36576	R

R denotes an observation with a large standardized residual.

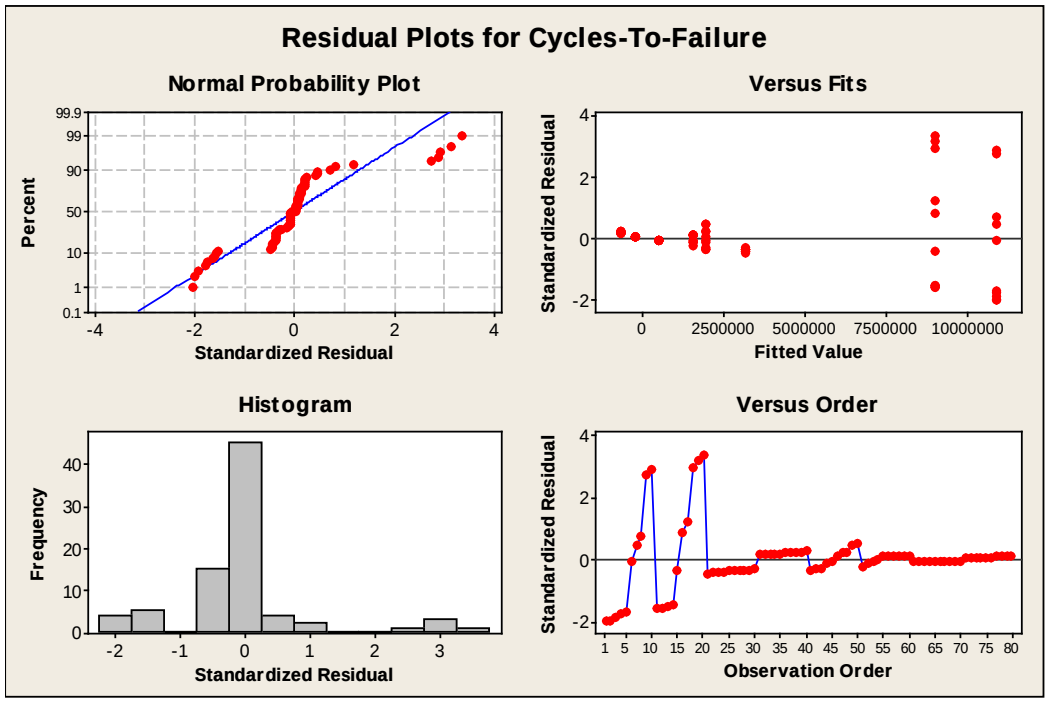

Figure 3.19 Residual Plots for Cycles-To-Failure

Table 3.23 General Regression Analysis: Cycles-To-Failure versus SnPb_SAC305, microStrain

Box-Cox transformation of the response with rounded lambda = -0.103461
The 95% CI for lambda is (-1.975, -1.965)

Regression Equation
Cycles-To-Failure^-0.103461 = 0.0164531 + 0.134384 SnPb_SAC305 - 0.000810863microStrain - 0.000580507SnPb_SAC305*microStrain

Coefficients

Term	Coef	SE Coef	T	P
Constant	0.016453	0.0522750	0.31474	0.754
SnPb_SAC305	0.134384	0.0739280	1.81777	0.073
microStrain	-0.000811	0.0001667	-4.86510	0.000
SnPb_SAC305*microStrain	-0.000581	0.0002357	-2.46284	0.016

Summary of Model
S = 0.0330326 R-Sq = 63.72% R-Sq(adj) = 62.29%
PRESS = 0.0925354 R-Sq(pred) = 59.51%

Analysis of Variance

Source	DF	Seq SS	Adj SS	Adj MS	F	P
Regression	3	0.145633	0.145633	0.0485443	44.4891	0.0000000
SnPb_SAC305	1	0.043764	0.003605	0.0036055	3.3043	0.0730405
microStrain	1	0.095251	0.025827	0.0258266	23.6692	0.0000060
SnPb_SAC305*microStrain	1	0.006618	0.006618	0.0066185	6.0656	0.0160473
Error	76	0.082927	0.082927	0.0010912		
Lack-of-Fit	4	0.009547	0.009547	0.0023867	2.3418	0.0629679
Pure Error	72	0.073381	0.073381	0.0010192		
Total	79	0.228560				

Fits and Diagnostics for Unusual Observations for Transformed Response

Obs	Cycles-To-Failure^-0.103461	Fit	SE Fit	Residual	St Resid	
1	-0.310574	-0.207297	0.0079719	-0.103277	-3.22175	R
41	-0.336054	-0.233098	0.0079719	-0.102956	-3.21174	R
42	-0.308507	-0.233098	0.0079719	-0.075409	-2.35239	R

Fits for Unusual Observations for Original Response

Obs	Cycles-To-Failure	Fit	
1	81000	4031618	R
41	37800	1297354	R
42	86400	1297354	R

R denotes an observation with a large standardized residual.

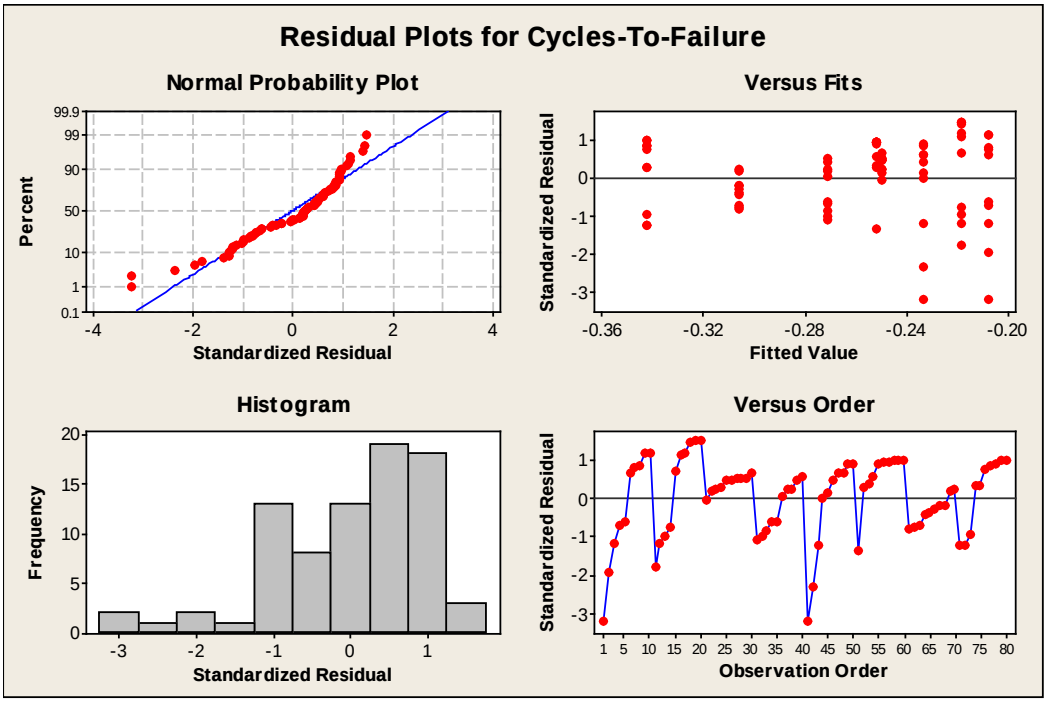

Figure 3.20 Residual Plots for Cycles-To-Failure

3.7 S-N Curve development

The goal for S-N curve development is to further refine the affect vibration levels have on cycles to failure by measuring the strain at the point of failure. In this dissertation only a Sn-Pb card set is available with no preconditioning and ENIG finish. The first step in the S-N curve development is to compare the two tin-lead vibration levels for datasets using the LR test to demonstrate whether they are from different distributions or not. The data in Table 3.1 columns 2 and 4 are compared by using the complete set of failures. Table 3.24 shows the two distributions as one and failures truncated to the first ten failures use Tables 3.25, 3.26, and 3.27 to calculate the LR test. In both cases

the null hypothesis is rejected and tin-lead at the 220 mils input and 260 mils input vibration are from different distributions. Figures 3.21 through 3.24 show the distributions for the LR test.

The actual S-N curve will map the strain level at the point of failure, in this case the strain at the individual components. In this dissertation both strain using strain gauges and displacement using a Laser Vibrometer (LV) Figure 3.26 are measured using the test vehicle in Figure 3.25 showing the 9 labeled strain gauges which also act as the LV targets. Figure 3.27 shows the 20 BGAs of the test vehicle and Figure 3.28 shows the relative position of the LV system to the test vehicle on the shaker with all the strain gauges connected to the signal conditioners.

Table 3.28 are the LV measurements at the strain gauge locations for three levels of vibration, the input vibration levels are in peak-to-peak units, but the LV measures peak displacement in one direction of circuit board bending. In Tables 3.29 and 3.30 both the LV and strain gauge measurements for 220 mils and 260 mils are used to map displacement and strain to the failure times in succession. Equation (5) is used to calculate the Bezier strains in these tables because the first set of strains are linearly interpolated from the measured strains to the 20 BGAs.

Figures 3.29 and 3.30 for 260 mils and Figures 3.32 and 3.33 for 220 mils shows a comparison between the interpolated strains and the Bezier smoothing algorithm with equation fits both logarithmic and power equations. Figure 3.35 shows a composite of the results and the best seem to be a power fit with Bezier smoothing. In addition, the S-N curves show shorter failure times for the higher

vibration levels due to higher bending and shearing than at lower vibration levels where non-linear affects are less pronounced. As described by Cheung, Zhu, and Iu (1998), because the test vibration amplitude between 110 mils and 130 mils is larger than the 90 mils thickness of the test vehicle boards; the vibration in these tests is nonlinear.

The LV measurement plots Figures 3.31 and 3.34 at 260 mils and 220 mils respectively, show a lot of dispersion. Figure 3.36 shows the targets for increasing the resolution of the LV measurement by taking 7 points at each of the 20 BGA locations which are tabulated for 220 mils and 260 mils peak displacements in Tables 3.31 and 3.32 respectively and plotted in Figures 3.37 and 3.39. Using equation (8) in an attempt to transform the LV displacements into strain shown in Figures 3.38 and 3.40 shows improvement. The summary results for the LV strains by BGA location are in Table 3.33.

Finally, the Bezier strain data is converted to displacement using equation (9) and applying Steinberg's equation's (10) and (11) to predict cycles-to-failure summarized in Tables 3.34 for 220 mils and Table 3.35 for 260 mils indicate how conservative Steinberg's equations compared to actual failure data for tin-lead. Steinberg's equations for linear systems have been applied to a non-linear vibration problem and are too conservative.

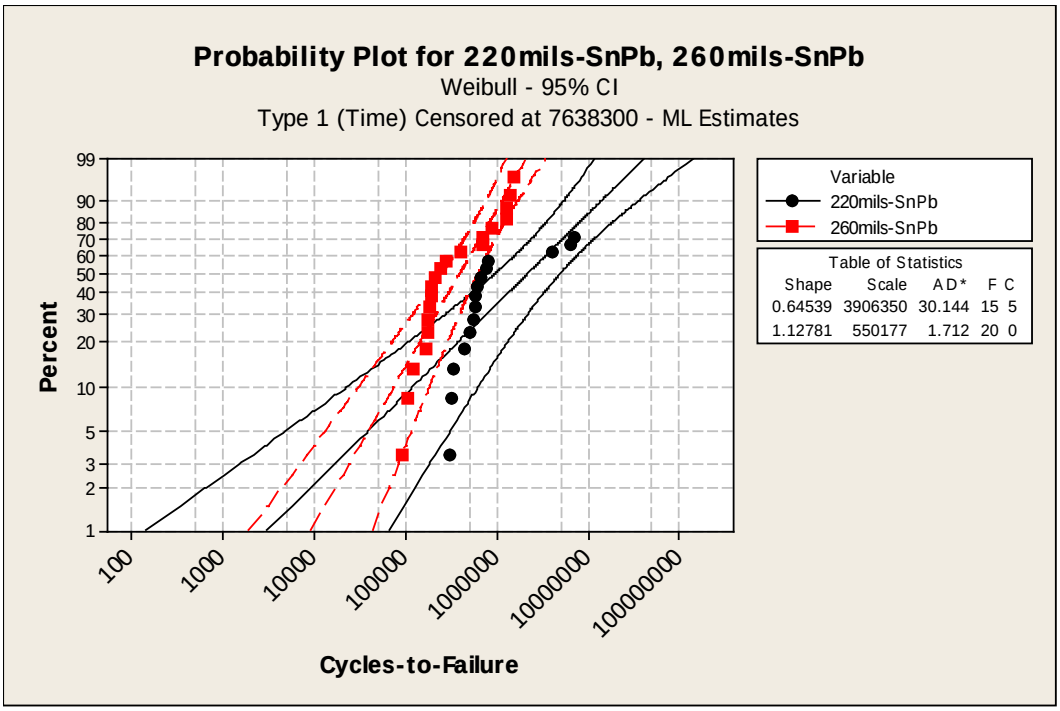

Figure 3.21 Probability plot for complete failure data of the 220mils-SnPb distribution, and 260mils-SnPb distribution

Table 3.24 Distribution Analysis: SnPb_220mils_260mils no preconditioning

Censoring Information	Count
Uncensored value	35
Right censored value	5

Type 1 (Time) Censored at 7638300
Estimation Method: Maximum Likelihood
Distribution: Weibull

Parameter Estimates

Parameter	Estimate	Standard Error	95.0% Normal CI Lower	Upper
Shape	0.635083	0.0820238	0.493054	0.818026
Scale	1628241	441753	956713	2771121

Log-Likelihood = -536.588

Goodness-of-Fit
Anderson-Darling (adjusted) = 18.657

Characteristics of Distribution

	Estimate	Standard Error	95.0% Normal CI Lower	Upper
Mean(MTTF)	2284128	647587	1310361	3981529
Standard Deviation	3745435	1376698	1822337	7697964
Median	914288	269687	512866	1629903
First Quartile(Q1)	228942	92847.1	103400	506908
Third Quartile(Q3)	2723226	725776	1615203	4591348
Interquartile Range(IQR)	2494284	672539	1470397	4231139

Table of Percentiles

Percent	Percentile	Standard Error	95.0% Normal CI Lower	Upper
1	1164.02	1191.20	156.633	8650.42
2	3494.81	3099.94	614.322	19881.6
3	6670.95	5388.48	1369.70	32489.9
4	10578.8	7952.99	2423.93	46169.7
5	15156.0	10738.7	3779.82	60771.4
6	20363.3	13711.5	5441.19	76208.1
7	26174.5	16848.2	7412.55	92424.7
8	32571.7	20132.1	9698.92	109385
9	39542.7	23550.8	12305.8	127064
10	47079.4	27094.7	15239.0	145447
20	153462	68416.8	64049.9	367693
30	321165	120009	154406	668028
40	565413	184644	298121	1072356
50	914288	269687	512866	1629903
60	1418850	390621	827168	2433767
70	2181008	581392	1293458	3677583
80	3444666	929350	2030010	5845155
90	6054274	1760185	3424432	10703740
91	6496180	1913213	3647267	11570403
92	7003501	2092650	3899201	12579249
93	7595308	2306740	4188230	13774007
94	8300026	2567933	4526134	15220587
95	9162594	2896205	4931308	17024517
96	10260010	3326347	5434804	19369198
97	11740490	3926618	6095383	22613688
98	13947990	4859152	7046493	27608971
99	18032783	6683832	8720991	37287195

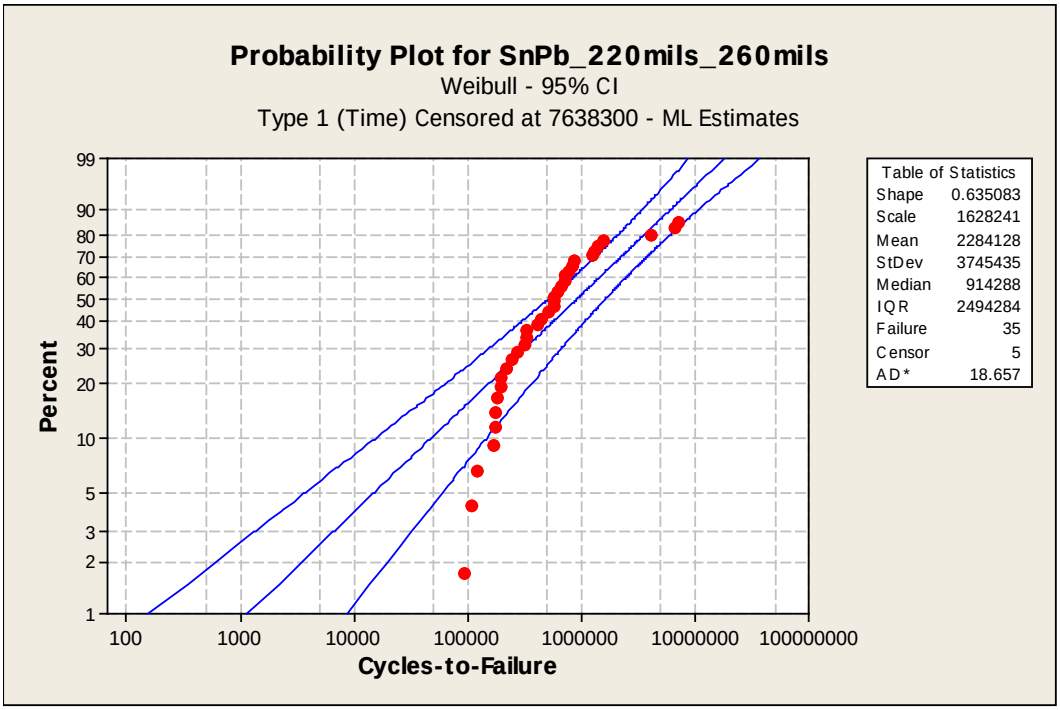

Figure 3.22 Probability Plot for SnPb_220mils_260mils

Table 3.25 Distribution Analysis: 220mils-SnPb no preconditioning

Censoring Information Count
Uncensored value 10
Estimation Method: Maximum Likelihood
Distribution: Weibull

Parameter Estimates

Parameter	Estimate	Standard Error	95.0% Normal CI Lower	Upper
Shape	4.80022	1.27330	2.85412	8.07328
Scale	549502	38022.8	479812	629316

Log-Likelihood = -131.365

Goodness-of-Fit
Anderson-Darling (adjusted) = 1.713

Characteristics of Distribution

	Estimate	Standard Error	95.0% Normal CI Lower	Upper
Mean(MTTF)	503346	37923.3	434245	583442
Standard Deviation	119663	25795.4	78427.8	182579
Median	509108	39617.5	437091	592991
First Quartile(Q1)	423885	47283.0	340643	527469
Third Quartile(Q3)	588195	38792.3	516873	669360
Interquartile Range(IQR)	164310	37900.9	104549	258231

Table of Percentiles

Percent	Percentile	Standard Error	95.0% Normal CI Lower	Upper
1	210754	59673.2	120995	367102
2	243751	59909.3	150570	394598
3	265517	59477.3	171166	411876
4	282219	58869.0	187513	424758
5	295968	58205.6	201301	435155
6	307762	57529.3	213354	443944
7	318155	56857.5	224141	451604
8	327494	56197.9	233958	458426
9	336006	55553.8	243003	464602
10	343851	54926.5	251420	470263
20	402035	49512.5	315817	511792
30	443300	45306.0	362830	541616
40	477745	42023.2	402090	567635
50	509108	39617.5	437091	592991
60	539586	38214.7	469652	619932
70	571168	38139.7	501101	651033
80	606771	40093.7	533065	690669
90	653774	46047.8	569475	750552
91	659896	47081.0	573781	758937
92	666494	48254.4	578321	768110
93	673686	49601.3	583158	778267
94	681641	51170.1	588378	789686
95	690616	53034.5	594114	802792
96	701030	55316.0	600580	818280
97	713643	58237.7	608160	837422
98	730097	62287.9	617676	862980
99	755335	68968.0	631565	903360

Table 3.26 Distribution Analysis: 260mils-SnPb

Censoring Information Count
Uncensored value 10
Estimation Method: Maximum Likelihood
Distribution: Weibull

Parameter Estimates

Parameter	Estimate	Standard Error	95.0% Normal CI Lower	Upper
Shape	5.27371	1.42094	3.11007	8.94259
Scale	180664	11330.2	159767	204293

Log-Likelihood = -119.606

Goodness-of-Fit
Anderson-Darling (adjusted) = 1.735

Characteristics of Distribution

	Estimate	Standard Error	95.0% Normal CI Lower	Upper
Mean(MTTF)	166390	11454.4	145388	190425
Standard Deviation	36298.9	8029.03	23529.6	55998.0
Median	168534	11883.6	146781	193512
First Quartile(Q1)	142649	14494.2	116891	174084
Third Quartile(Q3)	192207	11529.9	170887	216187
Interquartile Range(IQR)	49557.6	11758.9	31127.1	78900.9

Table of Percentiles

Percent	Percentile	Standard Error	95.0% Normal CI Lower	Upper
1	75517.0	19664.4	45331.0	125804
2	86207.1	19468.4	55375.0	134206
3	93186.7	19167.0	62269.5	139455
4	98507.4	18856.6	67690.8	143353
5	102866	18555.1	72232.4	146492
6	106591	18266.7	76180.9	149139
7	109862	17991.8	79698.5	151442
8	112794	17729.6	82887.2	153490
9	115459	17479.1	85815.4	155342
10	117910	17239.4	88531.7	157038
20	135941	15272.4	109074	169426
30	148584	13813.4	123834	178281
40	159057	12696.7	136021	185995
50	168534	11883.6	146781	193512
60	177693	11401.8	156695	201506
70	187136	11343.9	166172	210744
80	197724	11914.2	175699	222511
90	211619	13686.8	186424	240219
91	213422	13993.5	187684	242689
92	215363	14341.5	189011	245389
93	217477	14740.2	190424	248374
94	219813	15203.9	191946	251727
95	222446	15753.9	193616	255569
96	225497	16425.3	195497	260102
97	229187	17282.9	197698	265693
98	233992	18467.8	200457	273138
99	241343	20413.0	204475	284859

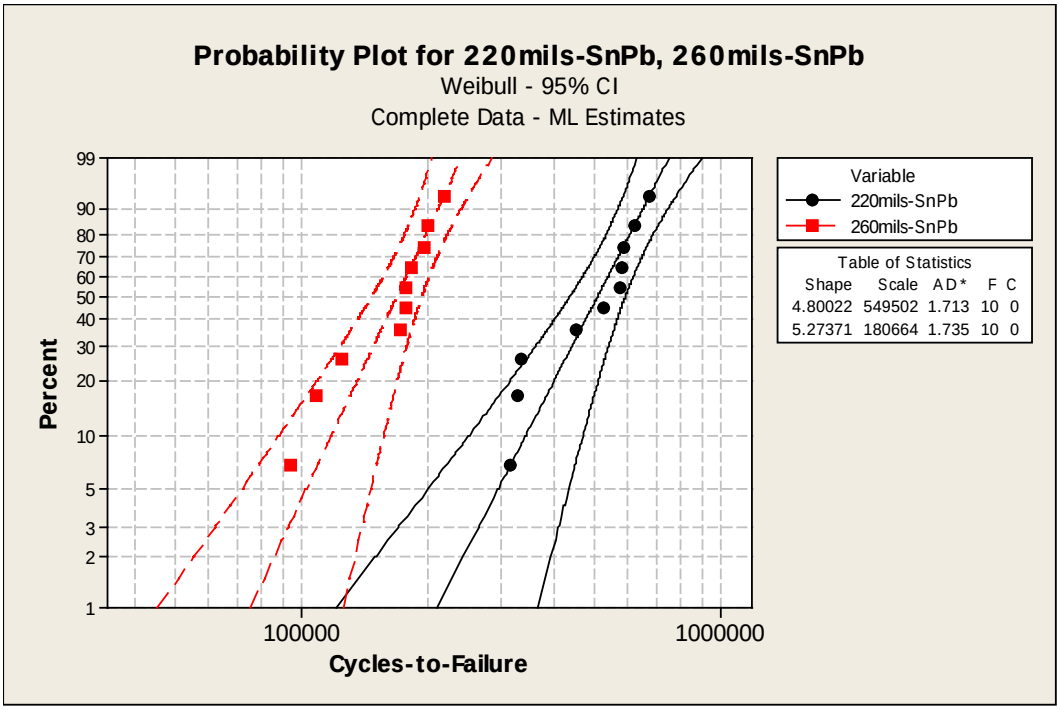

Figure 3.23 Probability Plot for 220mils-SnPb, 260mils-SnPb

Table 3.27 Distribution Analysis: Sn-Pb_220_260

```
Censoring Information  Count
Uncensored value          20
Estimation Method: Maximum Likelihood
Distribution:   Weibull
```

Parameter Estimates

Parameter	Estimate	Standard Error	95.0% Normal CI Lower	Upper
Shape	1.84633	0.327079	1.30472	2.61276
Scale	377322	48351.3	293519	485052

Log-Likelihood = -269.720

Goodness-of-Fit
Anderson-Darling (adjusted) = 1.369

Characteristics of Distribution

	Estimate	Standard Error	95.0% Normal CI Lower	Upper
Mean(MTTF)	335169	42225.9	261834	429044
Standard Deviation	188300	32832.4	133793	265014
Median	309386	44407.8	233520	409900
First Quartile(Q1)	192155	38776.1	129384	285378
Third Quartile(Q3)	450343	54746.5	354867	571506
Interquartile Range(IQR)	258189	40841.6	189361	352034

Table of Percentiles

Percent	Percentile	Standard Error	95.0% Normal CI Lower	Upper
1	31236.4	15561.7	11765.2	82932.1
2	45592.6	19765.1	19493.3	106636
3	56946.8	22542.1	26213.6	123712
4	66734.4	24638.0	32366.1	137597
5	75519.6	26324.1	38137.7	149543
6	83594.7	27733.1	43630.2	160166
7	91134.3	28940.9	48907.0	169821
8	98253.1	29995.6	54011.2	178735
9	105031	30929.3	58973.6	187059
10	111527	31765.2	63817.2	194903
20	167454	37137.3	108422	258626
30	215882	40091.7	150016	310666
40	262245	42263.1	191218	359655
50	309386	44407.8	233520	409900
60	359873	47188.0	278315	465331
70	417230	51518.0	327546	531470
80	488259	59161.6	385045	619140
90	592781	75269.1	462181	760285
91	607321	77938.4	472262	781006
92	623235	80969.9	483131	803968
93	640870	84459.4	494984	829752
94	660731	88546.4	508104	859204
95	683588	93446.9	522919	893622
96	710711	99521.6	540131	935164
97	744439	107444	561017	987829
98	789890	118719	588346	1060475
99	862854	138112	630507	1180821

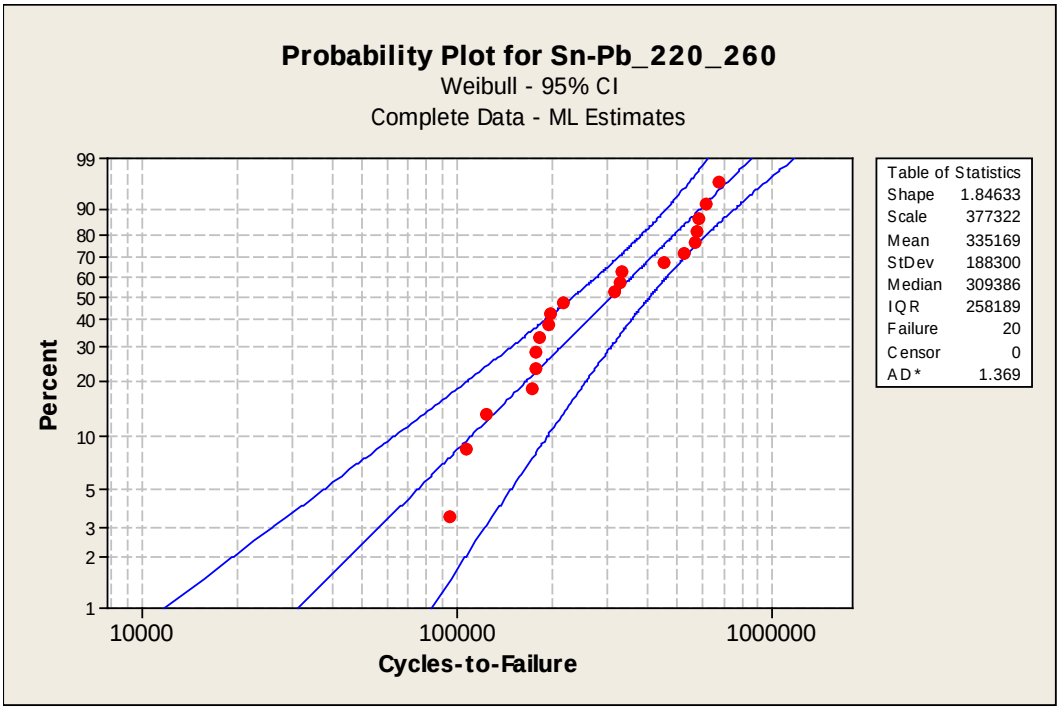

Figure 3.24 Probability Plot for Sn-Pb_220_260

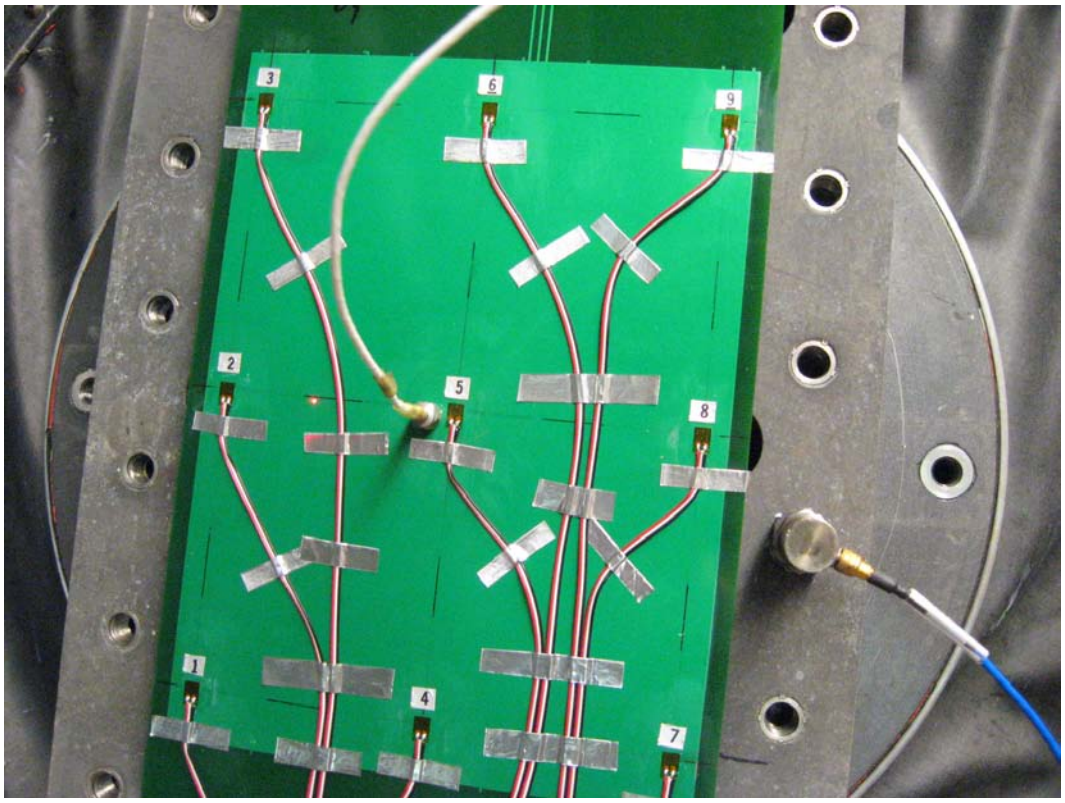

Figure 3.25 Test vehicle nine strain gauge locations also used as targets for the Laser Vibrometer

Figure 3.26 Laser Vibrometer system pointing at the test vehicle

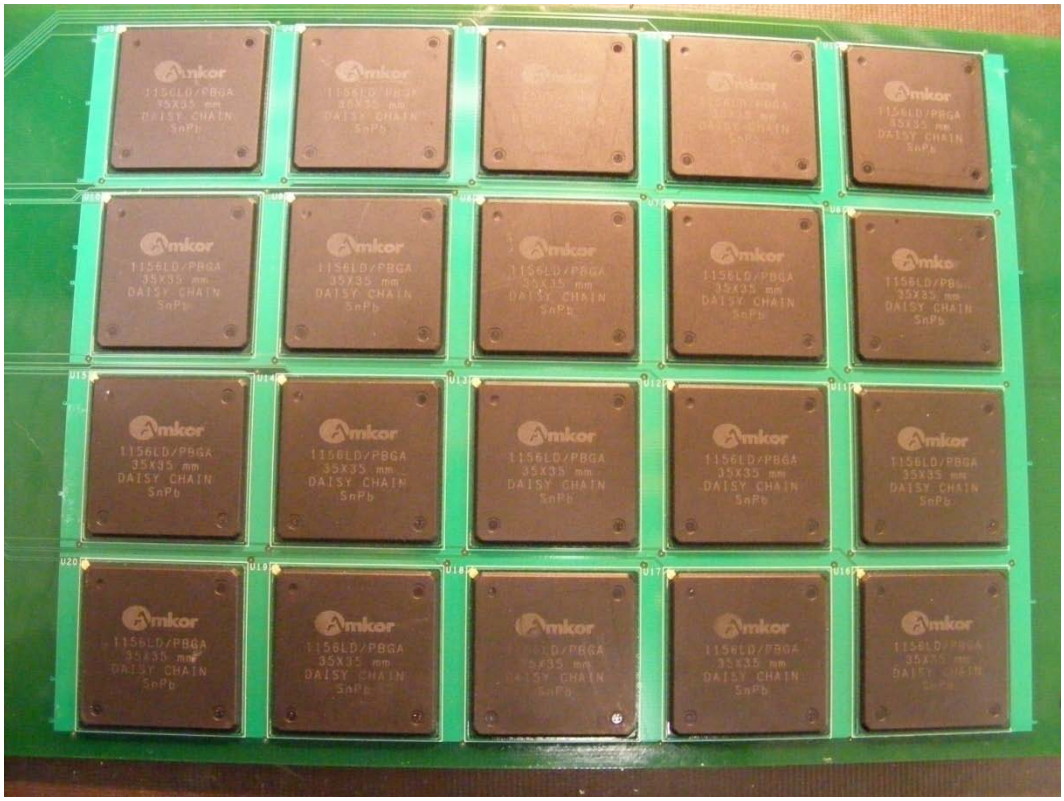

Figure 3.27 Test vehicle with 20 daisy chained 1156 BGAs 35mm x 35mm; location 1 is at the upper right hand corner and locations 2-5 proceed to the left in the upper row; locations 6-10 are in the second row; locations 11-15 are in the third row; and locations 16-20 are in the bottom row, where location 20 is on the bottom left hand corner. The numbers can be made out in the picture with designations going from U1-U20

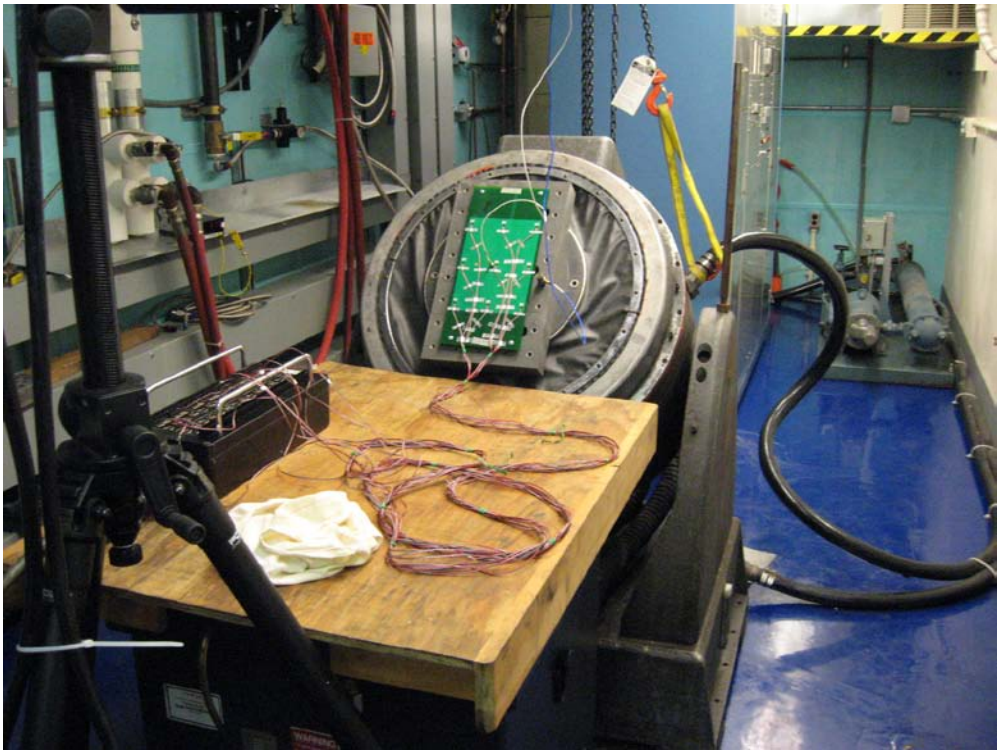

Figure 3.28 Test vehicle on the shaker with the Laser Vibrometer mounting tripod at left in photo

Table 3.28 Test vehicle measured displacements at the nine strain gauge locations using a laser vibrometer

	150 Mils P/P Scan		220 Mils P/P Scan		260 Mils P/P Scan	
Strain Gauge #	Peak Displacement		Peak Displacement		Peak Displacement	
	Milli Meters	**Mils**	**Milli Meters**	**Mils**	**Milli Meters**	**Mils**
1	1.585	62.4	2.163	85.15	2.448	96.37
2	1.902	74.88	2.832	111.49	2.886	113.62
3	1.136	44.72	1.623	63.89	1.417	55.78
4	1.47	57.87	2.246	88.42	2.635	103.74
5	1.864	73.38	2.141	84.29	2.577	101.45
6	1.313	51.69	1.507	59.33	1.873	73.74
7	1.458	57.4	2.15	84.64	2.495	98.22
8	1.915	75.39	2.804	110.39	2.349	92.48
9	1.203	47.36	0.949	37.36	0.762	30

Table 3.29 260 mils failure times and their measured LV displacements and strains including Bezier smoothed strains

Fail time	PCB chip location	PCB strain gauges	Micro strain reading at gauge locations	LV displacement (mils)	Bezier-micro strain
94500	18	8	447	92.48	447
108000	3	2	456	113.62	456
124200	8	5	325	101.45	340
172800	19	8,9	356	61.24	400
178200	13	5	325	101.45	338
178200	17	7,8	362	95.35	405
183600	2	1,2	361.5	104.995	408
197100	12	4,5	236.5	102.595	295
199800	4	2,3	363.5	84.7	410
218700	14	5,6	231.5	87.595	291
248400	9	5,6	231.5	87.595	293
280800	7	4,5	236.5	102.595	296
407700	5	3	271	55.78	271
718200	1	1	267	96.37	267
718200	20	9	265	30	265
880200	16	7	277	98.22	277
1277100	10	6	138	73.74	153
1287900	11	4	148	103.74	163
1428300	6	4	148	103.74	161
1582200	15	6	138	73.74	152

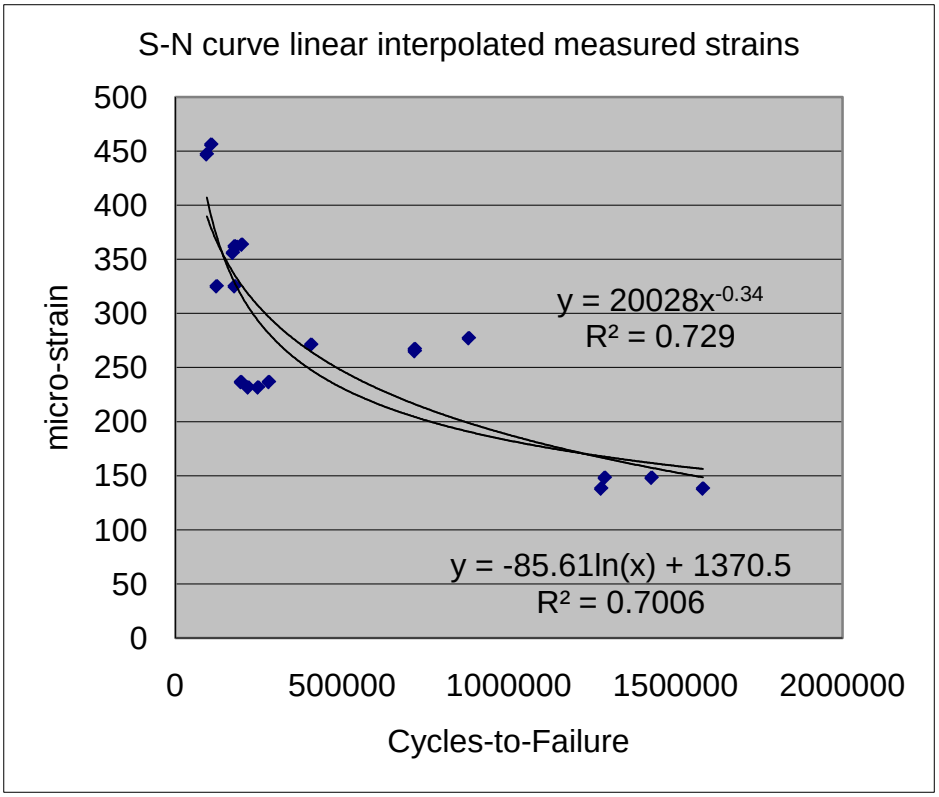

Figure 3.29 S-N curves using measured and linearly interpolated strain to the 20 BGA locations with logarithmic and power curve fits for 260 mils vibration input level and tin-lead solder

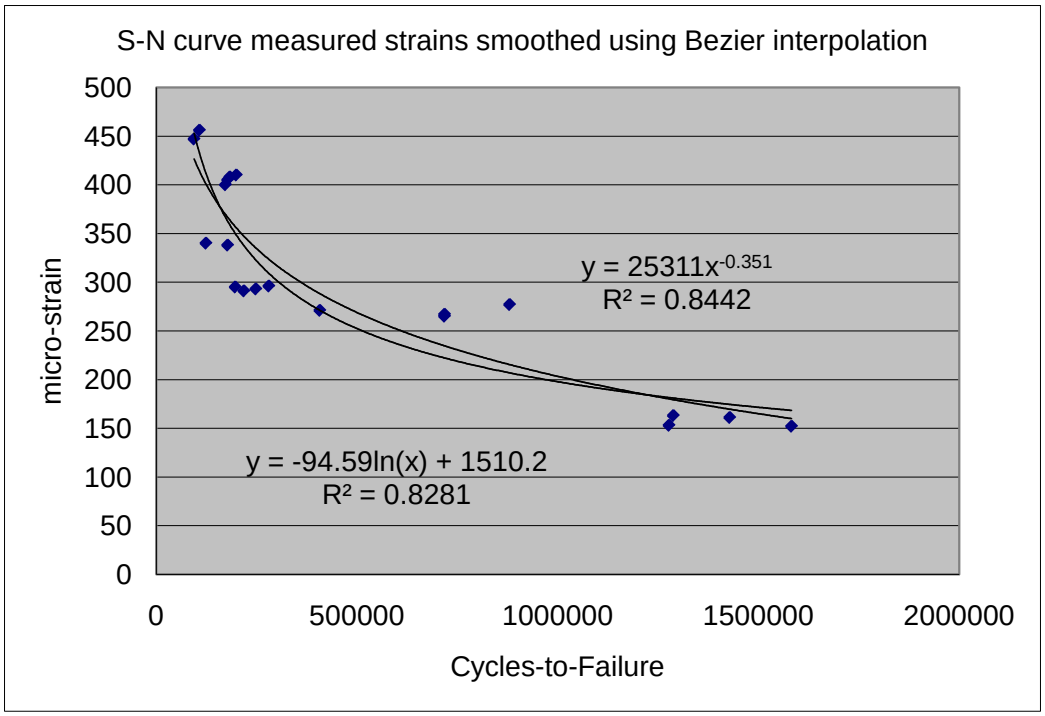

Figure 3.30 S-N curves using Bezier smoothed strains to the 20 BGA locations with logarithmic and power curve fits for 260 mils vibration input level and tin-lead solder

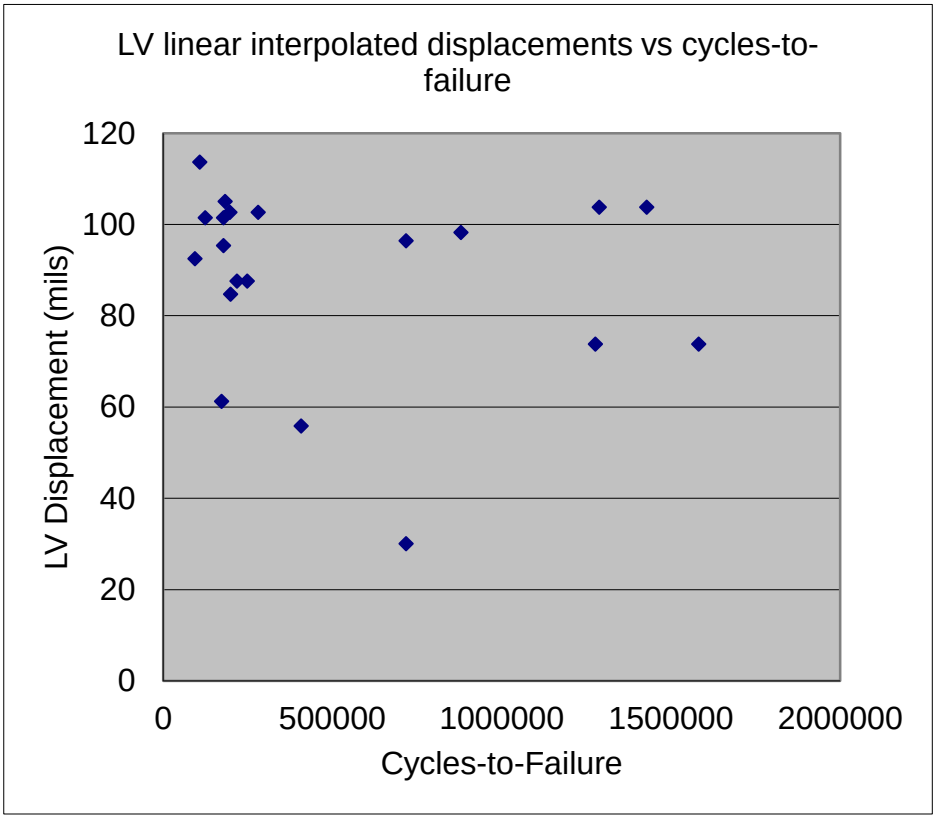

Figure 3.31 Laser Vibrometer measured displacements at the strain gauge locations and linearly interpolated to the 20 BGA locations for 260 mils tin-lead solder

Table 3.30 220 mils failure times and their measured LV displacements and strains including Bezier smoothed strains

Fail time	PCB chip location	PCB strain gauges	Micro strain reading at gauge locations	LV displacement (mils)	Bezier-micro strain
315900	4	2,3		87.69	347
329400	18	8	380	110.39	380
334800	3	2	386	111.49	386
453600	9	5,6		71.81	345
526500	13	5	276	84.29	382
575100	2	1,2		98.32	346
583200	8	5	276	84.29	384
588600	14	5,6		71.81	343
623700	17	7,8		97.515	345
677700	7	4,5		86.355	346
769500	12	4,5		86.355	345
826200	19	8,9		73.875	341
4158000	5	3	231	63.89	231
6666300	1	1	228	85.15	228
7219800	16	7	236	84.64	236
S7638300	6	4	126		231
S7638300	10	6	118		229
S7638300	11	4	126		233
S7638300	15	6	118		228
S7638300	20	9	226		226

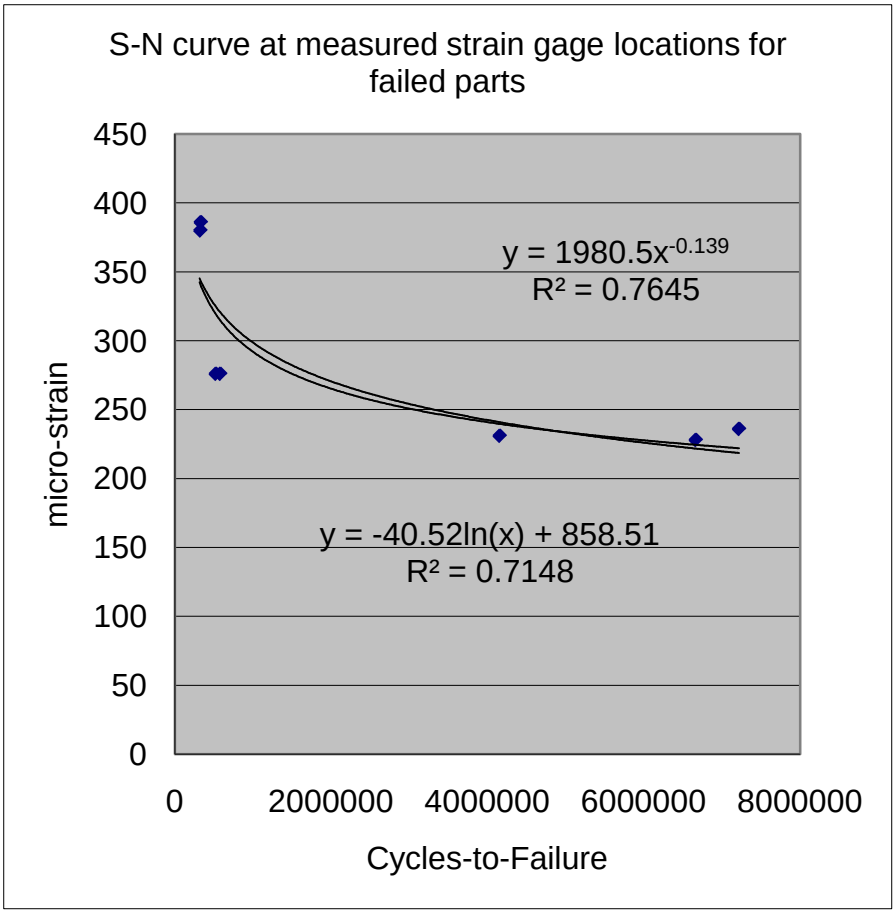

Figure 3.32 S-N curves using measured strains at the nine strain gauge locations with logarithmic and power curve fits for 220 mils vibration input level and tin-lead solder

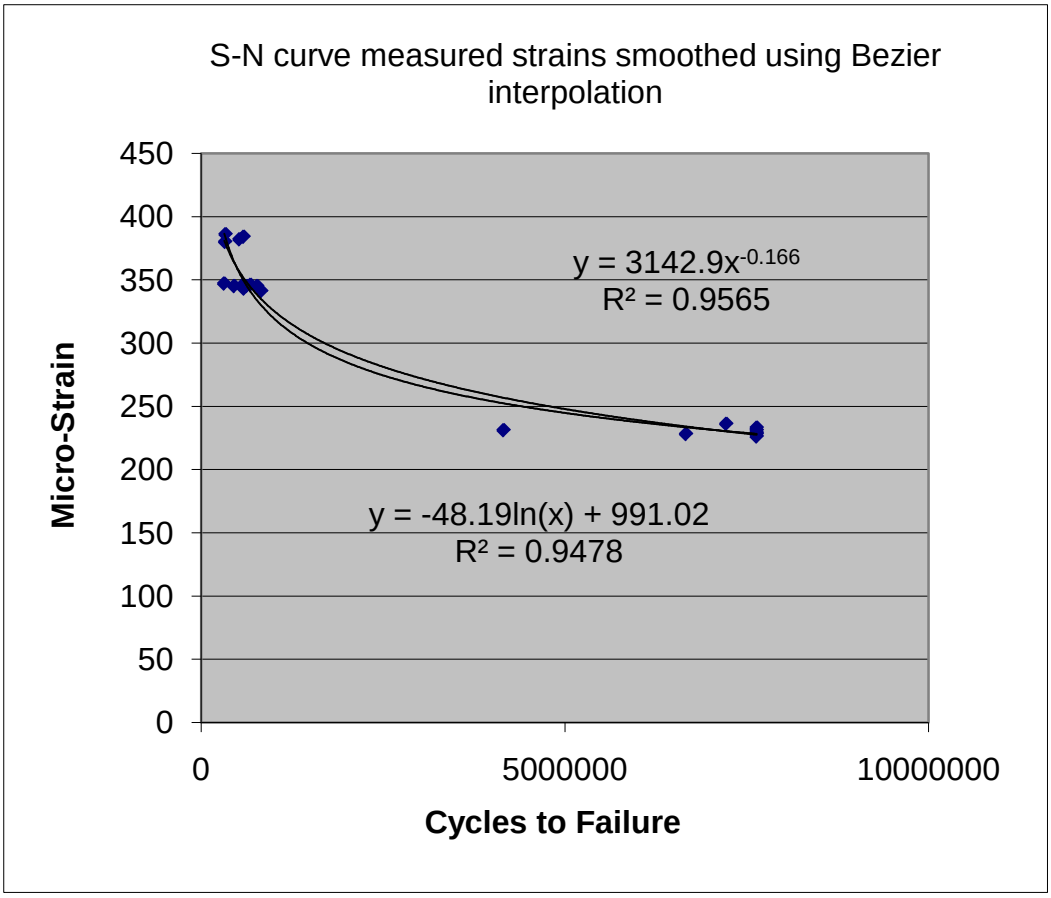

Figure 3.33 S-N curves using Bezier smoothed strains to the 20 BGA locations with logarithmic and power curve fits for 220 mils vibration input level and tin-lead solder

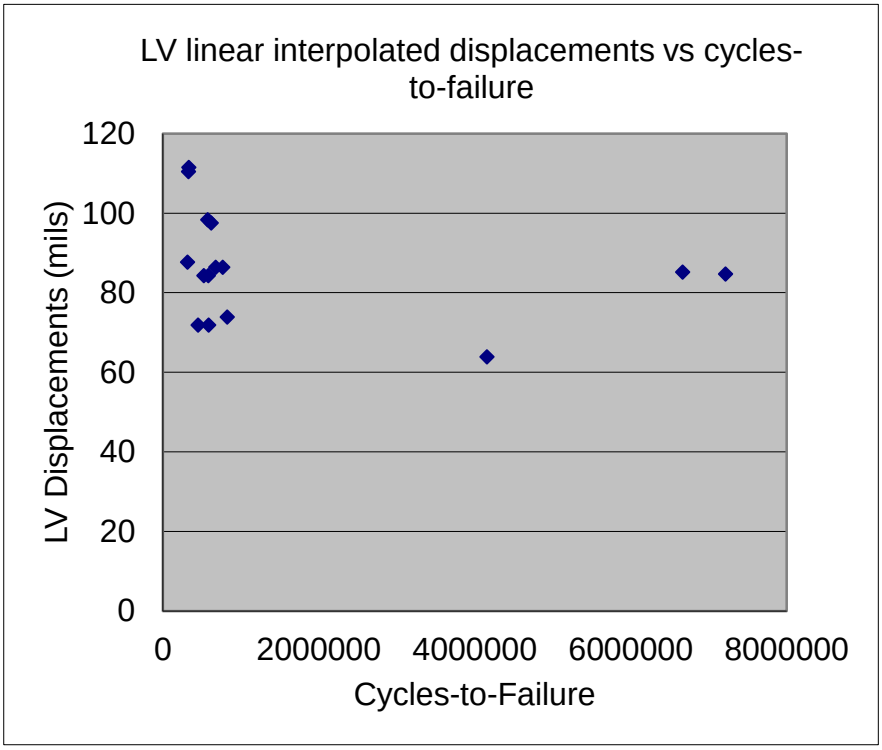

Figure 3.34 Laser Vibrometer measured displacements at the strain gauge locations and linearly interpolated to the 20 BGA locations for 220 mils tin-lead solder

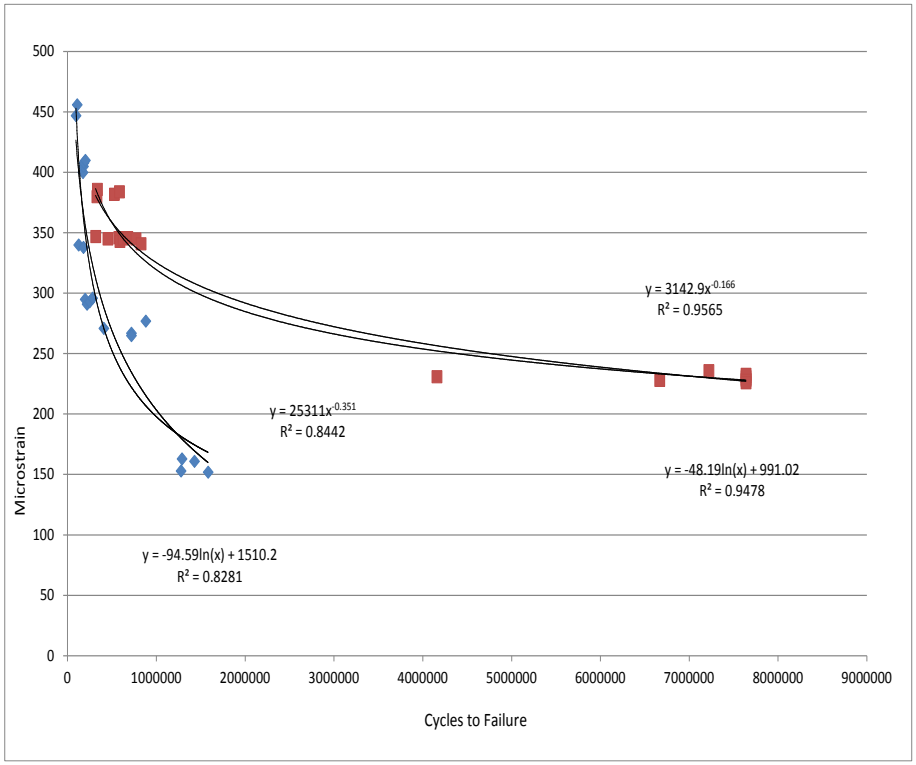

Figure 3.35 S-N logrithmic and power curves using Bezier smoothing for 220 mils and 260 mils vibration input levels for tin-lead solder

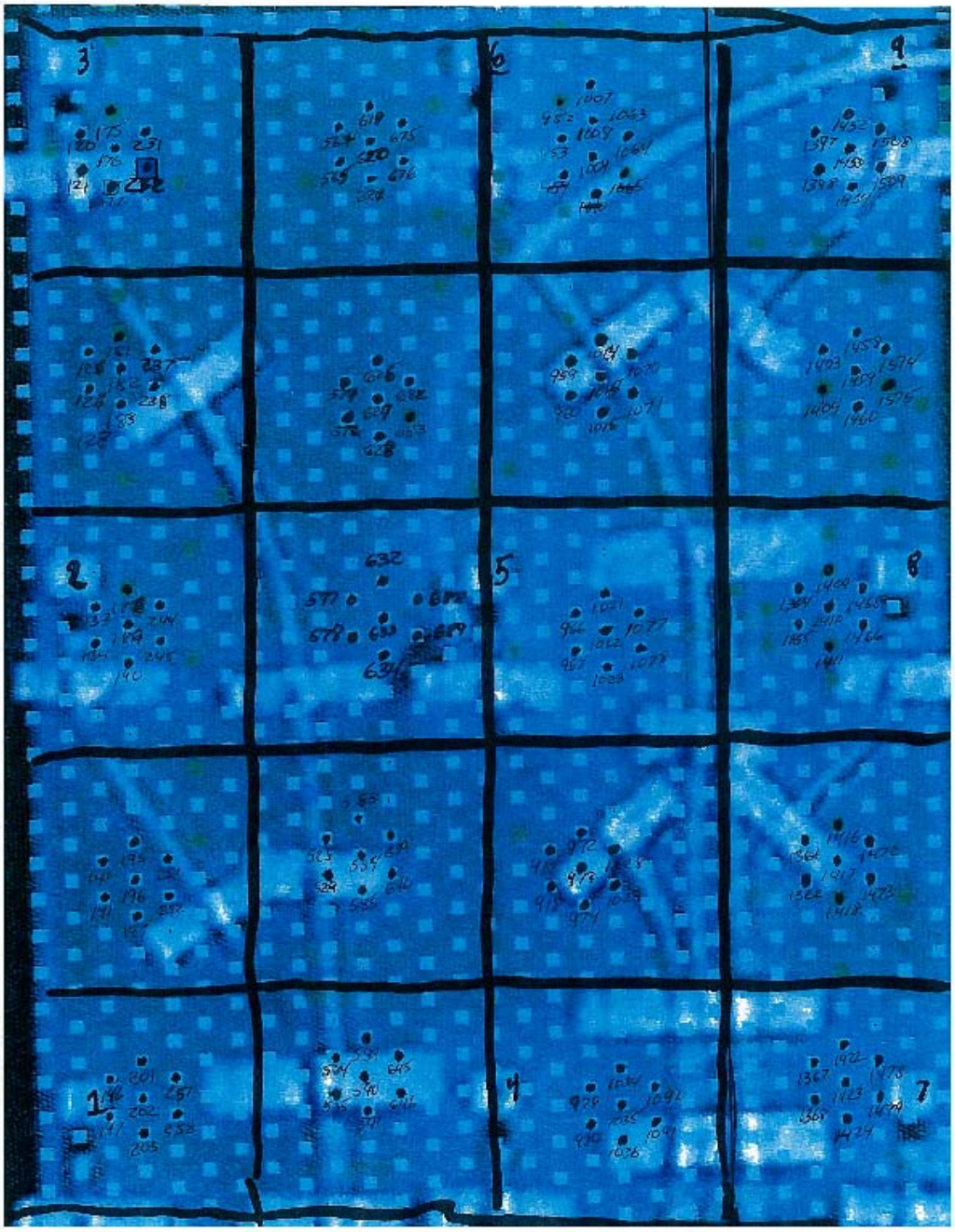

Figure 3.36 Seven displacement laser points per BGA for their 20 locations measured on the reverse side of the components

Table 3.31 Peak displacements for 220 mils at the dot locator numbers.

220 Mils Pk-Pk Scan

	Dot Locator #'s	Milli Meters	Mils	Dot Locator #'s	Milli Meters	Mils		Dot Locator #'s	Milli Meters	Mils	Dot Locator #'s	Milli Meters	Mils	
	120	1.845	72.64	564	1.321	52.008		952	1.413	55.63	1397	0.81	31.8897	
Strain Gauge 3	121	1.814	71.42	565	1.417	55.787	**Strain Gauge 6**	953	1.46	57.48	1398	0.957	37.6771	**Strain Gauge 9**
	175	1.534	60.39	619	1.12	44.094		1007	1.296	51.024	1452	0.847	33.3464	
	176	1.626	64.02	620	1.265	49.803		1008	1.365	53.74	1453	1.047	41.2204	
	177	1.911	75.24	621	1.559	61.378		1009	1.409	55.472	1454	1.262	49.6849	
	231	1.15	45.28	675	1.135	44.685		1063	1.222	48.11	1508	1.107	43.5826	
	232	1.449	57.05	676	1.488	58.583		1064	1.377	54.212	1509	1.377	54.2125	
	126	2.181	85.87	571	2.2	86.614		959	2.035	80.118	1403	1.205	47.4409	
	127	2.303	90.67	572	2.235	87.992		960	2.009	79.094	1404	1.062	41.8109	
	181	2.01	79.13	626	2.011	79.173		1014	2.261	89.016	1458	1.387	54.6062	
	182	2.032	80	627	2.167	85.315		1015	2.16	85.039	1459	1.333	52.4802	
	183	2.113	83.19	628	2.291	90.197		1016	2.304	90.708	1460	1.211	47.6771	
	237	1.884	74.17	682	1.905	75		1070	2.286	90	1514	1.68	66.1416	
	238	1.836	72.28	683	2.01	79.134		1071	2.219	87.362	1515	1.522	59.9211	
	133	2.875	113.2	577	2.931	115.39		966	2.738	107.8	1354	2.368	93.2282	
	134	2.881	113.4	578	2.92	114.96		967	2.766	108.9	1355	1.877	73.8975	
Strain Gauge 2	188	2.712	106.8	632	2.847	112.09	**Strain Gauge 5**	1021	2.857	112.48	1409	2.54	99.9998	**Strain Gauge 8**
	189	2.581	101.6	633	2.913	114.68		1022	2.963	116.65	1410	2.215	87.2046	
	190	2.441	96.1	634	2.888	113.7		1023	2.878	113.31	1411	1.772	69.7636	
	244	2.339	92.09	688	2.694	106.06		1077	2.928	115.28	1465	2.727	107.362	
	245	1.978	77.87	689	2.701	106.34		1078	2.948	116.06	1466	2.369	93.2675	
	140	2.547	100.3	528	2.78	109.45		917	2.568	101.1	1361	2.376	93.5431	
	141	2.604	102.5	529	2.678	105.43		918	2.777	109.33	1362	2.588	101.89	
	195	2.421	95.31	583	2.707	106.57		972	2.585	101.77	1416	1.956	77.0077	
	196	2.354	92.68	584	2.701	106.34		973	2.79	109.84	1417	2.523	99.3305	
	197	2.429	95.63	585	2.626	103.39		974	2.748	108.19	1418	2.346	92.362	
	251	2.041	80.35	639	2.677	105.39		1028	2.792	109.92	1472	2.294	90.3148	
	252	2.081	81.93	640	2.632	103.62		1029	2.752	108.35	1473	2.623	103.268	
	146	2.288	90.08	534	2.392	94.173		979	2.302	90.63	1367	2.22	87.4014	
	147	2.217	87.28	535	2.313	91.063		980	2.236	88.031	1368	2.064	81.2597	
	201	2.289	90.12	589	2.408	94.803		1034	2.425	95.472	1422	2.144	84.4093	
	202	2.284	89.92	590	2.338	92.047		1035	2.311	90.984	1423	1.87	73.6219	
Strain Guage 1	203	2.203	86.73	591	2.272	89.449	**Strain Gauge 4**	1036	2.231	87.834	1424	1.938	76.2991	**Strain Gauge 7**
	257	2.344	92.28	645	2.369	93.268		1090	2.351	92.559	1478	2.008	79.055	
	258	2.335	91.93	646	2.304	90.708		1091	2.241	88.228	1479	1.864	73.3857	

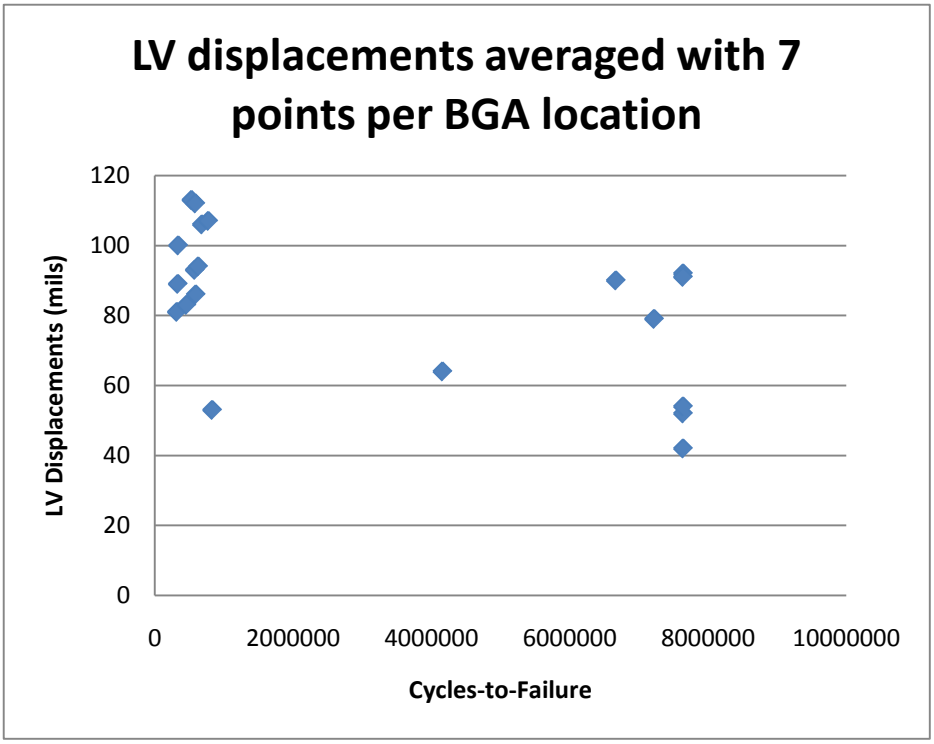

Figure 3.37 Laser Vibrometer displacements vs cycles-to-failure at each of the BGA locations each point averaged using 7 laser measurement points for 220 mils vibration level and tin-lead solder joints

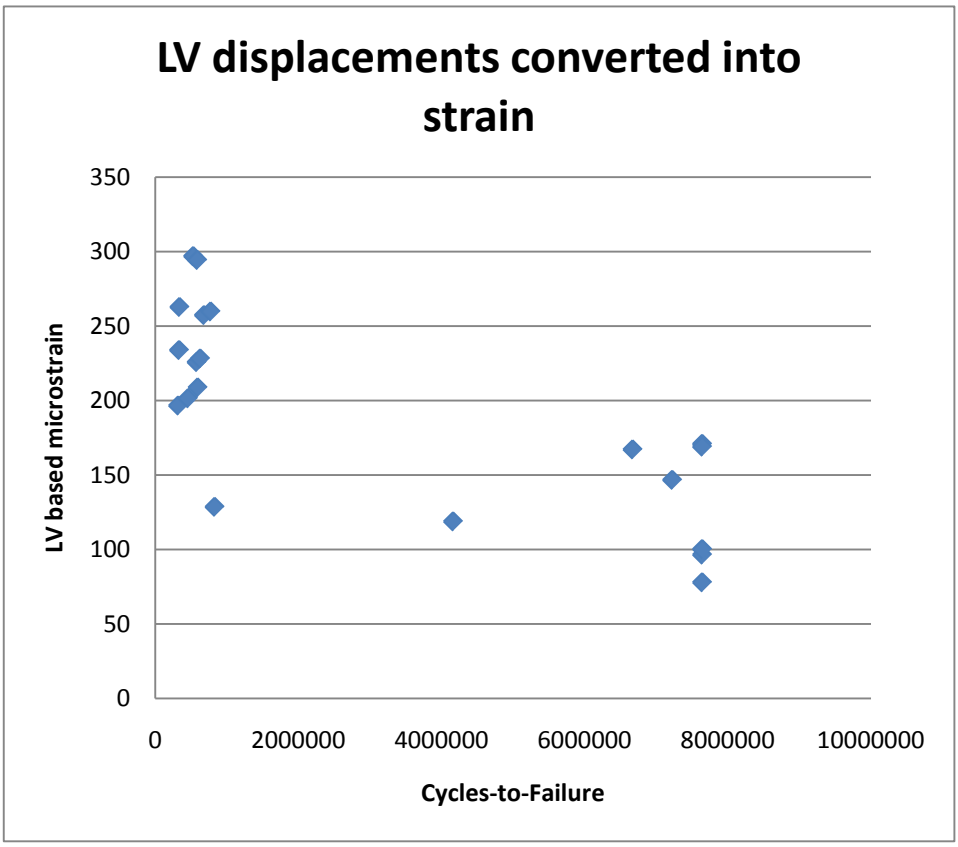

Figure 3.38 S-N curves based on transforming Laser Vibrometer displacements at each of the BGA locations each point averaged using 7 laser measurement points for 220 mils vibration level and tin-lead solder joints

Table 3.32 Peak displacements for 260 mils at the dot locator numbers

260 Mils Pk-Pk Scan

	Dot Locator #'s	Milli Meters		Dot Locator #'s	Milli Meters			Dot Locator #'s	Milli Meters		Dot Locator #'s	Milli Meters		
	120	1.314	51.73	564	1.859	73.189		952	1.892	74.488	1397	1.054	41.496	
Strain Gauge 3	121	1.4	55.12	565	1.897	74.685	**Strain Gauge 6**	953	1.599	62.953	1398	1.26	49.6062	**Strain Gauge 9**
	175	1.42	55.91	619	1.568	61.732		1007	1.534	60.394	1452	0.92	36.2204	
	176	1.251	49.25	620	1.634	64.331		1008	1.544	60.787	1453	1.193	46.9684	
	177	1.52	59.84	621	1.733	68.228		1009	1.566	61.653	1454	1.397	54.9999	
	231	1.282	50.47	675	1.424	56.063		1063	1.538	60.551	1508	1	39.37	
	232	1.385	54.53	676	1.722	67.795		1064	1.612	63.464	1509	1.382	54.4093	
	126	1.558	61.34	571	2.541	100.04		959	1.853	72.953	1403	2.207	86.8896	
	127	1.826	71.89	572	2.712	106.77		960	2.313	91.063	1404	2.325	91.5353	
	181	1.636	64.41	626	2.337	92.008		1014	2.181	85.866	1458	1.272	50.0786	
	182	1.898	74.72	627	2.441	96.102		1015	2.39	94.094	1459	1.661	65.3936	
	183	1.989	78.31	628	2.451	96.496		1016	2.71	106.69	1460	1.892	74.488	
	237	1.936	76.22	682	2.231	87.834		1070	2.59	101.97	1514	1.052	41.4172	
	238	2.143	84.37	683	2.194	86.378		1071	2.692	105.98	1515	1.422	55.9841	
	133	2.709	106.7	577	3.342	131.57		966	2.916	114.8	1354	2.977	117.204	
	134	2.966	116.8	578	3.34	131.5		967	2.996	117.95	1355	2.328	91.6534	
Strain Gauge 2	188	1.939	76.34	632	3.346	131.73	**Strain Gauge 5**	1021	3.181	125.24	1409	2.503	98.5431	**Strain Gauge 8**
	189	2.346	92.36	633	3.381	133.11		1022	3.116	122.68	1410	2.456	96.6927	
	190	2.471	97.28	634	3.392	133.54		1023	3.269	128.7	1411	2.248	88.5038	
	244	1.846	72.68	688	3.237	127.44		1077	3.187	125.47	1465	2.441	96.1022	
	245	1.958	77.09	689	3.008	118.42		1078	3.177	125.08	1466	2.292	90.236	
	140	2.486	97.87	528	3.248	127.87		917	2.661	104.76	1361	3.327	130.984	
	141	3.004	118.3	529	3.157	124.29		918	2.796	110.08	1362	3.347	131.771	
	195	2.194	86.38	583	3.283	129.25		972	2.994	117.87	1416	2.43	95.6691	
	196	2.306	90.79	584	3.217	126.65		973	3.095	121.85	1417	3.095	121.85	
	197	2.54	100	585	3.102	122.13		974	3.034	119.45	1418	2.915	114.764	
	251	2.395	94.29	639	3.246	127.8		1028	3.285	129.33	1472	2.472	97.3226	
	252	2.366	93.15	640	3.195	125.79		1029	3.133	123.35	1473	2.579	101.535	
	146	2.591	102	534	2.799	110.2		979	2.771	109.09	1367	2.796	110.079	
	147	2.47	97.24	535	2.74	107.87		980	2.694	106.06	1368	2.657	104.606	
	201	2.626	103.4	589	2.834	111.57		1034	2.863	112.72	1422	2.898	114.094	
	202	2.562	100.9	590	2.793	109.96		1035	2.728	107.4	1423	2.765	108.858	
Strain Gauge 1	203	2.464	97.01	591	2.697	106.18	**Strain Gauge 4**	1036	2.627	103.42	1424	2.675	105.315	**Strain Gauge 7**
	257	2.612	102.8	645	2.829	111.38		1090	2.774	109.21	1478	2.887	113.661	
	258	2.606	102.6	646	2.772	109.13		1091	2.625	103.35	1479	2.757	108.543	

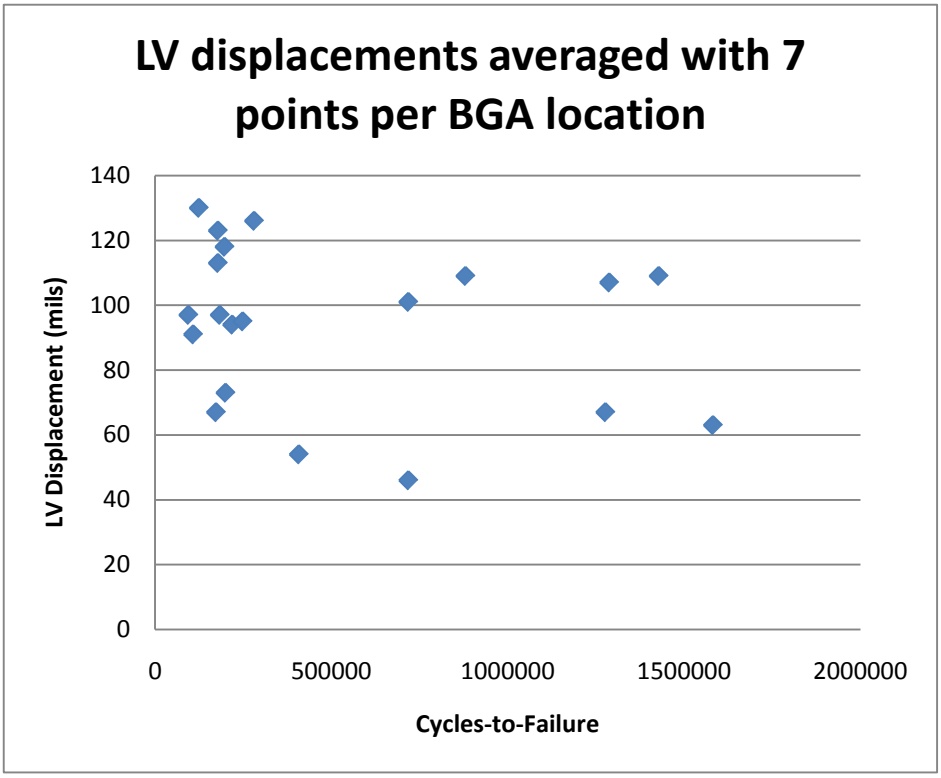

Figure 3.39 Laser vibrometer displacements vs cycles-to-failure at each of the BGA locations each point averaged using 7 laser measurement points for 260 mils vibration level and tin-lead solder joints

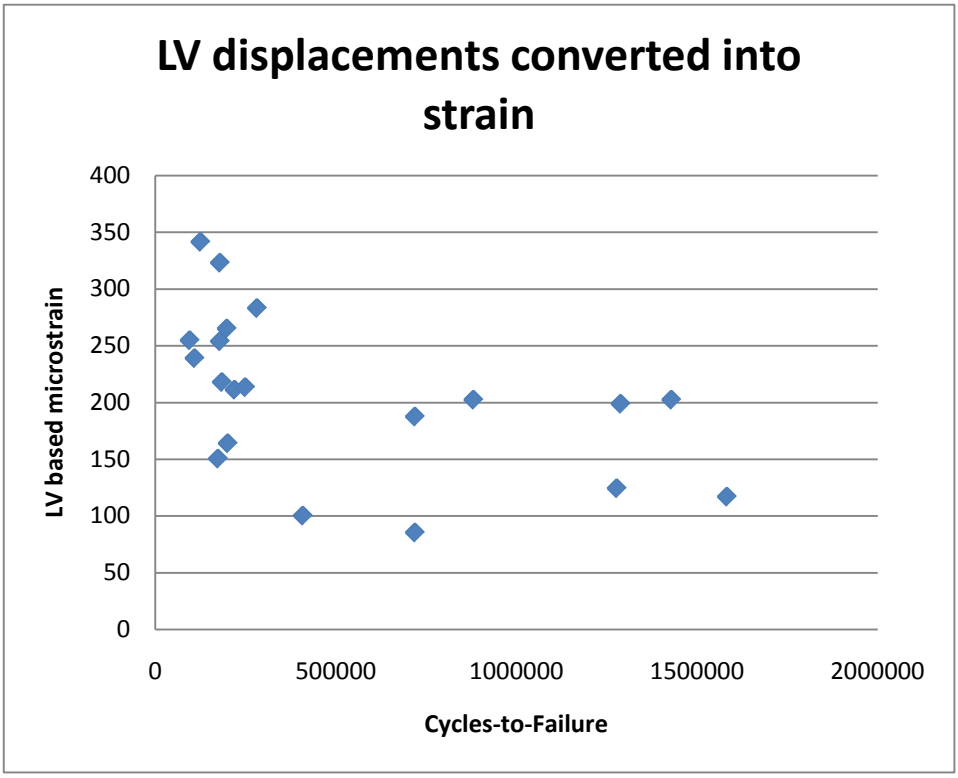

Figure 3.40 S-N curves based on transforming laser vibrometer displacements at each of the BGA locations each point averaged using 7 laser measurement points for 260 mils vibration level and tin-lead solder joints

Table 3.33 Summary results of using Laser Vibrometer based strains and strain gauges Bezier smoothing for both 220 mils and 260 mils vibration levels and tin-lead solder joints

	220 Mils P/P Scan			260 Mils P/P Scan		
BGA location	LV Displ, mils	LV micro-strain	Bezier micro-strain	LV Displ, mils	LV micro-strain	Bezier micro-strain
1	90	167.22	228	101	187.658	267
2	93	225.804	346	97	218.056	408
3	100	262.8	386	91	239.148	456
4	81	196.668	347	73	164.104	410
5	64	118.912	231	54	100.332	271
6	92	170.936	231	109	202.522	161
7	106	257.368	346	126	283.248	296
8	112	294.336	384	130	341.64	340
9	83	201.524	345	95	213.56	293
10	52	96.616	229	67	124.486	153
11	91	169.078	233	107	198.806	163
12	107	259.796	345	118	265.264	295
13	113	296.964	382	123	323.244	338
14	86	208.808	343	94	211.312	291
15	54	100.332	228	63	117.054	152
16	79	146.782	236	109	202.522	277
17	94	228.232	345	113	254.024	405
18	89	233.892	380	97	254.916	447
19	53	128.684	341	67	150.616	400
20	42	78.036	226	46	85.468	265

Table 3.34 220 mils failure times and their measured LV displacements and strains including Bezier smoothed strains

Fail time	PCB chip location	Bezier-micro strain	Bezier displacement, mils	Steinberg equation: N, cycles to failure
315900	4	347	142.91	1884
329400	18	380	144.59	1310
334800	3	386	146.87	1231
453600	9	345	142.09	1928
526500	13	382	145.35	1283
575100	2	346	142.50	1906
583200	8	384	146.11	1256
588600	14	343	141.26	1974
623700	17	345	142.09	1928
677700	7	346	142.50	1906
769500	12	345	142.09	1928
826200	19	341	140.44	2020
4158000	5	231	124.30	9594
6666300	1	228	122.69	10109
7219800	16	236	126.99	8806
S7638300	6	231	124.30	9594
S7638300	10	229	123.23	9933
S7638300	11	233	125.38	9268
S7638300	15	228	122.69	10109
S7638300	20	226	121.61	10471

Table 3.35 260 mils failure times and their measured LV displacements and strains including Bezier smoothed strains

Fail time	PCB chip location	Bezier-micro strain	Bezier displacement, mils	Steinberg equation: N, cycles to failure
94500	18	447	170.08	684
108000	3	456	173.51	632
124200	8	340	129.37	2044
172800	19	400	164.74	1067
178200	13	338	128.61	2093
178200	17	405	166.80	1015
183600	2	408	168.03	986
197100	12	295	121.49	3607
199800	4	410	168.85	967
218700	14	291	119.85	3809
248400	9	293	120.67	3706
280800	7	296	121.90	3558
407700	5	271	145.83	5065
718200	1	267	143.68	5375
718200	20	265	142.60	5539
880200	16	277	149.06	4640
1277100	10	153	82.33	49850
1287900	11	163	87.71	38697
1428300	6	161	86.64	40656
1582200	15	152	81.79	51175

Chapter 4

AVIONICS LINE REPLACEABLE UNIT MODELING AND ACCELERATED LIFE TESTING COMPARISON RESULTS BETWEEN TIN-LEAD AND LEAD-FREE SOLDER INTERCONNECTS UNDER VIBRATION

4.1 Introduction

The goal of this phase of the research is to develop and illustrate a methodology for comparing the vibration performance of avionics products made with tin-lead (the baseline) and lead-free solder. Another goal is to rationally assess how to accelerate qualification testing because of how long testing needs to be to precipitate failures, but vibration levels cannot be so high that other modes of failure occur.

An aircraft line removable unit (LRU) is selected as a candidate for testing and is a graphics generating computer. Two GG LRU computers with four circuit card assemblies (CCAs) each are tested one made with tin-lead solder the second with a lead-free 96.5%Sn 3.0%Ag 0.5%Cu (SAC305) solder alloy with the failure results shown in Tables 4.2 tin-lead solder LRU and Table 4.7 lead-free solder LRU. The first test was to a tin-lead configuration to qualification vibration levels with a power spectral density (PSD) level of 0.004 g^2/Hz at the resonance of the circuit boards between 63.5 Hz to 73.2 Hz with no failures after running 20 qualification cycles at 5 hours per three axis. The PSD level was then increased to 0.04 g^2/Hz and between 2 hours and 3 hours 17 minutes the first failure occurred in the graphics generator (GG) CCA due to a broken pin in the connector therefore the GG CCA was replaced and continued at the 0.04 g^2/Hz level. The

next failure due to fretting in the power supply connector after 3 hours 20 minutes and the connector was replaced before testing continued at 0.04 g^2/Hz. Testing continued for 1 minute 30 seconds and stopped because the new GG CCA had a component that needed thermal control.

Similarly, a LRU with a lead-free solder processor CCA has been tested beginning with the higher levels as the tin-lead LRU, but after precipitating power supply connector fretting errors and leaded component failures, the stress was stepped down to Qualification levels with no solder joint failures after 20 qualification cycles. This system level testing has shown that other faults are occurring before solder joint failures. The logic now is to compare qualification cycles of survival between LRUs. The challenge now is to transform the results of the step stress results of the systems level testing to perform a valid comparison.

In addition, the circuit cards of the LRU or the display electronics unit-II (DEU-II) tin-lead and lead-free were outfitted with strain gauges at the end of the test and all indications are that the lead-free designed cards are stiffer Figure 4.4 to Figure 4.11 versus Figure 4.12 to Figure 4.19. Both a finite element analysis and a commercially available code (CALCE PWA, 2011) are used to assess displacements to perform life calculations.

4.2 Literature Search

Boeing has recently published their recent finding for the Joint Committee on Aging Aircraft (Woodrow, 2006) showing card level tests. More work

continues led by NASA and DOD, and others (Starr, 2006), (CALCE, 2006), and (Woodrow, 2007) to build prediction models for systems based on coupon testing and do not consider repairable systems. No side-by-side product data exist for high performance systems in the literature with predictive models.

The current issues begin with how to relate the two products; also we are looking for ball grid array (BGA) failures, but instead have precipitated other failures which have been repaired in hopes of finding a BGA failure. Clearly these are repairable systems and the industry treats them as such and it would make sense to pursue comparisons of repairable system models. Rigdon, Ma, and Bodden (1998) and Wang, Kvam, and Lu (2007) discuss power law process of repairable systems, but does this make sense for small samples with very little failure history. Moving onto the issue of accelerated testing as evidenced by the step stress approach to precipitating failures (Tables 4.2 and 4.7), called partially accelerated life tests Wang, Cheng, and Lu (in press) develop a method for estimating the acceleration factor to a "qualification" level for a Weibull distribution, but here we have repairable systems. In addition, (Wang, Cheng, and Lu, in press), have large sample sizes and single component types.

System level vibration testing that precipitates other modes of failure like connector fretting, defective parts is done to put coupon testing in context like whether solder joint failures occur early or late in system tests when designing a black box. In real world commercial avionics applications black boxes see thermally induced failure in conjunction with vibration and for this reason all vibration testing is performed at laboratory room temperatures. Thermal modes

of failure are not considered part of the scope of this proposal. Software and electrical device design errors also affect system testing, but both these kinds of errors can be distinguished from failures due to vibration and not counted in the failure analysis.

4.3 Methodology

This section describes the LRU ALT methodology overview which begins by side-by-side tin-lead and lead-free SAC305 LRU test to failure at qualification and step-stress random vibration as discussed in Section 4.4. Finite element analysis (FEA) is performed on the LRU and a CALCE PWA analysis is also performed on the CCAs and with failure estimates. The strains measured in sections 4.5 and 4.6 are taken at the maximum strain locations found by the finite element analysis (FEA) and using the resulting FEA stiffness, stresses are calculated. In section 4.7, finite element displacements are calculated and in section 4.8, CALCE PWA (2011) software is used to also compute displacements. Ultimately, the data is used to calculate why tin-solder did not fail and the CALCE PWA code is conservative.

This section also describes how to calculate life given solder joint stress or displacements based on Steinberg (2000). Life using stress is calculated as follows and is called the cumulative damage index (CDI):

$$CDI = \sum_{i=1}^{3} \frac{n_i}{N_i} \tag{12}$$

where i = 1, 2, and 3 Sigma designators, and

n_i = (Frequency of CCA) x (total number of hours of three axis random vibration) x (3600 seconds/hour) x (1, 2, or 3-sigma probability factor) and also represents

the vibration condition for 1, 2, and 3-sigma stress levels applied to the CCA as a function of the CCA frequency using stresses found by multiplying the strains by the stiffness of the circuit board.

Calculating the CDI denominators, the N_i represent the 1, 2, and 3 Sigma levels of rms stress and are computed using the following equation

$$N_i = N\,(S/S_i)^4 \tag{13}$$

where $N = 20 \times 10^6$ cycles, and S is computed by an equation representing 3-sigma stresses for components expected to achieve a fatigue life of about 20 million stress reversals in a random vibration environment per the research published by Steinberg (2000) S_i = PWB rms stress responses from the measured strains.

Calculate life using displacements by

$$N_S = N\,(Z/Z_S)^4 \tag{14}$$

Where N = 10,000,000 cycles and

$$Z = (0.00022B)/(Chr\sqrt{l}) \tag{15}$$

Where Z is the maximum desired PCB displacement and Z_S is the rms displacement,

B = length of PWB edge parallel to component (in.),
l = length of electronic component (in.),
h = thickness of PWB (in.), all DEU-II PWBs are 0.090 inches thick.
C = constant for different types of electronic components,
= 1.75 for a BGA,
r = relative position factor for component on PWB,
= 1.0 when component is at top center of PWB.

4.4 Description of the DEU-II system and testing

The DEU-II LRU shown in its vibration fixture, Figure 4.1 includes an ARINC Specification 600-13 based design chassis rack interconnect circuit board with circuit cards installed: two I/O CCAs, one graphics card (GG) CCA, a power supply CCA, and one processor CCA. The life tests compared two versions of the DEU-II LRUs: one with tin-lead eutectic solder and the other with a lead-free solder alloy SAC305, but repairs to the lead-free CCAs used 96.6%Sn 3.0%Ag 0.4%Cu (SAC304). The weights of the circuit cards are tabulated in Table 4.1 showing that the lead-free LRUs are lighter. Only the I/O CCA in slot A5 is made with SAC305 solder for the lead-free LRU version; also slots A1 and A2 are in close physical proximity to each other as are slots A5 and A6. Slot A3 is unused. The weights in this table are used in subsequent analyses.

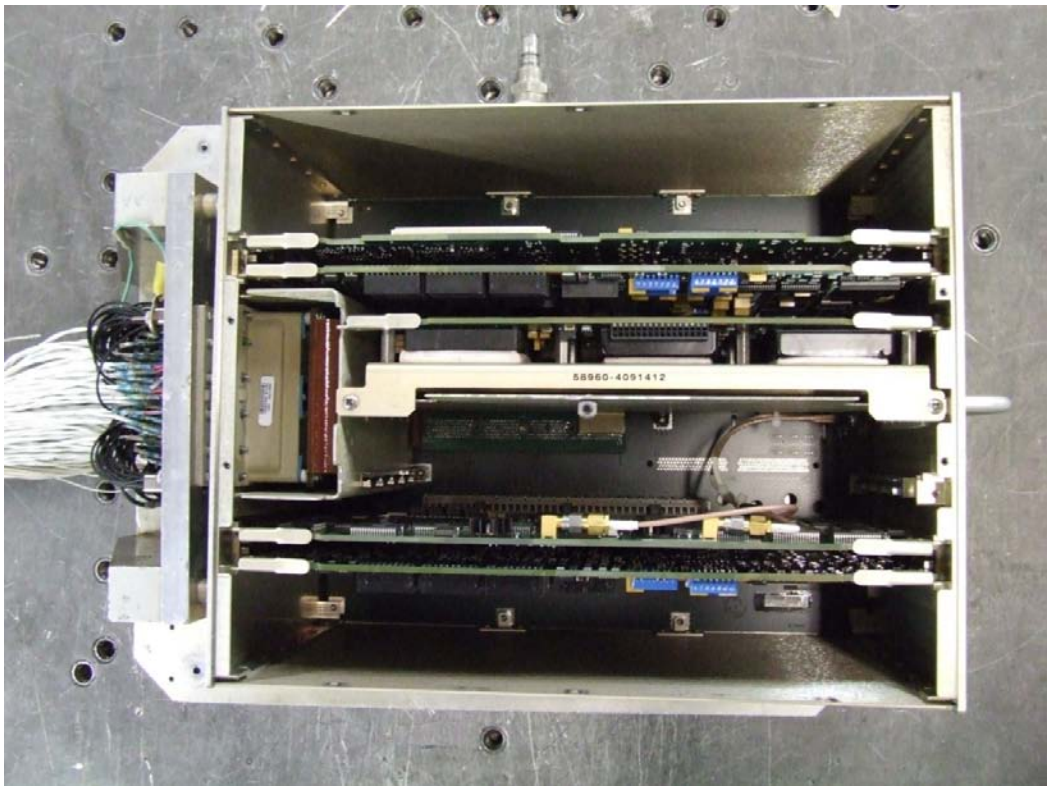

Figure 4.1 DEU-II circuit card set in the rack: starting from the bottom, I/O CCA (slot A1), GG CCA (slot A2), slot A3 is blank, PS CCA (slot A4), I/O CCA (slot A5), and Processor CCA (slot A6)

Table 4.1 Weights of DEU-II vibration test circuit cards for tin-lead and lead-free solder LRU test articles

Item & Location in LRU	Tin-Lead Solder Weight (lbs)	Lead-Free Solder Weight (lbs)
IO CCA Slot A1	1.2155	1.225 (tin-lead solder)
GG CCA Slot A2	1.1326	1.115
PS CCA Slot A4	2.5989	2.56
IO CCA Slot A5	1.2164	1.203
CPU CCA Slot A6	1.0621	1.048
Total LRU	15.681	15.492

The DEU-II Graphics Computer with four circuit test cards each were subjected to fatigue with one LRU made with tin-lead solder and the other with a lead-free tin-silver-copper (SAC) 305 alloy with failure results shown in Table 4.2 and Table 4.7 respectively. These tests were performed with real-time qualification software and hardware so that fault detection was continuous, although software coverage can never be 100 percent. In the photograph of the test installation in Figure 4.2, on the left side the computer screen shows "TEST IN PROGRESS" and the graphics displays driven through a cable assembly connected to the DEU-II which can be seen on the right side mounted in the vertical shaker axis. An accelerated test, or step stress curve, was used which raised the random vibration levels from 2.5 Grms to 8.0 Grms using the Unholtz-Dickie vibration shaker software to match the qualification signal acceleration power spectral density (PSD) levels until the PSD at resonance reaches 0.04 g^2/Hz as indicated in Figure 4.3.

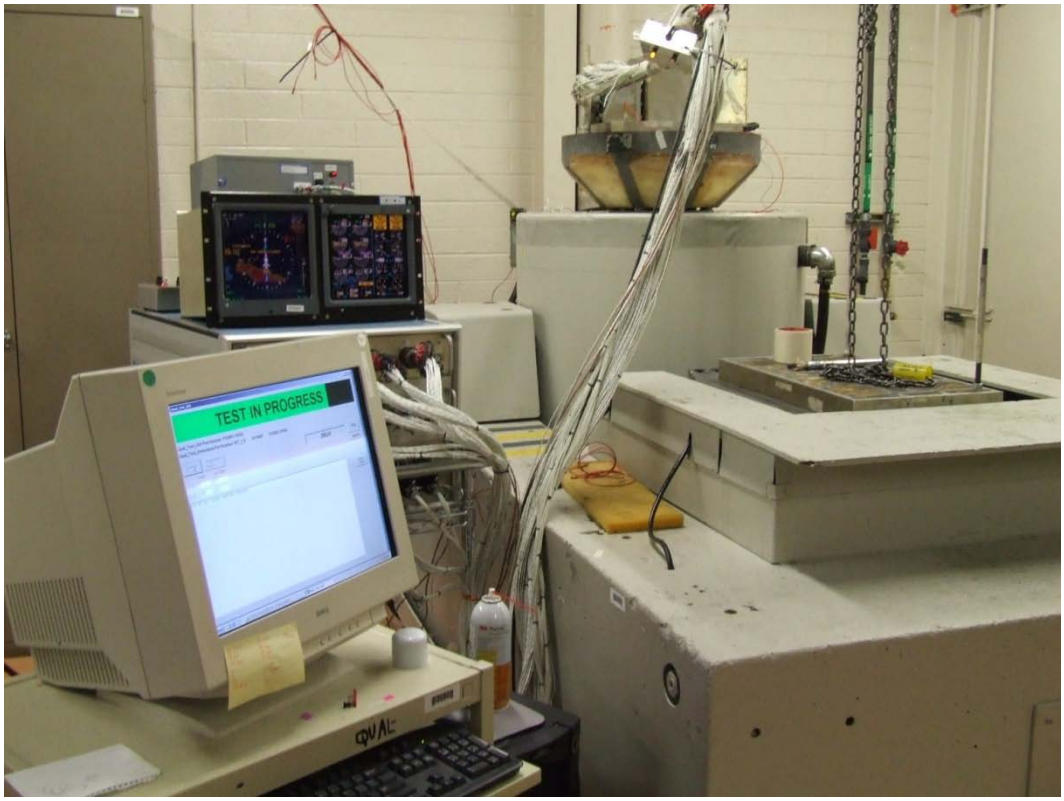

Figure 4.2 DEU-II functional testing using real-time qualification software

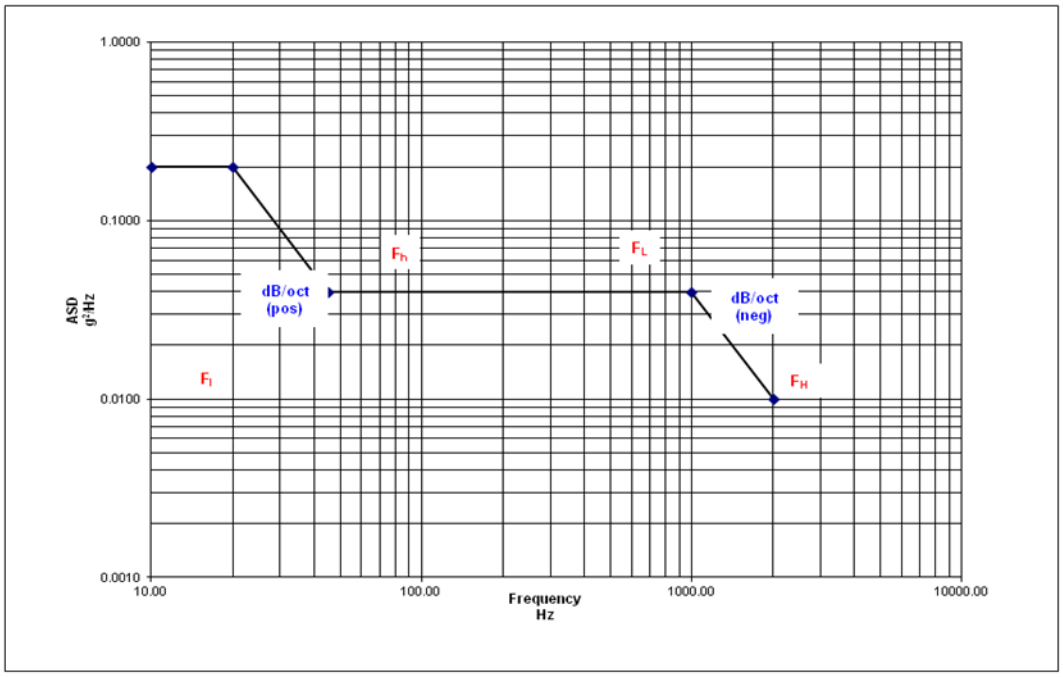

Figure 4.3 DEU-II random vibration test spectrum

4.5 DEU-II life testing for tin-lead solder connections

The first life test was a tin-lead solder configuration to qualification vibration levels (see the black-colored control curve in Figure 4.3) with a power spectral density of 0.004 g^2/Hz at the fundamental resonance of the circuit boards between 70 and 90 hertz. No failures were recorded after running 20 qualification cycles at 5 hours per three axes. These levels are also set using an industry standard equation proposed by Steinberg (2000, Chapters 8 and 9), but the equation proved to be too conservative. The PSD level was then increased to 0.04 g^2/Hz, and between 2 hours and 3 hours 17 minutes the first failure occurred in the graphics generator (GG) circuit card due to a broken pin in the connector. Therefore, the card was replaced and the test was continued with the input remaining at 0.04 g^2/Hz. The next failure occurred due to fretting in the power supply connector (refer to Figure below) after 3 hours 20 minutes. The connector was replaced and testing continued at 0.04 g^2/Hz. Testing continued for 1 minute 30 seconds and stopped because the new GG card had a component that needed thermal control.

Table 4.2 summarizes the tin-lead failures that occurred during the test, the cycles to failure were calculated by taking the resonant frequency and multiplying by 3,600 seconds/hour times the number of hours at that input level. At the conclusion of the test no failures had been observed that were attributable to a tin-lead solder joint.

Table 4.2 DEU-II LRU failure times for each axis of vibration with tin-lead solder connections for qualification and step stress input levels

Input PSD at Mode 1 Resonance (g^2/Hz)	Axis of Vibration	Time at Level (hr : min : sec)	Root Cause & Resolution
0.004	Vertical	100:00:00	No failures
0.004	Longitudinal	100:00:00	No failures
0.004	Lateral	100:00:00	No failures
0.04	Lateral	2:17:00 to 3:17:00	GG broken connector pin; replace card
0.04	Lateral	00:03:00	PS connector fretting; replace connector
0.04	Lateral	00:01:30	GG thermal control

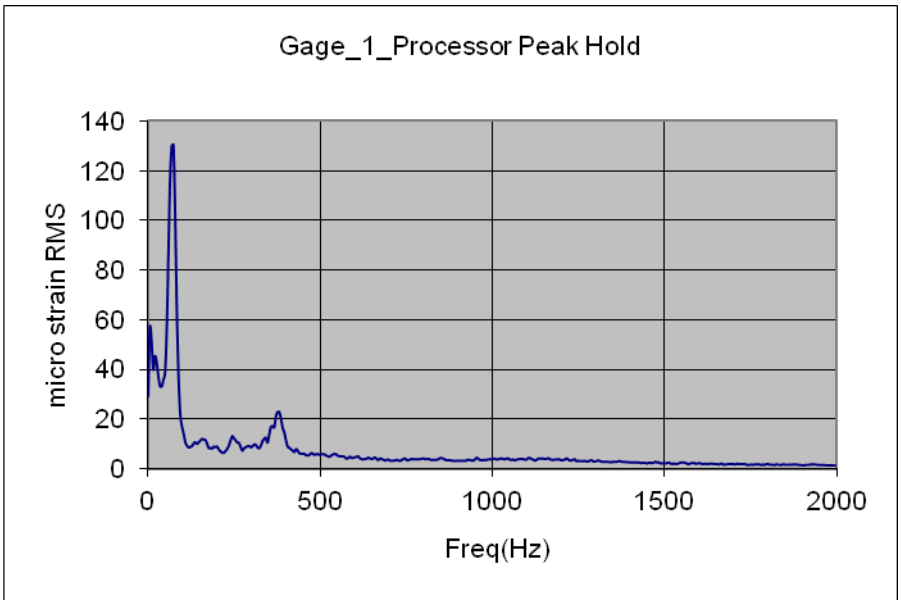

Figure 4.4 Tin-lead solder processor with 2.5 Grms input, maximum PCB strain response is 131 RMS micro strain at 73.2 hertz mode 1 frequency

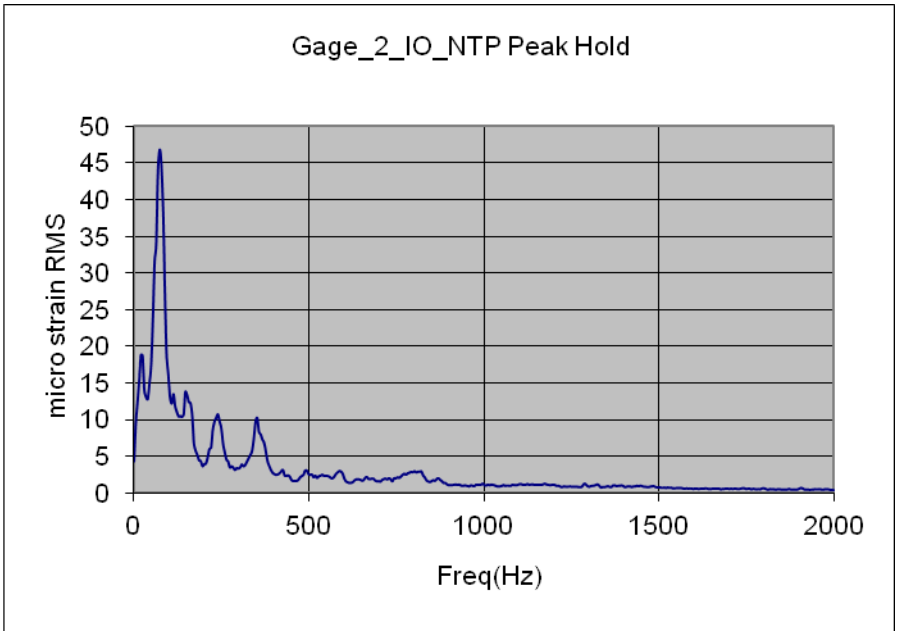

Figure 4.5 Tin-lead solder I/O next to processor with 2.5 Grms input, maximum PCB strain response is 46.8 RMS micro strain at 73.2 hertz mode 1 frequency

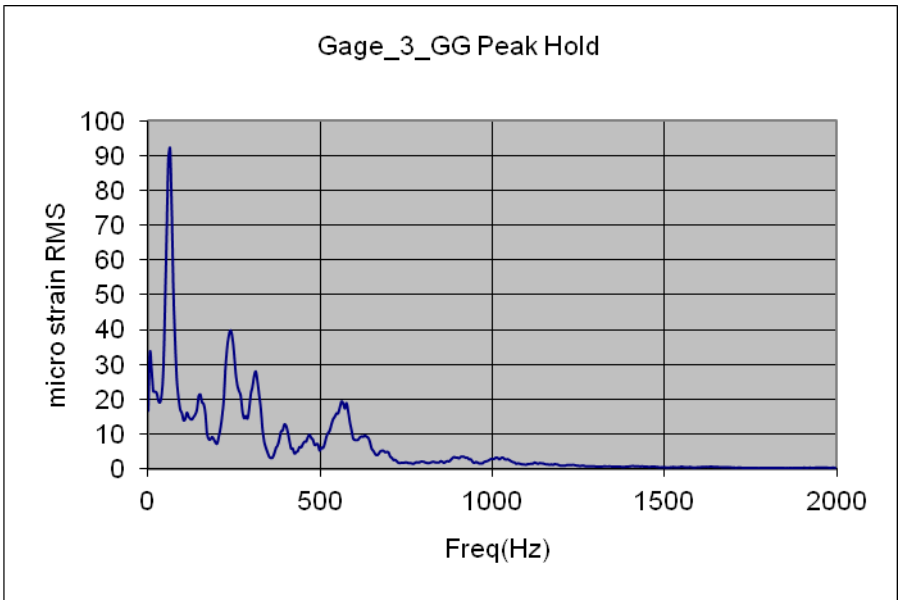

Figure 4.6 Tin-lead solder graphics generator with 2.5 Grms input, maximum PCB strain response is 92.3 RMS micro strain at 63.5 hertz mode 1 frequency

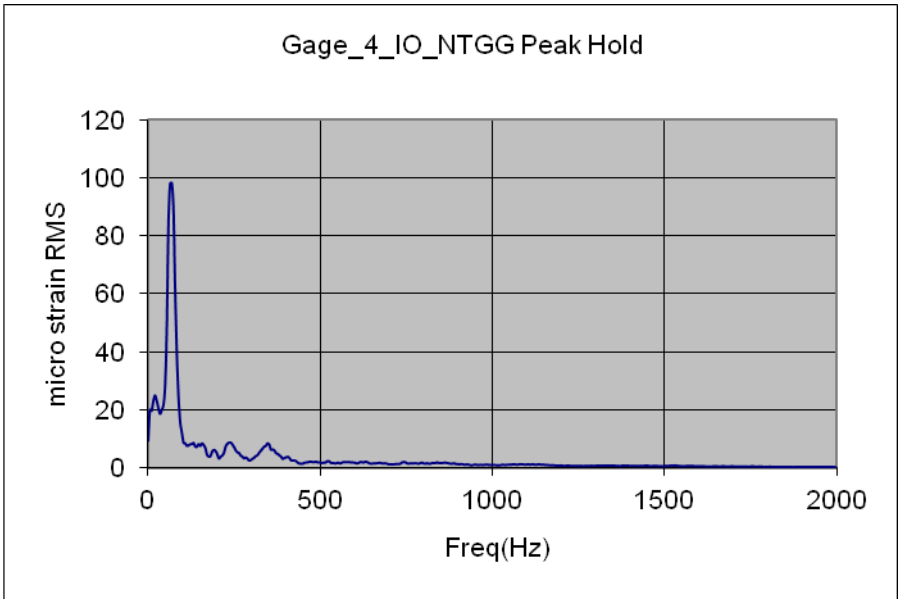

Figure 4.7 Tin-lead solder I/O next to graphics generator with 2.5 Grms input, maximum PCB strain response is 98.4 RMS micro strain at 68.4 hertz mode 1 frequency

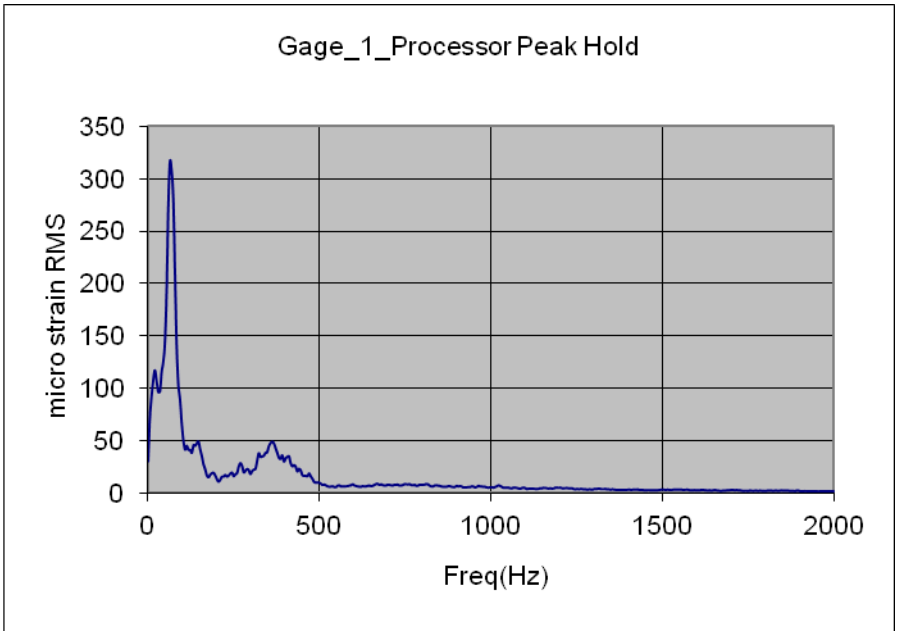

Figure 4.8 Tin-lead solder processor with 8.0 Grms input, maximum PCB strain response is 317 RMS micro strain at 63.5 hertz mode 1 frequency

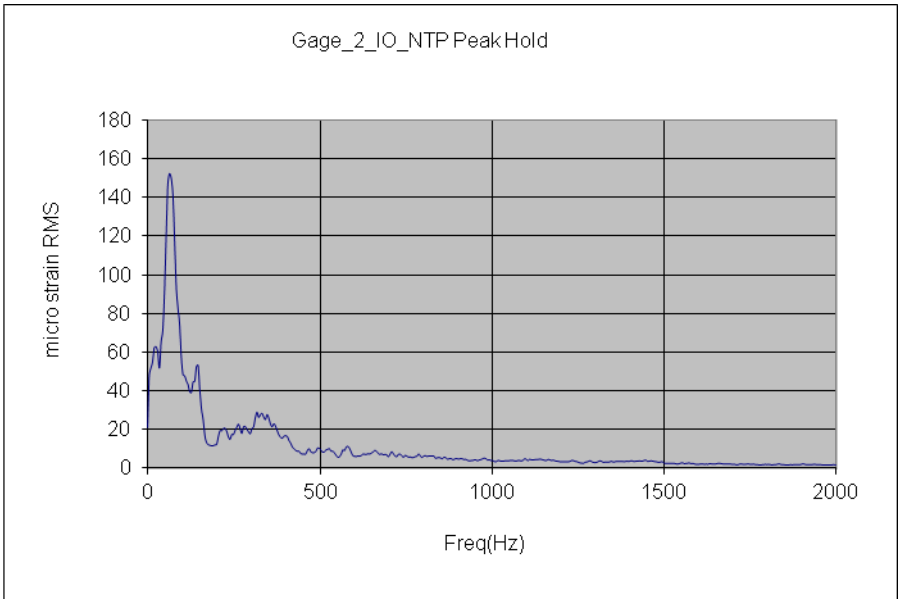

Figure 4.9 Tin-lead solder I/O next to processor with 8.0 Grms input, maximum PCB strain response is 153 RMS micro strain at 63.5 hertz mode 1 frequency

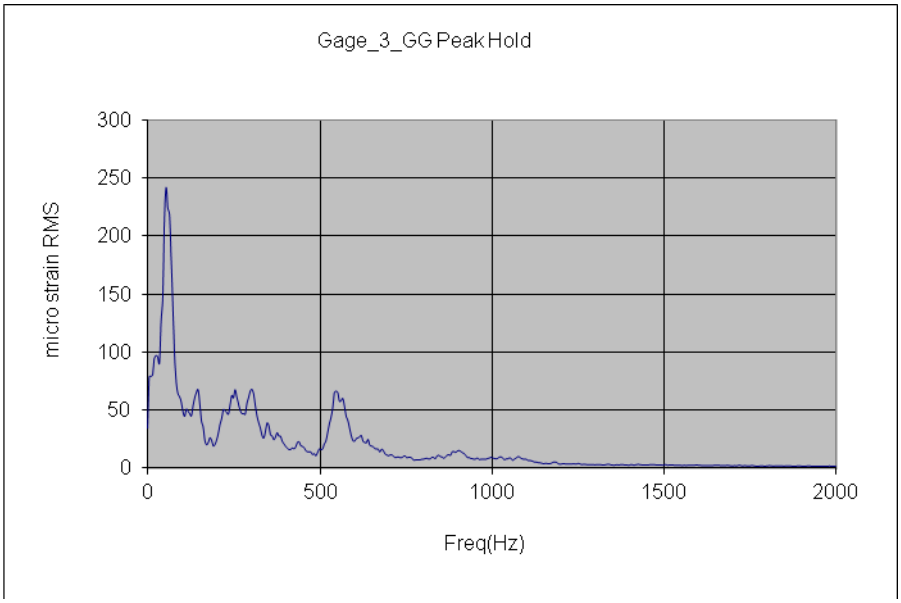

Figure 4.10 Tin-lead solder graphics generator with 8.0 Grms input, maximum PCB strain response is 242 RMS micro strain at 53.7 hertz mode 1 frequency

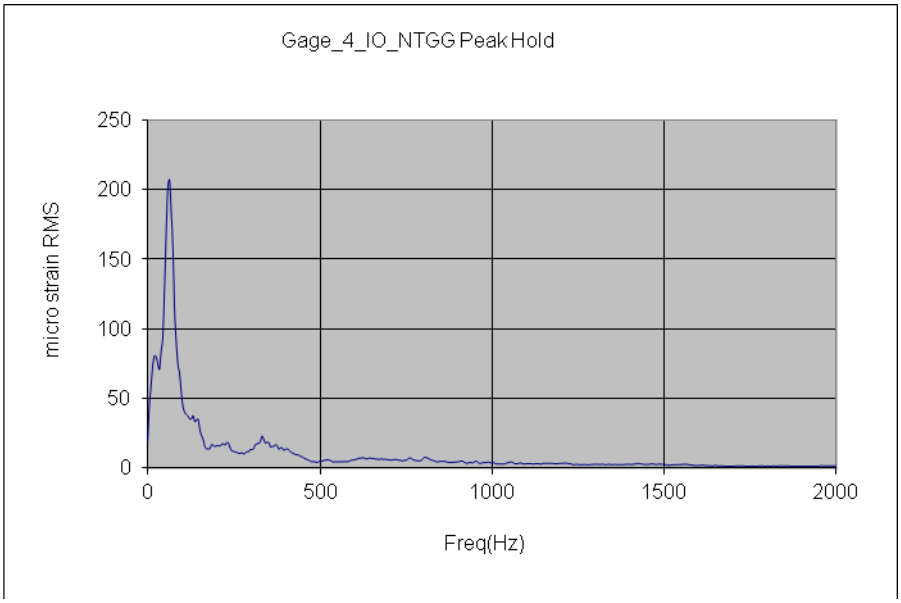

Figure 4.11 Tin-lead solder I/O next to graphics generator with 8.0 Grms input, maximum PCB strain response is 208 RMS micro strain at 63.5 hertz mode 1 frequency

Table 4.3 Processor cycles-to-failure and strains due to circuit card vibration with tin-lead solder connections

Input PSD at Mode 1 Resonance (g^2/Hz)	Mode 1 Frequency (Hz)	Time at Level (hr:min:sec)	Cycles-to-Failure	RMS Strain (micro strain)	Root Cause & Resolution
0.004	73.2	100:00:00	26,352,000	131	No failures
0.04	63.5	2:21:30 to 3:21:30	539,115 to 767,715	317	No failures

Table 4.4 I/O next to processor cycles-to-failure and strains due to circuit card vibration with tin-lead solder connections

Input PSD at Mode 1 Resonance (g^2/Hz)	Mode 1 Frequency (Hz)	Time at Level (hr:min:sec)	Cycles-to-Failure	RMS Strain (micro strain)	Root Cause & Resolution
0.004	73.2	100:00:00	26,352,000	46.8	No failures
0.04	63.5	2:21:30 to 3:21:30	539,115 to 767,715	153	No failures

Table 4.5 Graphics generator cycles-to-failure and strains due to circuit card vibration with tin-lead solder connections

Input PSD at Mode 1 Resonance (g^2/Hz)	Mode 1 Frequency (Hz)	Time at Level (hr:min:sec)	Cycles-to-Failure	RMS Strain (micro strain)	Root Cause & Resolution
0.004	63.5	100:00:00	22,860,000	92.3	No failures
0.04	53.7	2:17:00 to 3:17:00	441,414 to 634,734	242	GG broken connector pin; replace card
0.04	53.7	00:04:30	14,499	242	GG thermal control issues

Table 4.6 I/O next to graphics generator cycles-to-failure and strains due to circuit card vibration with tin-lead solder connections

Input PSD at Mode 1 Resonance (g^2/Hz)	Mode 1 Frequency (Hz)	Time at Level (hr:min:sec)	Cycles-to-Failure	RMS Strain (micro strain)	Root Cause & Resolution
0.004	68.4	100:00:00	24,624,000	98.4	No failures
0.04	63.5	2:21:30 to 3:21:30	539,115 to 767,715	208	No failures

4.6 DEU-II life testing for lead-free solder connections

Similarly, a lead-free LRU life test was conducted beginning with higher levels than the tin-lead LRU, but after precipitating power supply connector fretting errors and leaded component failures, the stress was stepped down to qualification levels with no solder joint failures after 20 qualification cycles. This system-level testing showed that other faults were occurring before failure of the solder joints occurred.

A summary of the failures observed in the lead-free circuit cards is shown in Table 4.7. Table 4.8 and Table 4.11 indicate no failures to those circuit cards. Table 4.9 is a failure due to lead failure and corroborated by accompanying photos, Figures 4.20 and 4.21. In Table 4.10 the only real lead-free solder joint failure occurred when a ferrite bead failed as shown in Figure 4.23.

Table 4.7 DEU-II LRU failure times for each axis of vibration with lead-free solder connections for qualification and step stress input levels

Input PSD at Mode 1 Resonance (g^2/Hz)	Axis of Vibration	Time at Level (hr:min:sec)	Root Cause & Resolution
0.04	Lateral	00:11:36	I/O next to Processor resistor package lead failure; replace (see Figure 4.20 & Figure 4.21)
0.04	Lateral	00:11:09	PS connector fretting; clean connector
0.04	Lateral	00:31:55	PS capacitor lead break; replace capacitor
0.04	Lateral	00:13:27	PS connector fretting; clean connector
0.004	Vertical	100:00:00	No failures
0.004	Longitudinal	100:00:00	No failures
0.004	Lateral	100:00:00	No failures
0.04	Lateral	00:09:56	PS connector fretting; replace PS
0.04	Lateral	00:05:38	MOBO PS connector fretting; new rack
0.04	Lateral	00:34:16	PS connector fretting; clean connector (see Figure 4.22)
0.04	Lateral	00:14:55	GG ferrite bead solder joint failure; replace choke (see Figure 4.23)
0.04	Lateral	00:17:47	PS intermittent failure

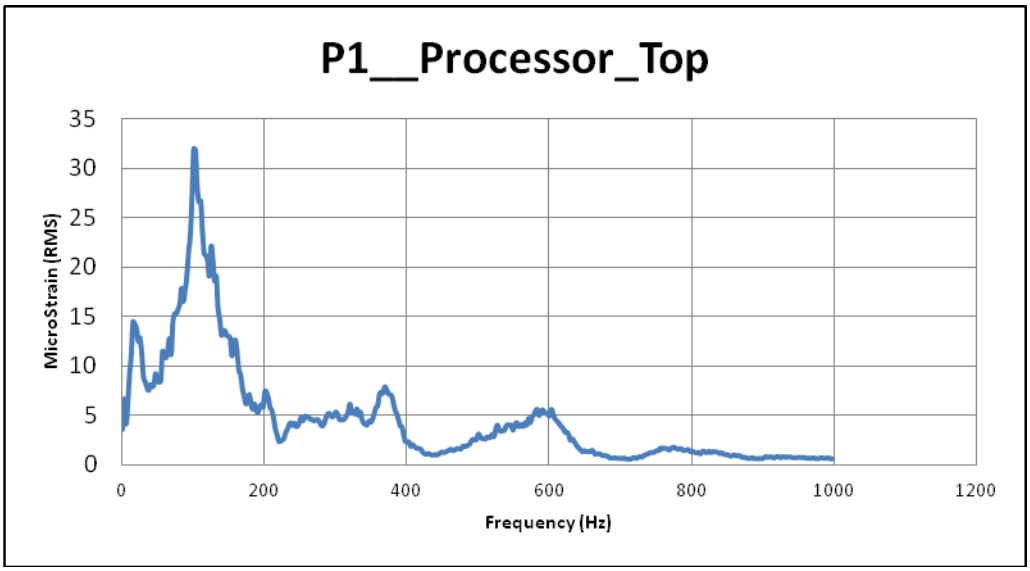

Figure 4.12 Lead-free solder processor with 2.5 Grms input, maximum PCB strain response is 32.0 RMS micro strain at 100 hertz mode 1 frequency

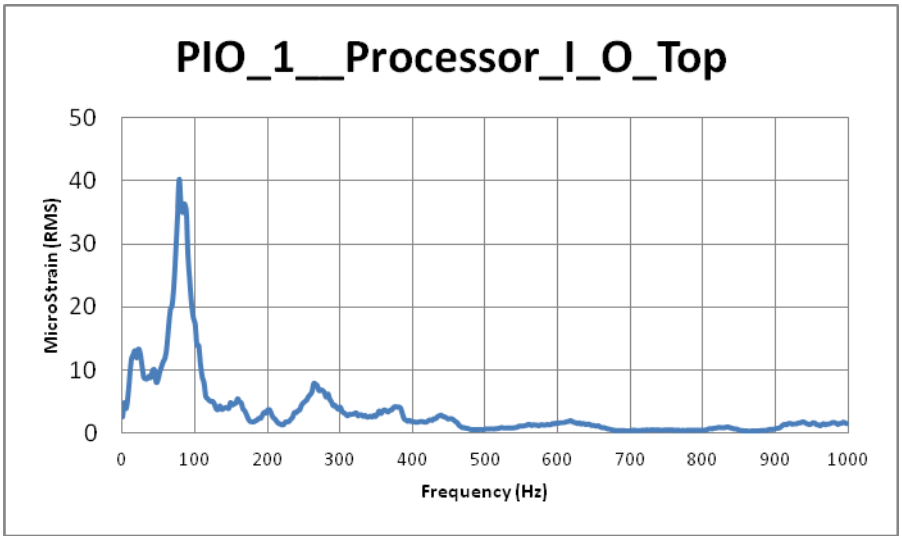

Figure 4.13 Lead free solder I/O next to processor with 2.5 Grms input, maximum PCB strain response is 40.3 RMS micro strain at 78.1 hertz mode 1 frequency

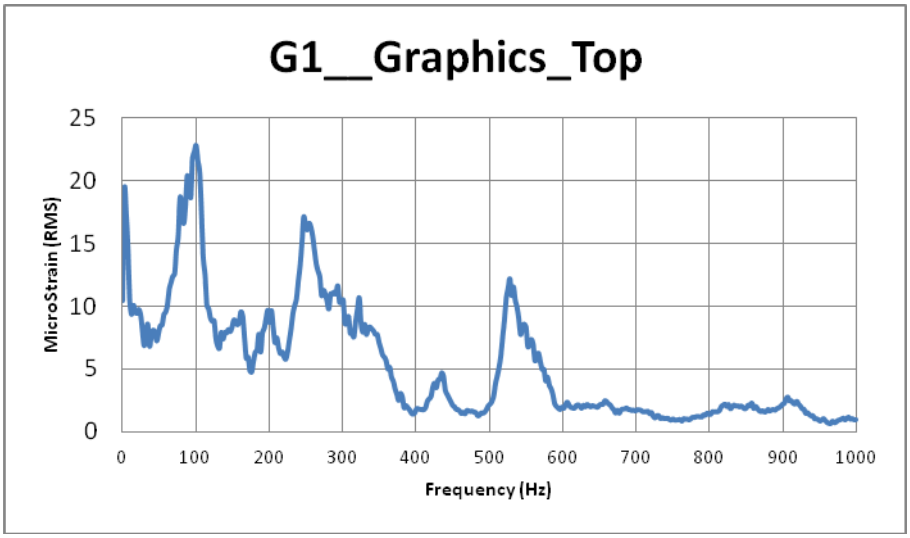

Figure 4.14 Lead-free solder graphics generator with 2.5 Grms input, maximum PCB strain response is 22.8 RMS micro strain at 100 hertz mode 1 frequency

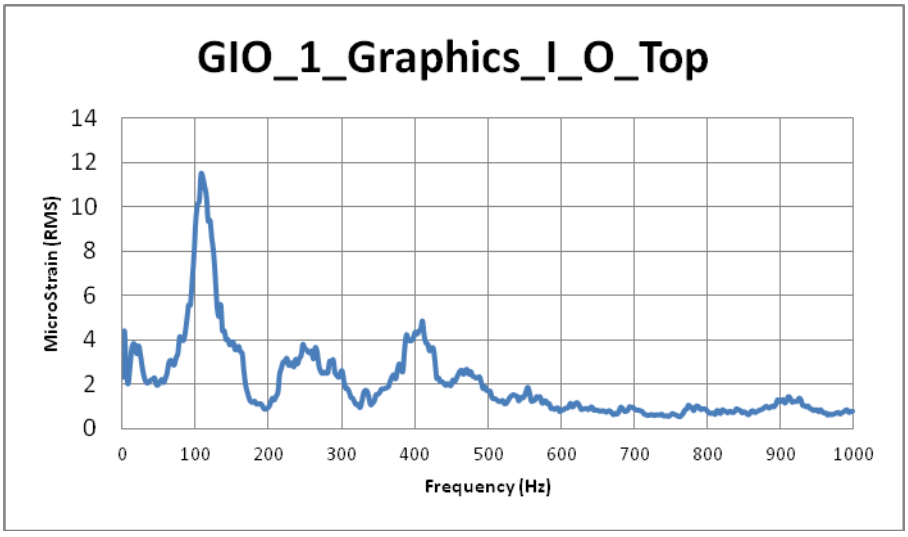

Figure 4.15 Tin-lead solder I/O next to graphics generator with 2.5 Grms input, maximum PCB strain response is 11.5 RMS micro strain at 107 hertz mode 1 frequency

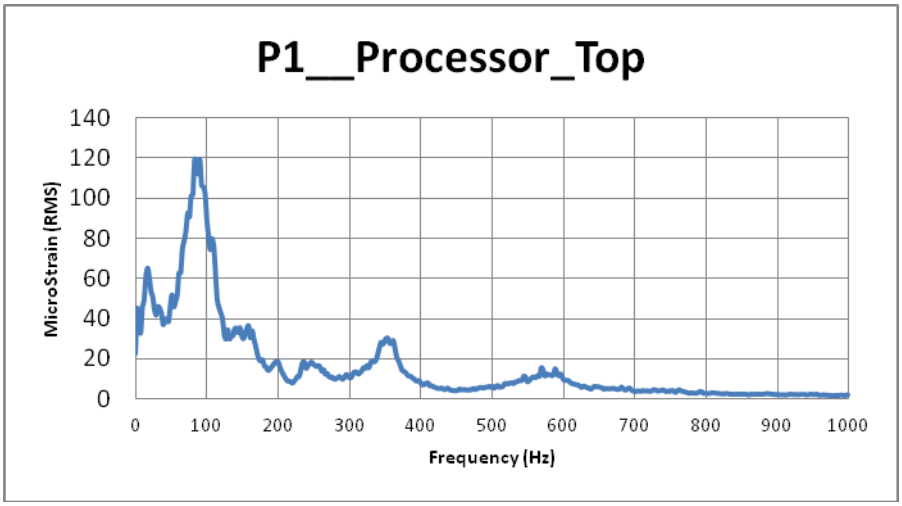

Figure 4.16 Lead-free solder processor with 8.0 Grms input, maximum PCB strain response is 119 RMS micro strain at 90.3 hertz mode 1 frequency

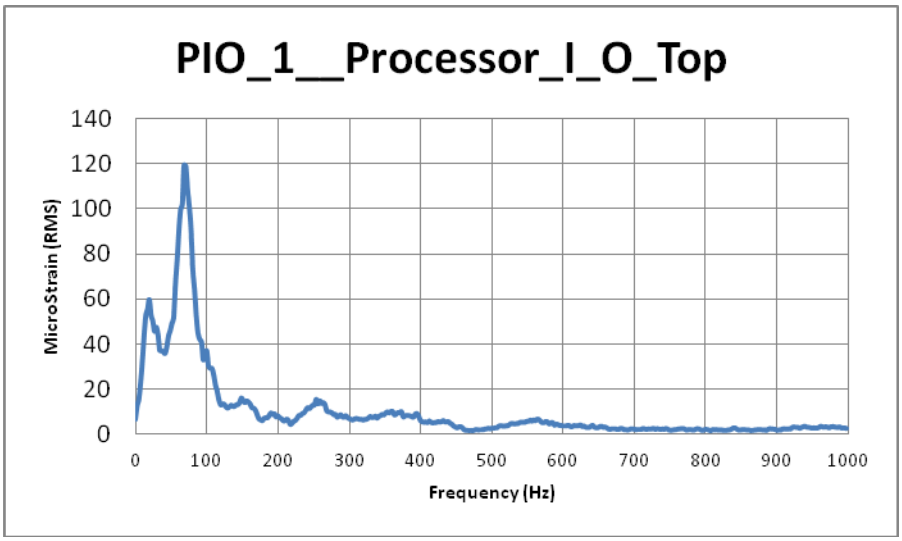

Figure 4.17 Lead-free solder I/O next to processor with 8.0 Grms input, maximum PCB strain response is 119 RMS micro strain at 68.3 hertz mode 1 frequency

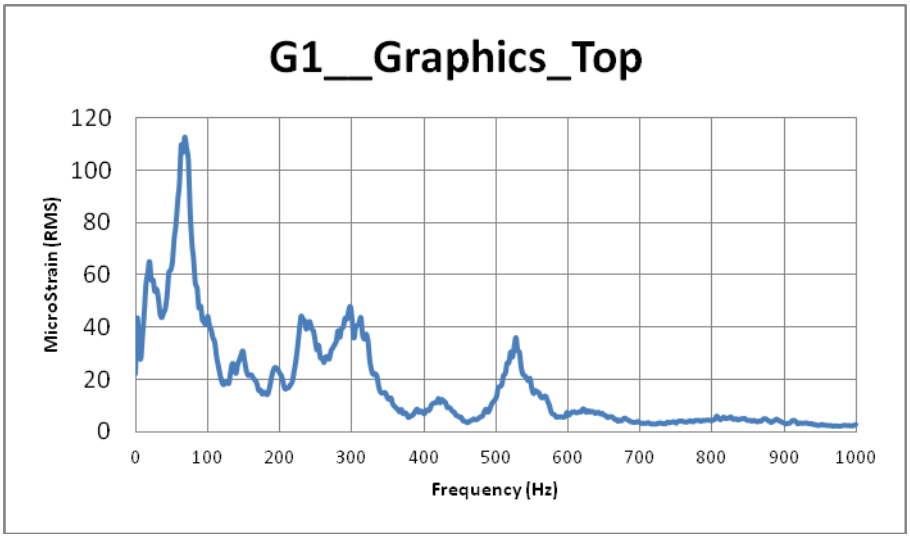

Figure 4.18 Lead-free solder graphics generator with 8.0 Grms input, maximum PCB strain response is 113 RMS micro strain at 68.4 hertz mode 1 frequency

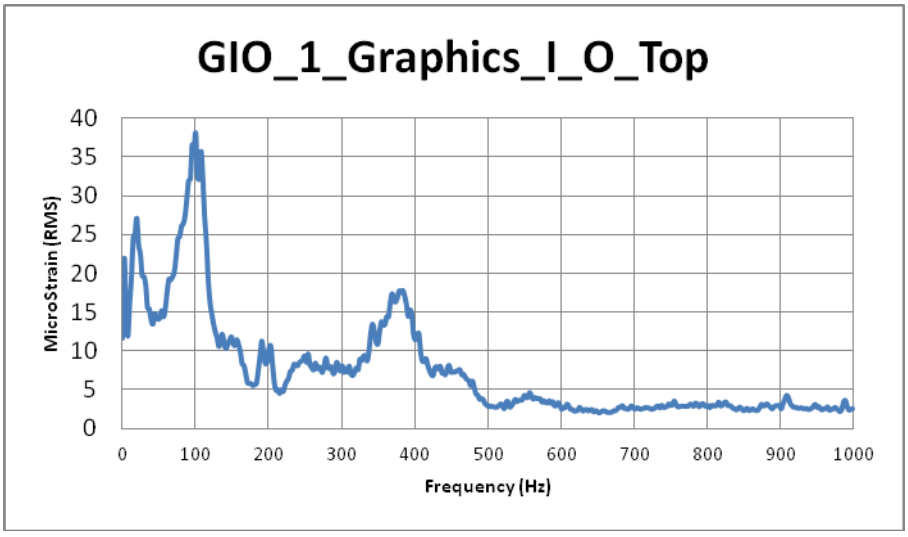

Figure 4.19 Tin-lead solder I/O next to graphics generator with 8.0 Grms input, maximum PCB strain response is 38.1 RMS micro strain at 100 hertz mode 1 frequency

Table 4.8 Processor cycles-to-failure and strains due to circuit card vibration with lead-free solder connections

Input PSD at Mode 1 Resonance (g^2/Hz)	Mode 1 Frequency (Hz)	Time at Level (hr:min:sec)	Cycles to Failure	RMS Strain (micro strain)	Root Cause & Resolution
0.004	100	100:00:00	36,000,000	32	No failures
0.04	90.3	02:30:39	816,222	119	No failures

Table 4.9 I/O next to processor cycles-to-failure and strains due to circuit card vibration with lead-free solder connections

Input PSD at Mode 1 Resonance (g^2/Hz)	Mode 1 Frequency (Hz)	Time at Level (hr:min:sec)	Cycles to Failure	RMS Strain (micro strain)	Root Cause & Resolution
0.04	68.3	00:11:36	47,537	119	I/O next to Processor resistor package lead failure; replace (see Figure 4.20 & Figure 4.21)
0.004	78.1	100:00:00	28,116,000	40.3	No failures
0.04	68.3	02:19:03	569,827	119	No failures

Table 4.10 Graphics generator cycles-to-failure and strains due to circuit card vibration with lead-free solder connections

Input PSD at Mode 1 Resonance (g^2/Hz)	Mode 1 Frequency (Hz)	Time at Level (hr:min:sec)	Cycles to Failure	RMS Strain (micro strain)	Root Cause & Resolution
0.004	100	100:00:00	36,000,000	22.8	No failures
0.04	68.4	02:12:52	545,285	113	GG ferrite bead solder joint failure; replace choke (see Figure 4.23)
0.04	68.4	00:17:47	72,983	113	No failures

Table 4.11 I/O next to graphics generator cycles-to-failure and strains due to circuit card vibration with tin-lead solder connections

Input PSD at Mode 1 Resonance (g^2/Hz)	Mode 1 Frequency (Hz)	Time at Level (hr:min:sec)	Cycles to Failure	RMS Strain (micro strain)	Root Cause & Resolution
0.004	107	100:00:00	38,520,000	11.5	No failures
0.04	100	02:30:39	903,900	38.1	No failures

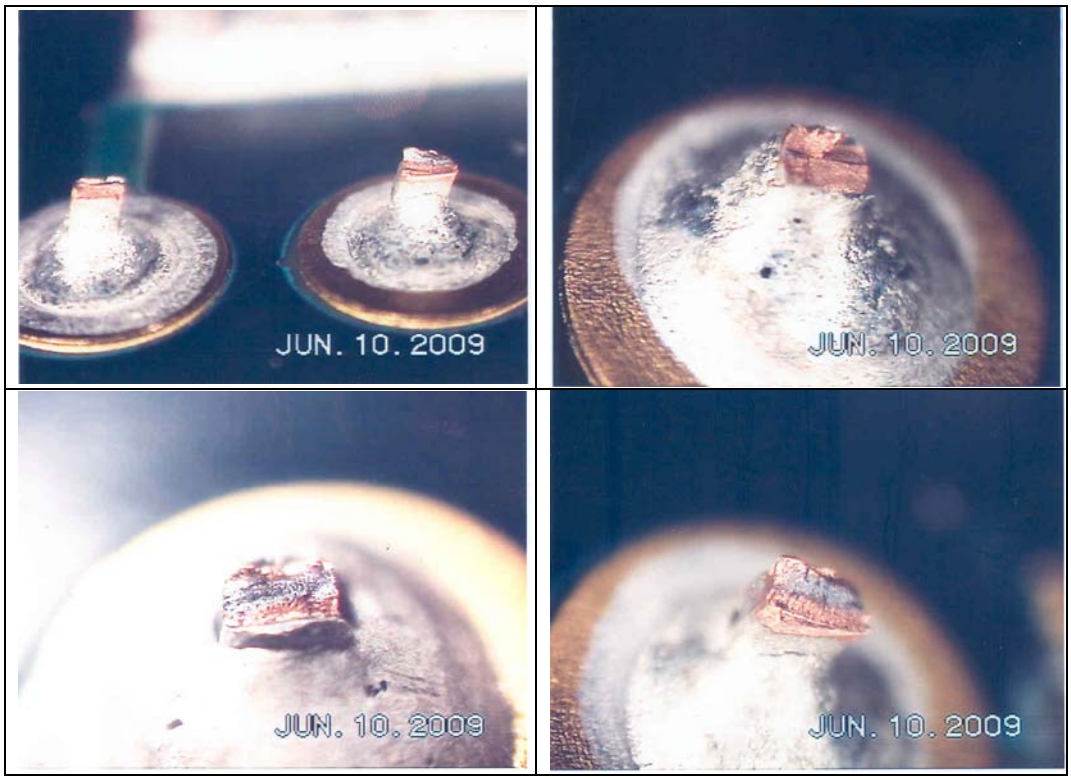

Figure 4.20 DEU-II I/O CCA resistor lead fatigue as seen from the SAC305 solder joint (4 photos)

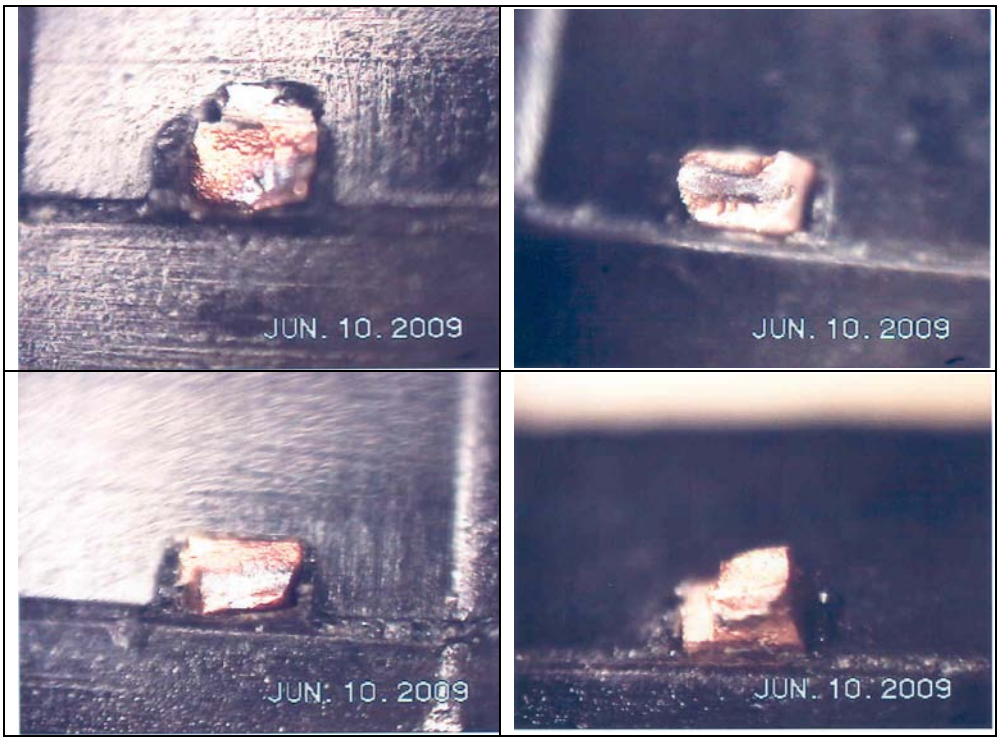

Figure 4.21 DEU-II I/O CCA resistor lead fatigue as seen from the resistor side (4 photos)

Figure 4.22 SAC305 DEU-II LRU with a Sn-Pb solder power supply showing connector fretting

Figure 4.23 DEU-II SAC solder failure to a graphics CCA ferrite bead (2 photos of same failure)

4.7 Finite element analysis circuit card assembly deflections and frequencies

Finite element analysis is performed on the entire DEU-II system with transmissibility through the chassis to the CCAs, Table 4.12 shows the 1-sigma RMS displacement and fundamental frequency for each CCA at the accelerated or step stress random vibration levels in Figure 4.3. The FEA stiffness in Table 4.12 is a global stiffness due to the CCA stack-up composite comprised of all the circuit layers made of copper and FR-4 board. FEA displacements are calculated using NASTRAN Multi-Point Constraint (MPC) equations in which multiple nodes are constrained to get the maximum displacements relative to the card edge boundaries. In this way, strain calculations are due to CCA bending only and rigid body translations are eliminated that would otherwise contribute to higher strains. This analysis is the baseline displacement model for which subsequent comparison will be made to CALCE_PWA displacement calculations in the next section. The FEA displacements and frequencies are close to those in the CALCE_PWA calculations shown in Table 4.13. Also, the first mode frequencies match well to the strain gauge frequencies shown in Figures 4.8 through 4.11. Good frequency agreement means that dynamic equations of the model and boundary conditions are similar and similar displacements mean that the transmissibility and damping are in agreement. The maximum FEA strains are calculated using equation (8) using a 12 inch long CCA and stresses are calculated by multiplying the FEA stiffness by the strain that in turn can be used to compute life. In this dissertation, the actual measured stresses are used to

calculate life, but the FEA strains are calculated to assess the performance of the measured strains.

Table 4.12 Finite element deflections for each circuit card assembly

CCA	FEA 1-sigma RMS displacements, mils	FEA stiffness, 10**6 psi	FEA Mode 1 Frequency, hertz
Processor	**16.62**	**4.36**	**79.55**
I/O next to Processor	**20.56**	**4.448**	**69.86**
GG	**17.78**	**4.121**	**77.18**
I/O next to GG	**20.84**	**4.448**	**69.13**

4.8 Analysis based on CALCE PWA Software

This section summarizes the analysis performed using the CALCE PWA software code module for vibration written by University of Maryland's Center for Advanced Life Cycle Engineering and is part of a software suite called the Simulation Assisted Reliability Assessment (SARA®) Software (CALCE, 2011) currently at version 6.1.6 released September 23, 2011. From the product literature on the website (CALCE, 2011), "The SARA® software can be used to assess life expectancy of electronic hardware under anticipated life cycle loading conditions, as well as under accelerated stress test conditions. The assessment of life expectancy under anticipated life cycle loading conditions is referred to as the virtual qualification (VQ™) process. The CALCE methodology uses physics-of-failure based principles and software to assess whether a part/system can meet defined life cycle requirements based on its materials, geometry, and operating

characteristics. The software implements math based physics models and allows for the creation of a computer model of the design. Thus, the design can be assessed prior to fabrication."

The goal of this analysis is to calculate CALCE PWA model frequencies and maximum displacements used in a Steinberg analysis for assessing life and component life calculations from CALCE PWA for reconciling Steinberg life calculations with test results.

Figures 4.24 and Figure 4.25 shows the qualification and step stress levels imparted to the I/O CCA, processor CCA and graphics CCA in that order based on transmissibility through the DEU-II chassis. Each circuit card was analyzed in succession: Figures 4.26 through 4.29 for the I/O CCA, Figures 4.30 through 4.33 for the processor CCA, and Figures 4.34 through 4.37 for the graphics CCA. The summary shown in Table 4.13 includes the first mode natural frequency for each CCA and the maximum 1-sigma RMS board displacement for both the 5.34 grms qualification level chassis transmission and 16.9 grms step stress level chassis transmission. Each set of CCA analyses begins with a slide containing a top side or main component side of the CCA layout followed by a bottom side or passive component side layout; and the next slide is structural boundary conditions for vibration analysis. Figures 4.27, 4.28, 4.31, 4.32 and 4.35, 4.36 show mode shape 1 and its frequency followed by the 1-sigma RMS displacements and its maximum value as a function of 5.34 grms qualification input due to chassis transmission. Figures 4.29, 4.33, and 4.37 show the mode 1 frequency 1-sigma

RMS displacements and its maximum value as a function of 16.9 Grms qualification input due to chassis transmission. The associated CALCE PWA estimated weights of the CCAs shown in Figures 4.38, 4.39, and 4.40 indicate that all CCAs are lighter than the actual weights of the CCAs shown in Table 4.1. On average, the I/O CCA is 20 percent lighter, the CPU CCA is 31 percent lighter, and the graphics CCA is 0.5 percent lighter. The CALCE PWA code frequencies and thus displacements cannot be easily weight scaled due to the nature of the mass distribution and concomitant stiffness. Fortunately, the graphics CCA weight is within the range of the GG-weighed cards and also has the highest calculated board deflection.

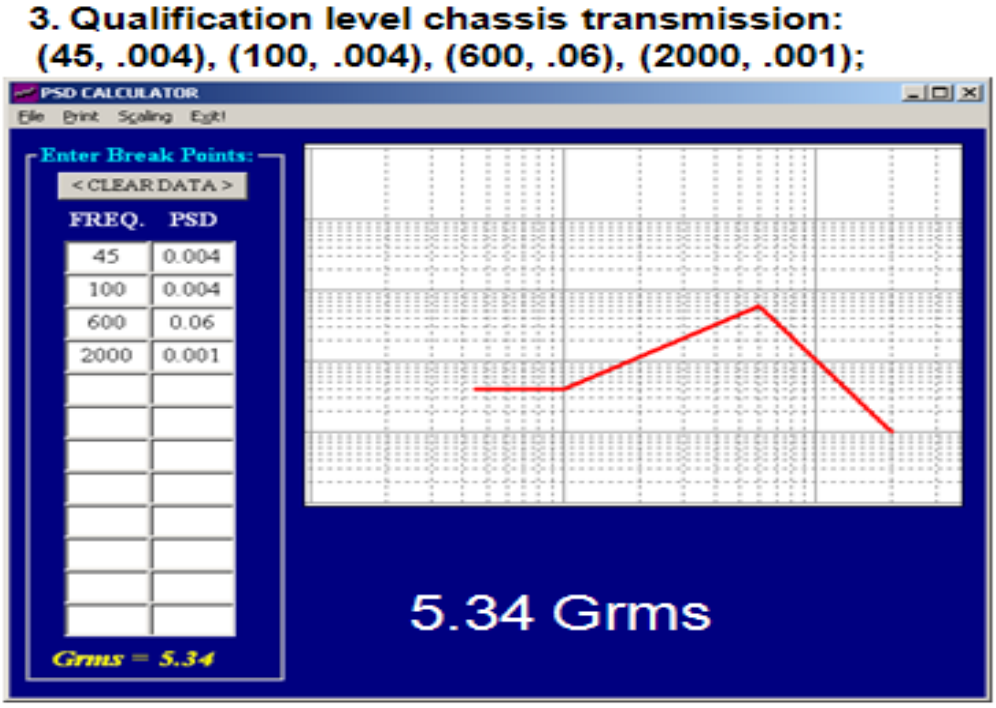

Figure 4.24 Input 5.34 Grms to the CCA boundary conditions at chassis card guides

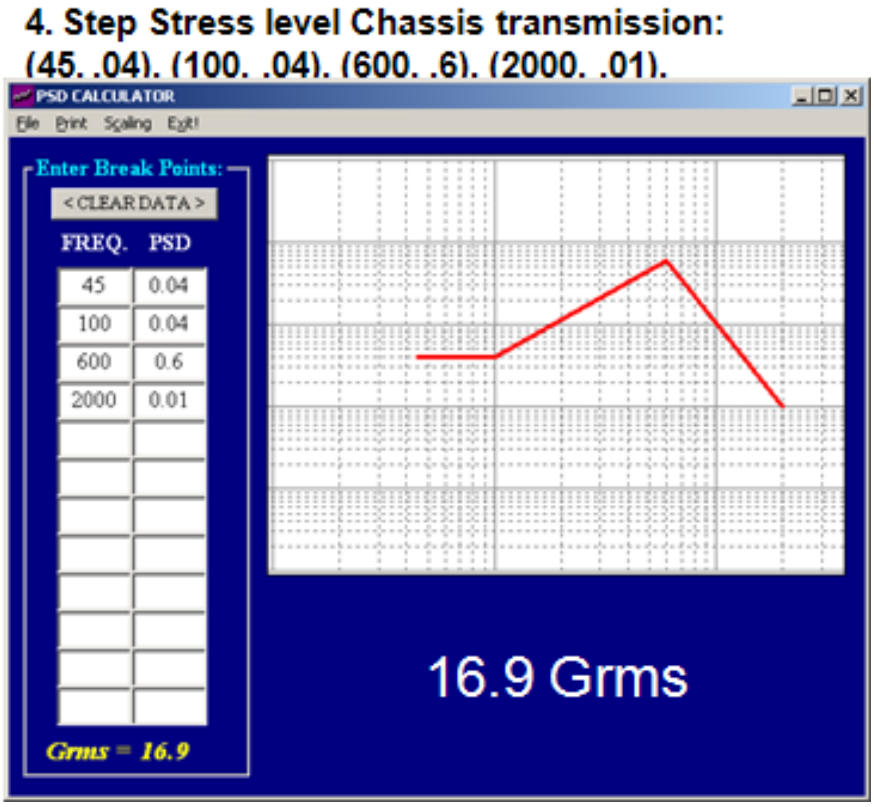

Figure 4.25 Input 16.9 Grms to the CCA boundary conditions at chassis card guides

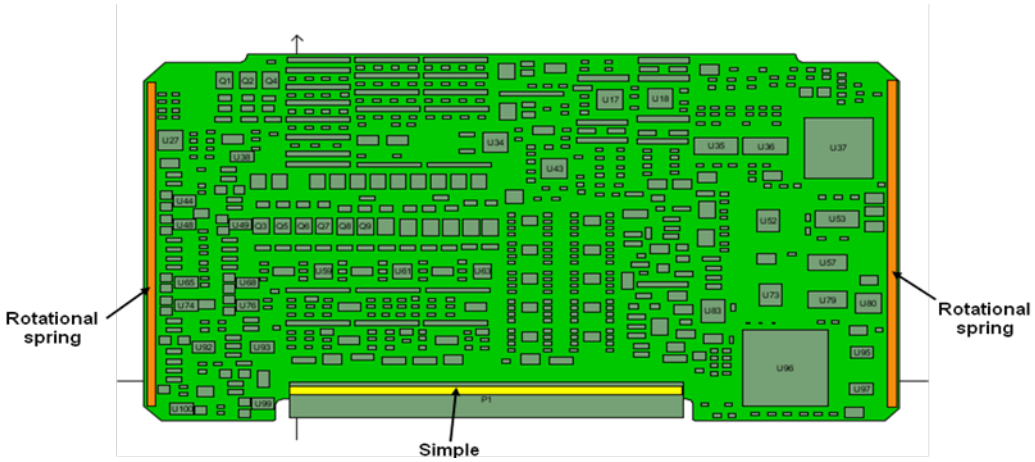

Figure 4.26 I/O CCA vibration boundary conditions

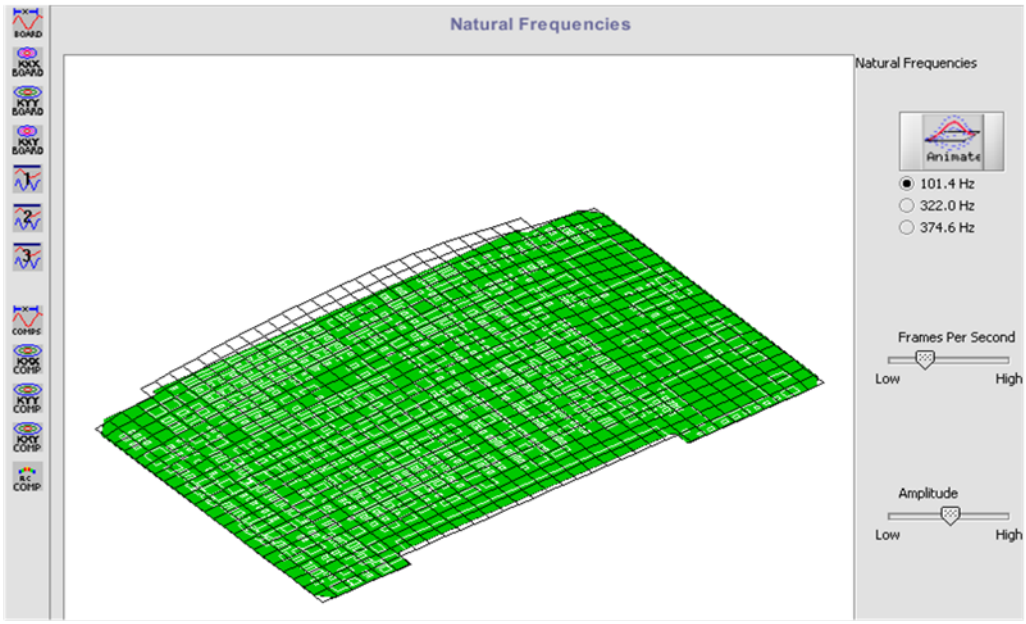

This Preliminary Analysis indicates that the DEU-II/ IO-CCA Assembly will sustain a 101.4 Hz (1st mode) Range of Dynamic Natural frequency at 5.34 G Vibration Environment.

Figure 4.27 I/O CCA vibration modal results for natural frequencies at 5.34 Grms input

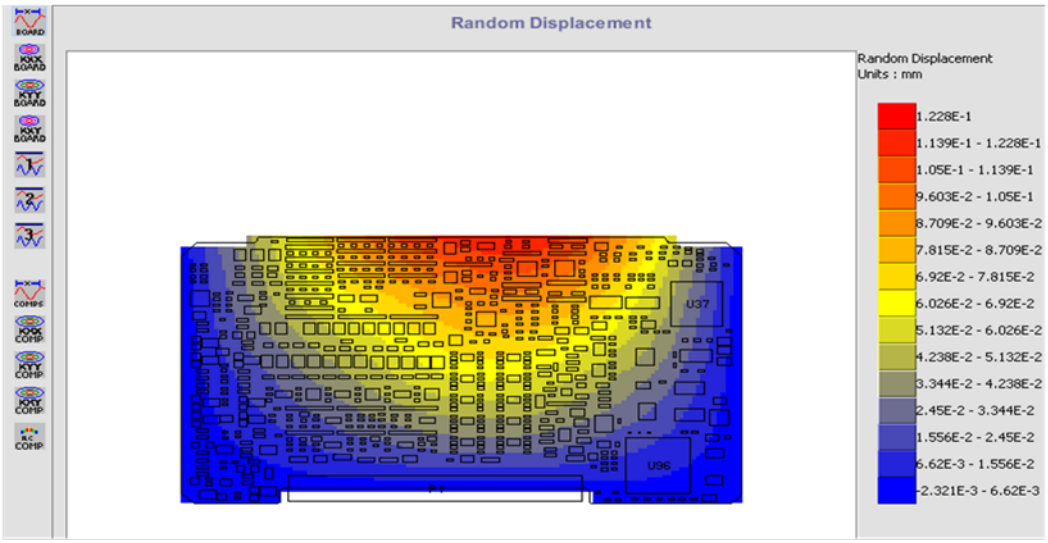

The Maximum board deflection is about 0.1228 mm (0.00483 inches)

Figure 4.28 I/O CCA 1-sigma random displacement for 5.34 Grms input

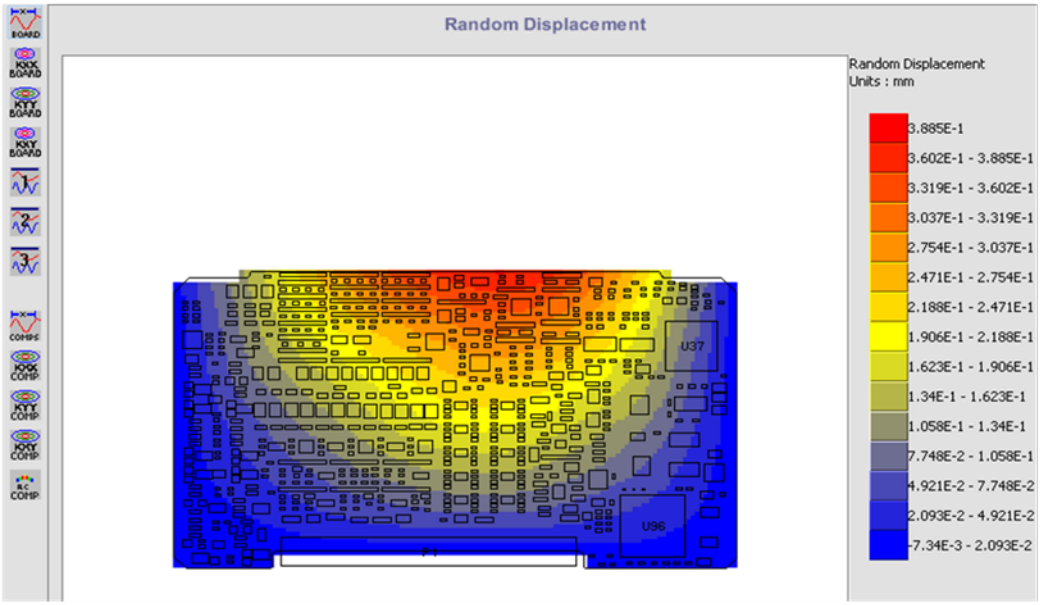

The Maximum board deflection is about 0.3885 mm (0.015275 inches)

Figure 4.29 I/O CCA 1-sigma random displacement for 16.9 Grms input

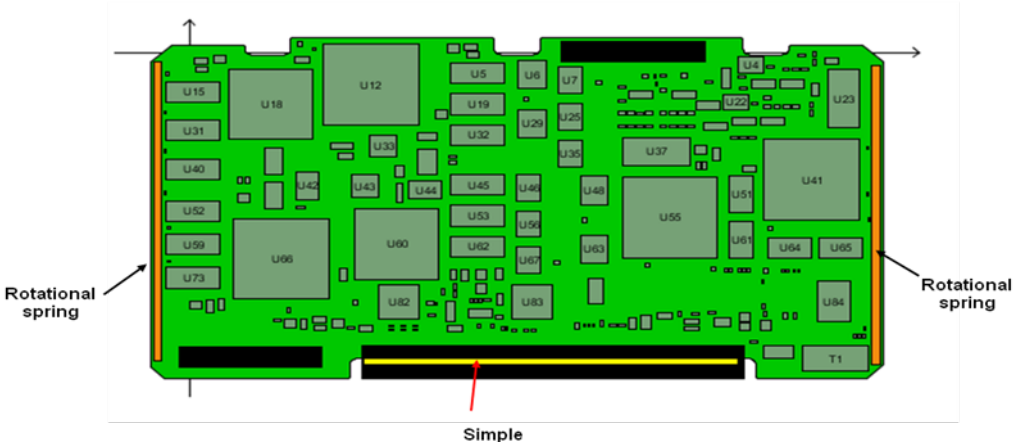

Figure 4.30 CPU vibration boundary conditions

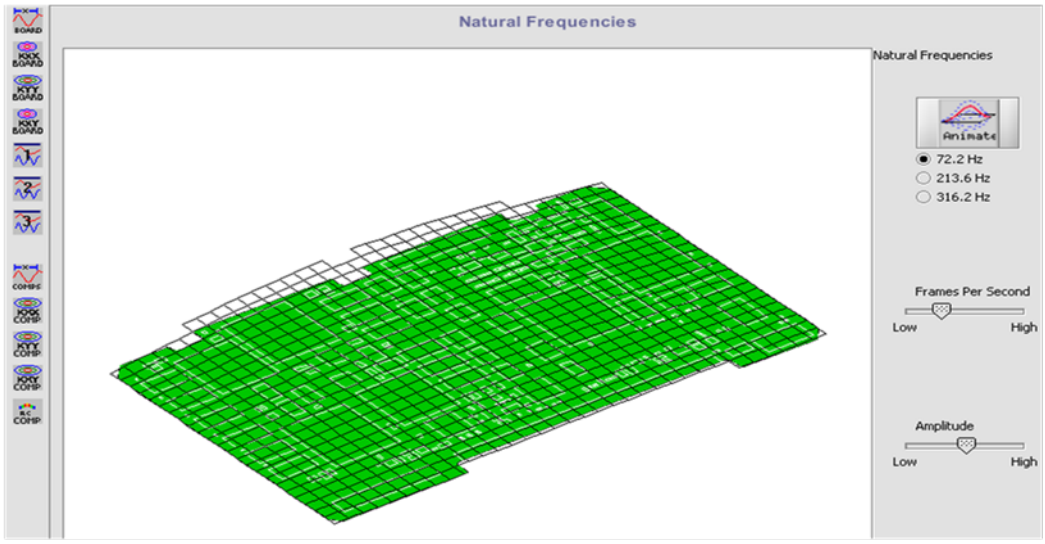

This Preliminary Analysis indicates that the DEU-II/ CPU-CCA Assembly will sustain a 72.2 Hz (1st mode) Range of Dynamic Natural frequency at 5.34 G Vibration Environment.

Figure 4.31 CPU CCA vibration modal results for natural frequencies at 5.34 Grms input

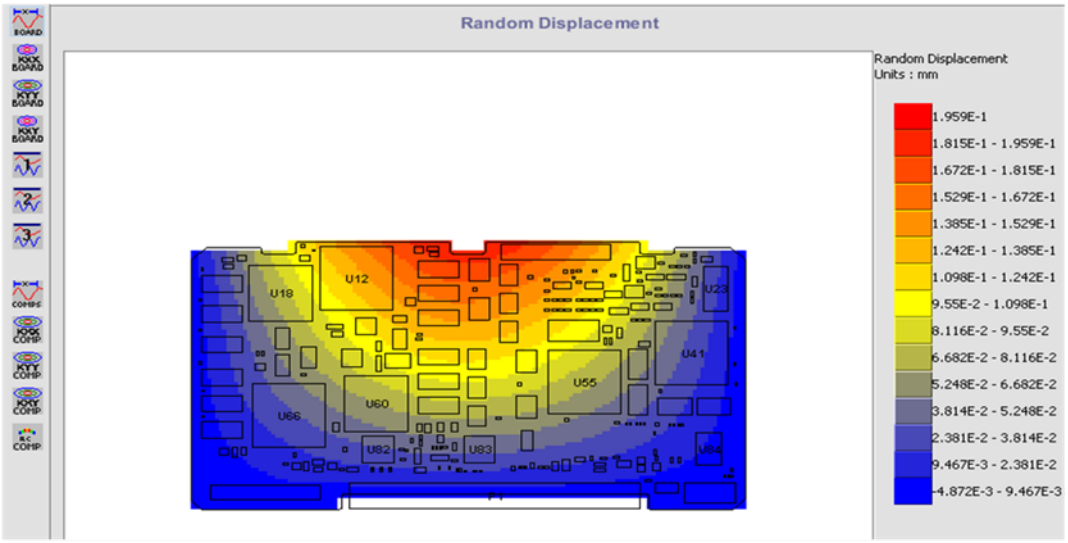

The Maximum board deflection is about 0.1959 mm (0.00771 inches)

Figure 4.32 CPU CCA 1-sigma random displacement for 5.34 Grms input

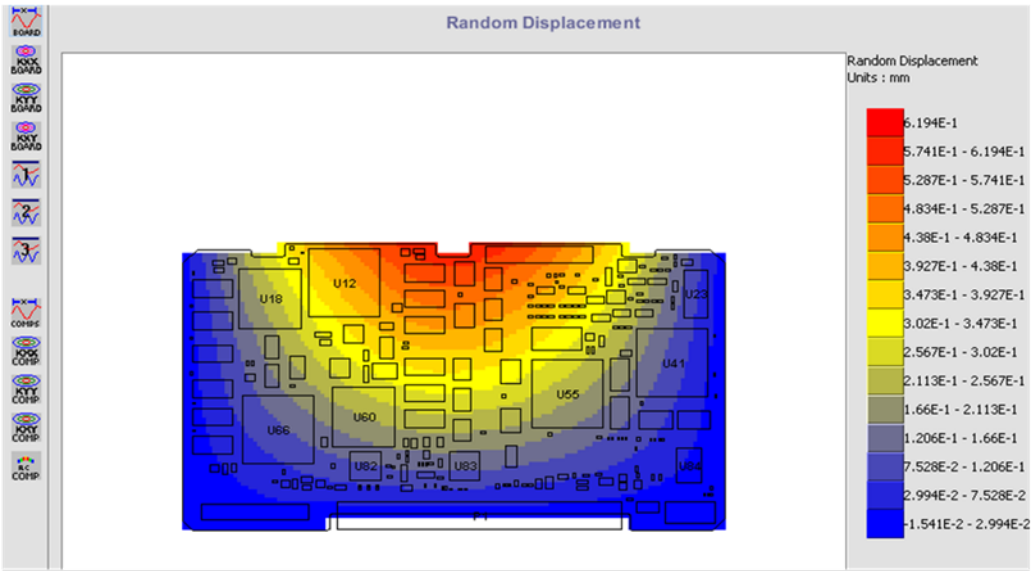

Figure 4.33 CPU CCA 1-sigma random displacement for 16.9 Grms input

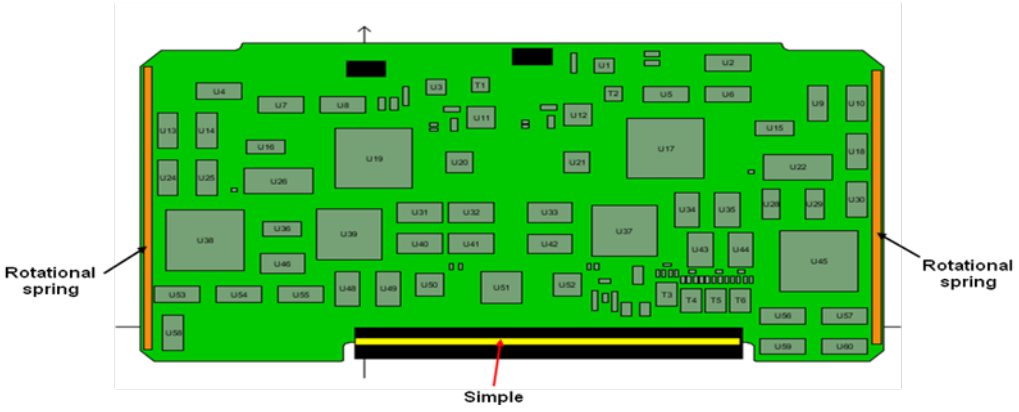

Figure 4.34 GG vibration boundary conditions

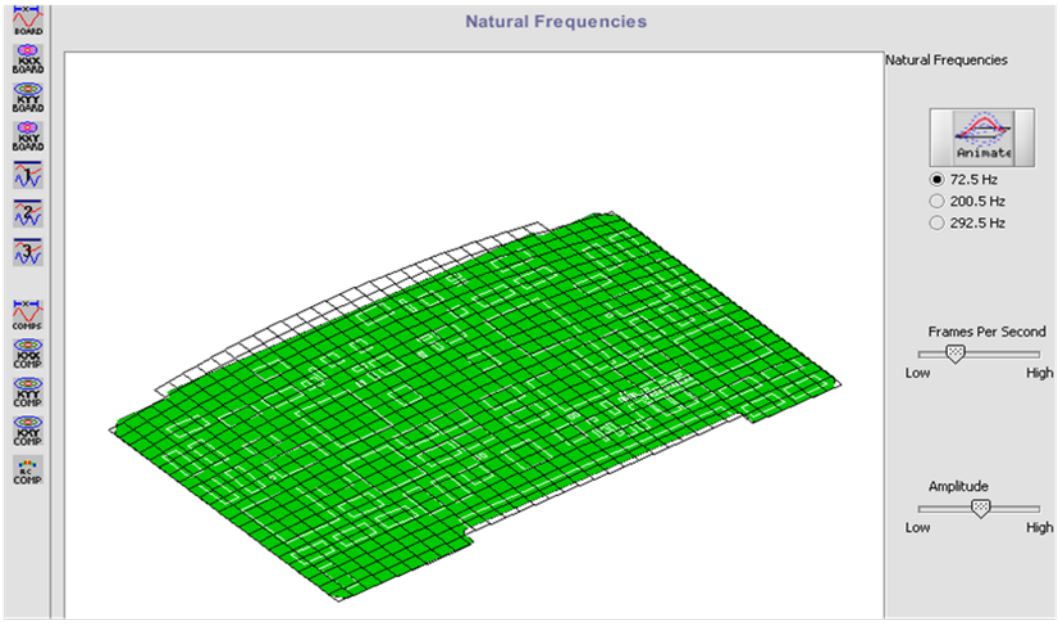

Figure 4.35 GG CCA vibration modal results for natural frequencies at 5.34 Grms input

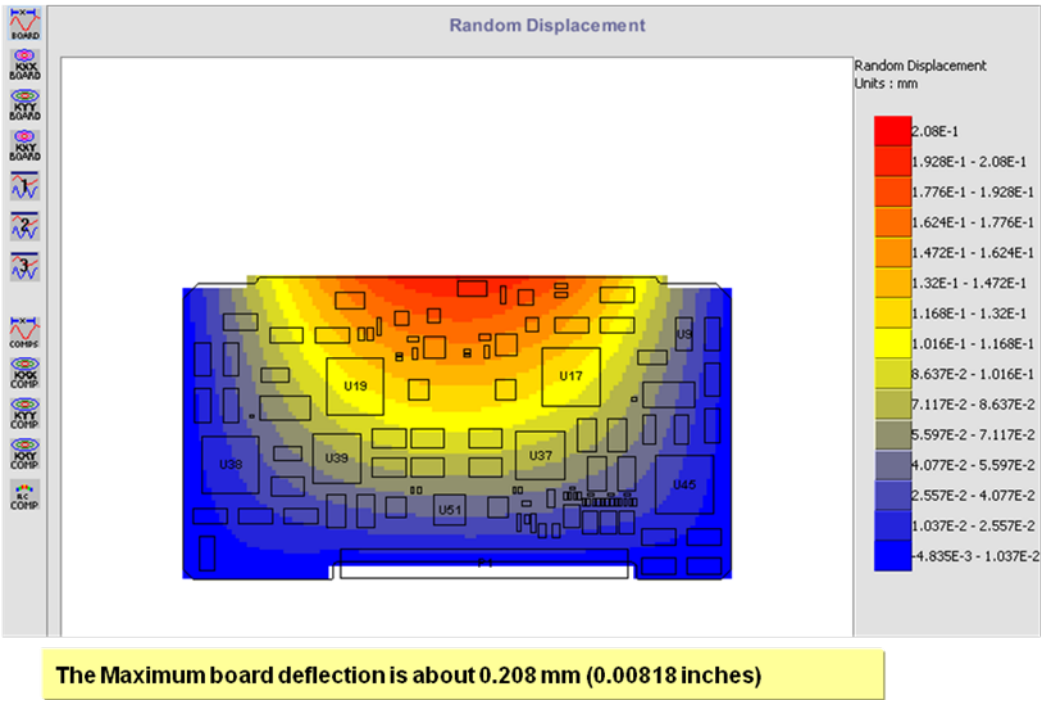

Figure 4.36 GG CCA 1-sigma random displacement for 5.34 Grms input

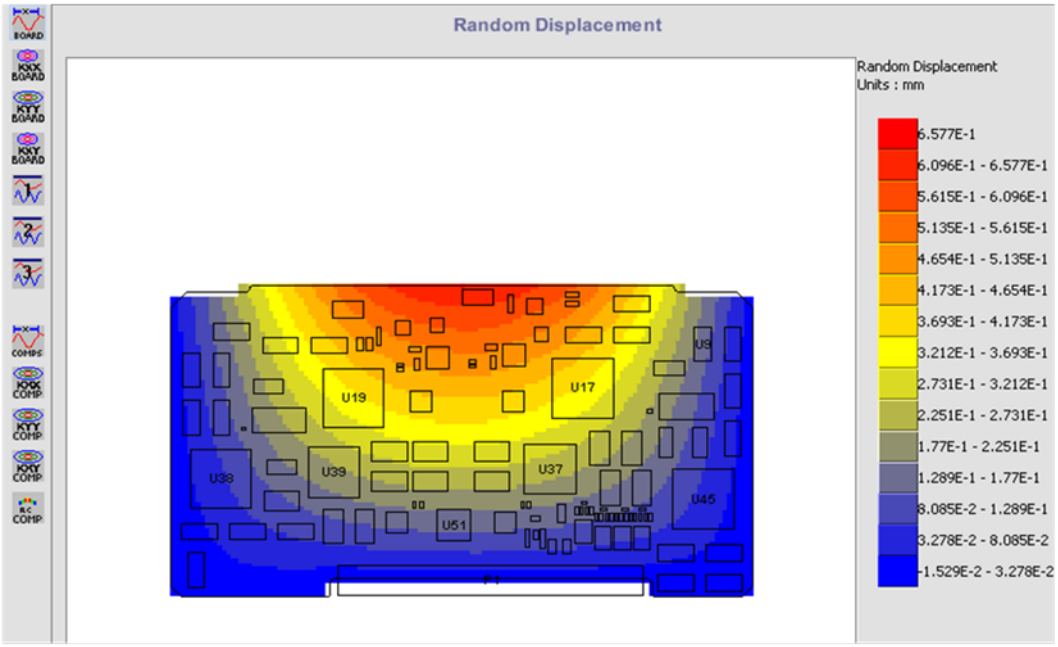

Figure 4.37 GG CCA 1-sigma random displacement for 16.9 Grms input

Table 4.13 Summary of the fundamental frequencies and 1-sigma random displacements

	5.34 Grms (Qualification level chassis transmission)		**16.9 Grms (Step Stress level chassis transmission)**	
CCA	1st Mode Nat. Frequency (Hz)	Max. board deflection (inch)	1st Mode Nat. Frequency (Hz)	Max. board deflection (inch)
I/O	101.4	0.00483	101.4	0.015275
CPU	72.2	0.00771	72.2	0.024385
Graphics	72.5	0.00818	72.5	0.02589

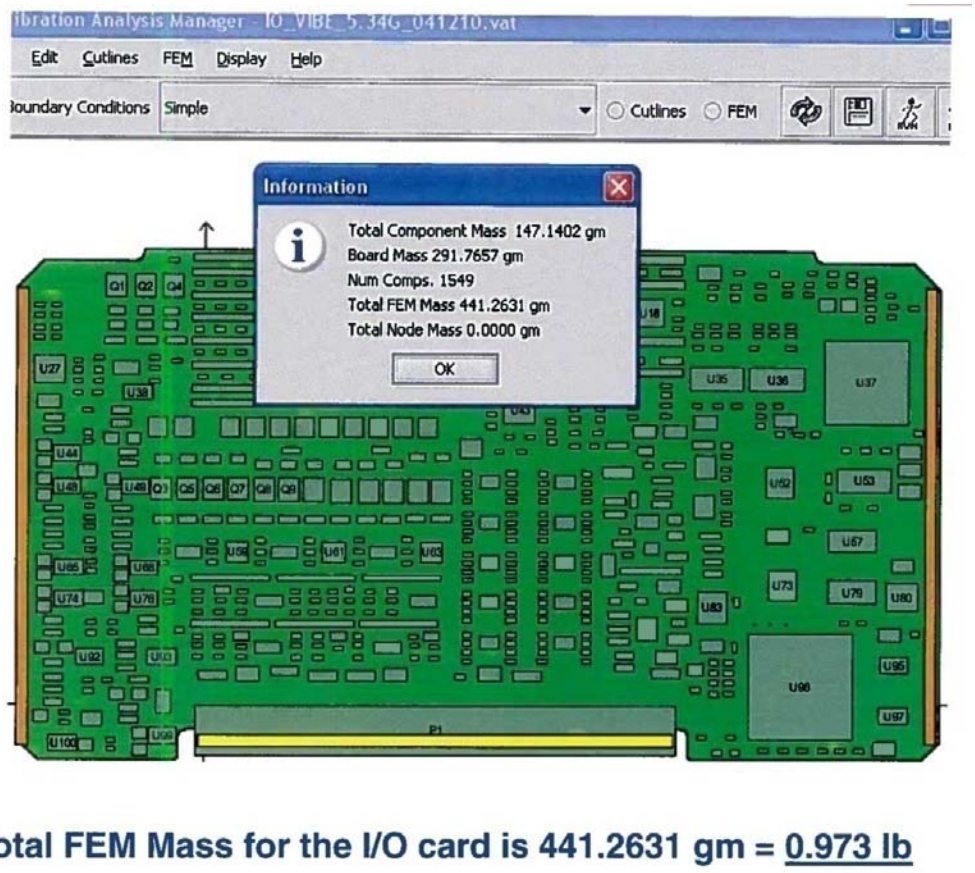

Figure 4.38 CALCE-estimated weights for I/O CCA

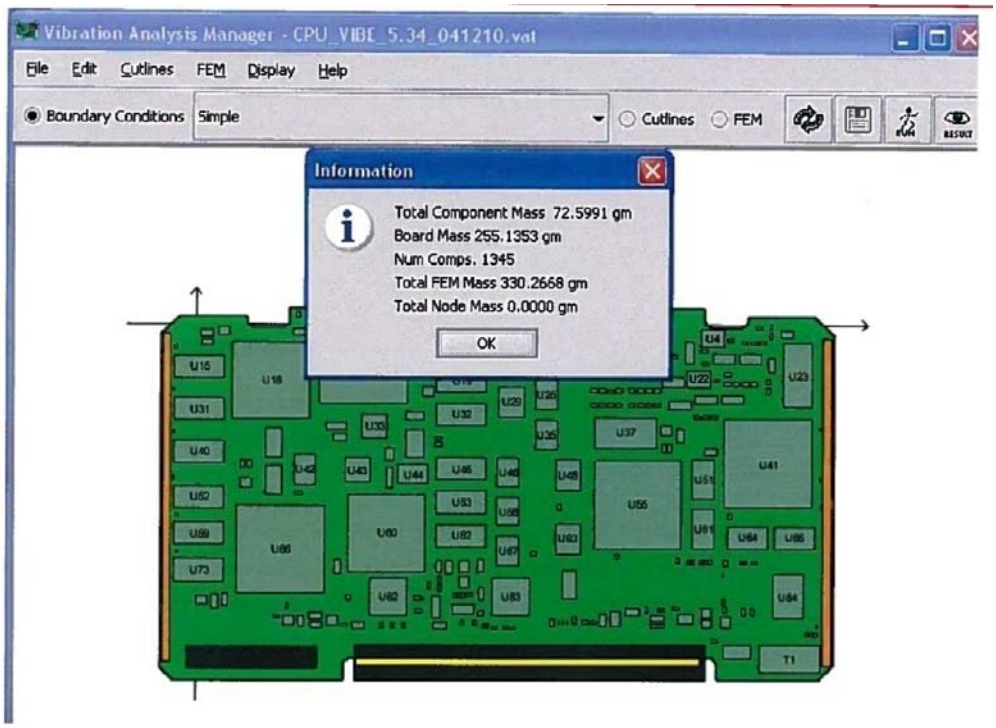

Figure 4.39 CALCE-estimated weights for CPU CCA

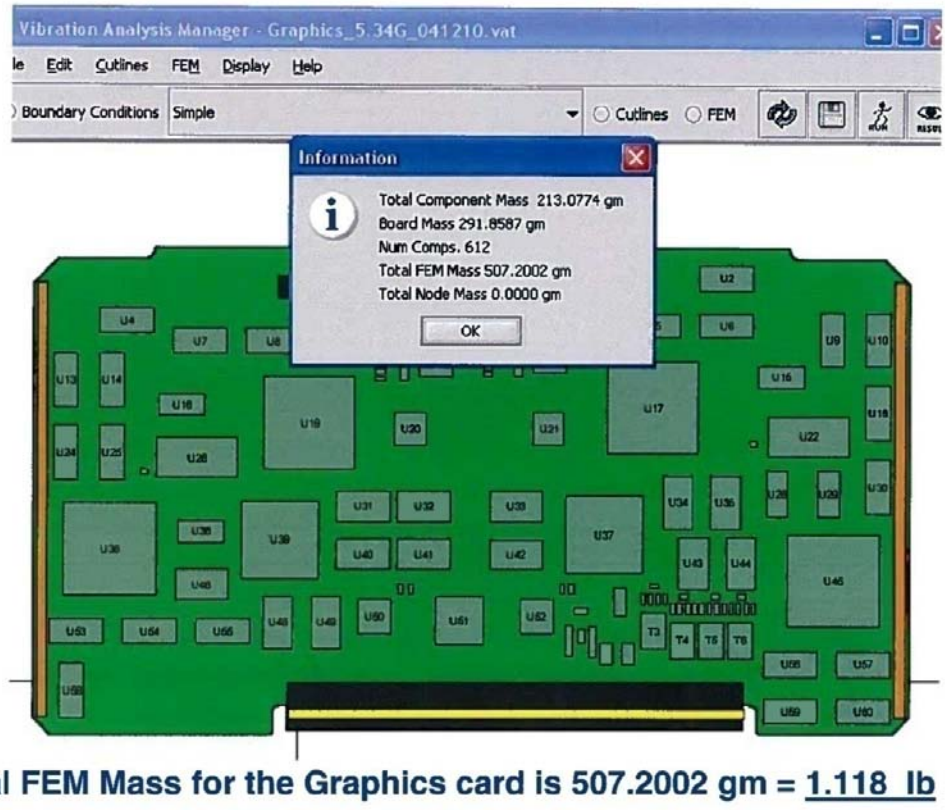

Figure 4.40 CALCE-estimated weights for graphics generator CCA

The CALCE PWA solder joint reliability results based on vibration tests are included in Figures 4.31, 4.32, and 4.33 herein show that the boards are not as populated as the previous analysis and have a considerably lower Mode 1 frequency which may be explained by the board thickness being 0.1 inch. A thickness of 0.085 inch would result in a 28 percent higher frequency, assuming the lower mass is counteracted by the stiffness those components would impose on the board. Tables 4.14, 4.15, and 4.16 vibration failures as a function of time comparisons between lead-free solder and tin-lead solder for selected components in the CPU CCA, graphics CCA, and I/O CCA both at 5.34 grms input and 16.9 grms input.

Parts Analyzed		
CPU CCA	Graphics CCA	I-O CCA
1902482	1902482	1902482
4087540-977	4084440-977	4075657-400
4088523-977	4087202-400	4087540-977
4088927-977	4087540-977	4089728-400
4089440-400	4088272-400	4089934-977
4089888-977	4090537-977	4091418-102
4089934-977	4090544-400	53000910-1
4090173-400	53001118-1	
4090531-400		
4090537-977		
53000493-1		
53000944-1		

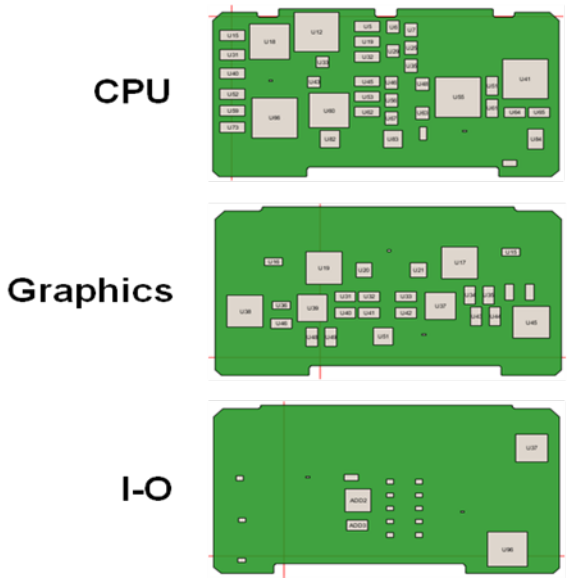

Figure 4.41 Thermally defined critical part types

Ref	Cu (oz)	Thck	Proposed Stackup: Electrical, Mechanical, and PWA DC	Copper Percentage
1		0.0006	Tin/Lead Plating Layer	N/A
2		0.0020	Plating Layer	N/A
3	1.0	0.0014	Layer 1 - Signal Layer	10%
4		0.0050	Core	0%
5	1.0	0.0014	Layer 2 - Ground Layer	70%
6		0.0100	B-Stage Dielectric	0%
7	1.0	0.0014	Layer 3 - Power Layer	70%
8		0.0060	Core	0%
9	1.0	0.0014	Layer 4 - Ground Layer	70%
10		0.0080	B-Stage Dielectric	0%
11	1.0	0.0014	Layer 5 - Signal Layer	5%
12		0.0080	Core	0%
13	1.0	0.0014	Layer 6 - Signal Layer	5%
14		0.0080	B-Stage Dielectric	0%
15	1.0	0.0014	Layer 7 - Ground Layer	70%
16		0.0060	Core	0%
17	1.0	0.0014	Layer 8 - Power Layer	70%
18		0.0100	B-Stage Dielectric	0%
19	1.0	0.0014	Layer 9 - Ground Layer	70%
20		0.0050	Core	0%
21	1.0	0.0014	Layer 10 - Signal Layer	10%
22		0.0020	Plating Layer	N/A
23		0.0006	Tin/Lead Plating Layer	N/A
Cu:	10.0	0.0852	Nominal thickness of PWB	
Planes	10.0	0.0100	PWB Tolerance +/-.010 if thickness <.100 or +/-8% if thickness >.100	
		0.0952	Total Maximum PWB Thickness	

Ef composite 4.155E+06

α composite 1.679E-05

υ composite 2.736E-01

ρ composite 7.937E-02

Composite k [W/(m·K)]	30.82
Btu/(hr·ft·°F)	17.81

Figure 4.42 Ten layer 0.085 inches thick

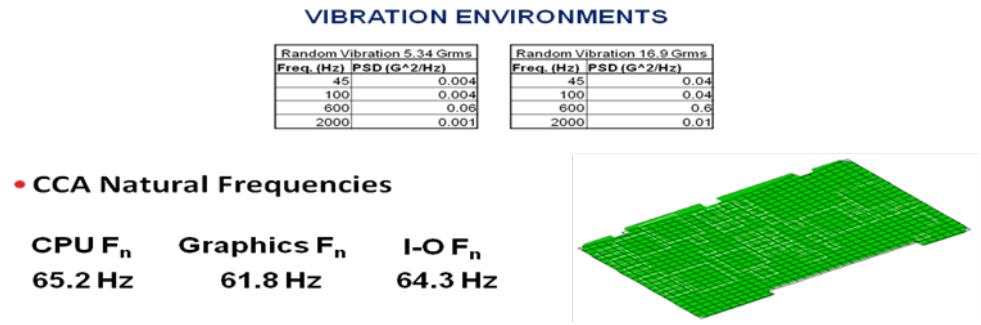

Figure 4.43 Vibration first natural frequencies for all three CCAs at both 5.34 Grms and 16.9 Grms input levels

Table 4.14 CPU CCA vibration solder joint reliability results

5.34 Grms Input

		Lead Free Solder	Lead Solder	Lead Free Solder	Lead Solder
		Mean Fatigue	Mean Fatigue	1% Weibull	1% Weibull
Component	Part Number	Hours to Failure	Hours to Failure	Hours to Failure	Hours to Failure
U41	4090531-400	158.00	2020.00	54.80	701.00
U55	4090531-400	158.00	2020.00	54.80	701.00
U66	4090173-400	397.00	5490.00	138.00	1900.00
U12	4090173-400	1460.00	22600.00	507.00	7850.00
U61	4087540-977	1490.00	23000.00	515.00	7980.00

16.9 Grms Input

		Lead Free Solder	Lead Solder	Lead Free Solder	Lead Solder
		Mean Fatigue	Mean Fatigue	1% Weibull	1% Weibull
Component	Part Number	Hours to Failure	Hours to Failure	Hours to Failure	Hours to Failure
U41	4090531-400	0.18	1.29	0.06	0.45
U55	4090531-400	0.18	1.29	0.06	0.45
U66	4090173-400	0.45	3.52	0.15	1.22
U12	4090173-400	1.64	14.60	0.57	5.05
U61	4087540-977	1.67	14.70	0.58	5.09

Table 4.15 GG CCA vibration solder joint reliability results

5.34 Grms Input

		Lead Free Solder	Lead Solder	Lead Free Solder	Lead Solder
		Mean Fatigue	Mean Fatigue	1% Weibull	1% Weibull
Component	Part Number	Hours to Failure	Hours to Failure	Hours to Failure	Hours to Failure
U39	4090544-400	503.00	9220.00	174.00	3200.00
U37	4090544-400	637.00	7120.00	221.00	2470.00
U45	4087202-400	762.00	11100.00	264.00	3850.00
U38	4087202-400	762.00	11100.00	264.00	3850.00
U46	4087540-977	1060.00	15800.00	366.00	5490.00

16.9 Grms Input

		Lead Free Solder	Lead Solder	Lead Free Solder	Lead Solder
		Mean Fatigue	Mean Fatigue	1% Weibull	1% Weibull
Component	Part Number	Hours to Failure	Hours to Failure	Hours to Failure	Hours to Failure
U39	4090544-400	0.40	5.93	0.14	2.06
U37	4090544-400	0.57	4.67	0.20	1.62
U45	4087202-400	0.86	7.00	0.30	2.43
U38	4087202-400	0.86	7.00	0.30	2.43
U46	4087540-977	1.18	9.98	0.41	3.46

Table 4.16 I/O CCA vibration solder joint reliability results

5.34 Grms Input

		Lead Free Solder	Lead Solder	Lead Free Solder	Lead Solder
		Mean Fatigue	Mean Fatigue	1% Weibull	1% Weibull
Component	Part Number	Hours to Failure	Hours to Failure	Hours to Failure	Hours to Failure
U96	4091418-102	681.00	9920.00	236.00	3440.00
U37	4075657-400	1450.00	22500.00	505.00	7800.00
ADD2	4089728-400	3800.00	63800.00	1320.00	22100.00
R24	1902482	4160.00	70300.00	1440.00	24400.00
R27	1902482	6190.00	108000.00	2150.00	37400.00

16.9 Grms Input

		Lead Free Solder	Lead Solder	Lead Free Solder	Lead Solder
		Mean Fatigue	Mean Fatigue	1% Weibull	1% Weibull
Component	Part Number	Hours to Failure	Hours to Failure	Hours to Failure	Hours to Failure
U96	4091418-102	0.64	6.87	0.22	2.38
U37	4075657-400	1.63	14.00	0.57	4.87
ADD2	4089728-400	4.22	39.50	1.47	13.70
R24	1902482	4.67	43.90	1.62	15.20
R27	1902482	6.90	66.70	2.40	23.10

4.9 LRU test and analysis results

In this section, calculations are presented showing why the tin-lead LRU did not fail and why analysis results from the commercial CALCE PWA code are conservative. Since the only solder joint failure occurred in the GG CCA of the lead-free LRU, comparisons between tin-lead and lead-free are made here for the GG CCA data only by performing life calculations using stress for the tin-lead CCA and displacement for lead-free. This is done because of the reliability of the strain measurements in the case of the tin-lead and for lead-free the CALCE PWA code calculates displacements. Tables 4.17 and 4.18 are summary tables for data in sections 4.6 and 4.8. The last column takes the CALCE PWA deflections using equation (8) and computes the strain for the appropriate CCA boundary conditions using (Steinberg, 2000) to show that the code is giving good estimates but are based on board stack-ups and distributed component masses. Table 4.19 takes the finite element data in section 4.7 and using equation (8) shows that the strains are comparable to the CALCE PWA strains. Next the FEA CCA stiffness's are then used to calculate the CCA stresses from the strains in Table 4.18.

The tin-lead GG CCA no failure calculation proceeds by applying equation (13) as follows:

$$N_{SnPb} = N \times (S / S_{SnPb})^4,$$

where S_{SnPb} = 997 psi GG stress from Table 4.19, N = 1000 cycles-to-failure, S = 6500 psi, and exponent = 4 using Steinberg's (2000) for tin-lead solder. Therefore, N_{SnPb} = 1.8 million predicted cycles-to-failure for Sn-Pb solder, but the actual GG CCA had only between 456,000 to 649,000 cycles (Table 4.5) and thus did not expect failure of this GG CCA.

The following calculation shows why the CALCE PWA code is conservative for lead-free LRU applications, applying equation (14):

$$N_i = N \times (Z / Z_i)^b,$$

where $N = 20 \times 10^6$ cycles, and Z is computed by an equation representing 3 sigma displacements for components expected to achieve a fatigue life of about 20 million stress reversals in a random vibration environment per the research published by Steinberg (2000). Z_i = 0.07767 3-sigma CCA RMS displacement responses (Table 4.13) calculated using CALCE PWA and N_i = 545,300 cycles-to-failure SAC305 failure time from Table 4.10. This calculation leads to an exponent b = 2.8 for the failed part, but exponents this small show early failure due to manufacturing issues like low solder as evidenced by the photograph in Figure 4.23. At the this point, the test was stopped with only one failure, but the CALCE PWA showed that several of the BGA, TSOPs, and PQFP should have failed before the time the first failure actually occurred.

Table 4.17 Comparing qualification 2.5 Grms level random vibration Sn-Pb and SAC305 to CALCE PWA maximum 3-Sigma Grms strains

CCA	Strain Gauge Sn-Pb Mode 1 Frequency (Hz)	Sn-Pb measured strain (micro-strain)	Strain Gauge SAC305 Mode 1 Frequency (Hz)	SAC305 measured strain (micro-strain)	CALCE PWA Mode 1 Frequency (Hz)	Calculated CALCE PWA strain from deflections (micro-strain)
Processor	73.2	131	100	32	72.2	71.3
I/O next to Processor	73.2	46.8	78.1	40.3	101.4	44.7
GG	63.5	92.3	100	22.8	72.5	75.7
I/O next to GG (Sn-Pb)	68.4	98.4	107	11.5	101.4	44.7

Table 4.18 Comparing step stress 8 Grms level random vibration Sn-Pb and SAC305 to CALCE PWA maximum 3-Sigma Grms strains

CCA	Strain Gauge Sn-Pb Mode 1 Frequency (Hz)	Sn-Pb measured strain (micro-strain)	Strain Gauge SAC305 Mode 1 Frequency (Hz)	SAC305 measured strain (micro-strain)	CALCE PWA Mode 1 Frequency (Hz)	Calculated CALCE PWA strain from deflections (micro-strain)
(Processor	63.5	317	90.3	119	72.2	226
I/O next to Processor	63.5	153	68.3	119	101.4	141
GG	53.7	242	68.4	113	72.5	240
I/O next to GG (Sn-Pb)	63.5	208	100	38.1	101.4	141

Table 4.19 FEA strain calculations and CCA stresses using FEA calculated boards stack up stiffness's

CCA	FEA stiffness, (psi 10**6)	FEA Mode 1 Frequency, (Hz)	FEA 1-sigma RMS displacement, (mils)	Calculated FEA step stress 3-sigma RMS strain, (micro-strain)	Qualification Sn-Pb 3-sigma stress, (psi)	Qualification SAC305 3-sigma stress, (psi)	Step stress Sn-Pb 3-sigma stress, (psi)	Step stress SAC305 3-sigma stress, (psi)
Processor	4.36	79.55	16.62	153.8	571	140	1382	519
I/O next to Processor	4.448	69.86	20.56	190.2	208	179	681	529
GG	4.121	77.18	17.78	164.5	380	94.0	997	466
I/O next to GG	4.448	69.13	20.84	192.8	438	51.2	912	169

Chapter 5

CONCLUSION AND RECOMMENDATIONS

5.1 Summary of Research Performed

In chapter 2, accelerated testing was performed on hundreds of samples to show the failure relationship between and actual re-flow oven and an accelerated thermal machine called an IST tester. The data is shown to be Weibull and comparisons using the likelihood ratio test are performed to prove when distributions of failed coupons are similar.

In chapter 3, 16 large test vehicles with 20 large 1156 I/O BGAs are subjected to vibration 8 boards made of tin-lead solder and the 8 boards made of lead-free solder alloy SAC305. The LR test was used to find differences between tin-lead and SAC305 boards and then these results are used to subsequently perform statistical analysis. A regression analysis and a two-way ANOVA are performed to reach conclusions about significant factors in a vibration environment. S-N curves are developed to show how finer granularity between failure time and strain may be used to model failure prediction using both strain gauges and laser vibrometry.

In chapter 4, side-by-side testing of a tin-lead solder LRU and a lead-free solder LRU is performed with measurements of strain showing the differences in stiffness between the two solders. A finite element model is used to reconcile the measurements and a commercial vibration code for circuit board durability is used to predict life.

5.2 Major Conclusions and Recommendations to Practitioners

In chapter 2, a fundamental finding of the study showed IST preconditioning is independent of the quality of suppliers or the number of cycles to failure that a test vehicle will attain. A theory is developed that allows a practitioner to set the IST parameters given only the actual preconditioning cycles, re-flow oven peak temperature, and ramp time to cycle time ratio. Using equation (4) find the joule equivalent for re-flow then make adjustments to the parameters for IST until the joule equivalent difference is less than 123 JE. This means that the distribution of failure will be similar had an LR test been used to compare both sets of coupons.

In chapter 3, the use of the LR test together with regression analysis can be a powerful way to identify significant factors. In the case of ENIG finish boards preconditioning may not be needed and for OSP finishes there is evidence that SAC305 and tin-lead may behave similarly at lower vibration levels when the boards are preconditioned. S-N curves were developed for tin-lead and can be recommended for use in LRU tests.

In chapter 4, Side-by-side testing is showing that the solder joint failures for both tin-lead and lead-free occur late compared to other failure modes like pins breaking and fretting, or vulnerable lead failures. Commercial codes do not appear to model low strain conditions well and are conservative.

5.3 Recommendations for Further Research

Calculating an equivalent IST cycles to failure for a PTH design. Recall 350 IST cycles presented in chapter 2 and the industry report by Slough (2005) say for example, "customers specify greater than 300 cycles for accept/reject criteria." The literature review has not come up with software or models that take as input an IST PTH design and calculates the mean cycles to failure, but papers that calculated mean cycles to failure of PTH designs with models based on Modified Coffin-Manson equations validated with thermal cycling data from either MIL-T-CYCLE (single chamber cycling between -65^{o}C and 125^{o}C) and/or IEC OIL-T-SHOCK (between 25^{o} C and 260^{o} C), (IPC-TR-579,1988), (Yoder, Bhandarkar, and Dasgupta, 1993), (Mirman, 1988), and (Fu, Ume, and McDowell, 1998). In addition, the software package suite (CALCE, 2011) gives acceptable results for the current airline studies and design examples, but the temperature and ramp time, for which the models have been validated using an air circulating single chamber (Bhandarkar, Dasgupta, Barker, Pecht, and Engelmaier, 1992) and (Yoder, Bhandarkar, and Dasgupta, 1993) are out of the range of current accelerated test methods IPC-6012B with Amendment 1 (2007) and IPC-TM-650 (2004) like the air-to-air dual chamber (Figure 2.9.3) or thermal shock test that cycles between -65^{o}C and 125^{o}C for the same PTH designs. More recently Narayanaswamy, and Gonzalez (2007) used the CALCE PTH model to compare thermal cycling and IST, but the "results did not show a good correlation." Dual chamber thermal shock testing data has been correlated with

IST by taking specific designed coupons then performed side-by-side comparisons defining failures when the coupons achieved 10% increase in elevated resistance from an initial elevated resistance measurement. The testing of similar coupon designs cited in Chen, Bjorndahl, Parrish, Birch, and Carter (2003); Dancer (2000); and Estes and White (2005) showed that 100 thermal shock cycles equaled between 250 and 300 IST cycles. A starting point for future work would be to use the Modified Coffin-Manson relation in IPC-TR-579 (1988, pp. 41-42) and apply it to both thermal shock and IST data. This should also lead to the relationship between single chamber thermal cycling results. In the mean time industry needs statistical methods for Polyimide materials operating at higher temperatures than the IST coupons used here. In addition, statistical methods for using IST for Microvias is needed.

Future research leads toward developing S-N curves for both tin-lead and lead-free test vehicles to corroborate failure results by studying differences in S-N curves beyond just failure time comparisons where all that is known are vibration levels, statistically significant differences, and characteristic life or scale parameters. To this end, the S-N curves use the same failure times, but now include the strain level at failure. This added dimension to the analysis leads to a finer level of fidelity data that shows where on the S-N curve differences occur. The data in this study has been higher strains than found on most commercial airplanes, and therefore can be analyzed using linear regression, but better models take into account the more non-linear nature of the data to address the very conservative methods currently used. This data and others are being reviewed for

conditions found in commercial airplanes such data should show higher dispersion at the low strain levels similar to more homogeneous metals. Future life studies are planned for vibration at much lower strains leading to very high cycles to failure requiring methods like RFL Pascual and Meeker (1999) and making linear regression of S-N curves so conservative to be unusable for very low strains.

Side-by-side testing continues to be needed to convince customers that lead-free solder is viable for high reliability applications, models need to be calibrated to lower vibration levels too. All testing has been vibration only. Further testing is needed with combined thermal and vibration to determine at what point interactions synergistic or antagonistic exist.

REFERENCES

ARINC Specification 600-13 (March 30, 2001). *Air transport avionics equipment interfaces.* Annapolis, MD: Aeronautical Radio, Inc.

Arnold, J. (2008, August). “Reliability testing of Ni-modified SnCu and SAC305-vibration”. Paper presented at Surface Mount Technology Association International, Orlando, FL.

Bhandarkar, S. M.; Dasgupta, A.; Barker, D.; Pecht, M.; and Engelmaier, W. (1992). "Influence of selected design variables on thermo-mechanical stress distributions in plated through hole structures". *Transaction of the ASME - Journal of Electronic Packaging, 114*, pp. 8-13.

Black, G.; Ard, D; Smith, J; and Schibik, T. (2010). “The impact of the Weibull distribution on the performance of the single-factor ANOVA model”. *International Journal of Industrial Engineering Computations, 1*, pp. 185-198. Retrieved from http://www.GrowingScience.com/ijiec

Blattau, M. D. (1999). *Evaluation of IST test technology for plated through hole reliability* (Unpublished master’s thesis). College Park: University of Maryland.

Blevins, R. D. (1979). *Formulas for natural frequency and mode shape.* New York, NY: Van Nostrand Reinhold.

Center for Advanced Life Cycle Engineering (CALCE), “Vibration durability investigation for SAC and SnPb solder: Based on JCAA/JG-PP lead-free solder project test results,” in NASA TEERM Project1, Chapter 10 Modeling, October 25, 2006.

Center for Advanced Life Cycle Engineering (CALCE) Simulation Assisted Reliability Assessment (SARA®) Software (Version calceSARA® 6.1.6 Release, September 23, 2011) [Computer software]. College Park: University of Maryland, http://www.calce.umd.edu/software/.

Chen, W.; Bjorndahl, B.; Parrish, B.; Birch, B.; and Carter, R. (2003). *Printed wiring board reliability evaluation methods correlations of IST vs thermal shock.* Redondo Beach, CA: Society for the Advancement of Material and Process Engineering (SAMPE).

Cheung, Y. K.; Zhu, D. S.; and Iu, V. P. (1998). “Nonlinear vibration of thin plates with initial stress by spline finite strip method”. *Thin-Walled Structures, 32,* pp. 275-287.

Clech, J.-P. (2008). Solder Reliability Solutions™ (Version SRS 1.1) [Computer software]. Montclair, NJ: Electronic Packaging Solutions International, Inc. (ESPI), http://www.jpclech.com.

Cluff, K. D. (1996). *Characterizing the humidity and thermal environments of commercial avionics for accelerated test tailoring* (Unpublished doctoral dissertation). College Park: University of Maryland.

Cluff, K.D. and Osterman, M. (2002, March). "Defining accelerated test requirements for PWBs: A physics-based approach". Paper presented at Association Connecting Electronics Industries (IPC) Printed Circuits Exposition, Long Beach, CA.

Dancer, J. (2000). "PTH reliability and accelerated test methods," Delco Electronic Systems company presentation, www.pwbcorp.com.

Dieter, G. E. (1976). *Mechanical metallurgy*, (2nd ed.). New York, NY: McGraw-Hill.

Dubal, D. (2004). *The art of the piano: Its performances, literature, and recordings,* (3rd ed., p. 383). Pompton Plains, NJ: Amadeus Press.

Estes, T. A. and White, V.W. (2005). "Via reliability test methods", IPC D-36 Subcommittee. Northbrook, IL: IPC.

Faux, I. D. and Pratt, M. J. (1979). *Computational geometry for design and manufacture*. New York, NY: Halstead Press.

Feynman, R. P.; Leighton, R. B.; and Sands, M. (1963). *The Feynman lectures on physics: Mainly mechanics, radiation, and heat*, (Vol. 1). Reading, MA: Addison-Wesley.

Fu, C.; Ume, I. C.; and McDowell, D. L. (1998). "Thermal stress and fatigue analysis of plated-through holes using an internal state variable constitutive model". *Finite Elements in Analysis and Design, 30, pp. 1-17.*

George, E.; Das, D.; Osterman, M.and Pecht, M. (2011), "Thermal Cycling Reliability of Lead-Free Solders (SAC305 and Sn3.5Ag) for High Temperature Applications," *IEEE Transactions on Device and Materials Reliability, Vol. 11, No. 2,* pp. 328-338.

Government Engineering and Information Technology Association, GEIA-STD-0005-3_Test Protocol Draft 23, *Performance testing for aerospace and high performance electronic interconnects containing lead-free solder and finishes*. (2007).

Gu, C. (2000). Multivariate spline regression. In M. G. Schimek (Ed.), *Smoothing and regression: Approaches, computation, and application*, pp. 329-355. New York, NY: John Wiley & Sons.

IPC-6012B with Amendment 1, *Qualification and performance specification for rigid printed boards.* (2007, January). Bannockburn, IL: Association Connecting Electronics Industries (IPC), http://www.IPC.org

IPC-TM-650 *Test methods manual*, Test Methods Subcommittee (7-11). (2001, May). *DC current induced thermal cycling test* (Number 2.6.26). Northbrook, IL: Association Connecting Electronics Industries (IPC), http://www.IPC.org

IPC-TM-650 *Test methods manual*, Rigid Printed Board Performance Task Group. (2004, May). *Thermal shock, continuity and microsection, printed board* (Number 2.6.7.2). Northbrook, IL: Association Connecting Electronics Industries (IPC), http://www.IPC.org

IPC-TR-579 *Round robin reliability evaluation of small diameter plated through holes in printed wiring boards* (1988, September). Northbrook, IL: Association Connecting Electronics Industries (IPC), http://www.IPC.org

Joint Group on Pollution Prevention (JG-PP), "Joint Test Protocol J-01-EM-026-P1 for validation of alternatives to eutectic tin-lead solders used in manufacturing and rework of printed wiring assemblies," February 14, 2003 (Revised April 2004).

Juarez, J. M. and White, V. (2009). "Validating circuit board interconnect stress test preconditioning processes using statistical model comparisons of accelerated test data". *Quality Reliability Engineering International, 25*, pp. 885-895. doi:10.1002/qre.1008

Kessel, K., "Lead-free solder testing for high reliability (Project 1)," NASA Technology Evaluation for Environmental Risk Mitigation (TEERM) Principal Center Website, (http://teerm.nasa.gov/LeadFreeSolderTestingForHighRelaibility_Proj1.html) last updated 09/14/2010.

Lau, J. H. (1994). A brief introduction to fine pitch surface mount technology. In J. H. Lau (Ed.), *Handbook of fine pitch surface mount technology* (pp. 1-54). New York, NY: Van Nostrand Reinhold.

Meeker, W. Q. and Escobar, L. A. (1998). *Statistical methods for reliability data*. New York, NY: John Wiley & Sons.

MIL-STD-810F, Department of defense test method standard for environmental engineering considerations and laboratory tests. (2000). Wright-Patterson AFB, OH: Author.

Miner, M. A. (1945). "Cumulative damage in fatigue". *Journal of Applied Mechanics, 12*, pp. A159-A164.

Mirman, B.A. (1988). "Mathematical model of a plated-through hole under a load induced by thermal mismatch". *IEEE Transactions on Components, Hybrids, and Manufacturing Technology, 11*, pp. 506-511.

Monroe, E. M. and Pan, R. (2008). "Experimental design considerations for accelerated life tests with nonlinear constraints and censoring," *Journal of Quality Technology, 40*, pp. 355-67.

Montgomery, D.C. (2007). *Design and analysis of experiments*, (7th ed.). New York, NY: John Wiley & Sons.

Montgomery, D. C., Peck, E. A., and Vining, G. G. (2001). *Introduction to linear regression analysis*, (3rd ed.). New York, NY: John Wiley & Sons.

Montgomery, D. C. and Runger, G. C. (2003). *Applied statistics and probability for engineers*, (3rd ed.). New York, NY: John Wiley & Sons.

Narayanaswamy, M. and Gonzalez, R. (2007, February). "A DOE to assess PCB fabrication material design and process using IST (interconnect stress testing) to improve fine pitch BGA via reliability". Paper presented at the IPC Printed Circuits Exposition, APEX and the Designers Summit, Los Angeles, CA.

Nelson, W. (1990). *Accelerated testing: Statistical models, test plans, and data analyses*. New York, NY: John Wiley & Sons.

Office of Naval Research (2009, July 30). *The lead free electronics Manhattan project – Phase I* (U.S. Government Contract No. N00014-08-D-0758). Available from ACI Technologies.

Pascual, F. G. and Meeker, W. Q. (1999). "Estimating fatigue curves with the random fatigue-limit model". *Technometrics, 41*, pp. 277-290.

Popov, E. P. (1968). *Introduction to mechanics of solids.* Englewood Cliffs, NJ: Prentice-Hall.

Rigdon, S. E.; Ma, X.; and Bodden, K. M. (1998). "Statistical inference for repairable systems using the power law process". *Journal of Quality Technology, 30*, pp. 395-400.

RTCA/DO-160D (July 29, 1997). *Environmental Conditions and test procedures for airborne equipment.* Chapter 8, Vibration. Washington, DC: RTCA, Inc.

Scott, R. E. (1965). *Elements of linear circuits*. Reading, MA: Addison-Wesley.

Slough, B. (2005, May 27). *IST correlation study between Multek Asia, PWB Interconnect Solutions, and Multek Germany* (Report number MET161404, Tracking #1614). Jingan Town, Doumen, Zhuhai, Guangdong, PRC: Multek Asia Analytical & Materials Development Lab.

Starr, J.E. (2006). "JCAA/JG-PP lead-free solder project: Vibration test, solder comparison by component level life-use analysis". Chapter 10 Modeling in NASA TEERM Project1. Plymouth, MN: CirVibe Inc.

Steinberg, D. S. (1991). *Cooling techniques for electronic equipment*, (2nd ed.). New York, NY: John Wiley & Sons.

Steinberg, D. S. (2000). *Vibration analysis for electronic equipment*, (3rd ed.). New York, NY: John Wiley & Sons.

Tobias, P. A. and Trindade, D. C. (1995). *Applied reliability*, (2nd ed.). Boca Raton, FL: Chapman and Hall/CRC.

Van Vlack, L. H. (1975). *Elements of materials science and engineering*, (3rd ed.). Reading, MA: Addison-Wesley.

Wang, F.-K.; Cheng, Y.-F.; and Lu, W.-L. (in press). "Partially accelerated life tests for the Weibull distribution under multiply censored data". *Quality Reliability Engineering International*, to appear.

Wang, N.; Kvam, P.; and Lu, J.-C. (2007). "Detection and estimation of a mixture in power law processes for a repairable system". *Journal of Quality Technology, 39*, pp. 140-150.

Woodrow, T. A. (January 9, 2006). "JCAA/JG-PP lead-free solder project: vibration test," Boeing Electronics Materials and Processes Report – 582, Revision A.

Woodrow, T.A. (2007). "Modeling of the JCAA/JG-PP lead-free solder project vibration test data". IPC/JEDEC Global Conference on Lead free Reliability & Reliability Testing, Boston, MA.

Woodrow, T. A. (November 18, 2010). “NASA-DoD lead-free electronics project: vibration test,” Boeing Electronics Materials and Processes Report – 603, Revision A.

Yoder, D. D.; Bhandarkar S. M.; and Dasgupta A. (1993, after May). “Experimental and analytical investigations in Aramid PWBs-Part2”. Association Connecting Electronics Industries (IPC) *Review, pp. 20-27*.

Zhou, Y. (2008). *Harmonic and random vibration durability investigation for SAC305 (Sn3.0Ag0.5Cu)solder joint* (Unpublished doctoral dissertation). College Park: University of Maryland.

Zhou, Y.; Al-Bassyiouni, M.; and Dasgupta, A. (2010). “Harmonic and random vibration durability of SAC305 and Sn37Pb solder alloys”. *IEEE Transactions on Components and Packaging Technologies, Vol. 33, No. 2*, June 2010, pp. 319-328.

Zhou, Y. and Dasgupta, A. (2007, November). “Vibration durability assessment of Sn3.0Ag0.5Cu & Sn37Pb solders under harmonic excitation”. In Proceeding of ASME International Mechanical Engineering Conference and Exposition, Seattle, WA.

Zhou, Y.; Scanff, E.; and Dasgupta, A. (2006, November). “Vibration durability comparison of Sn37Pb vs. SnAgCu solders”. In Proceeding of ASME International Mechanical Engineering Conference and Exposition, Chicago, IL.

APPENDIX A

CHAPTER 3 MINITAB VERSION 16 PLOTS USED TO IDENTIFY THE DISTRIBUTIONS AND ACCOMPANY THE LIKELIHOOD RATIO TEST RESULTS IN APPENDIX B

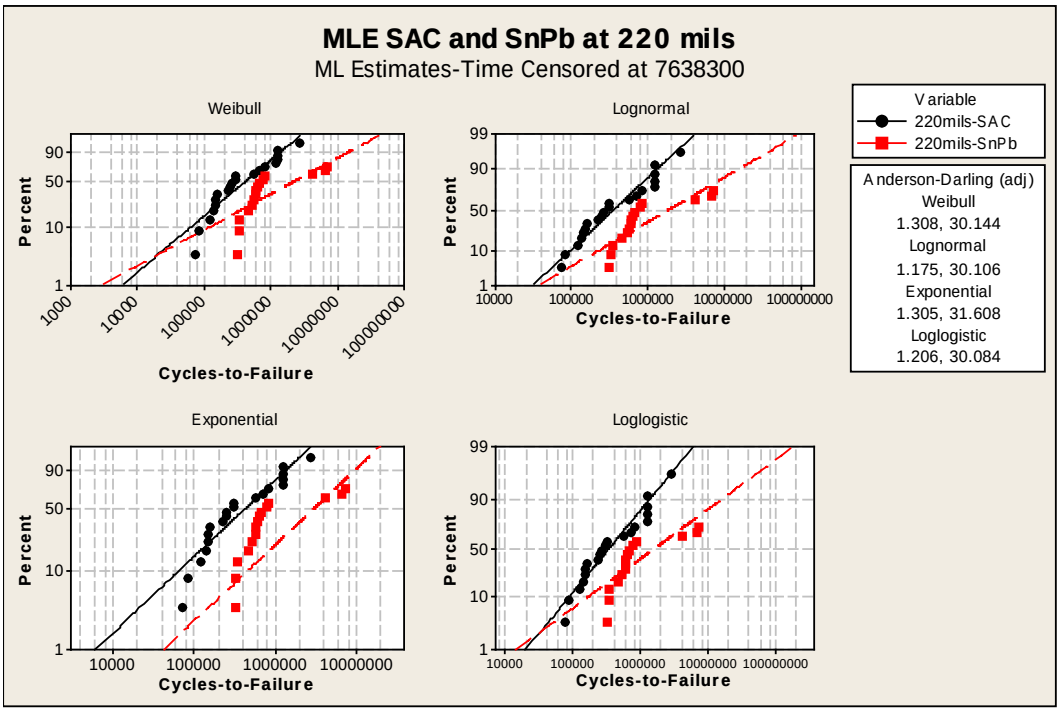
MLE SAC and SnPb at 220 mils
ML Estimates-Time Censored at 7638300
Weibull
Lognormal
Exponential
Loglogistic
Percent
Cycles-to-Failure
Variable
220mils-SAC
220mils-SnPb
Anderson-Darling (adj)
Weibull
1.308, 30.144
Lognormal
1.175, 30.106
Exponential
1.305, 31.608
Loglogistic
1.206, 30.084

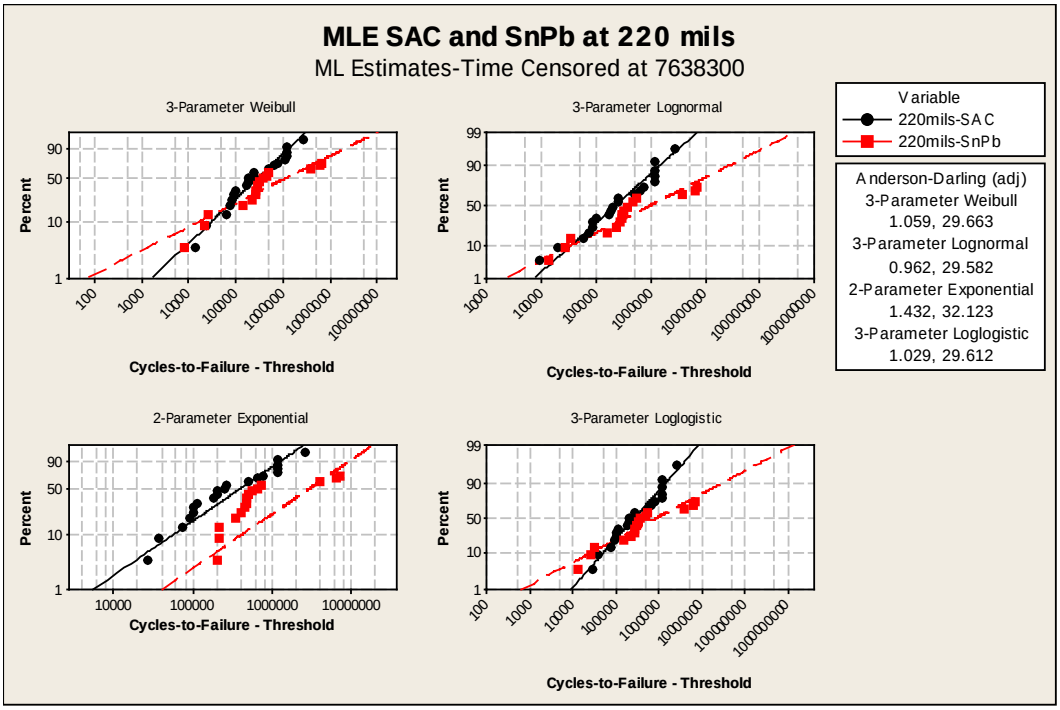
MLE SAC and SnPb at 220 mils
ML Estimates-Time Censored at 7638300
3-Parameter Weibull
3-Parameter Lognormal
2-Parameter Exponential
3-Parameter Loglogistic
Percent
Cycles-to-Failure - Threshold
Variable
220mils-SAC
220mils-SnPb
Anderson-Darling (adj)
3-Parameter Weibull
1.059, 29.663
3-Parameter Lognormal
0.962, 29.582
2-Parameter Exponential
1.432, 32.123
3-Parameter Loglogistic
1.029, 29.612

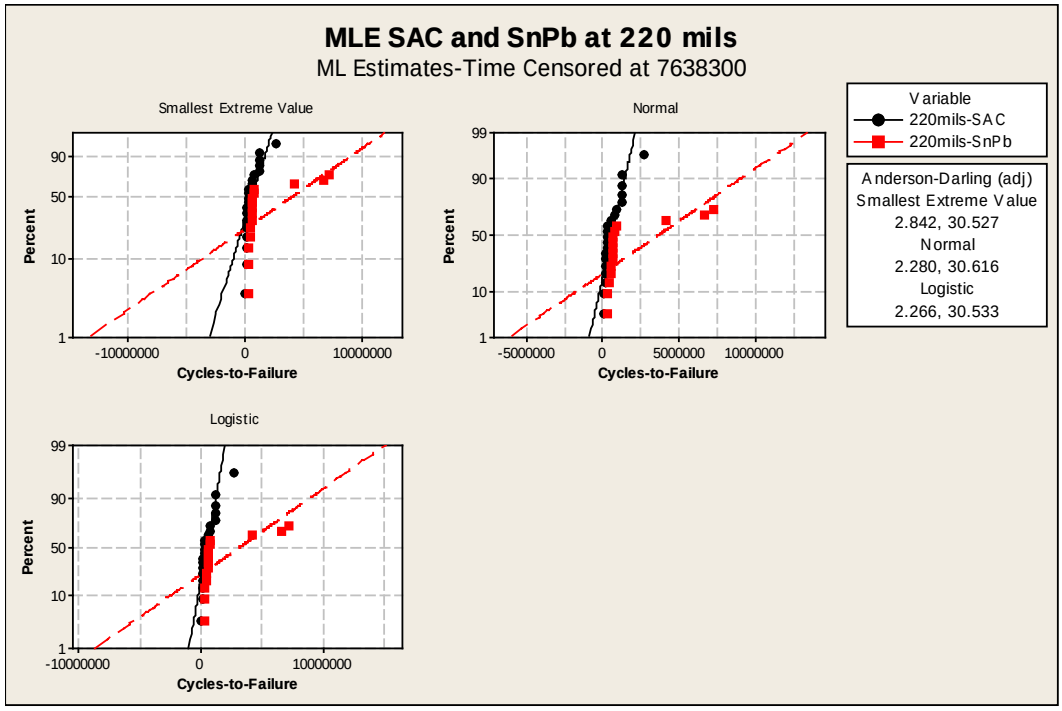
MLE SAC and SnPb at 220 mils
ML Estimates-Time Censored at 7638300
Smallest Extreme Value
Normal
Logistic
Percent
Cycles-to-Failure
Variable
220mils-SAC
220mils-SnPb
Anderson-Darling (adj)
Smallest Extreme Value
2.842, 30.527
Normal
2.280, 30.616
Logistic
2.266, 30.533

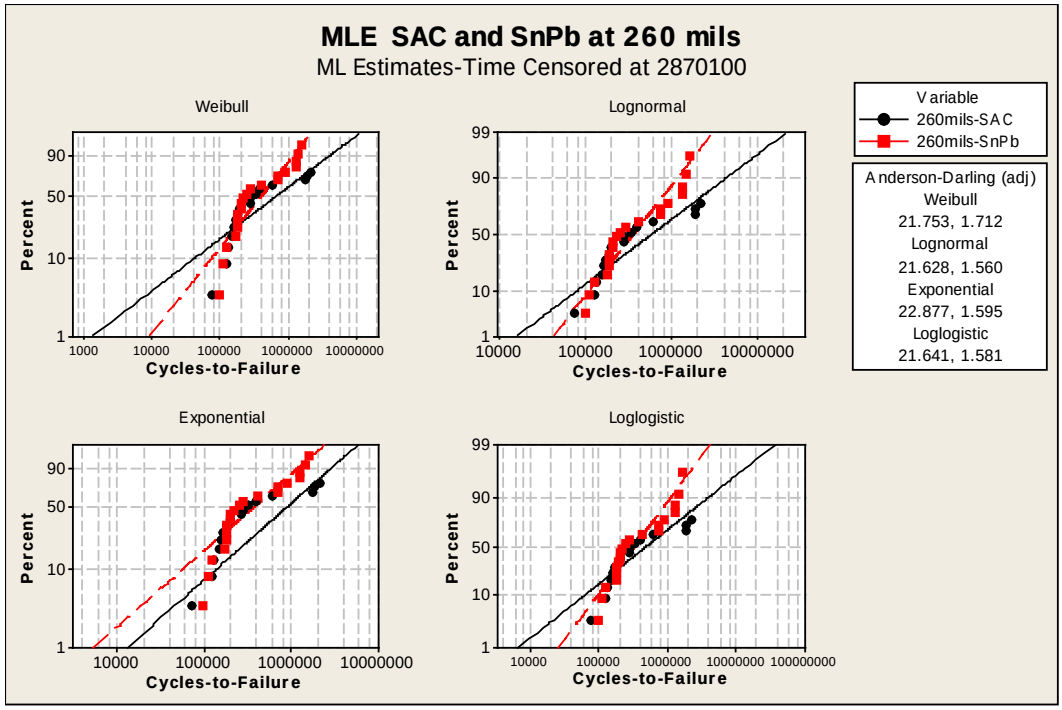
MLE SAC and SnPb at 260 mils
ML Estimates-Time Censored at 2870100
Weibull
Lognormal
Exponential
Loglogistic
Percent
Cycles-to-Failure
Variable
260mils-SAC
260mils-SnPb
Anderson-Darling (adj)
Weibull
21.753, 1.712
Lognormal
21.628, 1.560
Exponential
22.877, 1.595
Loglogistic
21.641, 1.581

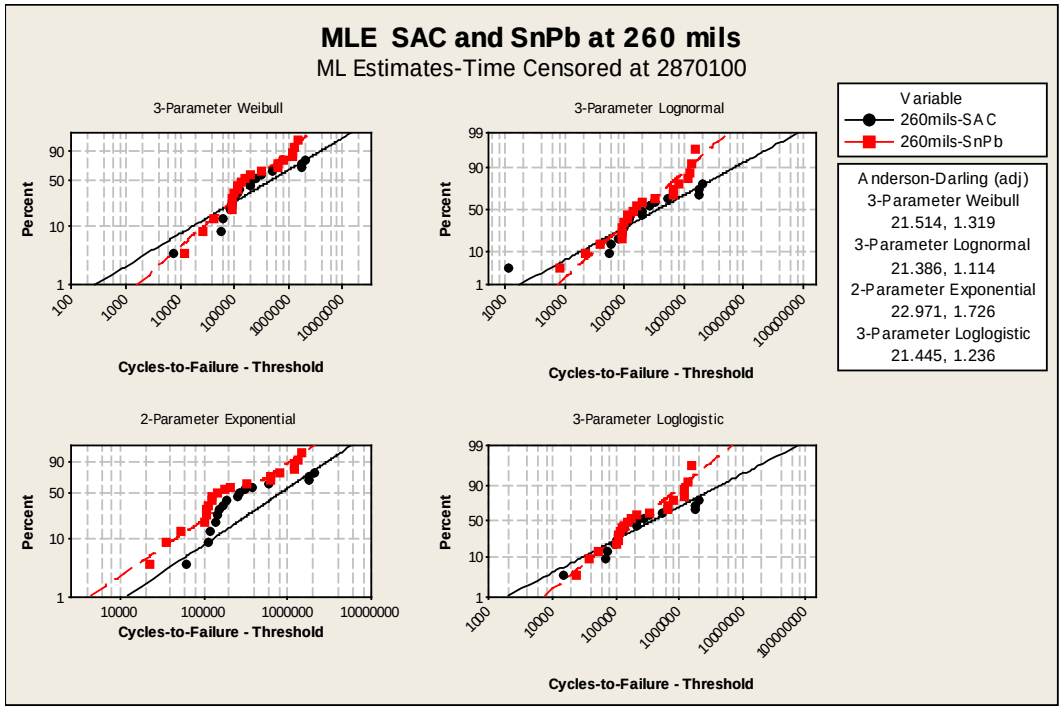
MLE SAC and SnPb at 260 mils
ML Estimates-Time Censored at 2870100
3-Parameter Weibull
3-Parameter Lognormal
2-Parameter Exponential
3-Parameter Loglogistic
Percent
Cycles-to-Failure - Threshold
Variable
260mils-SAC
260mils-SnPb
Anderson-Darling (adj)
3-Parameter Weibull
21.514, 1.319
3-Parameter Lognormal
21.386, 1.114
2-Parameter Exponential
22.971, 1.726
3-Parameter Loglogistic
21.445, 1.236

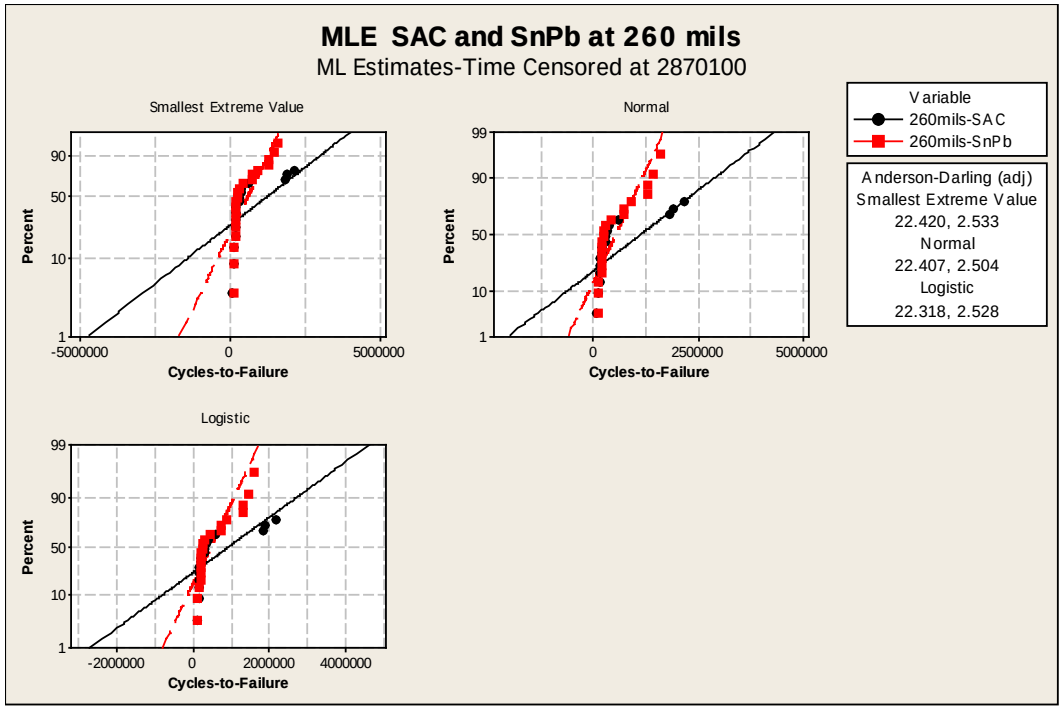
MLE SAC and SnPb at 260 mils
ML Estimates-Time Censored at 2870100
Smallest Extreme Value
Normal
Logistic
Percent
Cycles-to-Failure
Variable
260mils-SAC
260mils-SnPb
Anderson-Darling (adj)
Smallest Extreme Value
22.420, 2.533
Normal
22.407, 2.504
Logistic
22.318, 2.528

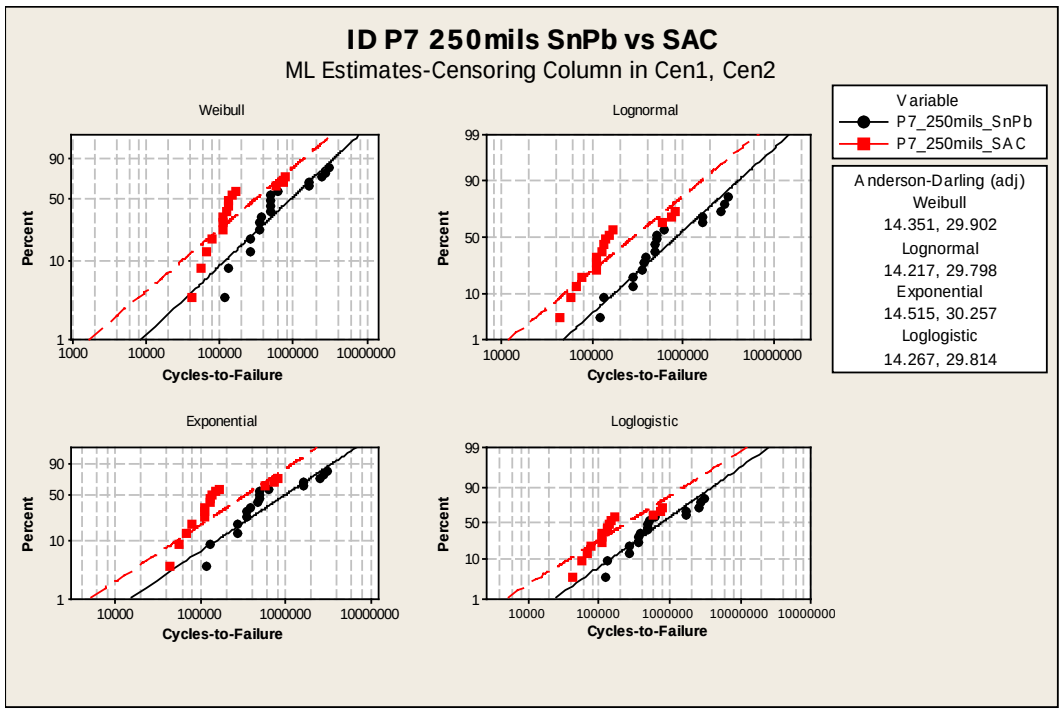
ID P7 250mils SnPb vs SAC
ML Estimates-Censoring Column in Cen1, Cen2
Weibull
Lognormal
Exponential
Loglogistic
Percent
Cycles-to-Failure
Variable
P7_250mils_SnPb
P7_250mils_SAC
Anderson-Darling (adj)
Weibull
14.351, 29.902
Lognormal
14.217, 29.798
Exponential
14.515, 30.257
Loglogistic
14.267, 29.814

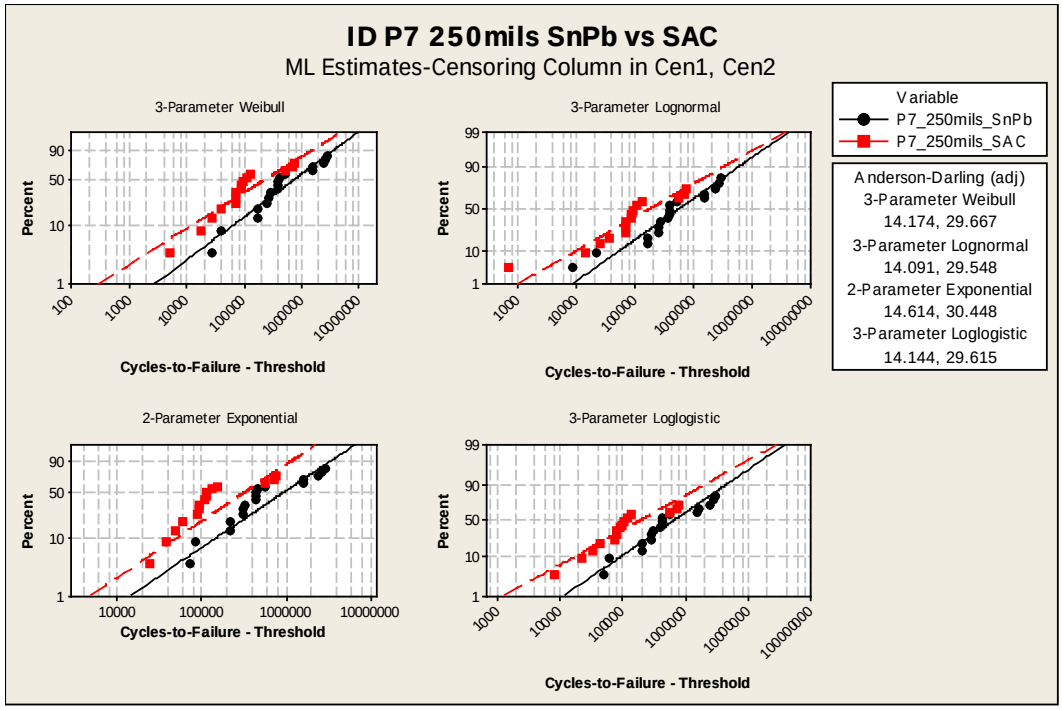
ID P7 250mils SnPb vs SAC
ML Estimates-Censoring Column in Cen1, Cen2
3-Parameter Weibull
3-Parameter Lognormal
2-Parameter Exponential
3-Parameter Loglogistic
Percent
Cycles-to-Failure - Threshold
Variable
P7_250mils_SnPb
P7_250mils_SAC
Anderson-Darling (adj)
3-Parameter Weibull
14.174, 29.667
3-Parameter Lognormal
14.091, 29.548
2-Parameter Exponential
14.614, 30.448
3-Parameter Loglogistic
14.144, 29.615

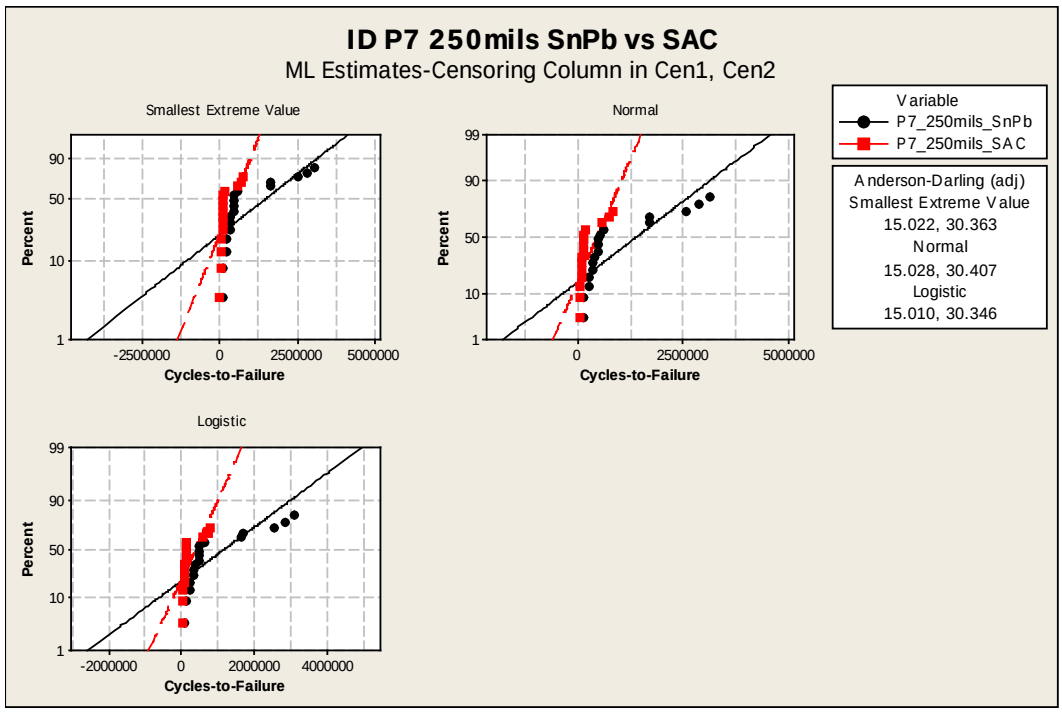
ID P7 250mils SnPb vs SAC
ML Estimates-Censoring Column in Cen1, Cen2
Smallest Extreme Value
Normal
Logistic
Percent
Cycles-to-Failure
Variable
P7_250mils_SnPb
P7_250mils_SAC
Anderson-Darling (adj)
Smallest Extreme Value
15.022, 30.363
Normal
15.028, 30.407
Logistic
15.010, 30.346

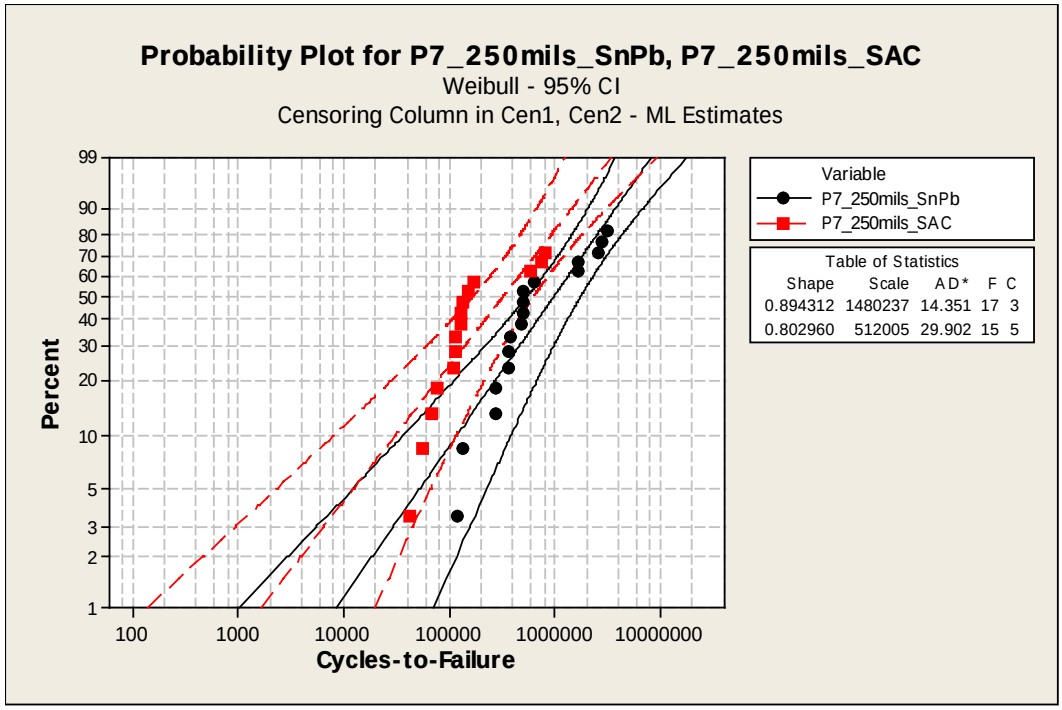
Probability Plot for P7_250mils_SnPb, P7_250mils_SAC
Weibull - 95% CI
Censoring Column in Cen1, Cen2 - ML Estimates
Percent
Cycles-to-Failure
Variable
P7_250mils_SnPb
P7_250mils_SAC
Table of Statistics
Shape Scale AD* F C
0.894312 1480237 14.351 17 3
0.802960 512005 29.902 15 5

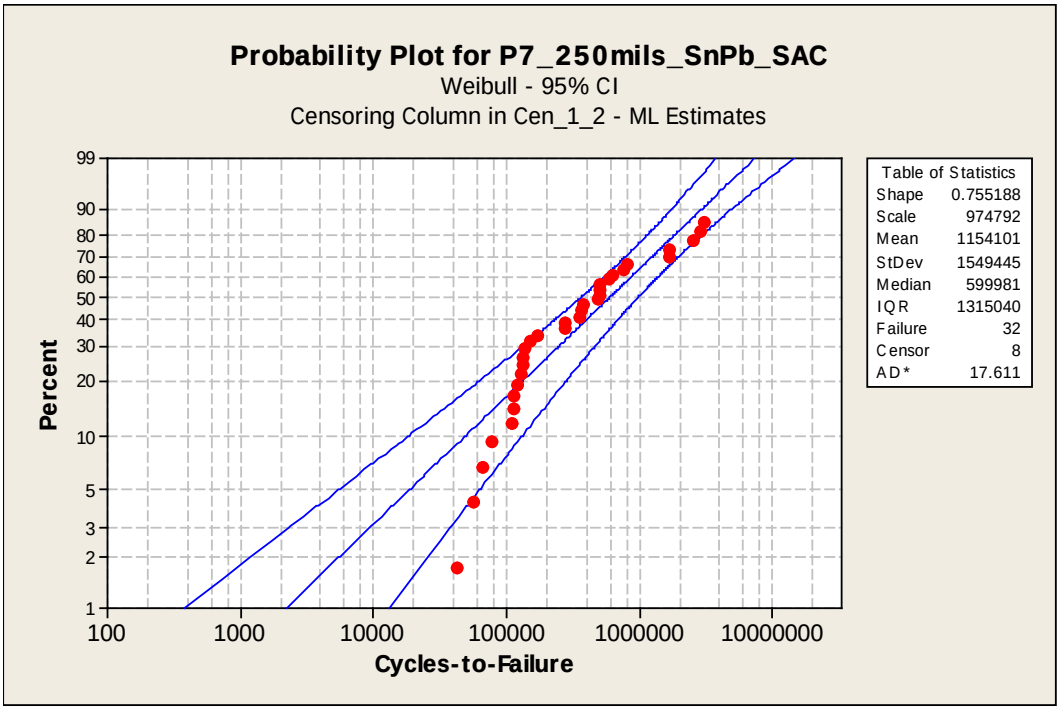
Probability Plot for P7_250mils_SnPb_SAC
Weibull - 95% CI
Censoring Column in Cen_1_2 - ML Estimates
Percent
Cycles-to-Failure
Table of Statistics
Shape 0.755188
Scale 974792
Mean 1154101
StDev 1549445
Median 599981
IQR 1315040
Failure 32
Censor 8
AD* 17.611

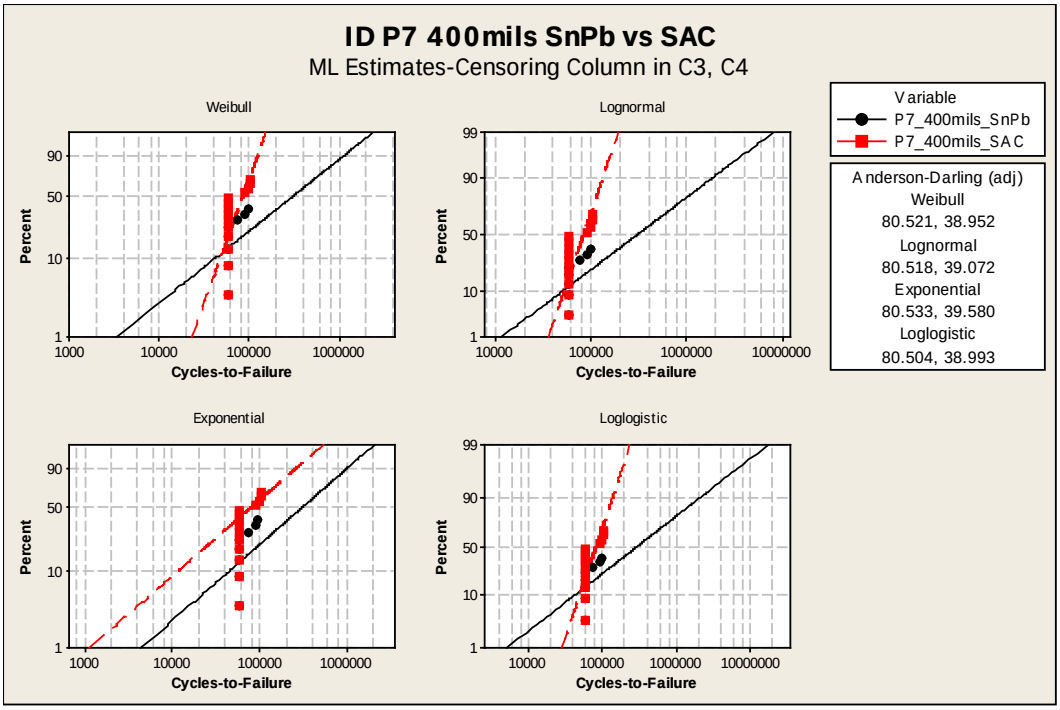
ID P7 400mils SnPb vs SAC
ML Estimates-Censoring Column in C3, C4
Weibull
Lognormal
Exponential
Loglogistic
Percent
Cycles-to-Failure
Variable
P7_400mils_SnPb
P7_400mils_SAC
Anderson-Darling (adj)
Weibull
80.521, 38.952
Lognormal
80.518, 39.072
Exponential
80.533, 39.580
Loglogistic
80.504, 38.993

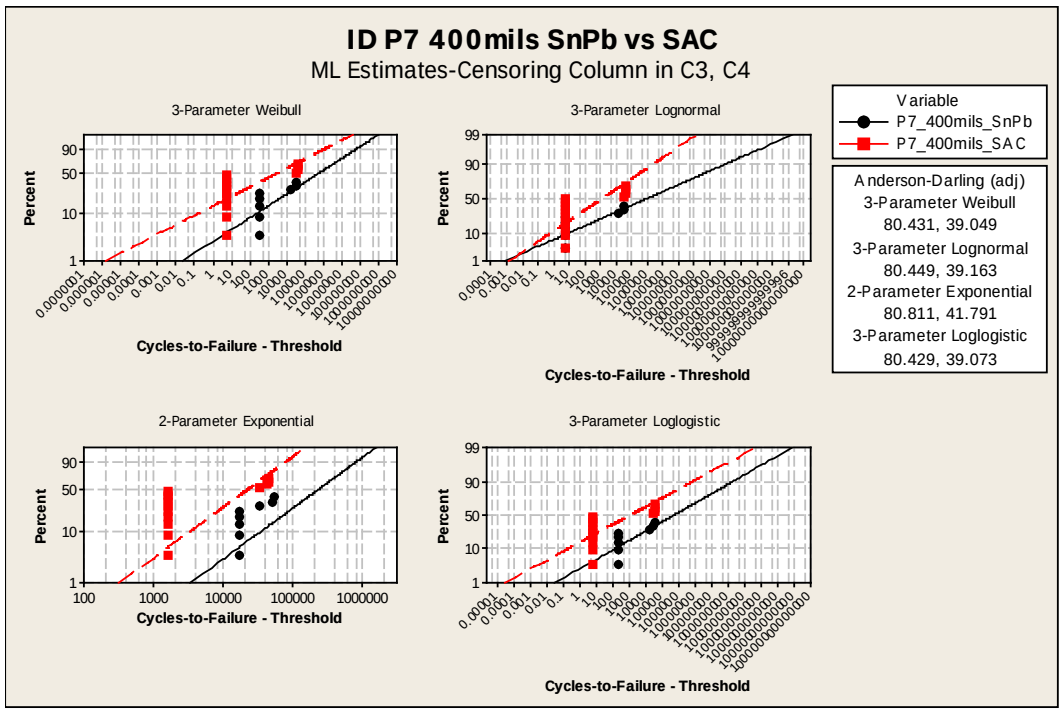
ID P7 400mils SnPb vs SAC
ML Estimates-Censoring Column in C3, C4
3-Parameter Weibull
3-Parameter Lognormal
2-Parameter Exponential
3-Parameter Loglogistic
Percent
Cycles-to-Failure - Threshold
Variable
P7_400mils_SnPb
P7_400mils_SAC
Anderson-Darling (adj)
3-Parameter Weibull
80.431, 39.049
3-Parameter Lognormal
80.449, 39.163
2-Parameter Exponential
80.811, 41.791
3-Parameter Loglogistic
80.429, 39.073

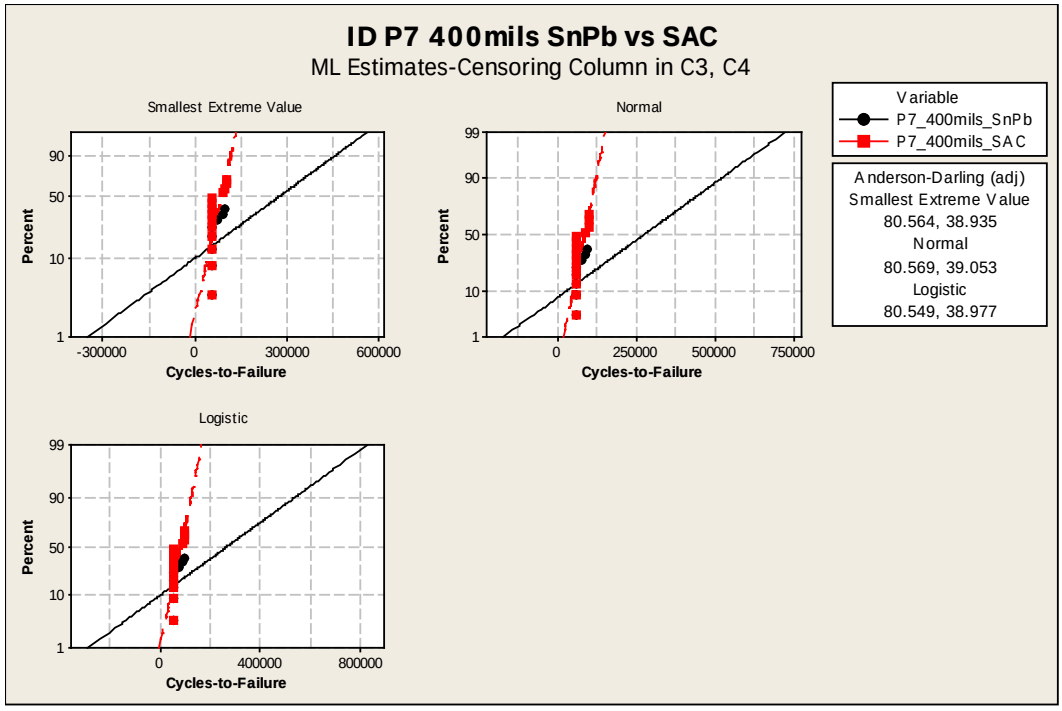
ID P7 400mils SnPb vs SAC
ML Estimates-Censoring Column in C3, C4
Smallest Extreme Value
Normal
Logistic
Percent
Cycles-to-Failure
Variable
P7_400mils_SnPb
P7_400mils_SAC
Anderson-Darling (adj)
Smallest Extreme Value
80.564, 38.935
Normal
80.569, 39.053
Logistic
80.549, 38.977

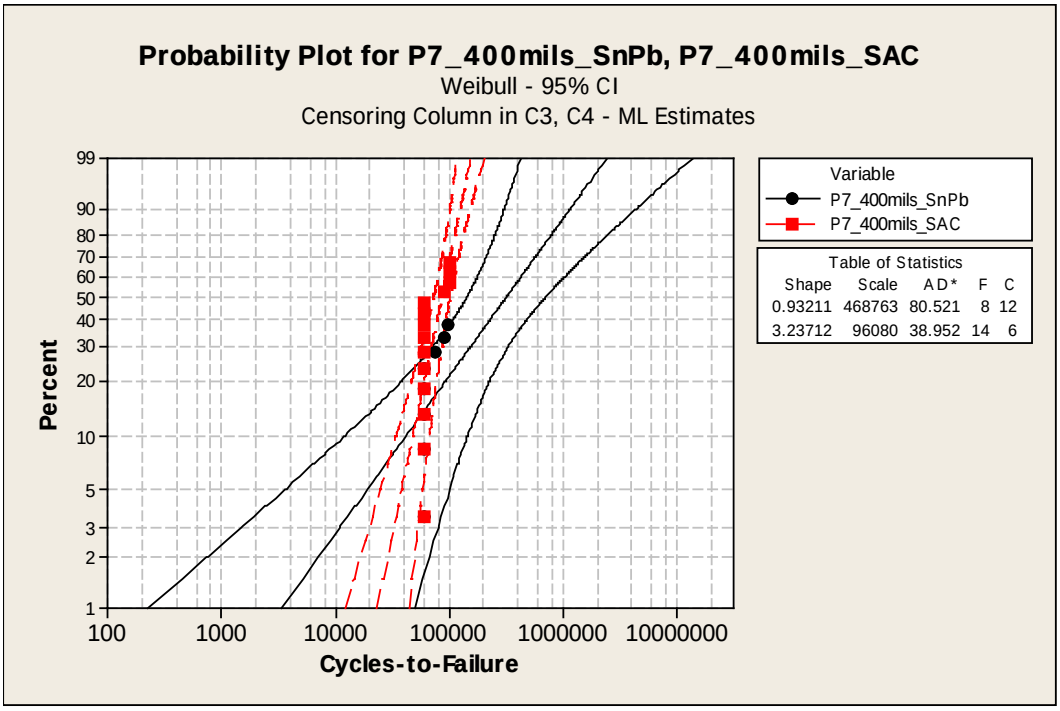
Probability Plot for P7_400mils_SnPb, P7_400mils_SAC
Weibull - 95% CI
Censoring Column in C3, C4 - ML Estimates
Percent
Cycles-to-Failure
Variable
P7_400mils_SnPb
P7_400mils_SAC
Table of Statistics
Shape Scale AD* F C
0.93211 468763 80.521 8 12
3.23712 96080 38.952 14 6

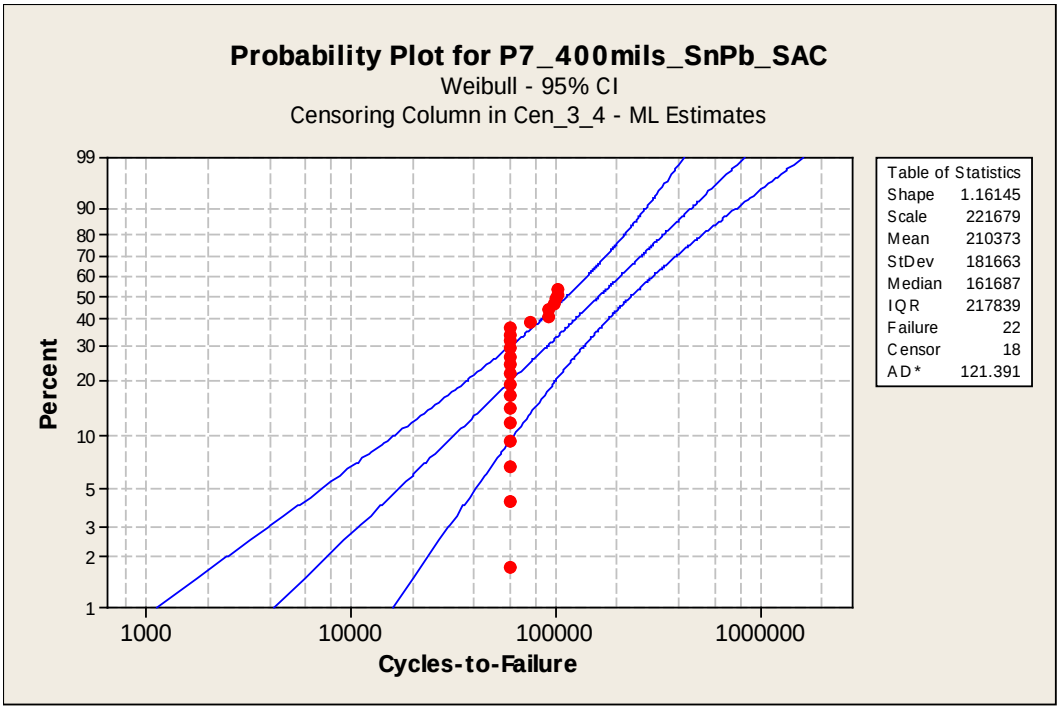
Probability Plot for P7_400mils_SnPb_SAC
Weibull - 95% CI
Censoring Column in Cen_3_4 - ML Estimates
Percent
Cycles-to-Failure
Table of Statistics
Shape 1.16145
Scale 221679
Mean 210373
StDev 181663
Median 161687
IQR 217839
Failure 22
Censor 18
AD* 121.391

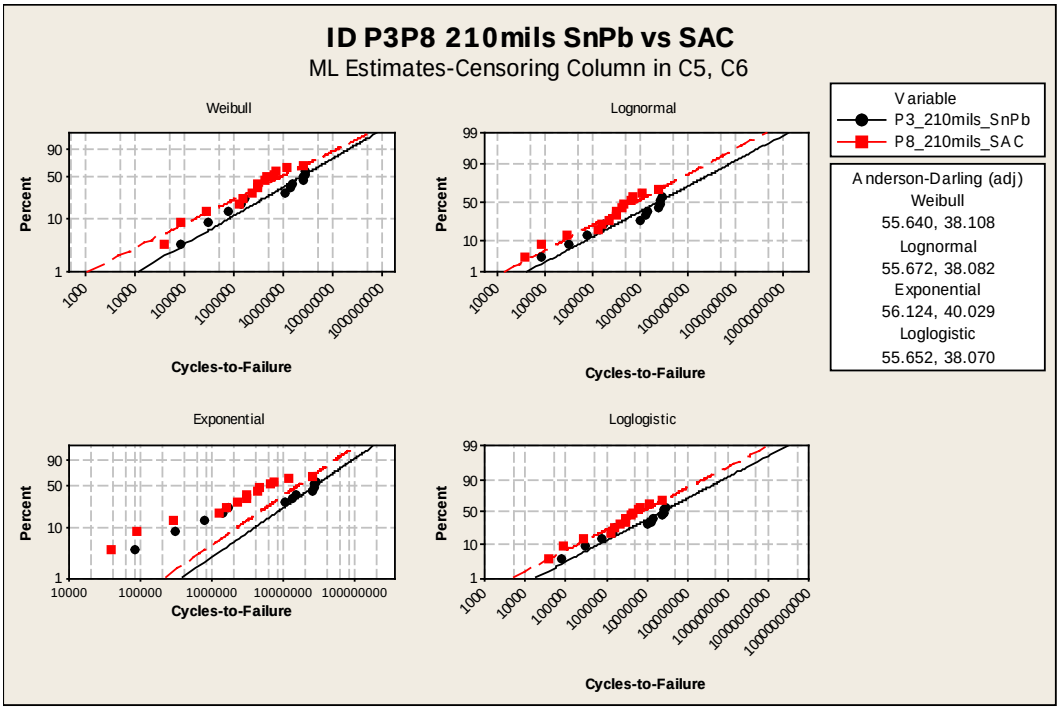
ID P3P8 210mils SnPb vs SAC
ML Estimates-Censoring Column in C5, C6
Weibull
Lognormal
Exponential
Loglogistic
Percent
Cycles-to-Failure
Variable
P3_210mils_SnPb
P8_210mils_SAC
Anderson-Darling (adj)
Weibull
55.640, 38.108
Lognormal
55.672, 38.082
Exponential
56.124, 40.029
Loglogistic
55.652, 38.070

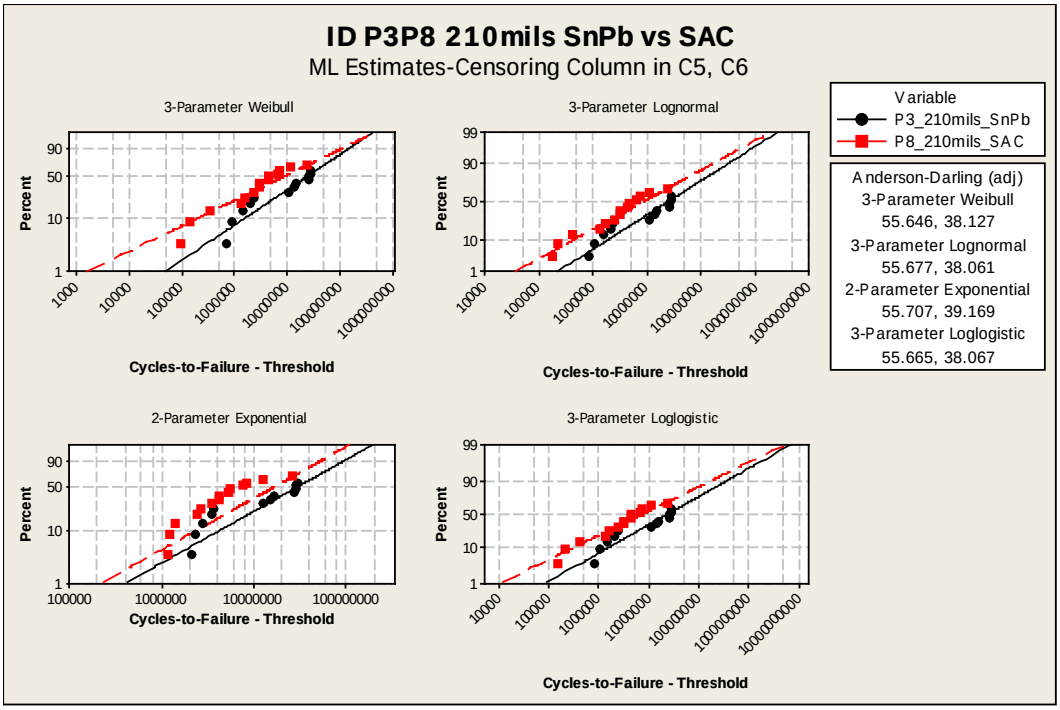
ID P3P8 210mils SnPb vs SAC
ML Estimates-Censoring Column in C5, C6
3-Parameter Weibull
3-Parameter Lognormal
2-Parameter Exponential
3-Parameter Loglogistic
Percent
Cycles-to-Failure - Threshold
Variable
P3_210mils_SnPb
P8_210mils_SAC
Anderson-Darling (adj)
3-Parameter Weibull
55.646, 38.127
3-Parameter Lognormal
55.677, 38.061
2-Parameter Exponential
55.707, 39.169
3-Parameter Loglogistic
55.665, 38.067

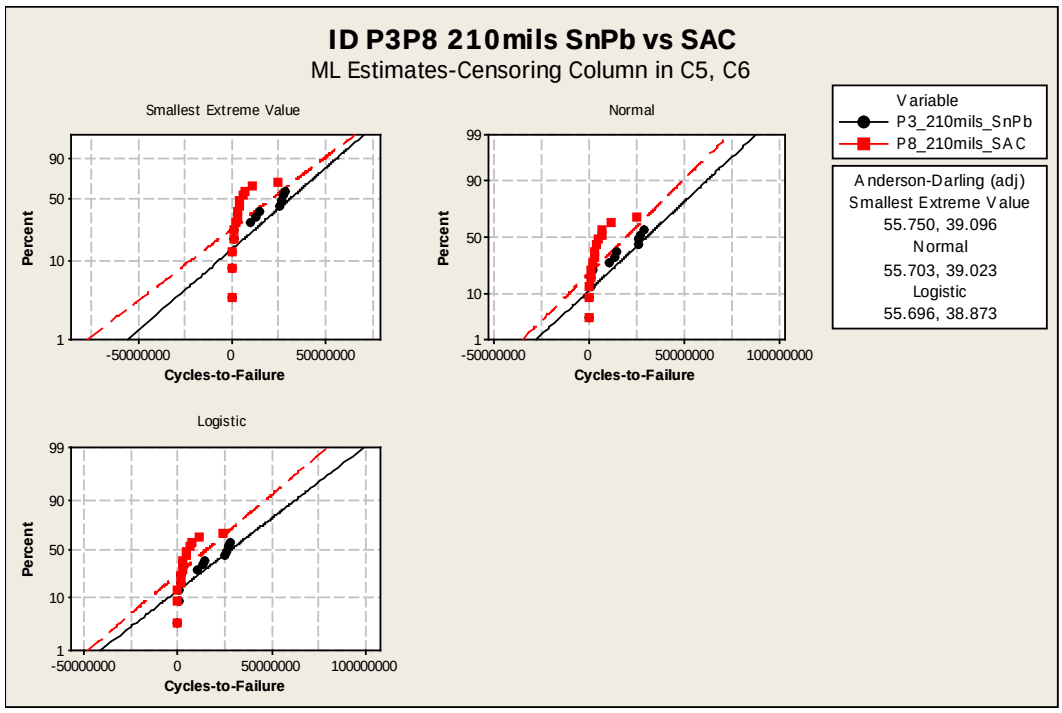
ID P3P8 210mils SnPb vs SAC
ML Estimates-Censoring Column in C5, C6
Smallest Extreme Value
Normal
Logistic
Percent
Cycles-to-Failure
Variable
P3_210mils_SnPb
P8_210mils_SAC
Anderson-Darling (adj)
Smallest Extreme Value
55.750, 39.096
Normal
55.703, 39.023
Logistic
55.696, 38.873

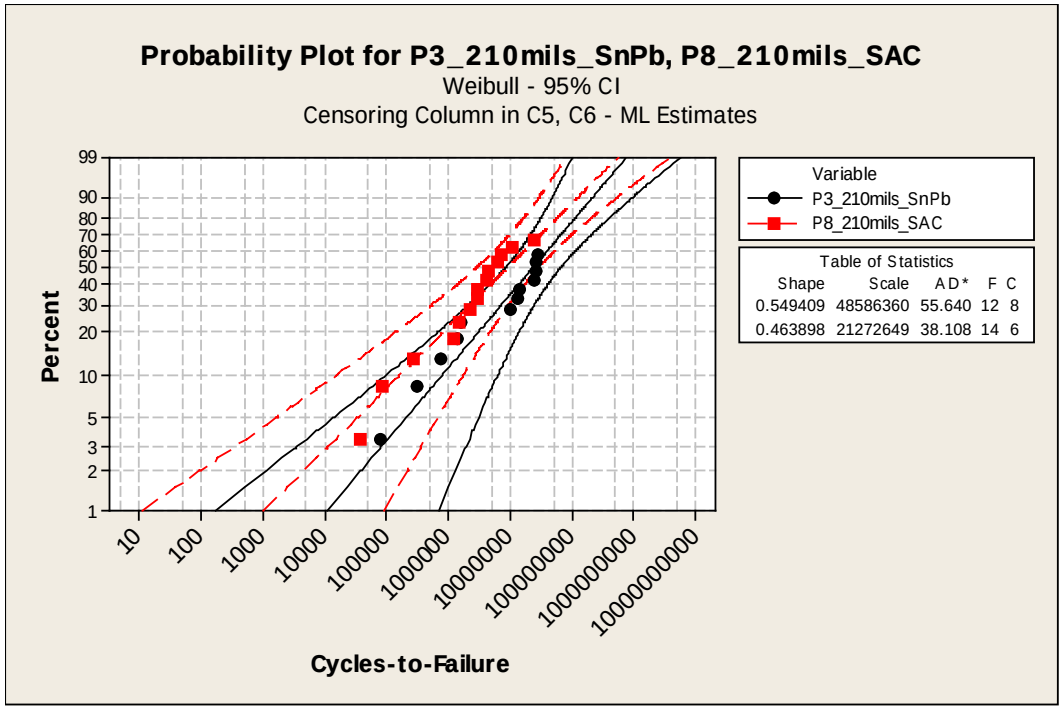
Probability Plot for P3_210mils_SnPb, P8_210mils_SAC
Weibull - 95% CI
Censoring Column in C5, C6 - ML Estimates
Percent
Cycles-to-Failure
Variable
P3_210mils_SnPb
P8_210mils_SAC
Table of Statistics
Shape Scale AD* F C
0.549409 48586360 55.640 12 8
0.463898 21272649 38.108 14 6

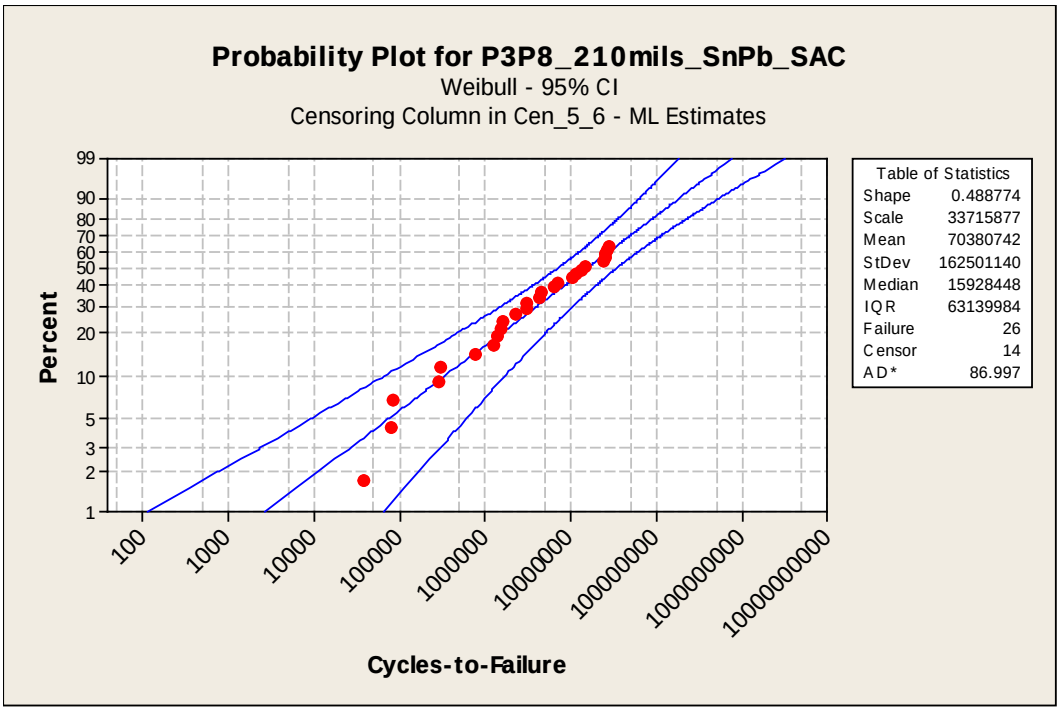
Probability Plot for P3P8_210mils_SnPb_SAC
Weibull - 95% CI
Censoring Column in Cen_5_6 - ML Estimates
Percent
Cycles-to-Failure
Table of Statistics
Shape 0.488774
Scale 33715877
Mean 70380742
StDev 162501140
Median 15928448
IQR 63139984
Failure 26
Censor 14
AD* 86.997

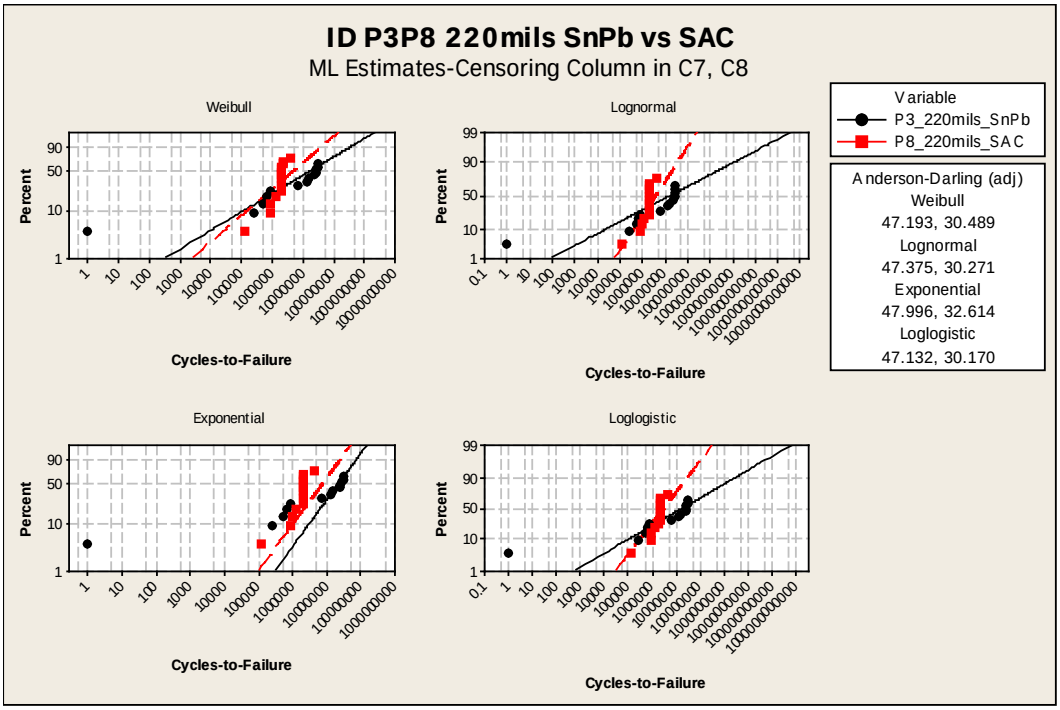
ID P3P8 220mils SnPb vs SAC
ML Estimates-Censoring Column in C7, C8
Weibull
Lognormal
Exponential
Loglogistic
Percent
Cycles-to-Failure
Variable
P3_220mils_SnPb
P8_220mils_SAC
Anderson-Darling (adj)
Weibull
47.193, 30.489
Lognormal
47.375, 30.271
Exponential
47.996, 32.614
Loglogistic
47.132, 30.170

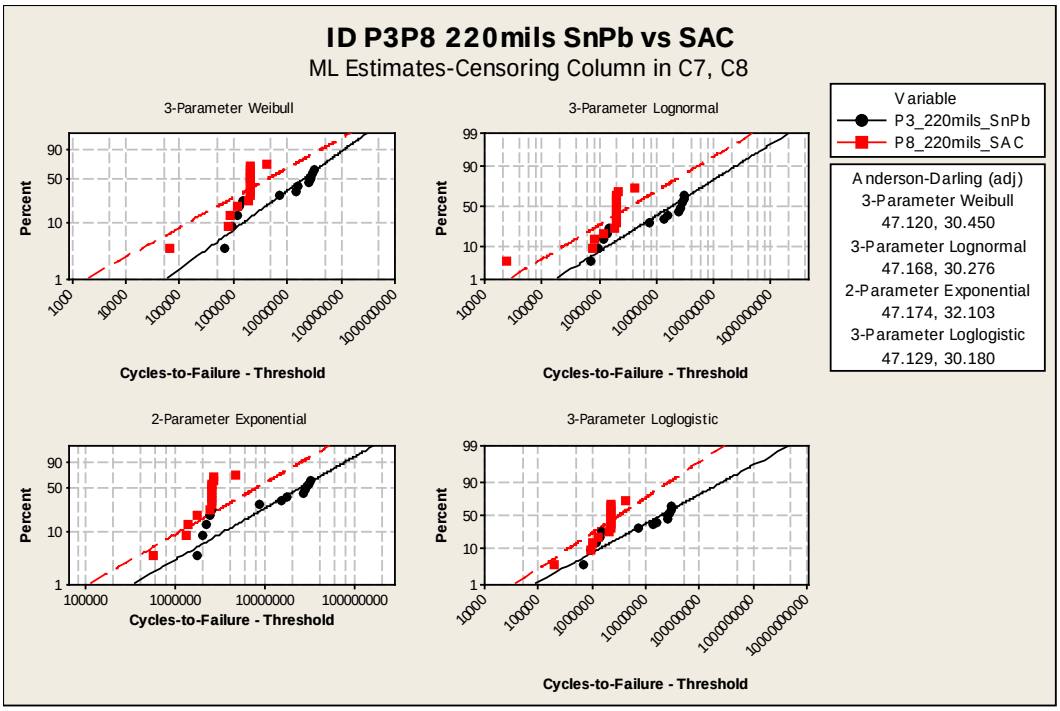
ID P3P8 220mils SnPb vs SAC
ML Estimates-Censoring Column in C7, C8
3-Parameter Weibull
3-Parameter Lognormal
2-Parameter Exponential
3-Parameter Loglogistic
Percent
Cycles-to-Failure - Threshold
Variable
P3_220mils_SnPb
P8_220mils_SAC
Anderson-Darling (adj)
3-Parameter Weibull
47.120, 30.450
3-Parameter Lognormal
47.168, 30.276
2-Parameter Exponential
47.174, 32.103
3-Parameter Loglogistic
47.129, 30.180

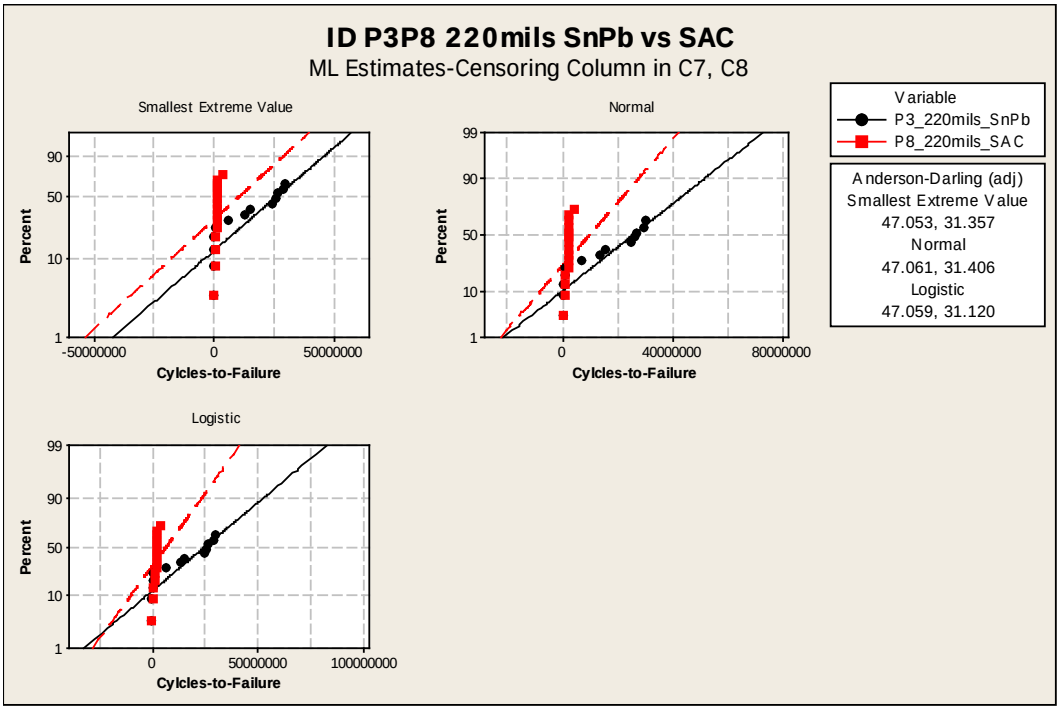
ID P3P8 220mils SnPb vs SAC
ML Estimates-Censoring Column in C7, C8
Smallest Extreme Value
Normal
Logistic
Percent
Cyclcles-to-Failure
Variable
P3_220mils_SnPb
P8_220mils_SAC
Anderson-Darling (adj)
Smallest Extreme Value
47.053, 31.357
Normal
47.061, 31.406
Logistic
47.059, 31.120

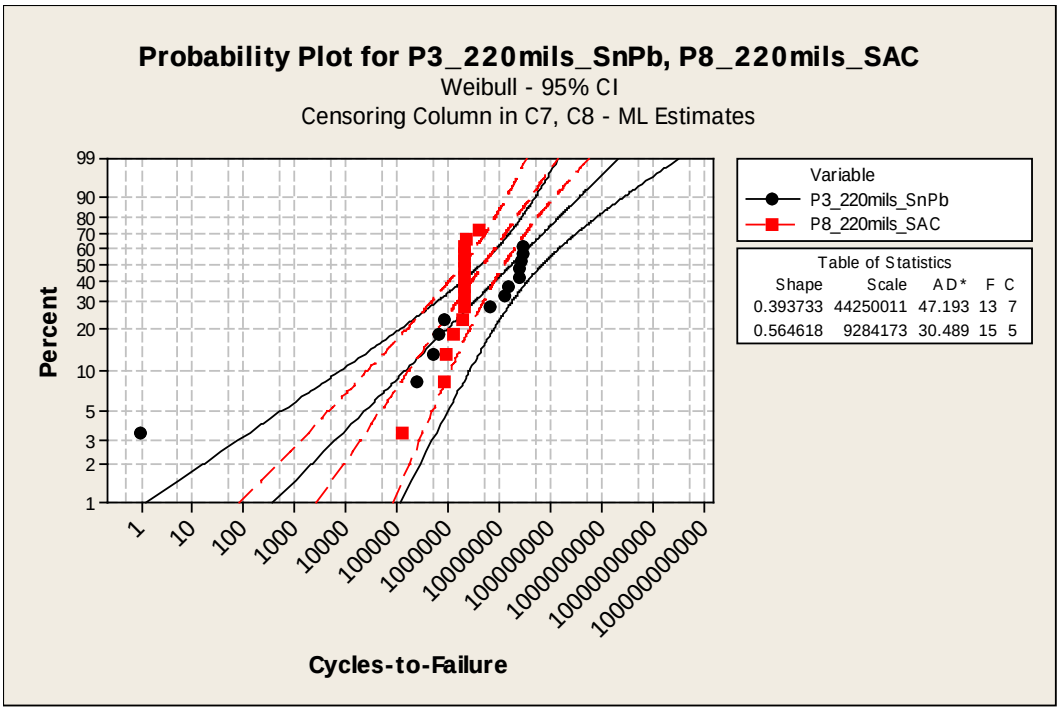
Probability Plot for P3_220mils_SnPb, P8_220mils_SAC
Weibull - 95% CI
Censoring Column in C7, C8 - ML Estimates
Percent
Cycles-to-Failure
Variable
P3_220mils_SnPb
P8_220mils_SAC
Table of Statistics
Shape Scale AD* F C
0.393733 44250011 47.193 13 7
0.564618 9284173 30.489 15 5

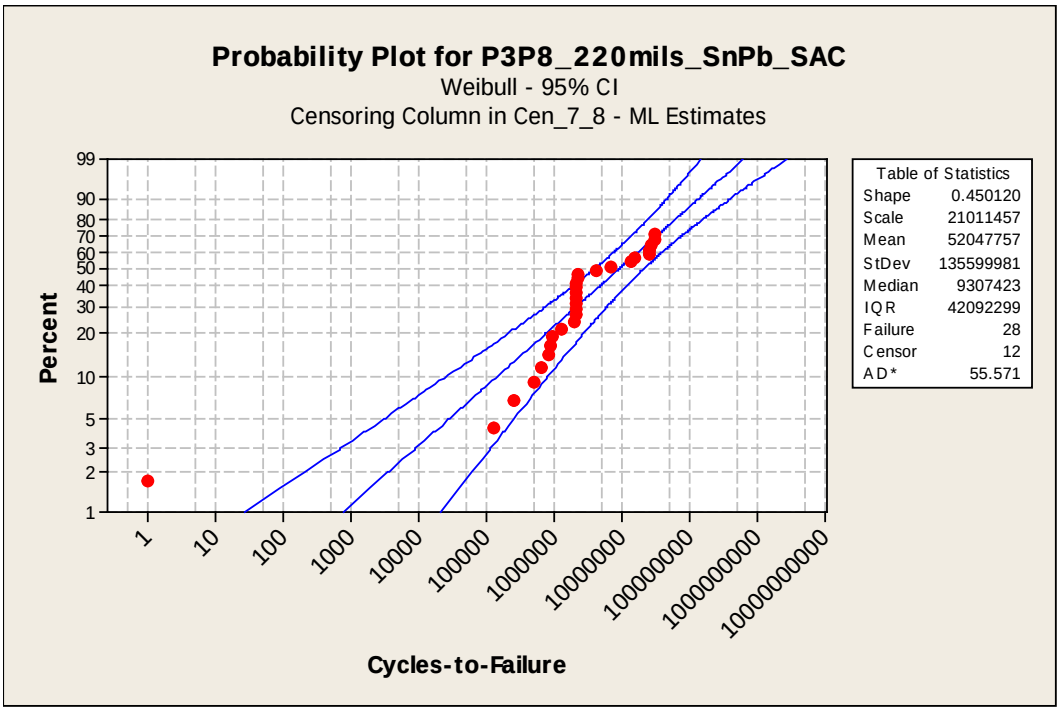
Probability Plot for P3P8_220mils_SnPb_SAC
Weibull - 95% CI
Censoring Column in Cen_7_8 - ML Estimates
Percent
Cycles-to-Failure
Table of Statistics
Shape 0.450120
Scale 21011457
Mean 52047757
StDev 135599981
Median 9307423
IQR 42092299
Failure 28
Censor 12
AD* 55.571

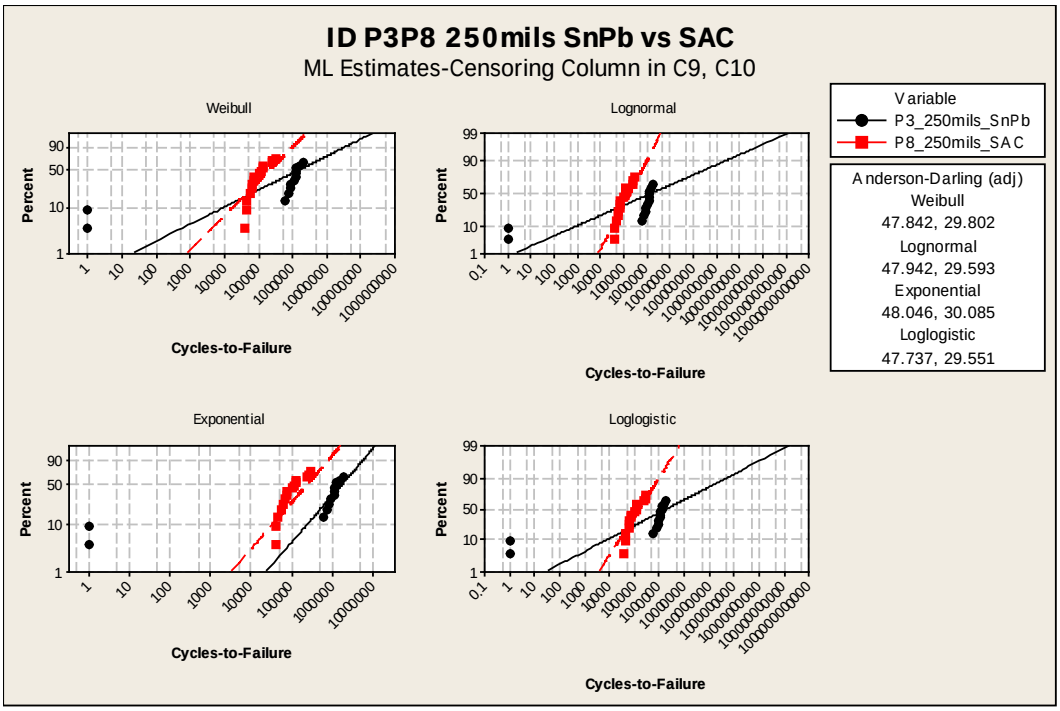
ID P3P8 250mils SnPb vs SAC
ML Estimates-Censoring Column in C9, C10
Weibull
Lognormal
Exponential
Loglogistic
Percent
Cycles-to-Failure
Variable
P3_250mils_SnPb
P8_250mils_SAC
Anderson-Darling (adj)
Weibull
47.842, 29.802
Lognormal
47.942, 29.593
Exponential
48.046, 30.085
Loglogistic
47.737, 29.551

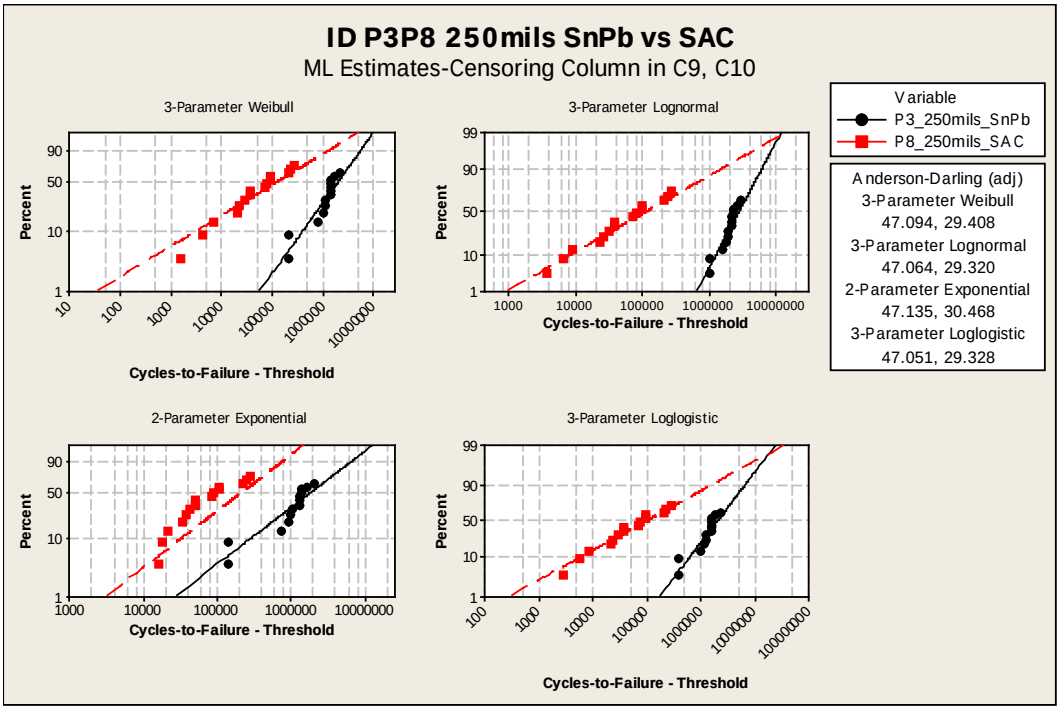
ID P3P8 250mils SnPb vs SAC
ML Estimates-Censoring Column in C9, C10
3-Parameter Weibull
3-Parameter Lognormal
2-Parameter Exponential
3-Parameter Loglogistic
Percent
Cycles-to-Failure - Threshold
Variable
P3_250mils_SnPb
P8_250mils_SAC
Anderson-Darling (adj)
3-Parameter Weibull
47.094, 29.408
3-Parameter Lognormal
47.064, 29.320
2-Parameter Exponential
47.135, 30.468
3-Parameter Loglogistic
47.051, 29.328

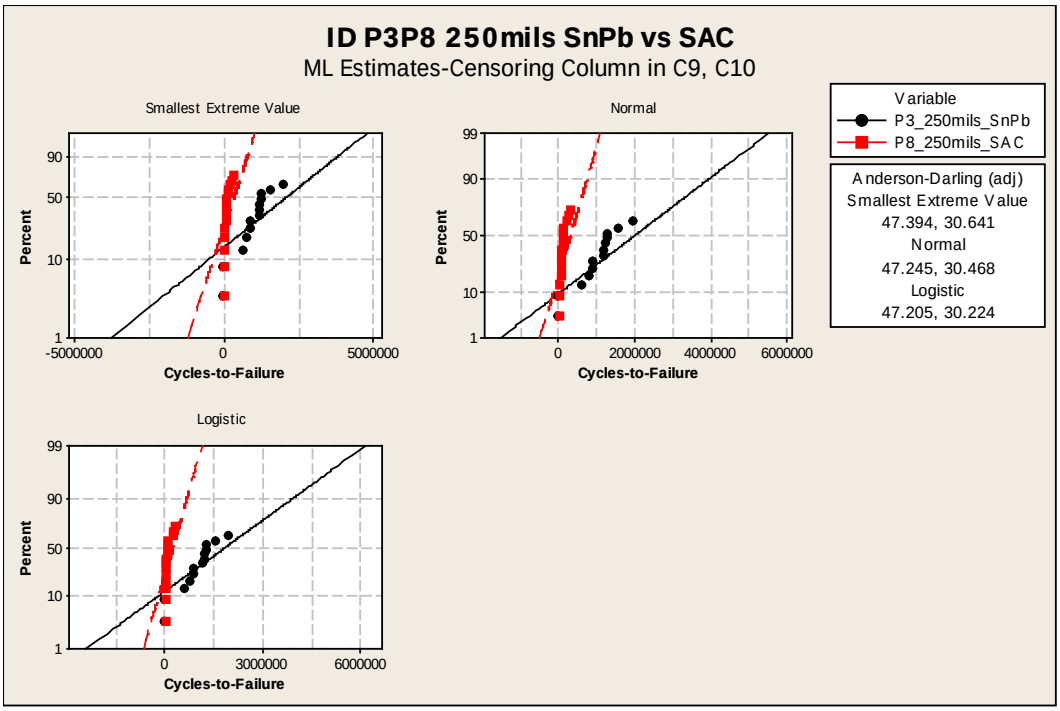
ID P3P8 250mils SnPb vs SAC
ML Estimates-Censoring Column in C9, C10
Smallest Extreme Value
Normal
Logistic
Percent
Cycles-to-Failure
Variable
P3_250mils_SnPb
P8_250mils_SAC
Anderson-Darling (adj)
Smallest Extreme Value
47.394, 30.641
Normal
47.245, 30.468
Logistic
47.205, 30.224

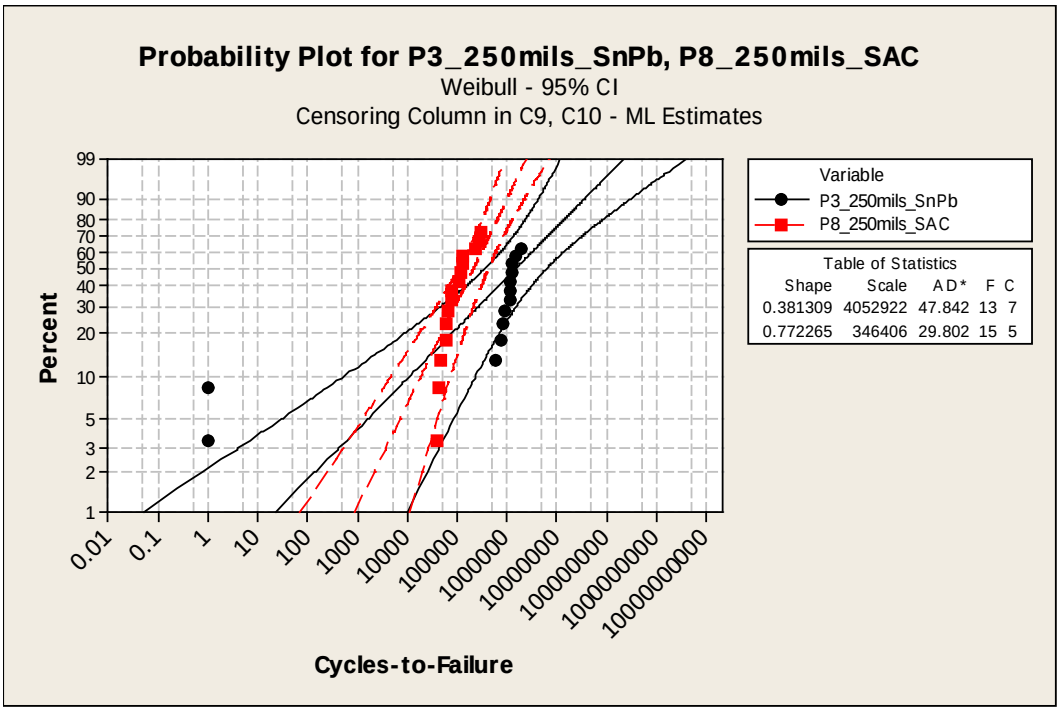
Probability Plot for P3_250mils_SnPb, P8_250mils_SAC
Weibull - 95% CI
Censoring Column in C9, C10 - ML Estimates
Percent
Cycles-to-Failure
Variable
P3_250mils_SnPb
P8_250mils_SAC
Table of Statistics
Shape Scale AD* F C
0.381309 4052922 47.842 13 7
0.772265 346406 29.802 15 5

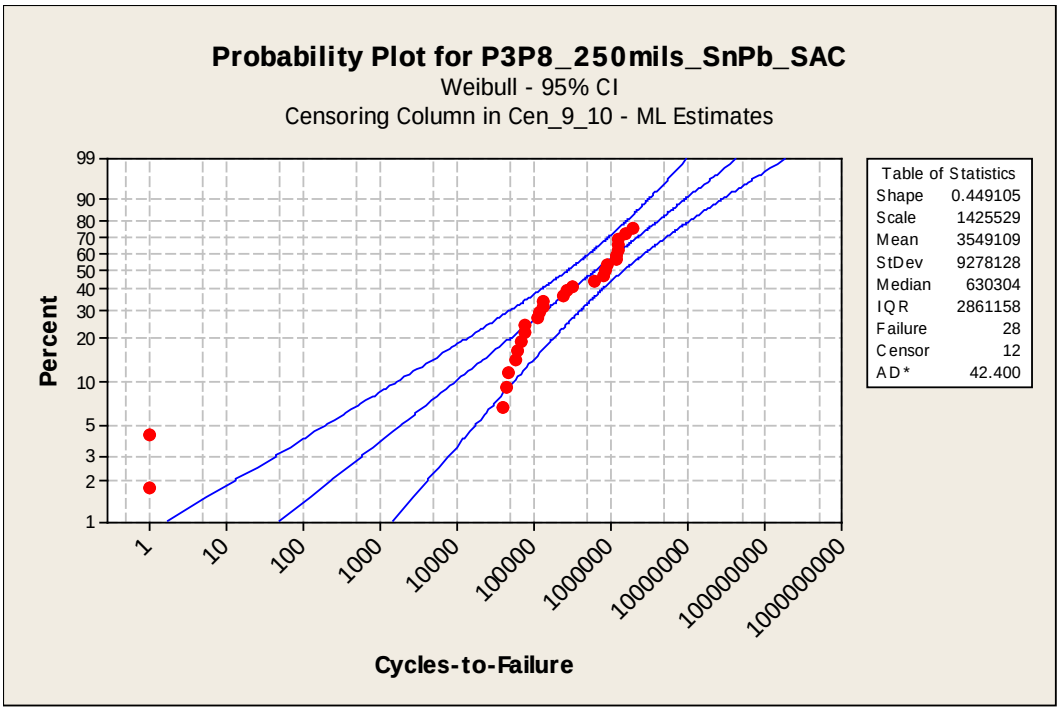
Probability Plot for P3P8_250mils_SnPb_SAC
Weibull - 95% CI
Censoring Column in Cen_9_10 - ML Estimates
Percent
Cycles-to-Failure
Table of Statistics
Shape 0.449105
Scale 1425529
Mean 3549109
StDev 9278128
Median 630304
IQR 2861158
Failure 28
Censor 12
AD* 42.400

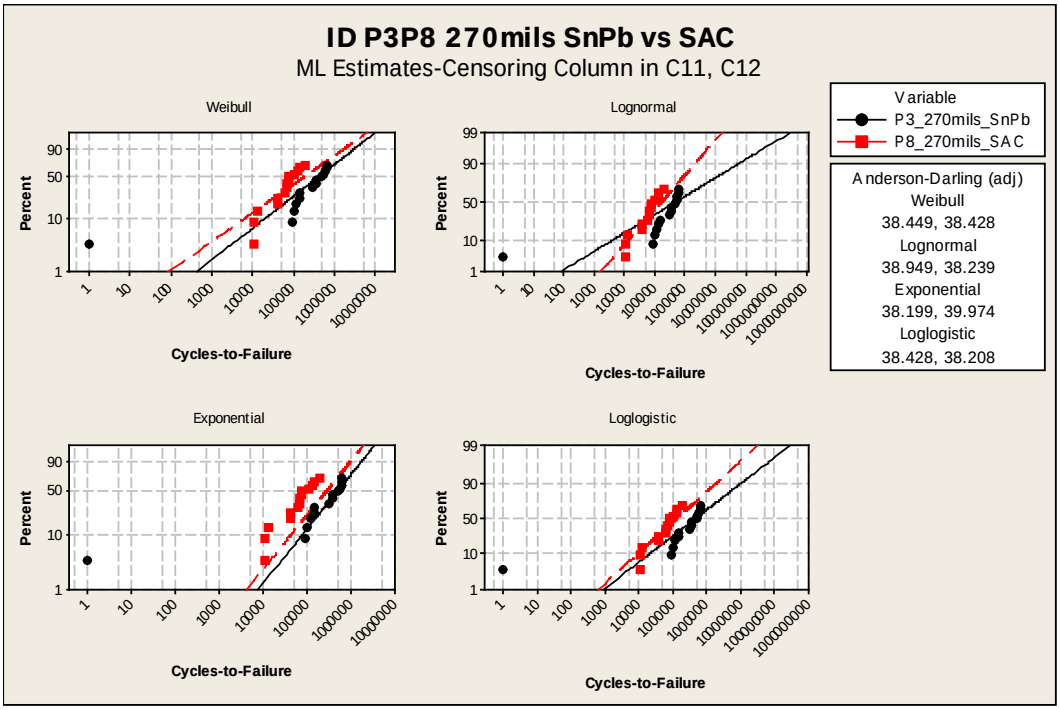
ID P3P8 270mils SnPb vs SAC
ML Estimates-Censoring Column in C11, C12
Weibull
Lognormal
Exponential
Loglogistic
Percent
Cycles-to-Failure
Variable
P3_270mils_SnPb
P8_270mils_SAC
Anderson-Darling (adj)
Weibull
38.449, 38.428
Lognormal
38.949, 38.239
Exponential
38.199, 39.974
Loglogistic
38.428, 38.208

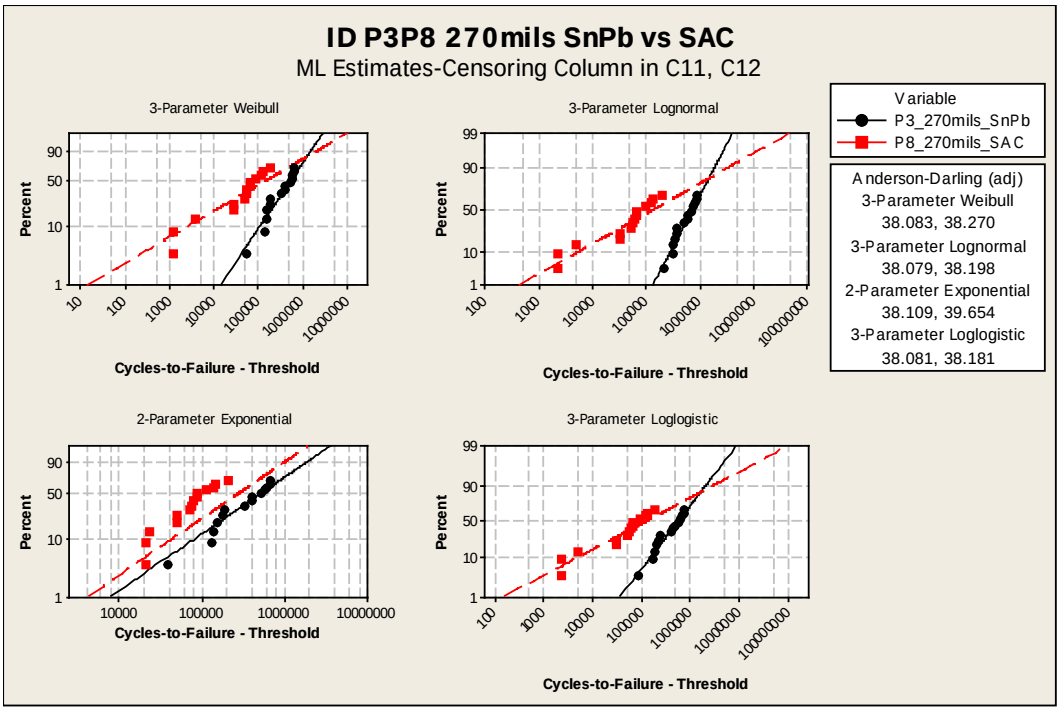
ID P3P8 270mils SnPb vs SAC
ML Estimates-Censoring Column in C11, C12
3-Parameter Weibull
3-Parameter Lognormal
2-Parameter Exponential
3-Parameter Loglogistic
Percent
Cycles-to-Failure - Threshold
Variable
P3_270mils_SnPb
P8_270mils_SAC
Anderson-Darling (adj)
3-Parameter Weibull
38.083, 38.270
3-Parameter Lognormal
38.079, 38.198
2-Parameter Exponential
38.109, 39.654
3-Parameter Loglogistic
38.081, 38.181

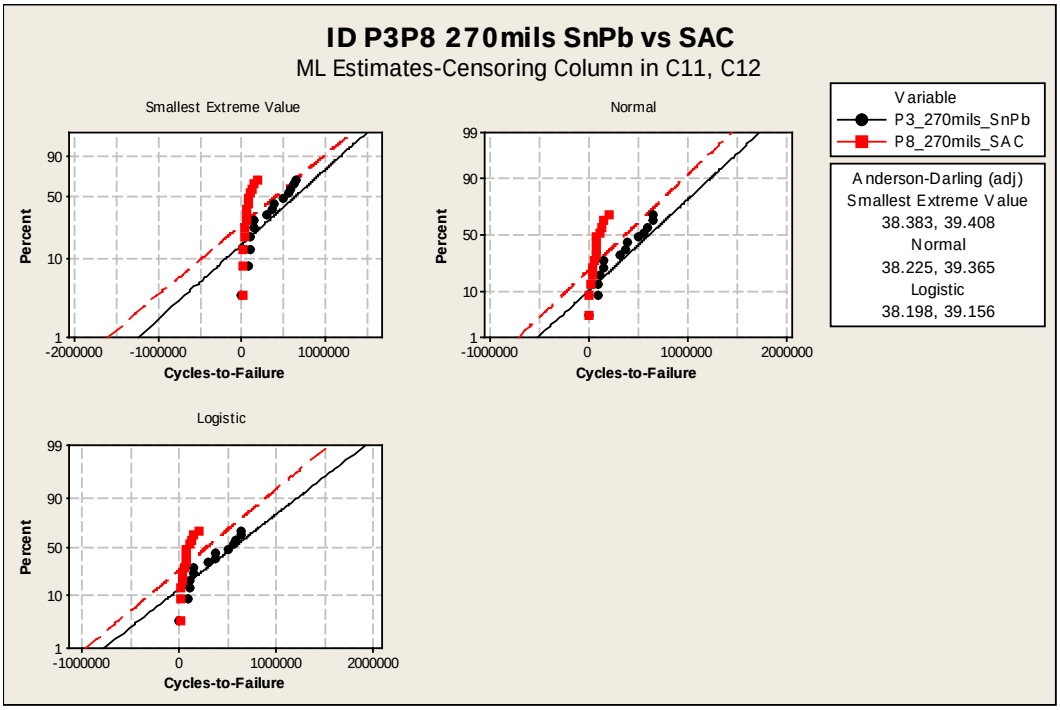
ID P3P8 270mils SnPb vs SAC
ML Estimates-Censoring Column in C11, C12
Smallest Extreme Value
Normal
Logistic
Percent
Cycles-to-Failure
Variable
P3_270mils_SnPb
P8_270mils_SAC
Anderson-Darling (adj)
Smallest Extreme Value
38.383, 39.408
Normal
38.225, 39.365
Logistic
38.198, 39.156

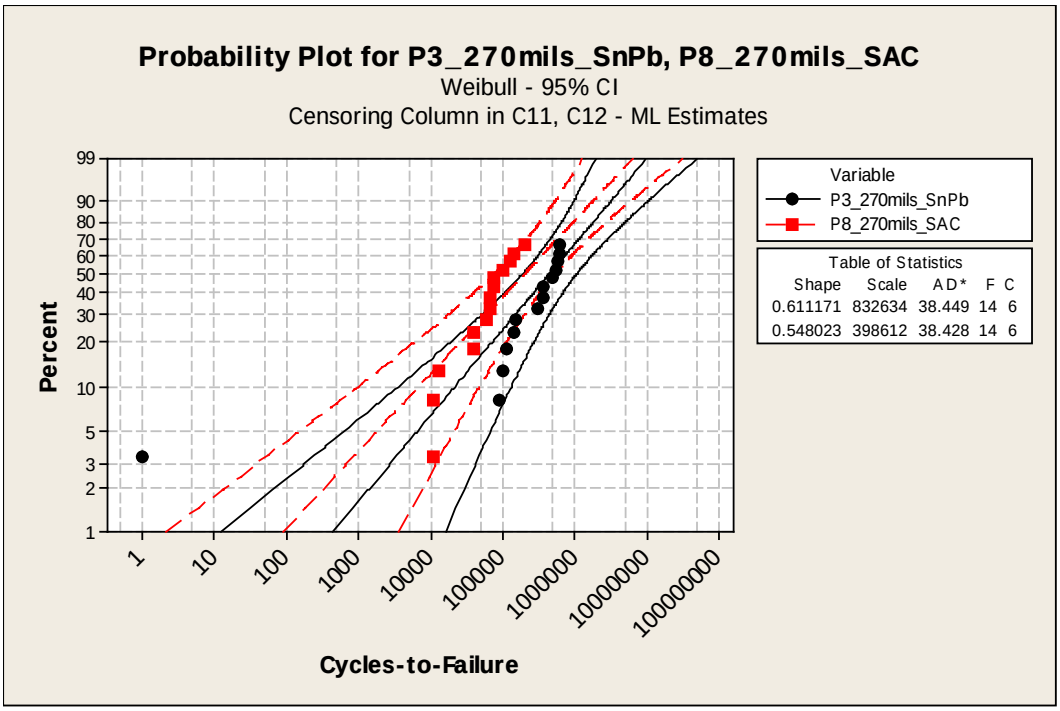
Probability Plot for P3_270mils_SnPb, P8_270mils_SAC
Weibull - 95% CI
Censoring Column in C11, C12 - ML Estimates
Percent
Cycles-to-Failure
Variable
P3_270mils_SnPb
P8_270mils_SAC
Table of Statistics
Shape Scale AD* F C
0.611171 832634 38.449 14 6
0.548023 398612 38.428 14 6

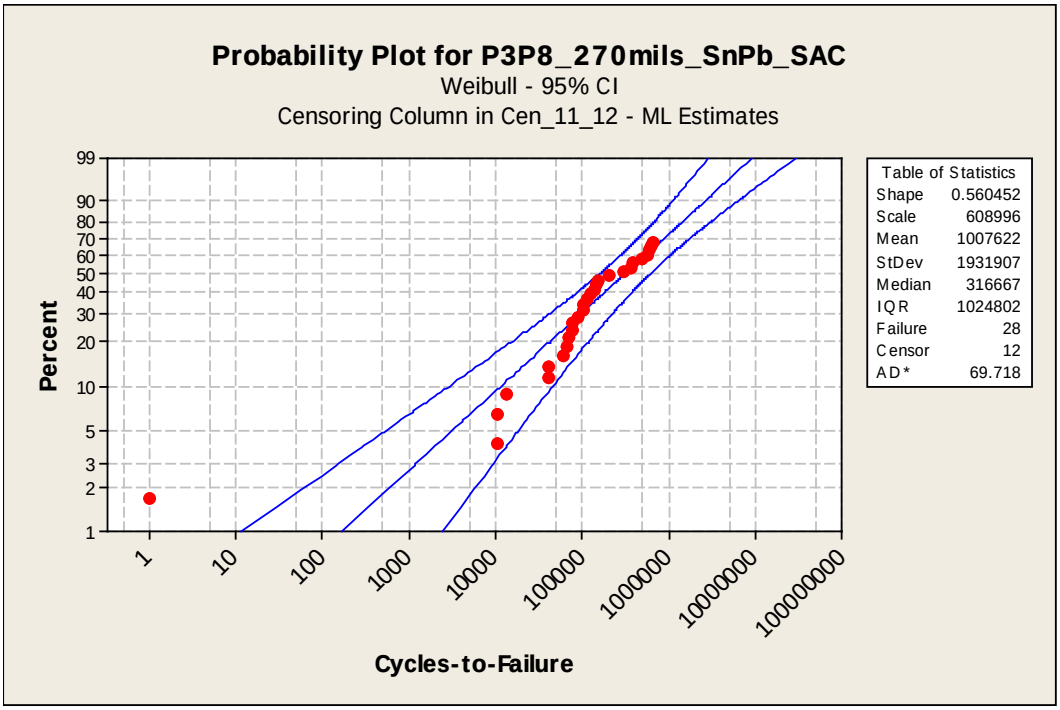
Probability Plot for P3P8_270mils_SnPb_SAC
Weibull - 95% CI
Censoring Column in Cen_11_12 - ML Estimates
Percent
Cycles-to-Failure
Table of Statistics
Shape 0.560452
Scale 608996
Mean 1007622
StDev 1931907
Median 316667
IQR 1024802
Failure 28
Censor 12
AD* 69.718

APPENDIX B

CHAPTER 3 MINITAB VERSION16 RESULTS USED TO CALCULATE THE LIKELIHOOD RATIOS

Distribution ID Plot: P7_250mils_SnPb, P7_250mils_SAC

Results for variable: P7_250mils_SnPb

3-Parameter Weibull

* WARNING * Variance/Covariance matrix of estimated parameters does not exist.
The threshold parameter is assumed fixed when calculating confidence intervals.

2-Parameter Exponential

* WARNING * Variance/Covariance matrix of estimated parameters does not exist.
The threshold parameter is assumed fixed when calculating confidence intervals.

3-Parameter Loglogistic

* WARNING * Variance/Covariance matrix of estimated parameters does not exist.
The threshold parameter is assumed fixed when calculating confidence intervals.

Goodness-of-Fit

Distribution	Anderson-Darling (adj)
Weibull	14.351
Lognormal	14.217
Exponential	14.515
Loglogistic	14.267
3-Parameter Weibull	14.174
3-Parameter Lognormal	14.091
2-Parameter Exponential	14.614
3-Parameter Loglogistic	14.144
Smallest Extreme Value	15.022
Normal	15.028
Logistic	15.010

Table of Percentiles

Distribution	Percent	Percentile	Standard Error	95% Normal CI Lower	Upper
Weibull	1	8638.02	9375.97	1029.19	72499.4
Lognormal	1	48013.2	26944.6	15983.5	144228
Exponential	1	15271.1	3703.79	9493.46	24565.1
Loglogistic	1	24671.4	17696.8	6048.23	100637
3-Parameter Weibull	1	95795.2	3697.72	92968.1	103324
3-Parameter Lognormal	1	121412	11498.1	112930	146175
2-Parameter Exponential	1	63071.4	3565.07	56457.1	70460.6
3-Parameter Loglogistic	1	84496.5	10316.3	72314.5	107340
Smallest Extreme Value	1	-4267107	1302068	-6819113	-1715102
Normal	1	-1779110	623321	-3000797	-557422
Logistic	1	-2564615	766895	-4067701	-1061529
Weibull	5	53450.3	39800.2	12420.1	230024
Lognormal	5	111188	48680.0	47139.7	262258
Exponential	5	77938.4	18902.8	48451.2	125371
Loglogistic	5	85694.5	43289.6	31838.9	230647
3-Parameter Weibull	5	117775	22209.8	92968.1	170440
3-Parameter Lognormal	5	142347	19860.3	112930	187115
2-Parameter Exponential	5	123392	18194.8	92420.9	164740
3-Parameter Loglogistic	5	124034	30854.1	76172.8	201968
Smallest Extreme Value	5	-2026717	896400	-3783628	-269805
Normal	5	-851133	485841	-1803363	101098
Logistic	5	-1208583	533343	-2253915	-163250
Weibull	10	119540	71763.8	36855.8	387720
Lognormal	10	173971	66082.9	82631.8	366274
Exponential	10	160092	38827.9	99522.6	257523
Loglogistic	10	150570	63384.8	65979.9	343610
3-Parameter Weibull	10	157699	46641.3	92968.1	281567
3-Parameter Lognormal	10	170017	37756.4	112930	262738
2-Parameter Exponential	10	202468	37373.7	141004	290723
3-Parameter Loglogistic	10	171833	49402.2	97810.2	301875
Smallest Extreme Value	10	-1037305	724924	-2458130	383520
Normal	10	-356432	421128	-1181828	468964
Logistic	10	-594747	441906	-1460867	271373
Weibull	50	982530	292330	548390	1760362
Lognormal	50	843900	236837	486860	1462773
Exponential	50	1053213	255442	654741	1694193
Loglogistic	50	789848	237263	438380	1423104
3-Parameter Weibull	50	889597	281921	478014	1655565
3-Parameter Lognormal	50	704801	255475	346358	1434195
2-Parameter Exponential	50	1062138	245874	674740	1671959

3-Parameter Loglogistic	50	754258	235997	408499 1392673
Smallest Extreme Value	50	1552075	365854	835015 2269135
Normal	50	1388631	309536	781952 1995310
Logistic	50	1210270	327764	567865 1852676

Table of MTTF

		Standard	95% Normal CI	
Distribution	Mean	Error	Lower	Upper
Weibull	1562930	436565	904020	2702098
Lognormal	1803003	732739	812959	3998750
Exponential	1519465	368524	944591	2444203
Loglogistic	2683743	2054830	598427	12035678
3-Parameter Weibull	1637842	530868	867710	3091499
3-Parameter Lognormal	3241834	3038380	516428	20350343
2-Parameter Exponential	1510927	354722	953688	2393761
3-Parameter Loglogistic	5010762	7850066	232475	108001848
Smallest Extreme Value	1262461	391804	494539	2030384
Normal	1388631	309536	781952	1995310
Logistic	1210270	327764	567865	1852676

Results for variable: P7_250mils_SAC

3-Parameter Weibull

* WARNING * Variance/Covariance matrix of estimated parameters does not exist.

The threshold parameter is assumed fixed when calculating confidence intervals.

2-Parameter Exponential

* WARNING * Variance/Covariance matrix of estimated parameters does not exist.

The threshold parameter is assumed fixed when calculating confidence intervals.

3-Parameter Loglogistic

* WARNING * Variance/Covariance matrix of estimated parameters does not exist.

The threshold parameter is assumed fixed when calculating confidence intervals.

Goodness-of-Fit

Distribution	Anderson-Darling (adj)
Weibull	29.902
Lognormal	29.798
Exponential	30.257
Loglogistic	29.814
3-Parameter Weibull	29.667
3-Parameter Lognormal	29.548
2-Parameter Exponential	30.448
3-Parameter Loglogistic	29.615
Smallest Extreme Value	30.363
Normal	30.407
Logistic	30.346

Table of Percentiles

Distribution	Percent	Standard Percentile	Error	95% Normal CI Lower	Upper
Weibull	1	1664.20	2107.62	139.062	19916.1
Lognormal	1	11813.6	7651.31	3319.58	42041.7
Exponential	1	5228.18	1349.91	3151.89	8672.22
Loglogistic	1	5163.66	4306.48	1007.07	26476.3
3-Parameter Weibull	1	38158.3	478.042	37866.0	39106.9
3-Parameter Lognormal	1	43525.8	1252.52	42521.4	46051.3
2-Parameter Exponential	1	23399.3	1286.18	21009.4	26060.9
3-Parameter Loglogistic	1	36054.4	1495.16	34676.7	39107.3
Smallest Extreme Value	1	-1340149	437425	-2197487	-482811
Normal	1	-595356	214938	-1016627	-174085
Logistic	1	-880577	271424	-1412558	-348596
Weibull	5	12670.5	10831.0	2372.29	67673.8
Lognormal	5	29892.1	14848.5	11291.0	79137.0
Exponential	5	26682.8	6889.46	16086.1	44259.9
Loglogistic	5	20914.6	12076.1	6744.74	64853.5
3-Parameter Weibull	5	41777.3	4308.45	37866.0	51135.7
3-Parameter Lognormal	5	47174.7	4597.32	42521.4	57103.4
2-Parameter Exponential	5	43841.0	6564.22	32691.3	58793.5
3-Parameter Loglogistic	5	42878.1	6168.62	34676.7	56845.1
Smallest Extreme Value	5	-631835	295625	-1211250	-52420.5
Normal	5	-288852	164689	-611636	33931.8

Logistic	5	-420484	186782	-786569	-54398.1
Weibull	10	31054.6	21163.3	8166.59	118089
Lognormal	10	49032.8	20892.7	21271.2	113027
Exponential	10	54808.5	14151.5	33042.2	90913.3
Loglogistic	10	39395.2	18741.8	15505.8	100090
3-Parameter Weibull	10	50162.4	10779.9	37866.0	76436.8
3-Parameter Lognormal	10	53058.7	9717.71	42521.4	75972.2
2-Parameter Exponential	10	70639.0	13483.4	48592.5	102688
3-Parameter Loglogistic	10	53066.8	11380.9	34855.5	80793.3
Smallest Extreme Value	10	-319026	235961	-781501	143448
Normal	10	-125456	141128	-402061	151149
Logistic	10	-212213	153486	-513040	88614.6
Weibull	50	324369	109281	167597	627787
Lognormal	50	280967	89266.4	150737	523711
Exponential	50	360575	93100.1	217378	598102
Loglogistic	50	253557	86675.2	129749	495505
3-Parameter Weibull	50	284281	105926	136955	590086
3-Parameter Lognormal	50	230835	99851.2	98878.0	538892
2-Parameter Exponential	50	361971	88704.9	223912	585154
3-Parameter Loglogistic	50	232291	85274.9	113124	476993
Smallest Extreme Value	50	499622	117546	269236	730008
Normal	50	450925	104694	245728	656121
Logistic	50	400218	112815	179106	621331

Table of MTTF

		Standard	95% Normal CI	
Distribution	Mean	Error	Lower	Upper
Weibull	578578	204856	289053	1158099
Lognormal	710561	369484	256440	1968869
Exponential	520200	134315	313611	862878
Loglogistic	1463532	2026385	97016	22078187
3-Parameter Weibull	664963	303769	271613	1627959
3-Parameter Lognormal	2408192	3985469	93969	61716083
2-Parameter Exponential	514060	127974	315580	837373
3-Parameter Loglogistic	*	*	*	*
Smallest Extreme Value	408059	124667	163717	652401
Normal	450925	104694	245728	656121
Logistic	400218	112815	179106	621331

ID P7 250mils SnPb vs SAC

ID P7 250mils SnPb vs SAC

ID P7 250mils SnPb vs SAC

Distribution Analysis: P7_250mils_SnPb

Variable: P7_250mils_SnPb

Censoring Information	Count
Uncensored value	17
Right censored value	3

Censoring value: Cen1 = 0

Estimation Method: Maximum Likelihood

Distribution: Weibull

Parameter Estimates

Parameter	Estimate	Standard Error	95.0% Normal CI Lower	Upper
Shape	0.894312	0.175432	0.608855	1.31360
Scale	1480237	406218	864447	2534687

Log-Likelihood = -258.805

Goodness-of-Fit
Anderson-Darling (adjusted) = 14.351

Characteristics of Distribution

	Estimate	Standard Error	95.0% Normal CI Lower	Upper
Mean(MTTF)	1562930	436565	904020	2702098
Standard Deviation	1751041	670280	826923	3707893
Median	982530	292330	548390	1760362
First Quartile(Q1)	367536	152843	162675	830383
Third Quartile(Q3)	2132804	581863	1249481	3640595

Interquartile Range(IQR) 1765268 511159 1000767 3113784

Table of Percentiles

Percent	Percentile	Standard Error	95.0% Normal CI Lower	Upper
1	8638.02	9375.97	1029.19	72499.4
2	18857.2	17686.5	2999.99	118532
3	29844.1	25430.4	5617.53	158552
4	41406.1	32772.0	8777.22	195331
5	53450.3	39800.2	12420.1	230024
6	65922.5	46572.0	16507.8	263256
7	78788.0	53127.2	21013.1	295414
8	92022.9	59496.0	25915.8	326759
9	105611	65701.8	31200.7	357480
10	119540	71763.8	36855.8	387720
20	276651	127132	112401	680917
30	467404	178246	221352	986963
40	698439	231002	365259	1335536
50	982530	292330	548390	1760362
60	1342387	373193	778463	2314823
70	1821693	494045	1070603	3099715
80	2520170	701328	1460672	4348177
90	3761429	1149667	2066266	6847302
91	3954396	1227028	2152568	7264463
92	4171298	1316118	2247512	7741771
93	4418648	1420330	2353311	8296588
94	4706021	1544707	2473175	8954737
95	5048314	1697205	2612035	9756946
96	5470599	1891402	2778056	10772807
97	6020120	2153332	2986342	12135865
98	6803641	2543076	3270227	14154839
99	8165032	3259888	3733497	17856651

Distribution Analysis: P7_250mils_SAC

Variable: P7_250mils_SAC

Censoring Information	Count
Uncensored value	15
Right censored value	5

Censoring value: Cen2 = 0

Estimation Method: Maximum Likelihood

Distribution: Weibull

Parameter Estimates

Parameter	Estimate	Standard Error	95.0% Normal CI Lower	Upper
Shape	0.802960	0.171239	0.528648	1.21961
Scale	512005	164648	272615	961609

Log-Likelihood = -211.846

Goodness-of-Fit
Anderson-Darling (adjusted) = 29.902

Characteristics of Distribution

	Estimate	Standard Error	95.0% Normal CI Lower	Upper
Mean(MTTF)	578578	204856	289053	1158099
Standard Deviation	726401	360673	274497	1922277
Median	324369	109281	167597	627787
First Quartile(Q1)	108495	50307.7	43723.6	269216
Third Quartile(Q3)	769023	255502	400991	1474840
Interquartile Range(IQR)	660529	234983	328910	1326498

Table of Percentiles

Percent	Percentile	Standard Error	95.0% Normal CI Lower	Upper
1	1664.20	2107.62	139.062	19916.1
2	3970.50	4320.30	470.602	33499.4
3	6620.79	6517.86	961.485	45590.8
4	9534.40	8688.69	1598.07	56884.3
5	12670.5	10831.0	2372.29	67673.8
6	16004.5	12945.7	3278.83	78120.2
7	19519.8	15034.4	4313.91	88324.4
8	23205.1	17098.9	5474.81	98355.6
9	27052.1	19141.2	6759.53	108264
10	31054.6	21163.3	8166.59	118089

20	79069.0	40675.7	28848.3	216716
30	141801	60180.8	61719.8	325786
40	221799	81907.0	107553	457399
50	324369	109281	167597	627787
60	459188	148152	243983	864216
70	645169	209583	341319	1219512
80	926114	318914	471570	1818788
90	1446686	562296	675352	3098977
91	1529584	604914	704601	3320500
92	1623315	654183	736844	3576268
93	1730882	712057	772853	3876485
94	1856714	781456	813749	4236427
95	2007737	866999	861258	4680371
96	2195657	976611	918241	5250155
97	2442666	1125564	990002	6026874
98	2799275	1349349	1088269	7200369
99	3429845	1766791	1249687	9413428

Probability Plot for P7_250mils_SnPb, P7_250mils_SAC

Distribution Analysis: P7_250mils_SnPb_SAC

Variable: P7_250mils_SnPb_SAC

Censoring Information	Count
Uncensored value	32
Right censored value	8

Censoring value: Cen_1_2 = 0

Estimation Method: Maximum Likelihood

Distribution: Weibull

Parameter Estimates

		Standard	95.0% Normal CI	
Parameter	Estimate	Error	Lower	Upper
Shape	0.755188	0.105326	0.574564	0.992595
Scale	974792	229596	614364	1546673

Log-Likelihood = -473.357

Goodness-of-Fit
Anderson-Darling (adjusted) = 17.611

Characteristics of Distribution

		Standard	95.0% Normal CI	
	Estimate	Error	Lower	Upper
Mean(MTTF)	1154101	288261	707356	1882997
Standard Deviation	1549445	521225	801376	2995821
Median	599981	151298	366006	983528
First Quartile(Q1)	187249	64980.9	94847.5	369668
Third Quartile(Q3)	1502288	355399	944894	2388491
Interquartile Range(IQR)	1315040	323476	812005	2129702

Table of Percentiles

		Standard	95.0% Normal CI	
Percent	Percentile	Error	Lower	Upper
1	2205.22	1998.84	373.175	13031.4
2	5558.79	4350.02	1199.15	25768.3
3	9573.97	6802.85	2378.29	38540.7
4	14109.0	9308.17	3871.93	51411.8
5	19090.1	11845.2	5657.79	64412.4
6	24472.2	14403.2	7721.36	77562.3
7	30224.7	16976.0	10052.6	90875.8
8	36326.4	19560.0	12644.1	104365
9	42761.5	22153.1	15490.9	118040
10	49518.6	24754.1	18589.0	131910
20	133760	51226.7	63144.4	283344
30	248911	79364.6	133242	464994
40	400511	111383	232216	690774
50	599981	151298	366006	983528
60	868236	206522	544712	1383910
70	1246415	291943	787570	1972587
80	1830563	443181	1138959	2942126
90	2941362	784643	1743735	4961540
91	3120890	845204	1835502	5306427
92	3324619	915475	1937996	5703361
93	3559337	998358	2054072	6167689
94	3835082	1098195	2187907	6722340
95	4167588	1221885	2345973	7403661
96	4583535	1381308	2539101	8274108

97	5133684	1599460	2787578	9454337
98	5934093	1930078	3136888	11225604
99	7364859	2554480	3731880	14534540

Probability Plot for P7_250mils_SnPb_SAC

Distribution ID Plot: P7_400mils_SnPb, P7_400mils_SAC

Results for variable: P7_400mils_SnPb

3-Parameter Weibull

* WARNING * Variance/Covariance matrix of estimated parameters does not exist.
The threshold parameter is assumed fixed when calculating confidence intervals.

3-Parameter Lognormal

* WARNING * Variance/Covariance matrix of estimated parameters does not exist.
The threshold parameter is assumed fixed when calculating confidence intervals.

2-Parameter Exponential

* WARNING * Variance/Covariance matrix of estimated parameters does not exist.
The threshold parameter is assumed fixed when calculating confidence intervals.

3-Parameter Loglogistic

* WARNING * Variance/Covariance matrix of estimated parameters does not exist.
The threshold parameter is assumed fixed when calculating confidence intervals.

Goodness-of-Fit

Distribution	Anderson-Darling (adj)

Weibull	80.521
Lognormal	80.518
Exponential	80.533
Loglogistic	80.504
3-Parameter Weibull	80.431
3-Parameter Lognormal	80.449
2-Parameter Exponential	80.811
3-Parameter Loglogistic	80.429
Smallest Extreme Value	80.564
Normal	80.569
Logistic	80.549

Table of Percentiles

			Standard	95% Normal CI	
Distribution	Percent	Percentile	Error	Lower	Upper
Weibull	1	3370.00	4632.61	227.780	49859.2
Lognormal	1	11809.7	9312.08	2517.98	55388.7
Exponential	1	4450.29	1573.41	2225.58	8898.84
Loglogistic	1	5179.61	5673.49	605.248	44326.3
3-Parameter Weibull	1	59059.5	0.119534	59059.5	59059.8
3-Parameter Lognormal	1	59394.1	0.0043095	59394.1	59394.1
2-Parameter Exponential	1	45963.6	1195.08	43680.0	48366.7
3-Parameter Loglogistic	1	59166.9	0.158640	59166.9	59167.2
Smallest Extreme Value	1	-347323	190129	-719969	25322.0
Normal	1	-170779	108441	-383320	41761.0
Logistic	1	-286467	150756	-581944	9010.48
Weibull	5	19367.2	16383.7	3689.69	101658
Lognormal	5	30560.0	16878.5	10352.1	90214.8
Exponential	5	22712.7	8030.14	11358.6	45416.5
Loglogistic	5	22158.4	15449.5	5650.10	86900.4
3-Parameter Weibull	5	59075.2	49.9027	59059.5	59173.1
3-Parameter Lognormal	5	59394.5	1.47476	59394.1	59397.4
2-Parameter Exponential	5	59835.0	6099.28	48999.1	73067.2
3-Parameter Loglogistic	5	59180.2	38.7619	59166.9	59256.3
Smallest Extreme Value	5	-105225	117023	-334586	124136
Normal	5	-40241.4	75921.1	-189044	108561
Logistic	5	-85998.1	95956.7	-274070	102074
Weibull	10	41922.9	26530.3	12127.7	144918
Lognormal	10	50731.3	22748.7	21066.1	122171
Exponential	10	46653.6	16494.6	23331.4	93289.1
Loglogistic	10	42784.2	23176.5	14797.2	123705

3-Parameter Weibull	10	59339.1	663.862	59059.5	60654.6
3-Parameter Lognormal	10	59405.3	32.6023	59394.1	59469.3
2-Parameter Exponential	10	78019.5	12528.4	56953.1	106878
3-Parameter Loglogistic	10	59364.0	444.464	59166.9	60241.5
Smallest Extreme Value	10	1691.46	87559.6	-169922	173305
Normal	10	29347.9	61607.3	-91400.2	150096
Logistic	10	4748.14	74570.9	-141408	150904
Weibull	50	316363	128650	142575	701987
Lognormal	50	303225	133756	127729	719846
Exponential	50	306926	108515	153493	613731
Loglogistic	50	296162	131653	123921	707806
3-Parameter Weibull	50	583463	796355	59059.5	8468323
3-Parameter Lognormal	50	1327597	3634005	59394.1	283820392
2-Parameter Exponential	50	275711	82422.1	153459	495354
3-Parameter Loglogistic	50	600490	975237	59166.9	14484885
Smallest Extreme Value	50	281502	56287.6	171180	391823
Normal	50	274825	60570.8	156108	393541
Logistic	50	271592	61376.9	151296	391889

Table of MTTF

		95% Normal CI		
Distribution	Mean	Standard Error	Lower	Upper
Weibull	4.84237E+05	2.79916E+05	155961	1.50349E+06
Lognormal	8.02449E+05	7.29170E+05	135191	4.76308E+06
Exponential	4.42800E+05	1.56553E+05	221443	8.85427E+05
Loglogistic	2.23507E+06	6.03684E+06	11226	4.44990E+08
3-Parameter Weibull	5.46557E+07	1.80994E+08	82958	3.60093E+10
3-Parameter Lognormal	9.76870E+23	2.49638E+25	59394	*
2-Parameter Exponential	3.78916E+05	1.18910E+05	204843	7.00912E+05
3-Parameter Loglogistic	*	*	*	*
Smallest Extreme Value	2.50206E+05	5.34875E+04	145372	3.55040E+05
Normal	2.74825E+05	6.05708E+04	156108	3.93541E+05
Logistic	2.71592E+05	6.13769E+04	151296	3.91889E+05

Results for variable: P7_400mils_SAC

3-Parameter Weibull

* WARNING * Variance/Covariance matrix of estimated parameters does not exist.

The threshold parameter is assumed fixed when calculating

confidence intervals.

3-Parameter Lognormal

* WARNING * Variance/Covariance matrix of estimated parameters does not exist.

The threshold parameter is assumed fixed when calculating confidence intervals.

2-Parameter Exponential

* WARNING * Variance/Covariance matrix of estimated parameters does not exist.

The threshold parameter is assumed fixed when calculating confidence intervals.

3-Parameter Loglogistic

* WARNING * Variance/Covariance matrix of estimated parameters does not exist.

The threshold parameter is assumed fixed when calculating confidence intervals.

Goodness-of-Fit

Distribution	Anderson-Darling (adj)
Weibull	38.952
Lognormal	39.072
Exponential	39.580
Loglogistic	38.993
3-Parameter Weibull	39.049
3-Parameter Lognormal	39.163
2-Parameter Exponential	41.791
3-Parameter Loglogistic	39.073
Smallest Extreme Value	38.935
Normal	39.053
Logistic	38.977

Table of Percentiles

Distribution	Percent	Standard Percentile	95% Normal CI Error	Lower	Upper

Weibull	1	23199.4	7577.64	12230.6	44005.3
Lognormal	1	35959.6	6228.26	25608.6	50494.5
Exponential	1	1153.28	308.226	683.030	1947.27
Loglogistic	1	28310.9	6529.54	18015.0	44491.0
3-Parameter Weibull	1	59394.1	0.0000078	59394.1	59394.1
3-Parameter Lognormal	1	59394.1	0.0044579	59394.1	59394.1
2-Parameter Exponential	1	58114.0	86.4673	57944.7	58283.7
3-Parameter Loglogistic	1	59394.1	0.0001125	59394.1	59394.1
Smallest Extreme Value	1	-15149.6	25811.0	-65738.2	35439.1
Normal	1	19784.6	13652.3	-6973.50	46542.6
Logistic	1	967.254	18152.3	-34610.6	36545.1

Weibull	5	38384.1	8375.84	25027.1	58869.9
Lognormal	5	45919.1	6050.92	35467.2	59451.0
Exponential	5	5885.91	1573.07	3485.94	9938.17
Loglogistic	5	41402.2	6618.40	30265.9	56636.1
3-Parameter Weibull	5	59394.1	0.0192181	59394.1	59394.1
3-Parameter Lognormal	5	59394.1	0.192201	59394.1	59394.5
2-Parameter Exponential	5	59441.6	441.298	58583.0	60312.9
3-Parameter Loglogistic	5	59394.1	0.0423878	59394.1	59394.2
Smallest Extreme Value	5	24674.9	17244.5	-9123.65	58473.4
Normal	5	39044.7	10385.6	18689.4	59400.1
Logistic	5	30879.8	12574.9	6233.54	55526.2

Weibull	10	47942.9	8277.26	34179.5	67248.5
Lognormal	10	52311.4	5884.75	41960.5	65215.7
Exponential	10	12090.1	3231.22	7160.40	20413.8
Loglogistic	10	49175.1	6481.85	37979.3	63671.3
3-Parameter Weibull	10	59394.3	0.572146	59394.1	59395.4
3-Parameter Lognormal	10	59394.8	1.41208	59394.1	59397.6
2-Parameter Exponential	10	61182.1	906.462	59431.1	62984.8
3-Parameter Loglogistic	10	59394.3	0.605221	59394.1	59395.5
Smallest Extreme Value	10	42262.3	13644.8	15519.1	69005.5
Normal	10	49312.2	8865.04	31937.1	66687.4
Logistic	10	44420.4	10365.1	24105.1	64735.7

Weibull	50	85795.3	7284.80	72642.1	101330
Lognormal	50	82844.7	7075.96	70074.8	97941.7
Exponential	50	79538.6	21257.6	47106.9	134299
Loglogistic	50	81558.7	7721.20	67746.4	98187.0
3-Parameter Weibull	50	62086.6	3731.69	59394.1	69848.8
3-Parameter Lognormal	50	60901.6	2127.80	59394.1	65218.1
2-Parameter Exponential	50	80103.9	5963.44	69228.4	92687.7
3-Parameter Loglogistic	50	60602.6	1899.90	59394.1	64443.1
Smallest Extreme Value	50	88290.2	6715.12	75128.9	101452

Normal	50	85531.0	6727.22	72345.9 98716.1
Logistic	50	84237.1	7446.80	69641.7 98832.6

Table of MTTF

			95% Normal CI	
Distribution	Mean	Standard Error	Lower	Upper
Weibull	8.61033E+04	7.12354E+03	73214.6	1.01261E+05
Lognormal	8.83510E+04	8.35187E+03	73408.6	1.06335E+05
Exponential	1.14750E+05	3.06682E+04	67961.0	1.93752E+05
Loglogistic	8.91313E+04	9.60754E+03	72157.0	1.10099E+05
3-Parameter Weibull	2.25265E+06	5.38272E+06	59394.1	2.43582E+08
3-Parameter Lognormal	6.26985E+10	4.73768E+11	59394.1	1.69504E+17
2-Parameter Exponential	8.99819E+04	8.60343E+03	74605.2	1.08528E+05
3-Parameter Loglogistic	*	*	*	*
Smallest Extreme Value	8.31422E+04	7.07801E+03	69269.5	9.70148E+04
Normal	8.55310E+04	6.72722E+03	72345.9	9.87161E+04
Logistic	8.42371E+04	7.44680E+03	69641.7	9.88326E+04

ID P7 400mils SnPb vs SAC

ID P7 400mils SnPb vs SAC

ID P7 400mils SnPb vs SAC

Distribution Analysis: P7_400mils_SnPb

Variable: P7_400mils_SnPb

Censoring Information	Count
Uncensored value	8
Right censored value	12

Censoring value: C3 = 0

Estimation Method: Maximum Likelihood

Distribution: Weibull

Parameter Estimates

Parameter	Estimate	Standard Error	95.0% Normal CI Lower	Upper
Shape	0.932113	0.301247	0.494733	1.75617
Scale	468763	219258	187419	1172444

Log-Likelihood = -111.983

Goodness-of-Fit
Anderson-Darling (adjusted) = 80.521

Characteristics of Distribution

	Estimate	Standard Error	95.0% Normal CI Lower	Upper
Mean(MTTF)	484237	279916	155961	1503486
Standard Deviation	519895	444601	97272.1	2778705
Median	316363	128650	142575	701987
First Quartile(Q1)	123157	50618.4	55031.0	275619
Third Quartile(Q3)	665488	360592	230102	1924687
Interquartile Range(IQR)	542331	345030	155859	1887110

Table of Percentiles

Percent	Percentile	Standard Error	95.0% Normal CI Lower	Upper
1	3370.00	4632.61	227.780	49859.2
2	7127.60	8153.44	757.238	67089.5
3	11072.3	11191.1	1527.24	80273.2
4	15159.2	13907.2	2510.61	91532.2
5	19367.2	16383.7	3689.69	101658
6	23684.0	18671.6	5051.27	111048
7	28102.3	20806.3	6584.63	119937
8	32617.0	22814.4	8280.56	128478
9	37224.6	24716.6	10130.8	136778
10	41922.9	26530.3	12127.7	144918
20	93776.5	42414.8	38645.5	227557
30	155102	60247.9	72439.6	332092
40	228023	86988.5	107958	481619
50	316363	128650	142575	701987
60	426797	192345	176445	1032366
70	572060	290655	211329	1548548

80	781052	452958	250634	2433997
90	1146964	778497	303249	4338097
91	1203361	832322	310206	4668121
92	1266620	893689	317735	5049267
93	1338598	964721	325981	5496766
94	1422017	1048567	335155	6033426
95	1521110	1150162	345572	6695493
96	1642988	1277888	357754	7545435
97	1801021	1447706	372650	8704343
98	2025350	1696161	392327	10455680
99	2412704	2143111	423073	13759203

Distribution Analysis: P7_400mils_SAC

Variable: P7_400mils_SAC

Censoring Information	Count
Uncensored value	14
Right censored value	6

Censoring value: C4 = 0

Estimation Method: Maximum Likelihood

Distribution: Weibull

Parameter Estimates

		Standard	95.0% Normal CI	
Parameter	Estimate	Error	Lower	Upper
Shape	3.23712	0.733136	2.07673	5.04588
Scale	96080.5	7952.18	81693.0	113002

Log-Likelihood = -168.655

Goodness-of-Fit
Anderson-Darling (adjusted) = 38.952

Characteristics of Distribution

		Standard	95.0% Normal CI	
	Estimate	Error	Lower	Upper

Mean(MTTF)	86103.3	7123.54	73214.6	101261
Standard Deviation	29229.4	6271.81	19194.4	44510.6
Median	85795.3	7284.80	72642.1	101330
First Quartile(Q1)	65385.9	7578.76	52098.3	82062.6
Third Quartile(Q3)	106281	9288.58	89549.8	126139
Interquartile Range(IQR)	40895.3	9021.60	26539.7	63015.9

Table of Percentiles

		Standard	95.0% Normal CI	
Percent	Percentile	Error	Lower	Upper
1	23199.4	7577.64	12230.6	44005.3
2	28783.8	8049.16	16638.6	49794.3
3	32676.1	8245.51	19926.8	53582.5
4	35769.9	8337.13	22652.8	56482.4
5	38384.1	8375.84	25027.1	58869.9
6	40673.8	8383.85	27155.8	60921.2
7	42727.3	8372.59	29101.1	62733.8
8	44600.1	8348.59	30903.1	64368.1
9	46329.8	8315.93	32589.2	65863.7
10	47942.9	8277.26	34179.5	67248.5
20	60450.8	7798.48	46945.3	77841.6
30	69875.5	7399.48	56778.8	85993.0
40	78075.7	7203.45	65160.1	93551.3
50	85795.3	7284.80	72642.1	101330
60	93520.4	7721.23	79548.1	109947
70	101751	8615.76	86191.3	120120
80	111296	10167.5	93050.4	133120
90	124317	12999.0	101280	152593
91	126047	13425.6	102298	155309
92	127920	13899.1	103384	158280
93	129972	14431.0	104554	161570
94	132255	15038.1	105834	165271
95	134845	15745.8	107261	169523
96	137871	16596.5	108895	174557
97	141566	17667.8	110847	180796
98	146433	19130.2	113354	189165
99	154001	21509.7	117121	202494

Probability Plot for P7_400mils_SnPb, P7_400mils_SAC

Distribution Analysis: P7_400mils_SnPb_SAC

Variable: P7_400mils_SnPb_SAC

Censoring Information	Count
Uncensored value	22
Right censored value	18

Censoring value: Cen_3_4 = 0

Estimation Method: Maximum Likelihood

Distribution: Weibull

Parameter Estimates

Parameter	Estimate	Standard Error	95.0% Normal CI Lower	Upper
Shape	1.16145	0.206924	0.819124	1.64683
Scale	221679	42490.9	152254	322761

Log-Likelihood = -293.663

Goodness-of-Fit
Anderson-Darling (adjusted) = 121.391

Characteristics of Distribution

	Estimate	Standard Error	95.0% Normal CI Lower	Upper
Mean(MTTF)	210373	44555.5	138903	318616
Standard Deviation	181663	60388.7	94691.2	348517
Median	161687	29680.5	112830	231702
First Quartile(Q1)	75831.8	17321.4	48464.2	118654
Third Quartile(Q3)	293671	62144.5	193971	444617
Interquartile Range(IQR)	217839	57433.6	129932	365221

Table of Percentiles

Percent	Percentile	Standard Error	95.0% Normal CI Lower	Upper
1	4222.93	2854.14	1122.83	15882.3
2	7703.57	4418.23	2503.24	23707.3

3	10970.2	5641.52	4003.85	30057.5
4	14116.0	6670.82	5590.62	35642.3
5	17182.8	7569.12	7246.62	40743.0
6	20194.3	8371.03	8961.59	45506.4
7	23165.8	9098.25	10728.6	50021.0
8	26107.9	9765.57	12542.5	54345.2
9	29028.7	10383.7	14399.5	58520.3
10	31934.2	10960.7	16296.7	62576.8
20	60934.0	15449.9	37071.2	100157
30	91250.2	19205.3	60406.3	137843
40	124322	23584.2	85718.5	180311
50	161687	29680.5	112830	231702
60	205606	38706.6	142165	297358
70	260097	52468.3	175156	386229
80	333941	74764.6	215327	517895
90	454559	117858	273458	755596
91	472411	124798	281486	792836
92	492240	132653	290261	834768
93	514566	141674	299973	882672
94	540146	152228	310899	938434
95	570152	164890	323459	1004990
96	606533	180627	338349	1087288
97	652925	201263	356847	1194663
98	717428	230931	381757	1348247
99	825610	282969	421730	1616275

Probability Plot for P7_400mils_SnPb_SAC

Distribution ID Plot: P3_210mils_SnPb, P8_210mils_SAC

Results for variable: P3_210mils_SnPb

3-Parameter Weibull

* WARNING * Variance/Covariance matrix of estimated parameters does not exist.

The threshold parameter is assumed fixed when calculating confidence intervals.

3-Parameter Lognormal

* WARNING * Variance/Covariance matrix of estimated parameters does not exist.
The threshold parameter is assumed fixed when calculating confidence intervals.

2-Parameter Exponential

* WARNING * Variance/Covariance matrix of estimated parameters does not exist.
The threshold parameter is assumed fixed when calculating confidence intervals.

3-Parameter Loglogistic

* WARNING * Variance/Covariance matrix of estimated parameters does not exist.
The threshold parameter is assumed fixed when calculating confidence intervals.

Goodness-of-Fit

Distribution	Anderson-Darling (adj)
Weibull	55.640
Lognormal	55.672
Exponential	56.124
Loglogistic	55.652
3-Parameter Weibull	55.646
3-Parameter Lognormal	55.677
2-Parameter Exponential	55.707
3-Parameter Loglogistic	55.665
Smallest Extreme Value	55.750
Normal	55.703
Logistic	55.696

Table of Percentiles

			Standard	95% Normal CI	
Distribution	Percent	Percentile	Error	Lower	Upper
Weibull	1	11225.6	23789.9	176.317	714699
Lognormal	1	41441.3	55980.5	2934.94	585151
Exponential	1	392831	113400	223092	691713

Loglogistic	1	19386.9	34884.8	569.975	659418
3-Parameter Weibull	1	-580407	86460.3	-630991	-410948
3-Parameter Lognormal	1	-554729	230848	-784558	-102276
2-Parameter Exponential	1	-1616548	123282	-1858176	-1374921
3-Parameter Loglogistic	1	-616524	130925	-710947	-359916
Smallest Extreme Value	1	-55366990	23056514	-100556926	-10177054
Normal	1	-27173960	12495948	-51665568	-2682352
Logistic	1	-41528029	16731512	-74321190	-8734869

Weibull	5	218096	299950	14722.5	3230832
Lognormal	5	265658	268583	36622.7	1927063
Exponential	5	2004866	578755	1138583	3530256
Loglogistic	5	253511	308374	23366.0	2750481
3-Parameter Weibull	5	-66805.7	626812	-630991	1161724
3-Parameter Lognormal	5	123049	681270	-784558	1458314
2-Parameter Exponential	5	135955	629185	-1097225	1369134
3-Parameter Loglogistic	5	-4688.96	663582	-710947	1295908
Smallest Extreme Value	5	-21819824	15053292	-51323734	7684085
Normal	5	-10414999	9295734	-28634302	7804304
Logistic	5	-16176527	11293816	-38311999	5958945

Weibull	10	808452	860457	100392	6510446
Lognormal	10	715275	612042	133697	3826694
Exponential	10	4118155	1188809	2338740	7251426
Loglogistic	10	811704	793792	119393	5518432
3-Parameter Weibull	10	1005760	1409357	-630991	3768048
3-Parameter Lognormal	10	1102938	1197317	-784558	3449636
2-Parameter Exponential	10	2433389	1292396	-99659.9	4966438
3-Parameter Loglogistic	10	1045141	1330265	-710947	3652413
Smallest Extreme Value	10	-7004568	11718733	-29972861	15963726
Normal	10	-1480859	7818798	-16805422	13843704
Logistic	10	-4700652	9114957	-22565640	13164336

Weibull	50	24934167	13112243	8895486	69890810
Lognormal	50	23541349	16228441	6096041	90910657
Exponential	50	27092576	7820953	15386136	47705782
Loglogistic	50	24863225	15758967	7178662	86113539
3-Parameter Weibull	50	25948458	11365728	3672041	48224875
3-Parameter Lognormal	50	24195388	12705634	-707198	49097974
2-Parameter Exponential	50	27409728	8502430	10745271	44074185
3-Parameter Loglogistic	50	24861898	12766927	-160818	49884614
Smallest Extreme Value	50	31768292	5951048	20104452	43432132
Normal	50	30034407	6168872	17943640	42125175
Logistic	50	29044784	6390980	16518692	41570875

Table of MTTF

			95% Normal CI	
Distribution	Mean	Standard Error	Lower	Upper
Weibull	82852215	63722110	18350173	3.74083E+08
Lognormal	967787083	1910846071	20189517	4.63910E+10
Exponential	39086325	11283250	22197503	6.88249E+07
Loglogistic	*	*	*	*
3-Parameter Weibull	59283201	34611435	-630991	1.27120E+08
3-Parameter Lognormal	189584713	222864766	-784558	6.26392E+08
2-Parameter Exponential	40448574	12266414	16406844	6.44903E+07
3-Parameter Loglogistic	*	*	*	*
Smallest Extreme Value	27431678	6111167	15454011	3.94093E+07
Normal	30034407	6168872	17943640	4.21252E+07
Logistic	29044784	6390980	16518692	4.15709E+07

Results for variable: P8_210mils_SAC

3-Parameter Weibull

* WARNING * Variance/Covariance matrix of estimated parameters does not exist.
The threshold parameter is assumed fixed when calculating confidence intervals.

3-Parameter Lognormal

* WARNING * Variance/Covariance matrix of estimated parameters does not exist.
The threshold parameter is assumed fixed when calculating confidence intervals.

2-Parameter Exponential

* WARNING * Variance/Covariance matrix of estimated parameters does not exist.
The threshold parameter is assumed fixed when calculating confidence intervals.

3-Parameter Loglogistic

* WARNING * Variance/Covariance matrix of estimated parameters does not exist.

The threshold parameter is assumed fixed when calculating confidence intervals.

Goodness-of-Fit

Distribution	Anderson-Darling (adj)
Weibull	38.108
Lognormal	38.082
Exponential	40.029
Loglogistic	38.070
3-Parameter Weibull	38.127
3-Parameter Lognormal	38.061
2-Parameter Exponential	39.169
3-Parameter Loglogistic	38.067
Smallest Extreme Value	39.096
Normal	39.023
Logistic	38.873

Table of Percentiles

Distribution	Percent	Standard Percentile	Error	95% Normal CI Lower	Upper
Weibull	1	1050.09	2416.63	11.5430	95529.4
Lognormal	1	14243.1	18683.5	1089.00	186285
Exponential	1	222102	59359.1	131540	375012
Loglogistic	1	5404.27	9165.54	194.587	150093
3-Parameter Weibull	1	-56422.4	3700.52	-58121.0	-49169.5
3-Parameter Lognormal	1	-101004	43171.9	-139205	-16388.6
2-Parameter Exponential	1	-910631	63768.9	-1035615	-785646
3-Parameter Loglogistic	1	-107391	17888.1	-119394	-72331.0
Smallest Extreme Value	1	-76888852	23859879	-123653354	-30124349
Normal	1	-34543242	11406937	-56900427	-12186057
Logistic	1	-48113746	14168277	-75883058	-20344434
Weibull	5	35250.7	53982.8	1752.43	709079
Lognormal	5	90755.9	90577.6	12833.5	641806
Exponential	5	1133526	302948	671334	1913925
Loglogistic	5	73210.0	85138.6	7493.37	715260
3-Parameter Weibull	5	-9970.17	69878.3	-58121.0	126989
3-Parameter Lognormal	5	47780.4	160624	-139205	362598
2-Parameter Exponential	5	68503.6	325453	-569373	706380
3-Parameter Loglogistic	5	4175.90	126367	-119394	251851

Smallest Extreme Value	5	-38921680	15983529	-70248822	-7594538
Normal	5	-18778152	8642936	-35717994	-1838310
Logistic	5	-25099925	9559595	-43836388	-6363463
Weibull	10	166364	200935	15594.6	1774781
Lognormal	10	243573	207535	45852.9	1293872
Exponential	10	2328354	622279	1378973	3931354
Loglogistic	10	238187	225301	37304.9	1520793
3-Parameter Weibull	10	152776	241616	-58121.0	626334
3-Parameter Lognormal	10	296812	319448	-139205	922918
2-Parameter Exponential	10	1352094	668507	41844.6	2662344
3-Parameter Loglogistic	10	235663	295914	-119394	815645
Smallest Extreme Value	10	-22154440	12683431	-47013508	2704628
Normal	10	-10373841	7347044	-24773784	4026101
Logistic	10	-14682250	7734779	-29842138	477638
Weibull	50	9653781	5693878	3038448	30672066
Lognormal	50	7926175	5128327	2230111	28170912
Exponential	50	15317805	4093856	9072007	25863644
Loglogistic	50	7647222	4757839	2258995	25887615
3-Parameter Weibull	50	10007540	5654859	-58121.0	21090859
3-Parameter Lognormal	50	8501606	4786285	-139205	17882552
2-Parameter Exponential	50	15306526	4397982	6686639	23926413
3-Parameter Loglogistic	50	7791158	4438390	-119394	16490243
Smallest Extreme Value	50	21726936	6390614	9201563	34252310
Normal	50	19272448	5465898	8559484	29985412
Logistic	50	15951492	5640180	4896943	27006041

Table of MTTF

		Standard	95% Normal CI	
Distribution	Mean	Error	Lower	Upper
Weibull	49347538	39079717	10451408	233000130
Lognormal	318093862	559522036	10122909	9995516611
Exponential	22098921	5906185	13088139	37313351
Loglogistic	*	*	*	*
3-Parameter Weibull	44767102	33040382	-58121	109525061
3-Parameter Lognormal	130437098	175365633	-139205	474147422
2-Parameter Exponential	22591408	6344948	10155540	35027277
3-Parameter Loglogistic	*	*	*	*
Smallest Extreme Value	16818953	6715418	3656976	29980929
Normal	19272448	5465898	8559484	29985412
Logistic	15951492	5640180	4896943	27006041

ID P3P8 210mils SnPb vs SAC

ID P3P8 210mils SnPb vs SAC

ID P3P8 210mils SnPb vs SAC

Distribution Analysis: P3_210mils_SnPb

Variable: P3_210mils_SnPb

Censoring Information	Count
Uncensored value	12
Right censored value	8

Censoring value: C5 = 0

Estimation Method: Maximum Likelihood

Distribution: Weibull

Parameter Estimates

		Standard	95.0% Normal CI	
Parameter	Estimate	Error	Lower	Upper
Shape	0.549409	0.144837	0.327717	0.921070
Scale	48586360	26605393	16611358	142109660

Log-Likelihood = -218.569

Goodness-of-Fit
Anderson-Darling (adjusted) = 55.640

Characteristics of Distribution

		Standard	95.0% Normal CI	
	Estimate	Error	Lower	Upper
Mean(MTTF)	82852215	63722110	18350173	374083086
Standard Deviation	163036009	171066411	20852385	1274709855
Median	24934167	13112243	8895486	69890810

First Quartile(Q1)	5031082	3459648	1307159	19363965
Third Quartile(Q3)	88046228	53755513	26608501	291340666
Interquartile Range(IQR)	83015146	52718515	23911366	288210816

Table of Percentiles

		Standard	95.0% Normal CI	
Percent	Percentile	Error	Lower	Upper
1	11225.6	23789.9	176.317	714699
2	40006.2	71875.7	1182.62	1353344
3	84464.5	135925	3604.75	1979128
4	143930	212607	7957.80	2603213
5	218096	299950	14722.5	3230832
6	306840	396620	24358.5	3865197
7	410151	501653	37311.6	4508616
8	528098	614323	54017.2	5162931
9	660807	734070	74903.3	5829726
10	808452	860457	100392	6510446
20	3168462	2445836	697878	14385263
30	7440277	4658303	2181011	25381672
40	14306408	7892363	4852343	42180311
50	24934167	13112243	8895486	69890810
60	41439046	22264647	14456745	118781551
70	68115787	39440044	21897248	211887828
80	115528680	75086532	32319244	412969932
90	221715781	169353044	49616234	990762168
91	240526905	187503101	52192519	1108457565
92	262369495	209011064	55058171	1250273139
93	288162393	234959692	58289585	1424569485
94	319286312	266996748	61998353	1644297693
95	357944083	307787943	66356950	1930829637
96	407948835	362020132	71653305	2322603989
97	476730081	438991107	78424896	2897951829
98	581789900	561089974	87871928	3851963841
99	782911177	807133338	103794892	5905395722

Distribution Analysis: P8_210mils_SAC

Variable: P8_210mils_SAC

Censoring Information	Count
Uncensored value	14
Right censored value	6

Censoring value: C6 = 0

Estimation Method: Maximum Likelihood

Distribution: Weibull

Parameter Estimates

Parameter	Estimate	Standard Error	95.0% Normal CI Lower	Upper
Shape	0.463898	0.106834	0.295388	0.728536
Scale	21272649	12312609	6841418	66145002

Log-Likelihood = -242.982

Goodness-of-Fit
Anderson-Darling (adjusted) = 38.108

Characteristics of Distribution

	Estimate	Standard Error	95.0% Normal CI Lower	Upper
Mean(MTTF)	49347538	39079717	10451408	233000130
Standard Deviation	122901030	129644161	15547181	971537091
Median	9653781	5693878	3038448	30672066
First Quartile(Q1)	1450202	1168072	299105	7031256
Third Quartile(Q3)	43014203	26492800	12863225	143838080
Interquartile Range(IQR)	41564001	26021473	12184728	141781262

Table of Percentiles

Percent	Percentile	Standard Error	95.0% Normal CI Lower	Upper
1	1050.09	2416.63	11.5430	95529.4
2	4730.23	9307.58	99.9980	223756
3	11461.8	20330.9	354.323	370773
4	21547.6	35273.1	870.961	533090
5	35250.7	53982.8	1752.43	709079
6	52815.4	76347.3	3106.76	897871
7	74477.5	102281	5047.25	1098992
8	100468	131720	7692.29	1312211

9	131020	164616	11165.3	1537457
10	166364	200935	15594.6	1774781
20	838686	753250	144247	4876298
30	2305044	1693863	545976	9731618
40	4999889	3198030	1427298	17514832
50	9653781	5693878	3038448	30672066
60	17618898	10152901	5694732	54511003
70	31739690	18877870	9893092	101829427
80	59338734	38323125	16734055	210414359
90	128419444	95455121	29917576	551232957
91	141422051	107132528	32040546	624215212
92	156756403	121194921	34444972	713386268
93	175168492	138457967	37208573	824648690
94	197792446	160179548	40446002	967261282
95	226461249	188424643	44336441	1156716616
96	264394691	226884322	49182815	1421320681
97	317974852	283023010	55559129	1819827061
98	402559388	375245479	64771354	2501940287
99	572196555	570519277	81066014	4038793577

Probability Plot for P3_210mils_SnPb, P8_210mils_SAC

Distribution Analysis: P3P8_210mils_SnPb_SAC

Variable: P3P8_210mils_SnPb_SAC

Censoring Information	Count
Uncensored value	26
Right censored value	14

Censoring value: Cen_5_6 = 0

Estimation Method: Maximum Likelihood

Distribution: Weibull

Parameter Estimates

		Standard	95.0% Normal CI	
Parameter	Estimate	Error	Lower	Upper
Shape	0.488774	0.0849256	0.347704	0.687078
Scale	33715877	13765304	15146466	75051197

Log-Likelihood = -462.316

Goodness-of-Fit
Anderson-Darling (adjusted) = 86.997

Characteristics of Distribution

		Standard	95.0% Normal CI	
	Estimate	Error	Lower	Upper
Mean(MTTF)	70380742	40369153	22867550	216614759
Standard Deviation	162501140	125106285	35936341	734816617
Median	15928448	6450565	7202135	35227813
First Quartile(Q1)	2635145	1433706	907174	7654529
Third Quartile(Q3)	65775129	29245296	27516668	157227161
Interquartile Range(IQR)	63139984	28739079	25874249	154078196

Table of Percentiles

		Standard	95.0% Normal CI	
Percent	Percentile	Error	Lower	Upper
1	2756.91	4440.33	117.344	64771.5
2	11503.0	15777.9	782.119	169179
3	26645.2	32848.4	2378.23	298528
4	48507.9	55050.7	5245.65	448565
5	77392.8	81985.4	9704.82	617182
6	113594	113362	16065.7	803186
7	157407	148959	24632.3	1005874
8	209128	188606	35706.1	1224850
9	269061	232166	49587.4	1459927
10	337517	279534	66576.9	1711070
20	1567038	953882	475268	5166780
30	4090842	2027726	1548438	10807656
40	8530587	3695565	3649446	19940262
50	15928448	6450565	7202135	35227813
60	28194019	11381571	12780200	62197989
70	49291389	20970547	21410931	113476663
80	89264092	41947896	35536238	224224019
90	185739697	101620636	63562527	542760599
91	203544462	113587506	68178632	607673502
92	224435756	127923225	73438995	685894582
93	249383703	145422354	79526071	782035762
94	279857469	167304761	86710257	903240353

95	318221342	195563196	95416322	1061294553
96	368608229	233739915	106366672	1277392849
97	439163641	288952327	120939839	1594716053
98	549351185	378610785	142300079	2120776926
99	766995768	565366238	180866092	3252585948

Probability Plot for P3P8_210mils_SnPb_SAC

Distribution ID Plot: P3_220mils_SnPb, P8_220mils_SAC

Results for variable: P3_220mils_SnPb

3-Parameter Weibull

* WARNING * Variance/Covariance matrix of estimated parameters does not exist.
The threshold parameter is assumed fixed when calculating confidence intervals.

3-Parameter Lognormal

* WARNING * Variance/Covariance matrix of estimated parameters does not exist.
The threshold parameter is assumed fixed when calculating confidence intervals.

2-Parameter Exponential

* WARNING * Variance/Covariance matrix of estimated parameters does not exist.
The threshold parameter is assumed fixed when calculating confidence intervals.

3-Parameter Loglogistic

* WARNING * Variance/Covariance matrix of estimated parameters does not exist.
The threshold parameter is assumed fixed when calculating confidence intervals.

Goodness-of-Fit

Distribution	Anderson-Darling (adj)
Weibull	47.193
Lognormal	47.375
Exponential	47.996
Loglogistic	47.132
3-Parameter Weibull	47.120
3-Parameter Lognormal	47.168
2-Parameter Exponential	47.174
3-Parameter Loglogistic	47.129
Smallest Extreme Value	47.053
Normal	47.061
Logistic	47.059

Table of Percentiles

Distribution	Percent	Percentile	Standard Error	95% Normal CI Lower	Upper
Weibull	1	373.136	1094.37	1.18955	117045
Lognormal	1	102.690	256.725	0.764783	13788.6
Exponential	1	325373	90242.3	188930	560355
Loglogistic	1	674.036	1767.23	3.95321	114925
3-Parameter Weibull	1	-632282	95656.5	-693116	-444798
3-Parameter Lognormal	1	-513434	183362	-702934	-154051
2-Parameter Exponential	1	-1401120	97762.2	-1592731	-1209510
3-Parameter Loglogistic	1	-617299	121175	-709085	-379801
Smallest Extreme Value	1	-41766367	17895410	-76840726	-6692008
Normal	1	-21310113	9951852	-40815384	-1804842
Logistic	1	-32310008	13407674	-58588566	-6031451
Weibull	5	23428.0	44751.1	554.382	990058
Lognormal	5	3653.27	6939.54	88.2652	151208
Exponential	5	1660589	460564	964232	2859848
Loglogistic	5	28043.9	49537.0	879.562	894148
3-Parameter Weibull	5	-109994	601933	-693116	1069773
3-Parameter Lognormal	5	33750.3	538947	-702934	1090068
2-Parameter Exponential	5	45359.6	498943	-932551	1023270
3-Parameter Loglogistic	5	-63025.9	585617	-709085	1084763
Smallest Extreme Value	5	-15254218	11798110	-38378088	7869653
Normal	5	-7555833	7497264	-22250201	7138534
Logistic	5	-11607342	9190121	-29619647	6404964
Weibull	10	145787	215854	8006.02	2654725
Lognormal	10	24524.2	39853.2	1014.72	592712

Exponential	10	3410982	946036	1980609	5874356
Loglogistic	10	151629	214252	9506.75	2418413
3-Parameter Weibull	10	889088	1274342	-693116	3386752
3-Parameter Lognormal	10	816333	946376	-702934	2671195
2-Parameter Exponential	10	1941614	1024869	-67091.7	3950321
3-Parameter Loglogistic	10	853734	1151987	-709085	3111588
Smallest Extreme Value	10	-3545798	9243717	-21663151	14571554
Normal	10	-223478	6360663	-12690148	12243192
Logistic	10	-2235857	7489839	-16915671	12443957

Weibull	50	17443880	12338094	4361003	69774992
Lognormal	50	20255388	26223601	1601526	256181095
Exponential	50	22440215	6223795	13030055	38646290
Loglogistic	50	21679128	19036819	3877814	121198340
3-Parameter Weibull	50	20873345	8371860	4464801	37281888
3-Parameter Lognormal	50	18818680	9537942	124658	37512702
2-Parameter Exponential	50	22556568	6742421	9341666	35771471
3-Parameter Loglogistic	50	20280913	9977134	726089	39835737
Smallest Extreme Value	50	27096189	4558251	18162181	36030197
Normal	50	25641478	4921877	15994777	35288179
Logistic	50	25321503	5106569	15312811	35330194

Table of MTTF

			95% Normal CI	
Distribution	Mean	Standard Error	Lower	Upper
Weibull	1.53698E+08	1.76977E+08	16089491	1468222003
Lognormal	1.86632E+13	1.14180E+14	115711073	*
Exponential	3.23744E+07	8.97904E+06	18798395	55754811
Loglogistic	*	*	*	*
3-Parameter Weibull	4.34569E+07	2.15176E+07	1283192	85630612
3-Parameter Lognormal	1.41356E+08	1.52422E+08	-702934	440098801
2-Parameter Exponential	3.33186E+07	9.72726E+06	14253488	52383638
3-Parameter Loglogistic	*	*	*	*
Smallest Extreme Value	2.36690E+07	4.74851E+06	14362068	32975905
Normal	2.56415E+07	4.92188E+06	15994777	35288179
Logistic	2.53215E+07	5.10657E+06	15312811	35330194

Results for variable: P8_220mils_SAC

3-Parameter Weibull

* WARNING * Variance/Covariance matrix of estimated parameters does not exist.
The threshold parameter is assumed fixed when calculating confidence intervals.

2-Parameter Exponential

* WARNING * Variance/Covariance matrix of estimated parameters does not exist.
The threshold parameter is assumed fixed when calculating confidence intervals.

3-Parameter Loglogistic

* WARNING * Variance/Covariance matrix of estimated parameters does not exist.
The threshold parameter is assumed fixed when calculating confidence intervals.

Goodness-of-Fit

Distribution	Anderson-Darling (adj)
Weibull	30.489
Lognormal	30.271
Exponential	32.614
Loglogistic	30.170
3-Parameter Weibull	30.450
3-Parameter Lognormal	30.276
2-Parameter Exponential	32.103
3-Parameter Loglogistic	30.180
Smallest Extreme Value	31.357
Normal	31.406
Logistic	31.120

Table of Percentiles

			Standard	95% Normal CI	
Distribution	Percent	Percentile	Error	Lower	Upper
Weibull	1	2687.73	4726.59	85.6002	84390.7
Lognormal	1	63637.5	54715.5	11799.1	343222
Exponential	1	107923	27865.6	65063.2	179017
Loglogistic	1	32755.4	34048.6	4270.45	251241

3-Parameter Weibull	1	65646.8	3758.54	63579.8	73442.6
3-Parameter Lognormal	1	135121	38481.4	105916	236123
2-Parameter Exponential	1	-322635	29375.5	-380210	-265060
3-Parameter Loglogistic	1	-22058.2	39020.2	-61011.9	54419.9
Smallest Extreme Value	1	-53413451	14936228	-82687920	-24138982
Normal	1	-22493445	6716687	-35657910	-9328980
Logistic	1	-28218504	7856062	-43616101	-12820906
Weibull	5	48207.9	57323.4	4687.77	495759
Lognormal	5	215210	141620	59255.0	781627
Exponential	5	550801	142216	332059	913637
Loglogistic	5	171426	120683	43136.0	681264
3-Parameter Weibull	5	104003	49660.9	63579.8	265149
3-Parameter Lognormal	5	227177	101201	105916	543942
2-Parameter Exponential	5	144240	149922	-149602	438082
3-Parameter Loglogistic	5	132131	130938	-61011.9	388765
Smallest Extreme Value	5	-28512544	10126364	-48359852	-8665236
Normal	5	-13050711	5133935	-23113038	-2988384
Logistic	5	-15628160	5228970	-25876753	-5379567
Weibull	10	172504	163843	26812.0	1109858
Lognormal	10	412050	232089	136618	1242775
Exponential	10	1131389	292123	682076	1876684
Loglogistic	10	362623	206210	118962	1105354
3-Parameter Weibull	10	213858	147369	63579.8	825437
3-Parameter Lognormal	10	364928	202040	123295	1080114
2-Parameter Exponential	10	756288	307952	152713	1359863
3-Parameter Loglogistic	10	337677	218310	-61011.9	765556
Smallest Extreme Value	10	-17515689	8107565	-33406224	-1625154
Normal	10	-8016825	4388168	-16617476	583827
Logistic	10	-9928884	4179411	-18120379	-1737390
Weibull	50	4850959	2317817	1901597	12374759
Lognormal	50	4073953	1691650	1805373	9193165
Exponential	50	7443195	1921825	4487248	12346352
Loglogistic	50	3282805	1276155	1532321	7032996
3-Parameter Weibull	50	4733677	2296959	1828788	12252755
3-Parameter Lognormal	50	3872773	1842129	1524538	9837980
2-Parameter Exponential	50	7410104	2025959	3439297	11380910
3-Parameter Loglogistic	50	3297825	1265920	816667	5778984
Smallest Extreme Value	50	11264070	4126712	3175863	19352276
Normal	50	9740259	3209226	3450292	16030226
Logistic	50	6830147	2993657	962688	12697606

Table of MTTF

Distribution	Mean	Standard Error	95% Normal CI Lower	Upper
Weibull	15194145	8323324	5192658	44459323
Lognormal	20142295	16320866	4115274	98586888
Exponential	10738260	2772607	6473731	17812021
Loglogistic	*	*	*	*
3-Parameter Weibull	15657601	8902109	5137782	47717181
3-Parameter Lognormal	33491876	45711633	2307654	486080472
2-Parameter Exponential	10883715	2922841	5155052	16612377
3-Parameter Loglogistic	108468039	824411186	-61012	1724284272
Smallest Extreme Value	8045151	4365017	-510126	16600428
Normal	9740259	3209226	3450292	16030226
Logistic	6830147	2993657	962688	12697606

ID P3P8 220mils SnPb vs SAC

ID P3P8 220mils SnPb vs SAC

ID P3P8 220mils SnPb vs SAC

Distribution Analysis: P3_220mils_SnPb

Variable: P3_220mils_SnPb

Censoring Information	Count
Uncensored value	13
Right censored value	7

Censoring value: C7 = 0

Estimation Method: Maximum Likelihood

Distribution: Weibull

Parameter Estimates

Parameter	Estimate	Standard Error	95.0% Normal CI Lower	Upper

Shape	0.393733	0.101913	0.237071	0.653921
Scale	44250011	32139875	10657729	183722384

Log-Likelihood = -228.578

Goodness-of-Fit
Anderson-Darling (adjusted) = 47.193

Characteristics of Distribution

		Standard	95.0% Normal CI	
	Estimate	Error	Lower	Upper
Mean(MTTF)	153697576	176976644	16089491	1468222003
Standard Deviation	495651194	753102876	25225663	9738896041
Median	17443880	12338094	4361003	69774992
First Quartile(Q1)	1869236	1781509	288677	12103665
Third Quartile(Q3)	101437092	81762110	20897597	492376414
Interquartile Range(IQR)	99567856	81212265	20129770	492492361

Table of Percentiles

			95.0% Normal CI	
Percent	Percentile	Standard Error	Lower	Upper
1	373.136	1094.37	1.18955	117045
2	2197.89	5472.24	16.6996	289271
3	6235.53	13919.0	78.4913	495365
4	13118.2	26897.9	235.800	729797
5	23428.0	44751.1	554.382	990058
6	37724.2	67757.1	1116.25	1274904
7	56556.6	96157.4	2019.64	1583777
8	80474.1	130171	3379.03	1916547
9	110030	170004	5325.34	2273393
10	145787	215854	8006.02	2654725
20	980512	1051782	119779	8026489
30	3226850	2788678	593146	17554809
40	8035012	6045883	1838681	35112892
50	17443880	12338094	4361003	69774992
60	35439357	25321128	8735934	143768028
70	70902738	54260433	15821792	317738873
80	148191404	127151855	27572188	796479847
90	368015434	372102026	50723873	2670051640
91	412303193	425665167	54504117	3118918946
92	465470364	491339810	58800804	3684688735

93	530539408	573532709	63758387	4414667274
94	612170344	679141471	69590463	5385113364
95	718012610	819676267	76631725	6727528394
96	861740899	1016093160	85449726	8690459389
97	1071021122	1311687293	97123733	1.18106E+10
98	1414132003	1816051952	114120247	1.75234E+10
99	2140029328	2942841976	144509907	3.16914E+10

Distribution Analysis: P8_220mils_SAC

Variable: P8_220mils_SAC

Censoring Information	Count
Uncensored value	15
Right censored value	5

Censoring value: C8 = 0

Estimation Method: Maximum Likelihood

Distribution: Weibull

Parameter Estimates

		Standard	95.0% Normal CI	
Parameter	Estimate	Error	Lower	Upper
Shape	0.564618	0.117439	0.375584	0.848792
Scale	9284173	4245762	3788600	22751379

Log-Likelihood = -252.773

Goodness-of-Fit
Anderson-Darling (adjusted) = 30.489

Characteristics of Distribution

		Standard	95.0% Normal CI	
	Estimate	Error	Lower	Upper
Mean(MTTF)	15194145	8323324	5192658	44459323
Standard Deviation	28853583	21093800	6885213	120915534
Median	4850959	2317817	1901597	12374759
First Quartile(Q1)	1021923	664616	285649	3655979

Third Quartile(Q3)	16557123	7814887	6564802	41758811
Interquartile Range(IQR)	15535200	7501082	6030024	40023461

Table of Percentiles

		Standard	95.0% Normal CI	
Percent	Percentile	Error	Lower	Upper
1	2687.73	4726.59	85.6002	84390.7
2	9256.29	13992.8	478.269	179143
3	19153.2	26207.5	1310.80	279863
4	32172.4	40767.2	2684.64	385551
5	48207.9	57323.4	4687.77	495759
6	67203.0	75645.0	7400.48	610263
7	89130.4	95567.0	10898.2	728949
8	113983	116967	15253.0	851772
9	141768	139750	20534.9	978731
10	172504	163843	26812.0	1109858
20	651650	469132	158936	2671815
30	1495439	892259	464404	4815496
40	2825283	1473706	1016398	7853444
50	4850959	2317817	1901597	12374759
60	7952433	3647681	3236418	19540490
70	12898055	5957405	5216364	31891914
80	21566817	10535863	8278572	56184517
90	40669340	22327673	13866063	119283693
91	44023193	24577884	14738756	131492884
92	47908701	27239381	15719834	146009403
93	52485752	30444202	16838544	163598123
94	57994207	34393064	18137834	185431625
95	64816048	39410273	19684492	213422829
96	73611108	46065231	21590782	250967993
97	85661869	55485665	24067985	304884507
98	103980377	70381638	27592750	391839111
99	138811173	100266141	33696453	571827000

Probability Plot for P3_220mils_SnPb, P8_220mils_SAC

Distribution Analysis: P3P8_220mils_SnPb_SAC

Variable: P3P8_220mils_SnPb_SAC

Censoring Information Count

Uncensored value 28
Right censored value 12

Censoring value: Cen_7_8 = 0

Estimation Method: Maximum Likelihood

Distribution: Weibull

Parameter Estimates

Parameter	Estimate	Standard Error	95.0% Normal CI Lower	Upper
Shape	0.450120	0.0746429	0.325218	0.622992
Scale	21011457	8886164	9172043	48133372

Log-Likelihood = -483.517

Goodness-of-Fit
Anderson-Darling (adjusted) = 55.571

Characteristics of Distribution

	Estimate	Standard Error	95.0% Normal CI Lower	Upper
Mean(MTTF)	52047757	30974380	16212110	167095395
Standard Deviation	135599981	107493801	28674045	641254309
Median	9307423	3985421	4021116	21543304
First Quartile(Q1)	1319354	772512	418758	4156803
Third Quartile(Q3)	43411653	19683577	17850778	105573640
Interquartile Range(IQR)	42092299	19386909	17066932	103812541

Table of Percentiles

Percent	Percentile	Standard Error	95.0% Normal CI Lower	Upper
1	765.673	1299.06	27.5339	21292.1
2	3611.65	5232.57	211.097	61791.5
3	8991.70	11732.1	696.978	116002
4	17233.7	20734.4	1630.33	182172
5	28621.3	32189.7	3157.65	259427
6	43416.8	46060.3	5427.89	347284

7	61871.5	62317.6	8593.14	445481
8	84231.6	80941.8	12809.1	553900
9	110742	101920	18235.4	672523
10	141648	125247	25036.0	801409
20	750330	490873	208156	2704684
30	2127023	1134454	747793	6050105
40	4724397	2190211	1904289	11720873
50	9307423	3985421	4021116	21543304
60	17302476	7271596	7592406	39430933
70	31736315	13851616	13490918	74657164
80	60479690	28843098	23750177	154011188
90	134018553	73958361	45438913	395277335
91	148024416	83291684	49132828	445959016
92	164592474	94566992	53376504	507539466
93	184551234	108455731	58329600	583908646
94	209163251	125996013	64229947	681135008
95	240474421	148896839	71453304	809311031
96	282089176	180222661	80642906	986748958
97	341176765	226193533	93035661	1251150194
98	435062948	302215503	111497942	1697607733
99	625088905	464699527	145595206	2683715682

Probability Plot for P3P8_220mils_SnPb_SAC

Distribution ID Plot: P3_250mils_SnPb, P8_250mils_SAC

Results for variable: P3_250mils_SnPb

3-Parameter Weibull

* WARNING * Variance/Covariance matrix of estimated parameters does not exist.
The threshold parameter is assumed fixed when calculating confidence intervals.

3-Parameter Lognormal

* WARNING * Newton-Raphson algorithm has not converged after 50 iterations.
* WARNING * Convergence has not been reached for the parameter estimates criterion.
* WARNING * Variance/Covariance matrix of estimated parameters does not exist.
The threshold parameter is assumed fixed when calculating

confidence intervals.

2-Parameter Exponential

* WARNING * Variance/Covariance matrix of estimated parameters does not exist.

The threshold parameter is assumed fixed when calculating confidence intervals.

3-Parameter Loglogistic

* WARNING * Variance/Covariance matrix of estimated parameters does not exist.

The threshold parameter is assumed fixed when calculating confidence intervals.

Goodness-of-Fit

Distribution	Anderson-Darling (adj)
Weibull	47.842
Lognormal	47.942
Exponential	48.046
Loglogistic	47.737
3-Parameter Weibull	47.094
3-Parameter Lognormal	47.064
2-Parameter Exponential	47.135
3-Parameter Loglogistic	47.051
Smallest Extreme Value	47.394
Normal	47.245
Logistic	47.205

Table of Percentiles

Distribution	Percent	Percentile	Standard Error	95% Normal CI Lower	Upper
Weibull	1	23.3556	73.0431	0.0508520	10726.9
Lognormal	1	2.58772	7.14104	0.0115864	577.942
Exponential	1	26031.7	7219.89	15115.5	44831.5
Loglogistic	1	34.2300	103.310	0.0923392	12689.0
3-Parameter Weibull	1	-155055	54745.0	-214189	-47756.2
3-Parameter Lognormal	1	-336560	205911	-740139	67019.2
2-Parameter Exponential	1	-112096	7821.51	-127426	-96766.5

3-Parameter Loglogistic	1	-203156	105744	-382883	4098.47
Smallest Extreme Value	1	-3769028	1493677	-6696580	-841476
Normal	1	-1519114	759516	-3007738	-30489.4
Logistic	1	-2407942	979576	-4327876	-488009
Weibull	5	1678.18	3393.08	31.9020	88279.7
Lognormal	5	134.484	282.161	2.20171	8214.46
Exponential	5	132856	36847.7	77143.9	228804
Loglogistic	5	1872.62	3765.39	36.3824	96385.0
3-Parameter Weibull	5	18022.8	141419	-214189	295200
3-Parameter Lognormal	5	14776.4	236469	-448695	478247
2-Parameter Exponential	5	3629.94	39918.2	-74608.3	81868.1
3-Parameter Loglogistic	5	51216.8	172949	-287757	390191
Smallest Extreme Value	5	-1492583	988248	-3429515	444348
Normal	5	-486824	570189	-1604373	630726
Logistic	5	-871391	661512	-2167930	425148
Weibull	10	11083.9	17254.7	524.327	234307
Lognormal	10	1104.92	1984.40	32.7039	37330.3
Exponential	10	272898	75688.2	158460	469981
Loglogistic	10	11460.7	18205.5	509.406	257844
3-Parameter Weibull	10	210654	202370	-185985	607292
3-Parameter Lognormal	10	272492	250954	-219368	764353
2-Parameter Exponential	10	155341	81995.1	-5366.78	316048
3-Parameter Loglogistic	10	264188	207847	-143185	671561
Smallest Extreme Value	10	-487249	777038	-2010216	1035717
Normal	10	63486.6	481991	-881198	1008171
Logistic	10	-175840	534641	-1223717	872036
Weibull	50	1549977	1129208	371704	6463280
Lognormal	50	1861257	2667780	112140	30892424
Exponential	50	1795342	497938	1042477	3091918
Loglogistic	50	2358973	2171071	388439	14325932
3-Parameter Weibull	50	1850266	484588	900490	2800042
3-Parameter Lognormal	50	1824760	427157	987548	2661972
2-Parameter Exponential	50	1804650	539431	747385	2861915
3-Parameter Loglogistic	50	1709943	446937	833962	2585924
Smallest Extreme Value	50	2143800	391543	1376390	2911211
Normal	50	2004711	367303	1284810	2724611
Logistic	50	1869466	380510	1123679	2615252

Table of MTTF

95% Normal CI

Distribution	Mean	Standard Error	Lower	Upper
Weibull	1.54568E+07	1.94708E+07	1308796	182544108
Lognormal	3.69185E+13	2.73176E+14	18570649	*
Exponential	2.59013E+06	7.18373E+05	1503976	4460695
Loglogistic	*	*	*	*
3-Parameter Weibull	2.43190E+06	6.79593E+05	1099922	3763877
3-Parameter Lognormal	2.42655E+06	6.54326E+05	1144093	3709003
2-Parameter Exponential	2.66567E+06	7.78234E+05	1140358	4190979
3-Parameter Loglogistic	3.14995E+06	1.35467E+06	494840	5805068
Smallest Extreme Value	1.84953E+06	4.07353E+05	1051130	2647923
Normal	2.00471E+06	3.67303E+05	1284810	2724611
Logistic	1.86947E+06	3.80510E+05	1123679	2615252

Results for variable: P8_250mils_SAC

3-Parameter Weibull

* WARNING * Variance/Covariance matrix of estimated parameters does not exist.
The threshold parameter is assumed fixed when calculating confidence intervals.

3-Parameter Lognormal

* WARNING * Variance/Covariance matrix of estimated parameters does not exist.
The threshold parameter is assumed fixed when calculating confidence intervals.

2-Parameter Exponential

* WARNING * Variance/Covariance matrix of estimated parameters does not exist.
The threshold parameter is assumed fixed when calculating confidence intervals.

3-Parameter Loglogistic

* WARNING * Variance/Covariance matrix of estimated parameters does not exist.
The threshold parameter is assumed fixed when calculating confidence intervals.

Goodness-of-Fit

Distribution	Anderson-Darling (adj)
Weibull	29.802
Lognormal	29.593
Exponential	30.085
Loglogistic	29.551
3-Parameter Weibull	29.408
3-Parameter Lognormal	29.320
2-Parameter Exponential	30.468
3-Parameter Loglogistic	29.328
Smallest Extreme Value	30.641
Normal	30.468
Logistic	30.224

Table of Percentiles

Distribution	Percent	Percentile	Standard Error	95% Normal CI Lower	Upper
Weibull	1	896.651	1163.99	70.4107	11418.5
Lognormal	1	8619.57	5479.78	2479.39	29965.8
Exponential	1	3563.85	920.182	2148.52	5911.51
Loglogistic	1	4154.28	3312.12	870.662	19821.7
3-Parameter Weibull	1	38970.7	76.2704	38932.0	39120.4
3-Parameter Lognormal	1	37692.4	962.239	36705.1	39626.3
2-Parameter Exponential	1	27633.4	835.769	26042.9	29321.0
3-Parameter Loglogistic	1	37925.6	404.972	37612.0	38727.7
Smallest Extreme Value	1	-1211249	361495	-1919767	-502731
Normal	1	-489700	165914	-814885	-164515
Logistic	1	-651079	197770	-1038701	-263457
Weibull	5	7400.35	6490.24	1326.58	41283.0
Lognormal	5	21268.1	10352.9	8191.82	55217.7
Exponential	5	18188.6	4696.28	10965.3	30170.2
Loglogistic	5	15537.8	8513.84	5308.56	45477.9
3-Parameter Weibull	5	39816.9	1174.60	38932.0	42186.9
3-Parameter Lognormal	5	40687.3	2975.92	36705.1	46958.8
2-Parameter Exponential	5	40916.5	4265.46	33355.1	50192.0
3-Parameter Loglogistic	5	40123.6	2244.57	37612.0	44773.2
Smallest Extreme Value	5	-611903	244888	-1091874	-131932
Normal	5	-255881	126866	-504534	-7227.19
Logistic	5	-328555	133146	-589517	-67592.8

Weibull	10	18795.7	13155.4	4767.47	74101.7
Lognormal	10	34421.8	14348.6	15205.9	77921.1
Exponential	10	37360.8	9646.53	22523.6	61972.1
Loglogistic	10	28230.6	12663.3	11719.3	68004.8
3-Parameter Weibull	10	42458.2	3722.43	38932.0	50418.4
3-Parameter Lognormal	10	45080.7	5367.32	36705.1	56929.2
2-Parameter Exponential	10	58330.0	8761.60	43454.6	78297.7
3-Parameter Loglogistic	10	44053.3	4721.98	37612.0	54352.2
Smallest Extreme Value	10	-347217	195924	-731221	36786.6
Normal	10	-131233	108483	-343856	81390.1
Logistic	10	-182558	107404	-393065	27949.2

Weibull	50	215512	75347.8	108611	427633
Lognormal	50	188126	57958.2	102851	344103
Exponential	50	245790	63462.7	148178	407703
Loglogistic	50	163418	51841.8	87754.4	304320
3-Parameter Weibull	50	170338	68025.6	77871.4	372601
3-Parameter Lognormal	50	152064	55027.1	74817.3	309064
2-Parameter Exponential	50	247639	57641.0	156925	390793
3-Parameter Loglogistic	50	140349	50969.3	68878.9	285978
Smallest Extreme Value	50	345490	99313.3	150839	540140
Normal	50	308464	79532.1	152584	464344
Logistic	50	246754	76943.7	95947.5	397561

Table of MTTF

		Standard	95% Normal CI	
Distribution	Mean	Error	Lower	Upper
Weibull	402923	149351	194853	833174
Lognormal	452735	226139	170087	1205078
Exponential	354600	91557	213776	588191
Loglogistic	695437	733994	87874	5503673
3-Parameter Weibull	533314	307138	172493	1648899
3-Parameter Lognormal	973225	949662	143754	6588794
2-Parameter Exponential	346467	83158	216451	554582
3-Parameter Loglogistic	*	*	*	*
Smallest Extreme Value	268013	105088	62044	473982
Normal	308464	79532	152584	464344
Logistic	246754	76944	95948	397561

ID P3P8 250mils SnPb vs SAC

ID P3P8 250mils SnPb vs SAC

ID P3P8 250mils SnPb vs SAC

Distribution Analysis: P3_250mils_SnPb

Variable: P3_250mils_SnPb

Censoring Information	Count
Uncensored value	13
Right censored value	7

Censoring value: C9 = 0

Estimation Method: Maximum Likelihood

Distribution: Weibull

Parameter Estimates

		Standard	95.0% Normal CI	
Parameter	Estimate	Error	Lower	Upper
Shape	0.381309	0.103045	0.224517	0.647597
Scale	4052922	3078107	914743	17957157

Log-Likelihood = -195.732

Goodness-of-Fit
Anderson-Darling (adjusted) = 47.842

Characteristics of Distribution

		Standard	95.0% Normal CI	
	Estimate	Error	Lower	Upper
Mean(MTTF)	15456813	19470753	1308796	182544108
Standard Deviation	52646948	87554531	2022004	1370769129
Median	1549977	1129208	371704	6463280
First Quartile(Q1)	154433	152145	22395.1	1064948
Third Quartile(Q3)	9545332	8164271	1785440	51031334
Interquartile Range(IQR)	9390899	8124054	1723193	51177662

Table of Percentiles

Percent	Percentile	Standard Error	95.0% Normal CI Lower	Upper
1	23.3556	73.0431	0.0508520	10726.9
2	145.755	386.058	0.811080	26192.8
3	427.806	1014.00	4.10866	44544.5
4	922.085	2004.29	13.0185	65310.3
5	1678.18	3393.08	31.9020	88279.7
6	2744.52	5210.32	66.4516	113351
7	4169.27	7482.14	123.736	140482
8	6000.99	10232.2	212.250	169667
9	8289.05	13482.7	341.954	200928
10	11083.9	17254.7	524.327	234307
20	79323.0	88411.0	8926.40	704891
30	271382	241412	47466.0	1551603
40	696144	537155	153426	3158630
50	1549977	1129208	371704	6463280
60	3222543	2397644	749697	13851973
70	6594614	5323325	1355438	32084777
80	14118267	12923833	2347433	84912094
90	36115731	39306849	4278429	304865664
91	40612069	45166619	4591909	359183981
92	46030618	52381288	4947755	428238188
93	52689492	61450671	5357783	518158790
94	61080683	73159758	5839452	638904111
95	72014577	88823354	6420098	807791330
96	86945505	110845286	7146039	1057861758
97	108829108	144215921	8105266	1461244341
98	145000527	201642467	9498629	2213493423
99	222414012	331484540	11982194	4128458633

Distribution Analysis: P8_250mils_SAC

Variable: P8_250mils_SAC

Censoring Information	Count
Uncensored value	15
Right censored value	5

Censoring value: C10 = 0

Estimation Method: Maximum Likelihood

Distribution: Weibull

Parameter Estimates

Parameter	Estimate	Standard Error	95.0% Normal CI Lower	Upper
Shape	0.772265	0.162299	0.511538	1.16588
Scale	346406	115821	179882	667090

Log-Likelihood = -205.824

Goodness-of-Fit
Anderson-Darling (adjusted) = 29.802

Characteristics of Distribution

	Estimate	Standard Error	95.0% Normal CI Lower	Upper
Mean(MTTF)	402923	149351	194853	833174
Standard Deviation	527778	271333	192683	1445634
Median	215512	75347.8	108611	427633
First Quartile(Q1)	69013.8	32985.3	27045.9	176104
Third Quartile(Q3)	528778	182598	268742	1040426
Interquartile Range(IQR)	459764	168597	224076	943353

Table of Percentiles

Percent	Percentile	Standard Error	95.0% Normal CI Lower	Upper
1	896.651	1163.99	70.4107	11418.5
2	2214.48	2470.53	248.686	19719.4
3	3768.46	3804.58	520.959	27259.9
4	5506.08	5146.89	881.393	34396.6
5	7400.35	6490.24	1326.58	41283.0
6	9434.76	7831.40	1854.32	48004.1
7	11598.3	9168.88	2463.12	54613.6
8	13883.1	10502.1	3151.99	61149.0
9	16283.7	11830.9	3920.25	67637.9
10	18795.7	13155.4	4767.47	74101.7
20	49667.5	26302.3	17591.5	140230
30	91164.7	39935.9	38631.9	215133

40	145154	55485.8	68620.7	307047
50	215512	75347.8	108611	427633
60	309331	103741	160308	596887
70	440530	148798	227230	854056
80	641515	229438	318254	1293122
90	1020038	410773	463270	2245942
91	1080880	442745	484297	2412364
92	1149829	479776	507530	2604982
93	1229152	523367	533541	2831671
94	1322192	575758	563161	3104247
95	1434188	640505	597670	3441524
96	1574013	723720	639193	3876008
97	1758524	837209	691677	4470884
98	2026199	1008488	763869	5374591
99	2502752	1330078	883182	7092276

Probability Plot for P3_250mils_SnPb, P8_250mils_SAC

Distribution Analysis: P3P8_250mils_SnPb_SAC

Variable: P3P8_250mils_SnPb_SAC

Censoring Information	Count
Uncensored value	28
Right censored value	12

Censoring value: Cen_9_10 = 0

Estimation Method: Maximum Likelihood

Distribution: Weibull

Parameter Estimates

		Standard	95.0% Normal CI	
Parameter	Estimate	Error	Lower	Upper
Shape	0.449105	0.0753331	0.323271	0.623920
Scale	1425529	604916	620544	3274759

Log-Likelihood = -407.794

Goodness-of-Fit

Anderson-Darling (adjusted) = 42.400

Characteristics of Distribution

		Standard	95.0% Normal CI	
	Estimate	Error	Lower	Upper
Mean(MTTF)	3549109	2138975	1089226	11564341
Standard Deviation	9278128	7462293	1918000	44881985
Median	630304	270235	272024	1460469
First Quartile(Q1)	88953.7	52297.6	28101.3	281580
Third Quartile(Q3)	2950112	1346471	1205976	7216694
Interquartile Range(IQR)	2861158	1326979	1152822	7101030

Table of Percentiles

		Standard	95.0% Normal CI	
Percent	Percentile	Error	Lower	Upper
1	50.7611	87.0955	1.75810	1465.61
2	240.279	351.858	13.6219	4238.32
3	599.442	790.204	45.2551	7940.13
4	1150.60	1398.07	106.327	12451.0
5	1913.07	2172.22	206.646	17710.7
6	2904.75	3110.14	356.222	23686.3
7	4142.76	4209.95	565.305	30359.6
8	5643.87	5470.29	844.410	37722.5
9	7424.75	6890.31	1204.34	45773.4
10	9502.14	8469.58	1656.21	54516.3
20	50524.4	33229.9	13920.9	183373
30	143563	76798.2	50315.2	409626
40	319449	148307	128594	793561
50	630304	270235	272024	1460469
60	1173377	494435	513760	2679876
70	2155168	945499	912112	5092300
80	4113081	1977392	1603046	10553301
90	9130692	5093777	3059429	27250032
91	10087178	5739456	3307109	30767401
92	11218904	6519763	3591555	35044378
93	12582582	7481294	3923433	40352764
94	14264650	8696108	4318631	47116835
95	16405201	10282862	4802244	56042684
96	19251110	12454381	5417219	68412446
97	23293540	15642792	6246123	86868124
98	29719861	20918821	7480219	118080782

99 42735838 32205205 9757468 187174765

Probability Plot for P3P8_250mils_SnPb_SAC

Distribution ID Plot: P3_270mils_SnPb, P8_270mils_SAC

Results for variable: P3_270mils_SnPb

3-Parameter Weibull

* WARNING * Variance/Covariance matrix of estimated parameters does not exist.
The threshold parameter is assumed fixed when calculating confidence intervals.

3-Parameter Lognormal

* WARNING * Variance/Covariance matrix of estimated parameters does not exist.
The threshold parameter is assumed fixed when calculating confidence intervals.

2-Parameter Exponential

* WARNING * Variance/Covariance matrix of estimated parameters does not exist.
The threshold parameter is assumed fixed when calculating confidence intervals.

3-Parameter Loglogistic

* WARNING * Variance/Covariance matrix of estimated parameters does not exist.
The threshold parameter is assumed fixed when calculating confidence intervals.

Goodness-of-Fit

Distribution	Anderson-Darling (adj)
Weibull	38.449
Lognormal	38.949

Exponential	38.199
Loglogistic	38.428
3-Parameter Weibull	38.083
3-Parameter Lognormal	38.079
2-Parameter Exponential	38.109
3-Parameter Loglogistic	38.081
Smallest Extreme Value	38.383
Normal	38.225
Logistic	38.198

Table of Percentiles

			Standard	95% Normal CI	
Distribution	Percent	Percentile	Error	Lower	Upper
Weibull	1	448.347	821.926	12.3356	16295.5
Lognormal	1	81.1053	142.689	2.57946	2550.17
Exponential	1	7549.60	2017.71	4471.27	12747.3
Loglogistic	1	915.155	1449.78	41.0233	20415.5
3-Parameter Weibull	1	-42417.5	13890.4	-57270.7	-15192.8
3-Parameter Lognormal	1	-84105.3	48280.9	-178734	10523.4
2-Parameter Exponential	1	-32316.6	2172.91	-36575.5	-28057.8
3-Parameter Loglogistic	1	-52166.7	24129.1	-90729.7	-4874.55
Smallest Extreme Value	1	-1233472	463709	-2142326	-324619
Normal	1	-508671	234898	-969063	-48279.3
Logistic	1	-781152	301977	-1373016	-189288
Weibull	5	6454.32	7758.26	611.904	68079.6
Lognormal	5	1047.14	1412.00	74.5105	14716.1
Exponential	5	38530.4	10297.7	22819.7	65057.4
Loglogistic	5	8966.05	9548.64	1111.96	72295.6
3-Parameter Weibull	5	4219.91	38248.3	-57270.7	79185.1
3-Parameter Lognormal	5	3823.16	60370.1	-114500	122146
2-Parameter Exponential	5	1047.22	11089.8	-20688.3	22782.8
3-Parameter Loglogistic	5	11574.4	44124.0	-74907.0	98055.8
Smallest Extreme Value	5	-506895	309900	-1114289	100498
Normal	5	-181492	178234	-530824	167840
Logistic	5	-296233	206555	-701073	108607
Weibull	10	20958.3	19623.1	3344.89	131320
Lognormal	10	4094.97	4747.61	422.075	39729.4
Exponential	10	79144.6	21152.3	46873.6	133633
Loglogistic	10	25191.0	21401.3	4765.41	133166
3-Parameter Weibull	10	57885.3	56466.0	-52786.0	168557
3-Parameter Lognormal	10	71968.1	67136.8	-59617.6	203554

2-Parameter Exponential	10	44785.4	22779.3	138.818	89431.9
3-Parameter Loglogistic	10	68381.1	56079.7	-41533.2	178295
Smallest Extreme Value	10	-186021	245378	-666954	294911
Normal	10	-7074.59	151739	-304477	290327
Logistic	10	-76725.0	168373	-406730	253280

Weibull	50	457101	202039	192212	1087036
Lognormal	50	502812	455017	85332.4	2962762
Exponential	50	520677	139157	308372	879148
Loglogistic	50	525424	272016	190474	1449382
3-Parameter Weibull	50	537550	141878	259474	815627
3-Parameter Lognormal	50	525108	129428	271435	778782
2-Parameter Exponential	50	520280	149861	226559	814002
3-Parameter Loglogistic	50	492335	137049	223725	760945
Smallest Extreme Value	50	653736	122204	414220	893252
Normal	50	608186	113744	385252	831120
Logistic	50	568751	117805	337858	799644

Table of MTTF

			95% Normal CI	
Distribution	Mean	Standard Error	Lower	Upper
Weibull	1223538	721374	385271	3.88570E+06
Lognormal	576679787	1783675513	1343263	2.47576E+11
Exponential	751179	200761	444887	1.26834E+06
Loglogistic	*	*	*	*
3-Parameter Weibull	722418	194875	340470	1.10437E+06
3-Parameter Lognormal	752991	217872	325970	1.18001E+06
2-Parameter Exponential	768512	216203	344761	1.19226E+06
3-Parameter Loglogistic	1037818	495186	67272	2.00836E+06
Smallest Extreme Value	559812	128503	307951	8.11672E+05
Normal	608186	113744	385252	8.31120E+05
Logistic	568751	117805	337858	7.99644E+05

Results for variable: P8_270mils_SAC

3-Parameter Weibull

* WARNING * Variance/Covariance matrix of estimated parameters does not exist.

The threshold parameter is assumed fixed when calculating confidence intervals.

3-Parameter Lognormal

* WARNING * Variance/Covariance matrix of estimated parameters does not exist.
The threshold parameter is assumed fixed when calculating confidence intervals.

2-Parameter Exponential

* WARNING * Variance/Covariance matrix of estimated parameters does not exist.
The threshold parameter is assumed fixed when calculating confidence intervals.

3-Parameter Loglogistic

* WARNING * Variance/Covariance matrix of estimated parameters does not exist.
The threshold parameter is assumed fixed when calculating confidence intervals.

Goodness-of-Fit

Distribution	Anderson-Darling (adj)
Weibull	38.428
Lognormal	38.239
Exponential	39.974
Loglogistic	38.208
3-Parameter Weibull	38.270
3-Parameter Lognormal	38.198
2-Parameter Exponential	39.654
3-Parameter Loglogistic	38.181
Smallest Extreme Value	39.408
Normal	39.365
Logistic	39.156

Table of Percentiles

Distribution	Percent	Standard Percentile	Error	95% Normal CI Lower	Upper
Weibull	1	90.1667	170.999	2.19161	3709.62
Lognormal	1	1710.84	1655.19	256.857	11395.3

Exponential	1	4186.68	1118.94	2479.57	7069.09
Loglogistic	1	620.797	767.111	55.0975	6994.68
3-Parameter Weibull	1	9575.53	34.5108	9560.75	9643.41
3-Parameter Lognormal	1	8986.48	529.827	8548.20	10087.3
2-Parameter Exponential	1	-6458.22	1160.38	-8732.52	-4183.93
3-Parameter Loglogistic	1	8608.51	253.575	8444.77	9120.13
Smallest Extreme Value	1	-1604055	486162	-2556915	-651195
Normal	1	-706640	228106	-1153719	-259562
Logistic	1	-961578	279335	-1509065	-414091
Weibull	5	1765.00	2236.80	147.234	21158.2
Lognormal	5	6583.17	4832.64	1561.62	27752.0
Exponential	5	21367.3	5710.66	12654.8	36078.1
Loglogistic	5	4403.10	3708.63	844.912	22946.0
3-Parameter Weibull	5	10098.7	836.845	9560.75	11879.6
3-Parameter Lognormal	5	10935.8	2192.94	8548.20	16200.9
2-Parameter Exponential	5	11358.7	5922.15	-248.491	22965.9
3-Parameter Loglogistic	5	10244.2	1904.60	8444.77	14748.0
Smallest Extreme Value	5	-826166	325905	-1464928	-187405
Normal	5	-392379	172738	-730940	-53818.3
Logistic	5	-512288	186966	-878734	-145841
Weibull	10	6564.33	6586.73	918.511	46913.3
Lognormal	10	13502.6	8438.60	3966.87	45960.6
Exponential	10	43890.2	11730.1	25994.1	74107.2
Loglogistic	10	10688.0	7312.52	2795.88	40857.5
3-Parameter Weibull	10	12192.2	3231.52	9560.75	20497.0
3-Parameter Lognormal	10	14442.4	4615.25	8548.20	27017.9
2-Parameter Exponential	10	34715.7	12164.6	10873.6	58557.8
3-Parameter Loglogistic	10	13770.4	4577.06	8444.77	26416.3
Smallest Extreme Value	10	-482632	258791	-989853	24589.6
Normal	10	-224848	146752	-512476	62780.1
Logistic	10	-308908	150344	-603576	-14239.4
Weibull	50	204220	102127	76635.0	544214
Lognormal	50	170191	79728.7	67947.8	426281
Exponential	50	288745	77170.4	171010	487538
Loglogistic	50	145014	68523.3	57436.8	366123
3-Parameter Weibull	50	177274	101200	57906.0	542708
3-Parameter Lognormal	50	151394	84389.6	50773.5	451422
2-Parameter Exponential	50	288639	80028.4	131786	445492
3-Parameter Loglogistic	50	137878	74071.7	48106.9	395169
Smallest Extreme Value	50	416430	130937	159798	673062
Normal	50	366121	108840	152799	579444
Logistic	50	289143	109887	73767.1	504518

Table of MTTF

Distribution	Mean	Standard Error	95% Normal CI Lower	Upper
Weibull	682402	423827	202011	2305185
Lognormal	1202090	1220953	164202	8800260
Exponential	416571	111333	246715	703368
Loglogistic	*	*	*	*
3-Parameter Weibull	926855	745236	191693	4481450
3-Parameter Lognormal	3159538	4755821	165338	60377467
2-Parameter Exponential	421199	115457	194909	647490
3-Parameter Loglogistic	*	*	*	*
Smallest Extreme Value	315873	137542	46296	585450
Normal	366121	108840	152799	579444
Logistic	289143	109887	73767	504518

ID P3P8 270mils SnPb vs SAC

ID P3P8 270mils SnPb vs SAC

ID P3P8 270mils SnPb vs SAC

Distribution Analysis: P3_270mils_SnPb

Variable: P3_270mils_SnPb

Censoring Information	Count
Uncensored value	14
Right censored value	6

Censoring value: C11 = 0

Estimation Method: Maximum Likelihood

Distribution: Weibull

Parameter Estimates

		Standard	95.0% Normal CI	
Parameter	Estimate	Error	Lower	Upper
Shape	0.611171	0.151400	0.376099	0.993168
Scale	832634	370798	347847	1993061

Log-Likelihood = -200.989

Goodness-of-Fit
Anderson-Darling (adjusted) = 38.449

Characteristics of Distribution

		Standard	95.0% Normal CI	
	Estimate	Error	Lower	Upper
Mean(MTTF)	1223538	721374	385271	3885699
Standard Deviation	2102447	1736710	416482	10613379
Median	457101	202039	192212	1087036
First Quartile(Q1)	108424	65797.4	33004.3	356188
Third Quartile(Q3)	1420884	693398	545970	3697846
Interquartile Range(IQR)	1312460	674013	479681	3591037

Table of Percentiles

		Standard	95.0% Normal CI	
Percent	Percentile	Error	Lower	Upper
1	448.347	821.926	12.3356	16295.5
2	1405.27	2192.03	66.0689	29889.6
3	2751.11	3854.04	176.627	42850.9
4	4442.16	5724.50	355.362	55528.5
5	6454.32	7758.26	611.904	68079.6
6	8772.66	9926.71	954.891	80595.1
7	11387.5	12210.1	1392.31	93136.1
8	14292.4	14594.0	1931.70	105748
9	17483.4	17067.8	2580.25	118465
10	20958.3	19623.1	3344.89	131320
20	71549.3	48817.6	18786.1	272505
30	154128	84775.6	52443.3	452972
40	277414	132052	109131	705195
50	457101	202039	192212	1087036
60	721661	317536	304648	1709495
70	1128131	525101	453063	2809059
80	1813909	939065	657576	5003625
90	3259215	1981277	990074	10728979

91	3506760	2176416	1039013	11835617
92	3791761	2405935	1093301	13150502
93	4125243	2680610	1154339	14742318
94	4523674	3016737	1224176	16716238
95	5013146	3440500	1305974	19243596
96	5638478	3997577	1404998	22628097
97	6486206	4777759	1531063	27478207
98	7757893	5994842	1706025	35277847
99	10131167	8389613	1998849	51349821

Distribution Analysis: P8_270mils_SAC

Variable: P8_270mils_SAC

Censoring Information	Count
Uncensored value	14
Right censored value	6

Censoring value: C12 = 0

Estimation Method: Maximum Likelihood

Distribution: Weibull

Parameter Estimates

		Standard	95.0% Normal CI	
Parameter	Estimate	Error	Lower	Upper
Shape	0.548023	0.122158	0.354046	0.848277
Scale	398612	194998	152809	1039806

Log-Likelihood = -190.324

Goodness-of-Fit
Anderson-Darling (adjusted) = 38.428

Characteristics of Distribution

		Standard	95.0% Normal CI	
	Estimate	Error	Lower	Upper
Mean(MTTF)	682402	423827	202011	2305185
Standard Deviation	1347298	1125345	262113	6925303

Median	204220	102127	76635.0	544214
First Quartile(Q1)	41039.9	27749.7	10905.7	154439
Third Quartile(Q3)	723436	373931	262682	1992372
Interquartile Range(IQR)	682396	362263	241079	1931585

Table of Percentiles

		Standard	95.0% Normal CI	
Percent	Percentile	Error	Lower	Upper
1	90.1667	170.999	2.19161	3709.62
2	322.375	523.431	13.3748	7770.22
3	681.913	999.168	38.5933	12048.9
4	1163.57	1574.89	81.9758	16515.7
5	1765.00	2236.80	147.234	21158.2
6	2485.33	2975.56	237.837	25970.9
7	3324.56	3784.45	357.095	30951.7
8	4283.34	4658.40	508.214	36100.9
9	5362.77	5593.51	694.326	41420.5
10	6564.33	6586.73	918.511	46913.3
20	25815.8	19399.1	5919.11	112594
30	60752.5	37594.8	18064.4	204316
40	117010	63334.1	40503.6	338029
50	204220	102127	76635.0	544214
60	339838	165736	130662	883883
70	559314	280110	209588	1492606
80	949900	512986	329604	2737555
90	1826000	1126293	545095	6116875
91	1981333	1244507	578501	6785952
92	2161736	1384668	615996	7586251
93	2374814	1553877	658681	8562170
94	2631996	1762948	708172	9782097
95	2951520	2029385	766977	11358183
96	3364960	2383992	839314	13490731
97	3933851	2887934	933105	16584607
98	4803197	3688662	1066208	21638092
99	6468490	5306087	1295879	32288024

Probability Plot for P3_270mils_SnPb, P8_270mils_SAC

Distribution Analysis: P3P8_270mils_SnPb_SAC

Variable: P3P8_270mils_SnPb_SAC

Censoring Information	Count
Uncensored value	28
Right censored value	12

Censoring value: Cen_11_12 = 0

Estimation Method: Maximum Likelihood

Distribution: Weibull

Parameter Estimates

Parameter	Estimate	Standard Error	95.0% Normal CI Lower	Upper
Shape	0.560452	0.0933832	0.404306	0.776903
Scale	608996	207011	312804	1185650

Log-Likelihood = -392.027

Goodness-of-Fit
Anderson-Darling (adjusted) = 69.718

Characteristics of Distribution

	Estimate	Standard Error	95.0% Normal CI Lower	Upper
Mean(MTTF)	1007622	448697	420974	2411792
Standard Deviation	1931907	1176581	585575	6373675
Median	316667	108805	161486	620970
First Quartile(Q1)	65942.7	30994.2	26247.4	165671
Third Quartile(Q3)	1090744	398266	533239	2231128
Interquartile Range(IQR)	1024802	387064	488815	2148500

Table of Percentiles

Percent	Percentile	Standard Error	95.0% Normal CI Lower	Upper
1	165.943	226.826	11.3882	2418.01
2	576.768	673.005	58.5831	5678.45
3	1199.92	1260.63	153.069	9406.32
4	2023.34	1959.70	303.140	13505.0

5	3040.95	2752.71	515.810	17927.9
6	4249.64	3627.99	797.380	22648.4
7	5648.08	4577.13	1153.71	27650.6
8	7236.16	5593.83	1590.37	32924.5
9	9014.68	6673.20	2112.71	38464.5
10	10985.1	7811.45	2725.96	44268.0
20	41909.3	22020.5	14964.4	117371
30	96771.2	41414.0	41828.1	223885
40	183693	68305.1	88629.6	380721
50	316667	108805	161486	620970
60	521040	175915	268835	1009849
70	848118	297851	426110	1688070
80	1423565	547141	670227	3023658
90	2697155	1201178	1126739	6456374
91	2921300	1326711	1199505	7114594
92	3181134	1475351	1281771	7895024
93	3487414	1654527	1376163	8837661
94	3856283	1875535	1486551	10003635
95	4313460	2156638	1618987	11492336
96	4903400	2529909	1783692	13479530
97	5712561	3058910	2000034	16316404
98	6944168	3896478	2312055	20856541
99	9290216	5579572	2862900	30147088

Probability Plot for P3P8_270mils_SnPb_SAC

APPENDIX C

CHAPTER 3 PROBABILITY PLOTS FOR TRUNCATED FAILURE TIME DATA SETS USED IN THE REGRESSION AND ANOVA

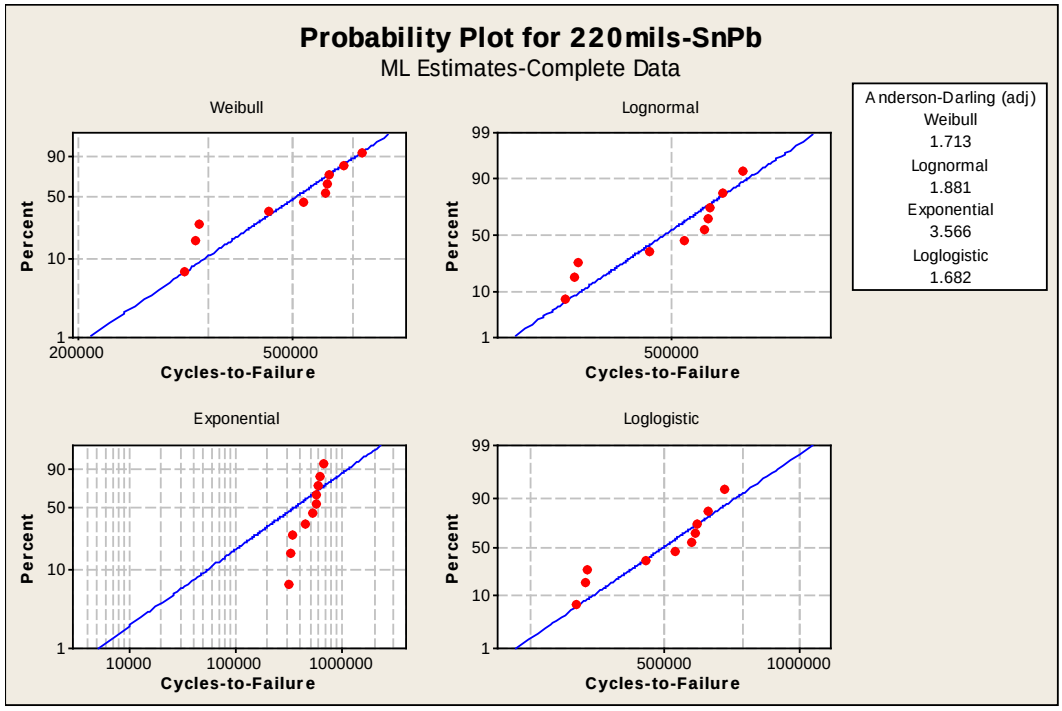
Probability Plot for 220mils-SnPb
ML Estimates-Complete Data
Weibull
Lognormal
Exponential
Loglogistic
Percent
Cycles-to-Failure
Anderson-Darling (adj)
Weibull
1.713
Lognormal
1.881
Exponential
3.566
Loglogistic
1.682

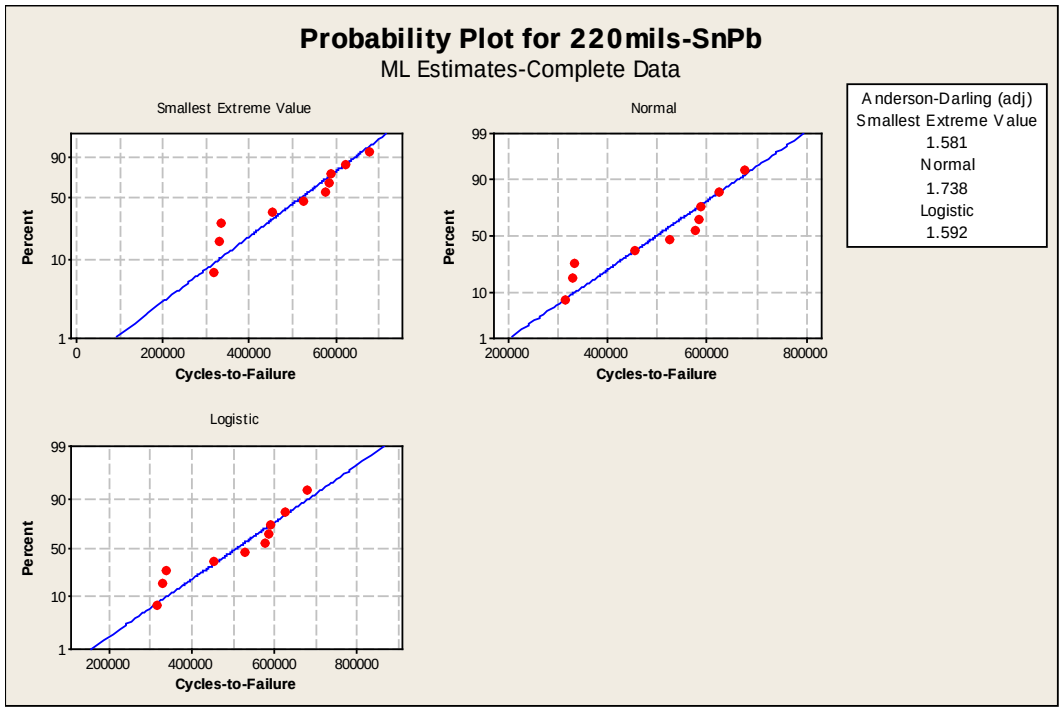
Probability Plot for 220mils-SnPb
ML Estimates-Complete Data
Smallest Extreme Value
Normal
Logistic
Percent
Cycles-to-Failure
Anderson-Darling (adj)
Smallest Extreme Value
1.581
Normal
1.738
Logistic
1.592

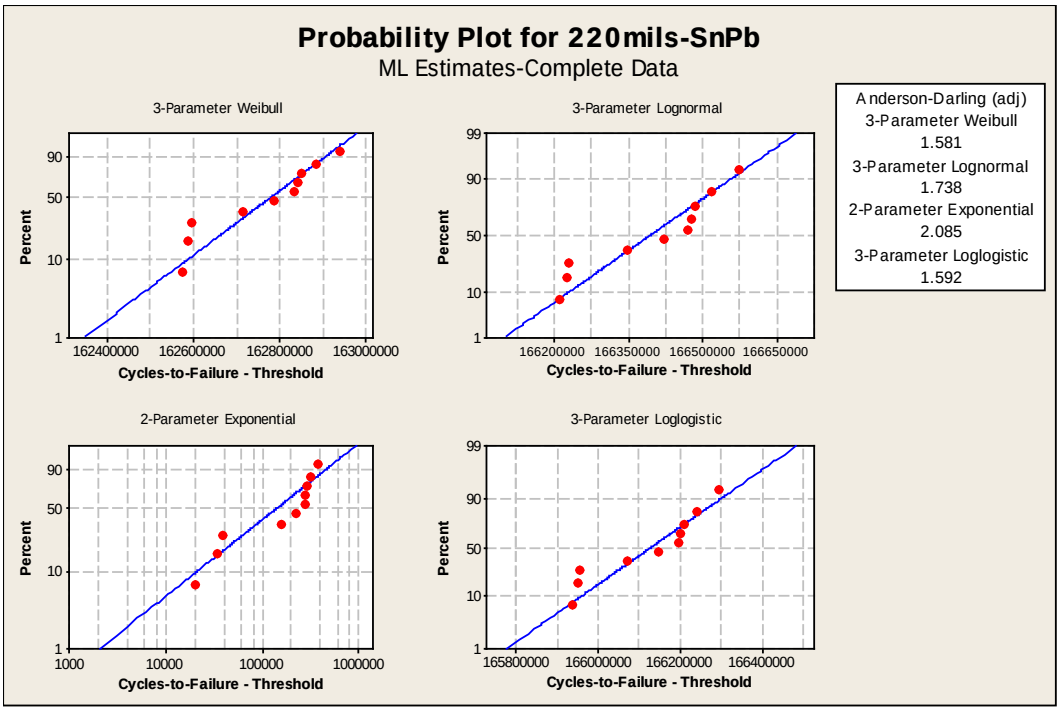
Probability Plot for 220mils-SnPb
ML Estimates-Complete Data
3-Parameter Weibull
3-Parameter Lognormal
2-Parameter Exponential
3-Parameter Loglogistic
Percent
Cycles-to-Failure - Threshold
Anderson-Darling (adj)
3-Parameter Weibull
1.581
3-Parameter Lognormal
1.738
2-Parameter Exponential
2.085
3-Parameter Loglogistic
1.592

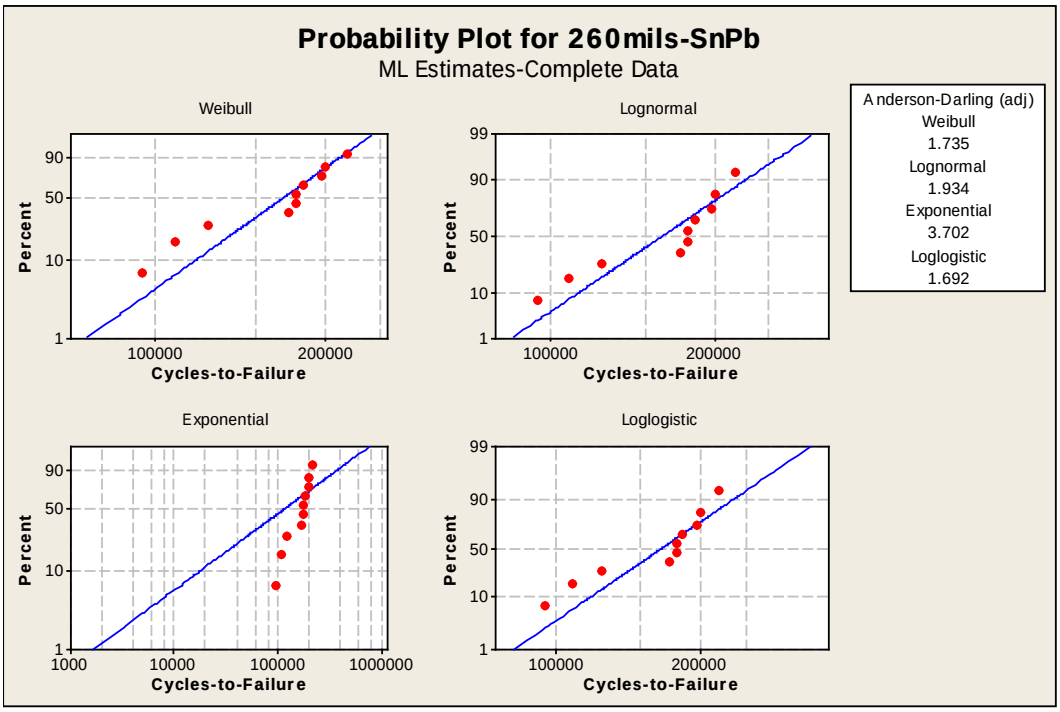
Probability Plot for 260mils-SnPb
ML Estimates-Complete Data
Weibull
Lognormal
Exponential
Loglogistic
Percent
Cycles-to-Failure
Anderson-Darling (adj)
Weibull
1.735
Lognormal
1.934
Exponential
3.702
Loglogistic
1.692

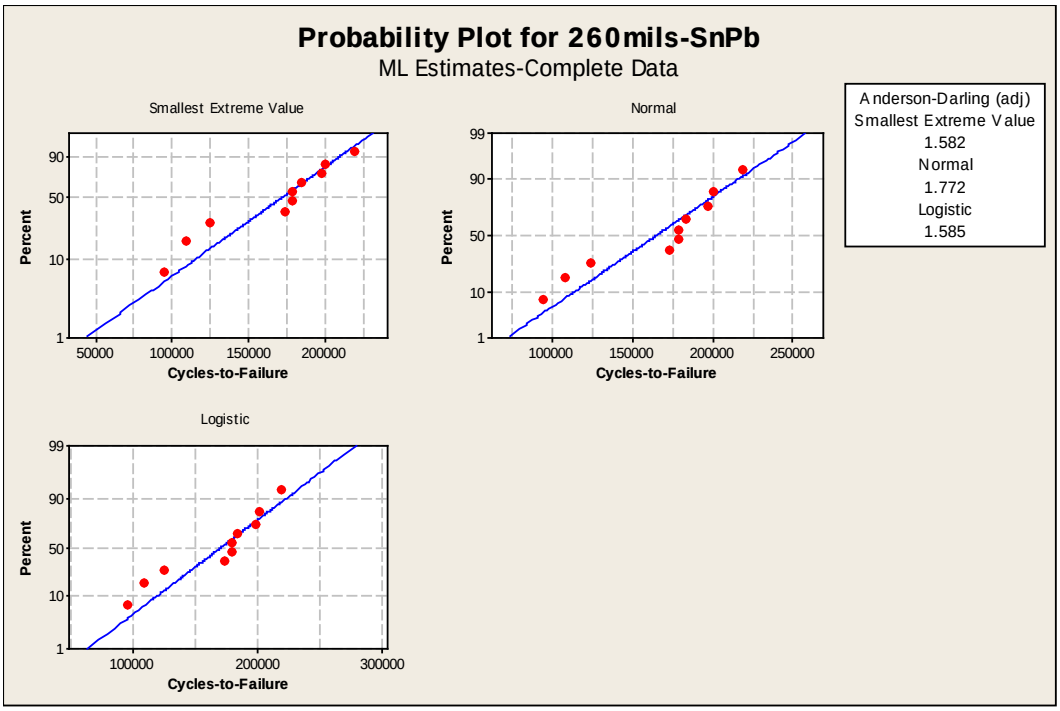
Probability Plot for 260mils-SnPb
ML Estimates-Complete Data
Smallest Extreme Value
Normal
Logistic
Percent
Cycles-to-Failure
Anderson-Darling (adj)
Smallest Extreme Value
1.582
Normal
1.772
Logistic
1.585

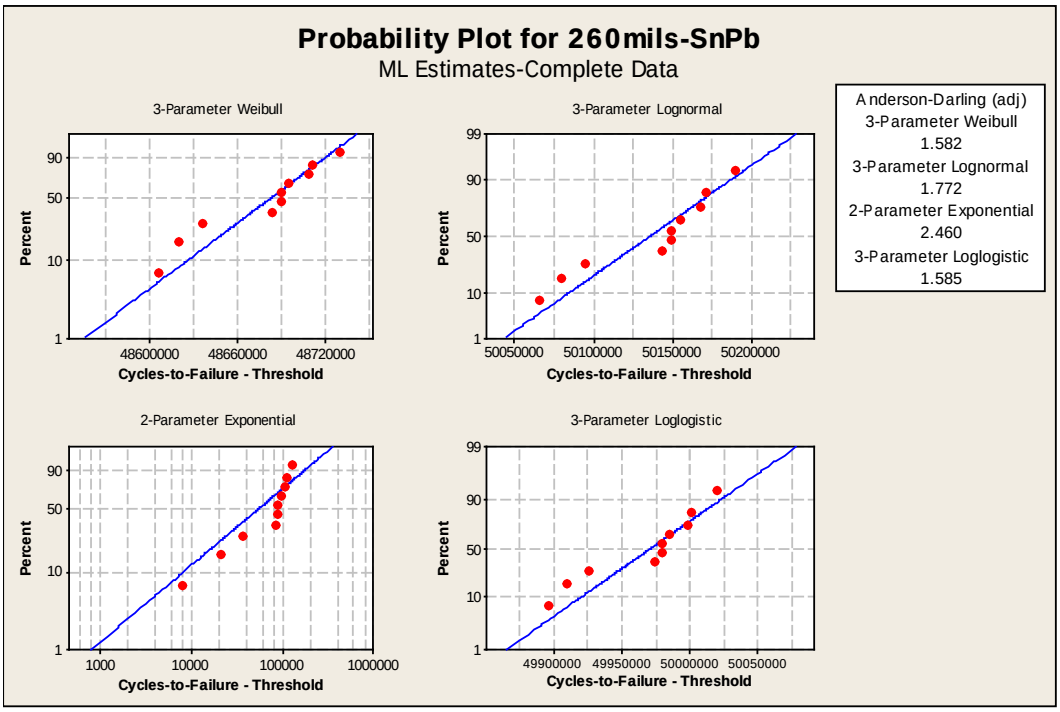
Probability Plot for 260mils-SnPb
ML Estimates-Complete Data
3-Parameter Weibull
3-Parameter Lognormal
2-Parameter Exponential
3-Parameter Loglogistic
Percent
Cycles-to-Failure - Threshold
Anderson-Darling (adj)
3-Parameter Weibull
1.582
3-Parameter Lognormal
1.772
2-Parameter Exponential
2.460
3-Parameter Loglogistic
1.585

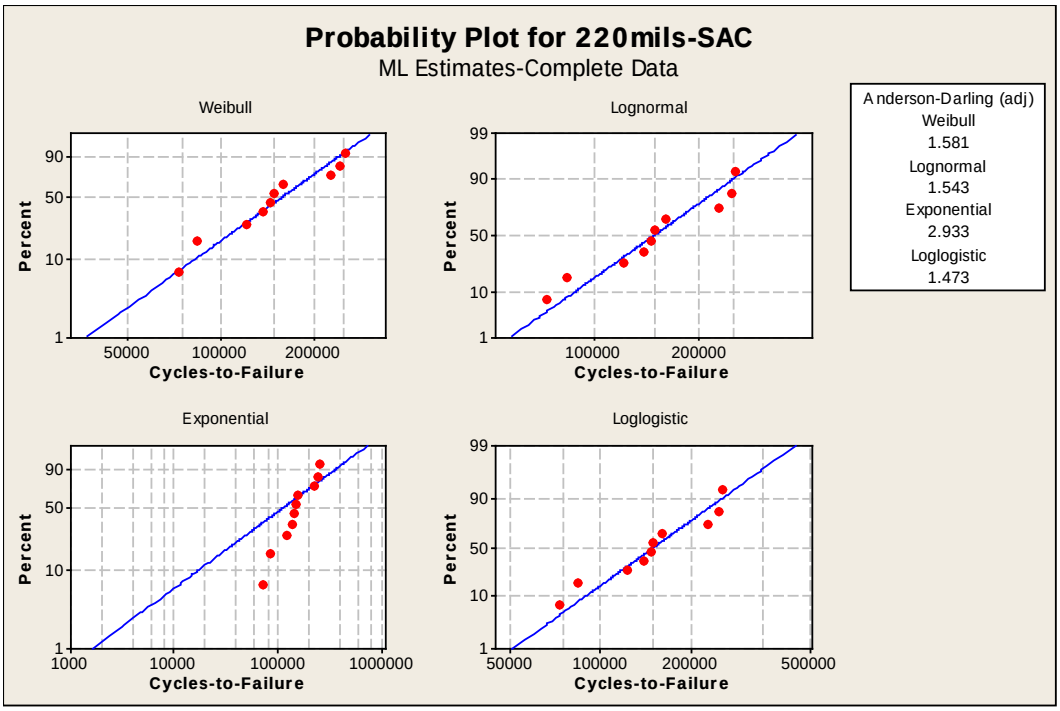
Probability Plot for 220mils-SAC
ML Estimates-Complete Data
Weibull
Lognormal
Exponential
Loglogistic
Percent
Cycles-to-Failure
Anderson-Darling (adj)
Weibull
1.581
Lognormal
1.543
Exponential
2.933
Loglogistic
1.473

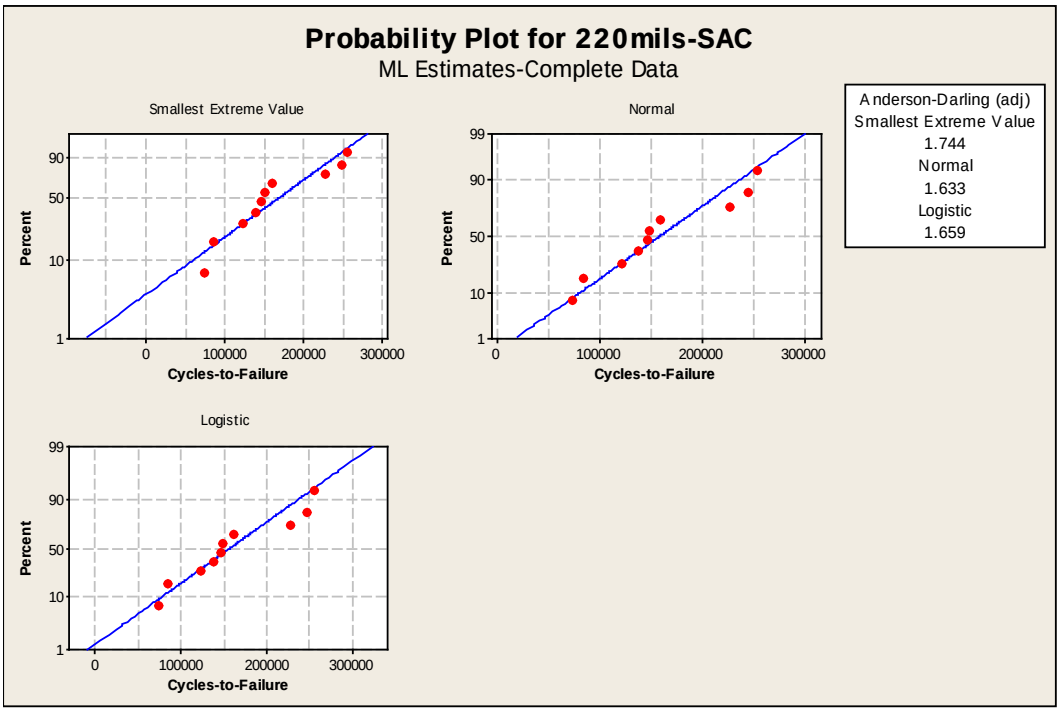
Probability Plot for 220mils-SAC
ML Estimates-Complete Data
Smallest Extreme Value
Normal
Logistic
Percent
Cycles-to-Failure
Anderson-Darling (adj)
Smallest Extreme Value
1.744
Normal
1.633
Logistic
1.659

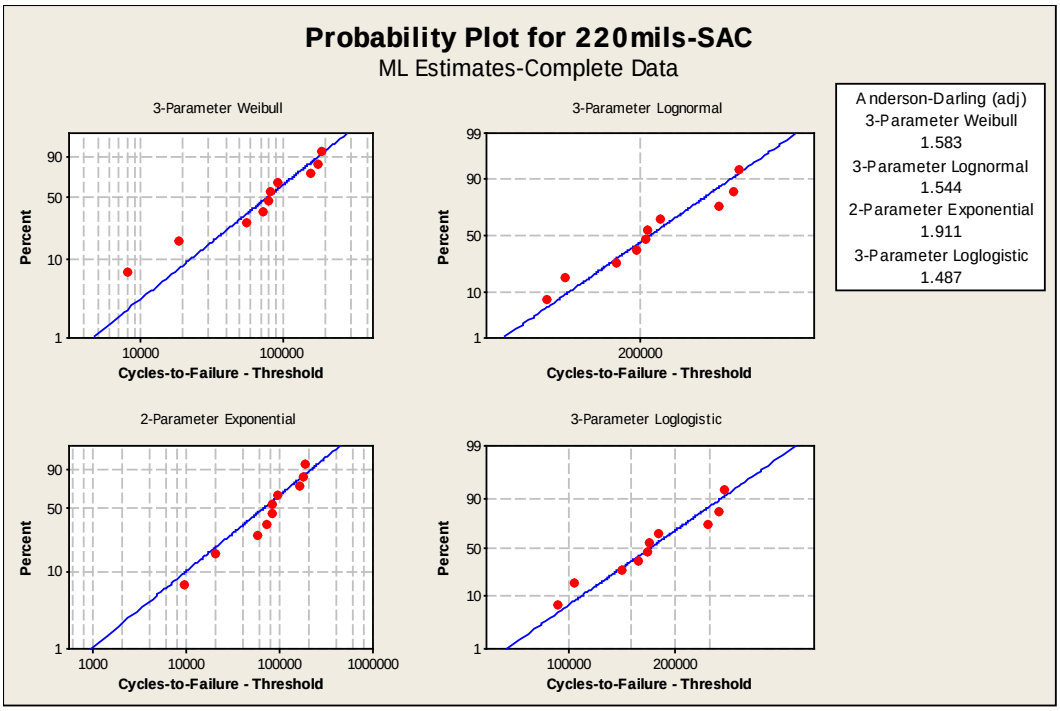
Probability Plot for 220mils-SAC
ML Estimates-Complete Data
3-Parameter Weibull
3-Parameter Lognormal
2-Parameter Exponential
3-Parameter Loglogistic
Percent
Cycles-to-Failure - Threshold
Anderson-Darling (adj)
3-Parameter Weibull
1.583
3-Parameter Lognormal
1.544
2-Parameter Exponential
1.911
3-Parameter Loglogistic
1.487

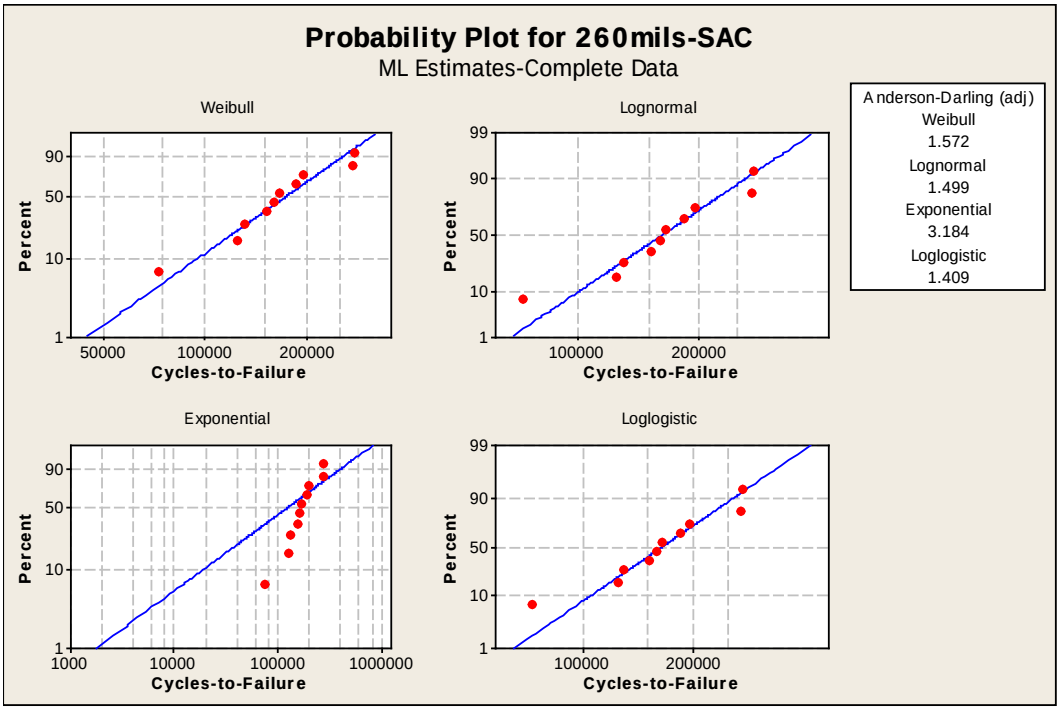
Probability Plot for 260mils-SAC
ML Estimates-Complete Data
Weibull
Lognormal
Exponential
Loglogistic
Percent
Cycles-to-Failure
Anderson-Darling (adj)
Weibull
1.572
Lognormal
1.499
Exponential
3.184
Loglogistic
1.409

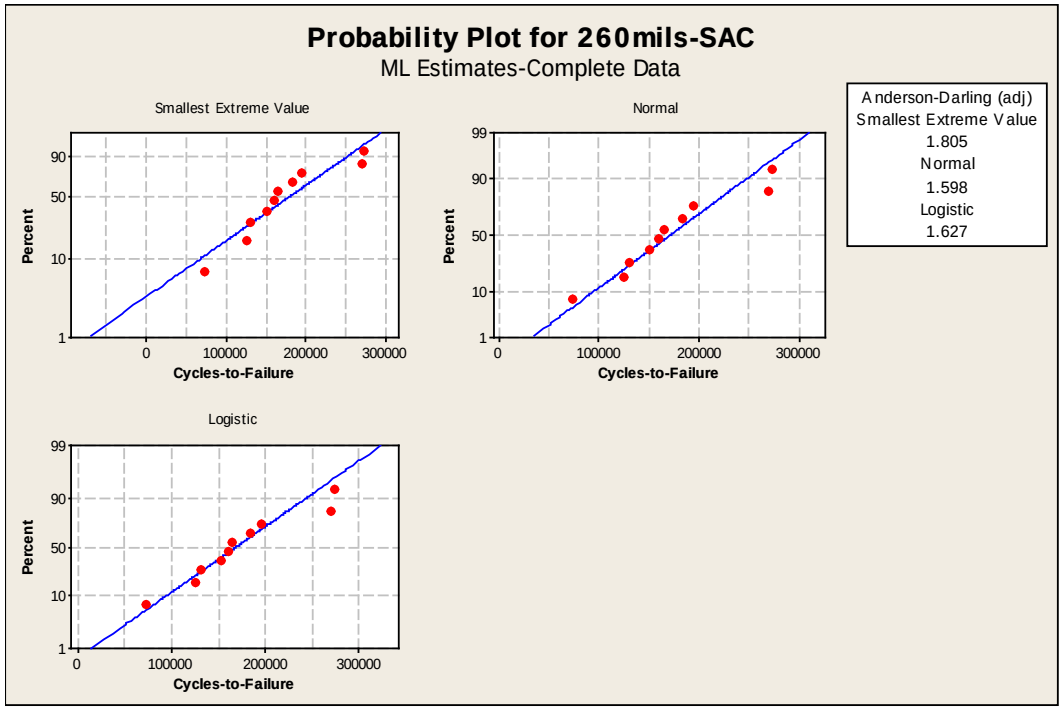
Probability Plot for 260mils-SAC
ML Estimates-Complete Data
Smallest Extreme Value
Normal
Logistic
Percent
Cycles-to-Failure
Anderson-Darling (adj)
Smallest Extreme Value
1.805
Normal
1.598
Logistic
1.627

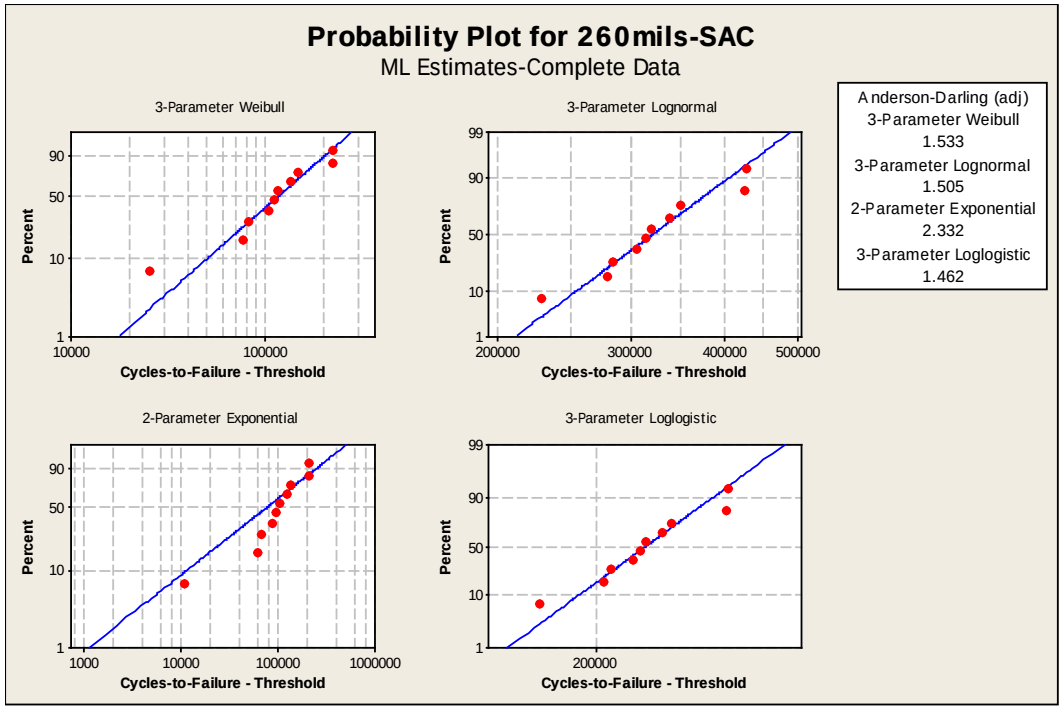
Probability Plot for 260mils-SAC
ML Estimates-Complete Data
3-Parameter Weibull
3-Parameter Lognormal
2-Parameter Exponential
3-Parameter Loglogistic
Percent
Cycles-to-Failure - Threshold
Anderson-Darling (adj)
3-Parameter Weibull
1.533
3-Parameter Lognormal
1.505
2-Parameter Exponential
2.332
3-Parameter Loglogistic
1.462

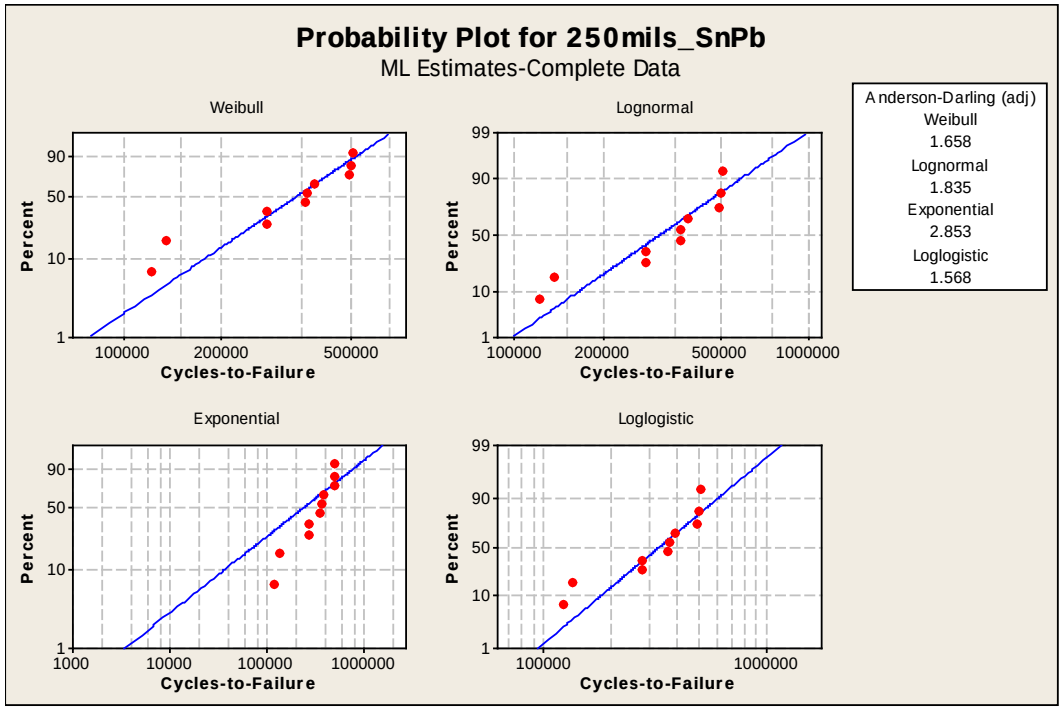
Probability Plot for 250mils_SnPb
ML Estimates-Complete Data
Weibull
Lognormal
Exponential
Loglogistic
Percent
Cycles-to-Failure
Anderson-Darling (adj)
Weibull
1.658
Lognormal
1.835
Exponential
2.853
Loglogistic
1.568

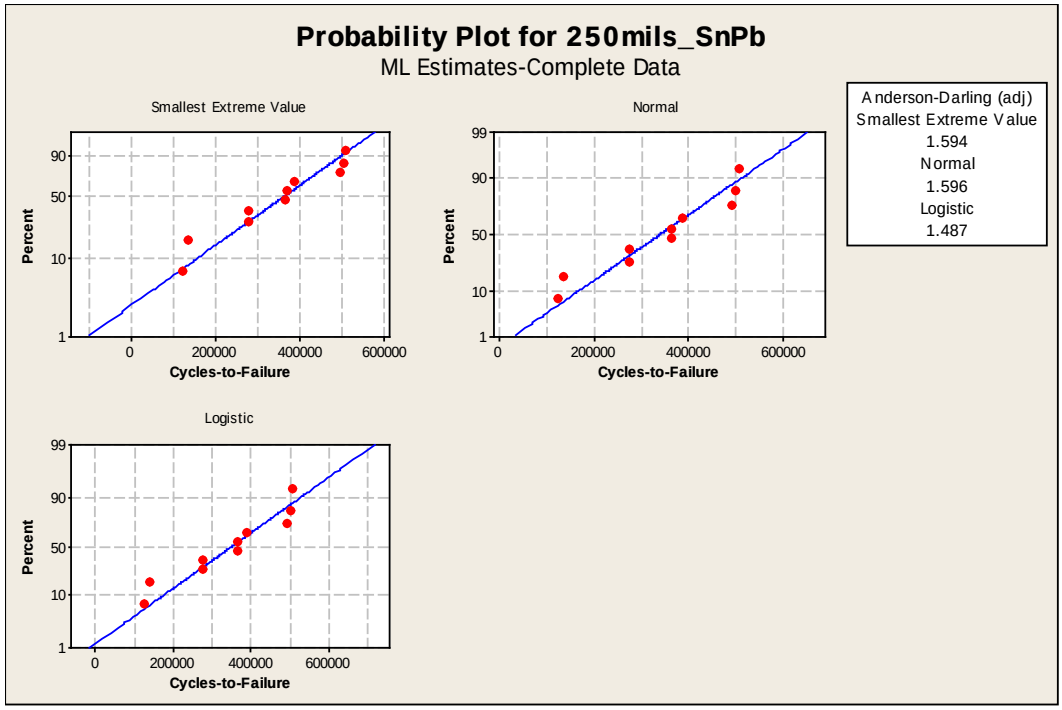
Probability Plot for 250mils_SnPb
ML Estimates-Complete Data
Smallest Extreme Value
Normal
Logistic
Percent
Cycles-to-Failure
Anderson-Darling (adj)
Smallest Extreme Value
1.594
Normal
1.596
Logistic
1.487

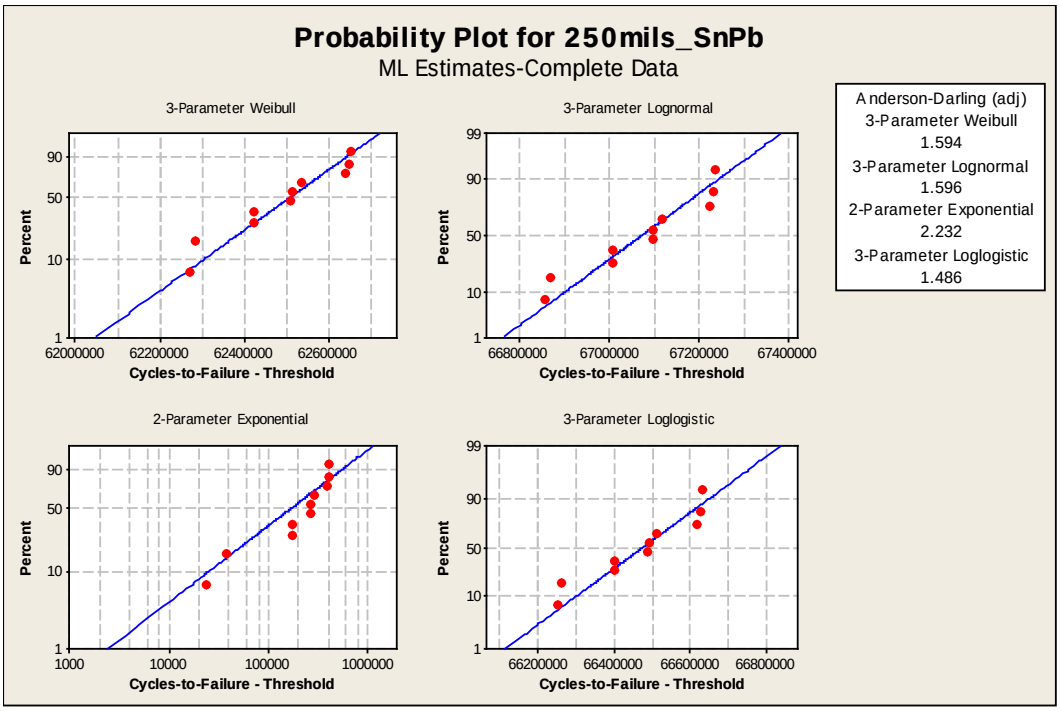
Probability Plot for 250mils_SnPb
ML Estimates-Complete Data
3-Parameter Weibull
3-Parameter Lognormal
2-Parameter Exponential
3-Parameter Loglogistic
Percent
Cycles-to-Failure - Threshold
Anderson-Darling (adj)
3-Parameter Weibull
1.594
3-Parameter Lognormal
1.596
2-Parameter Exponential
2.232
3-Parameter Loglogistic
1.486

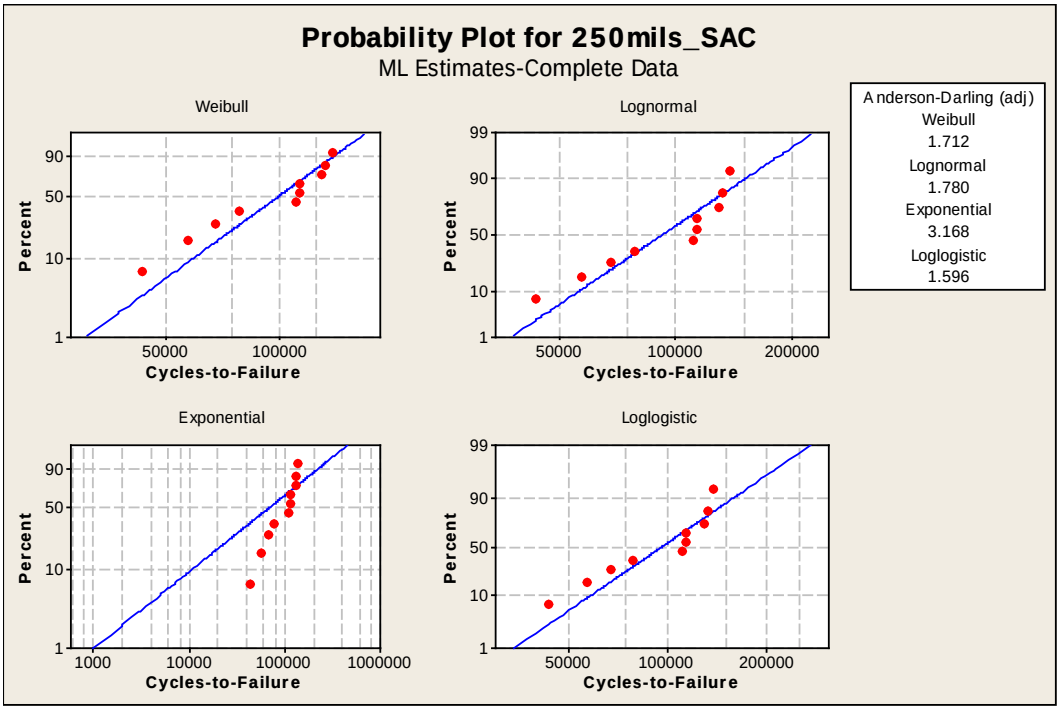
Probability Plot for 250mils_SAC
ML Estimates-Complete Data
Weibull
Lognormal
Exponential
Loglogistic
Percent
Cycles-to-Failure
Anderson-Darling (adj)
Weibull
1.712
Lognormal
1.780
Exponential
3.168
Loglogistic
1.596

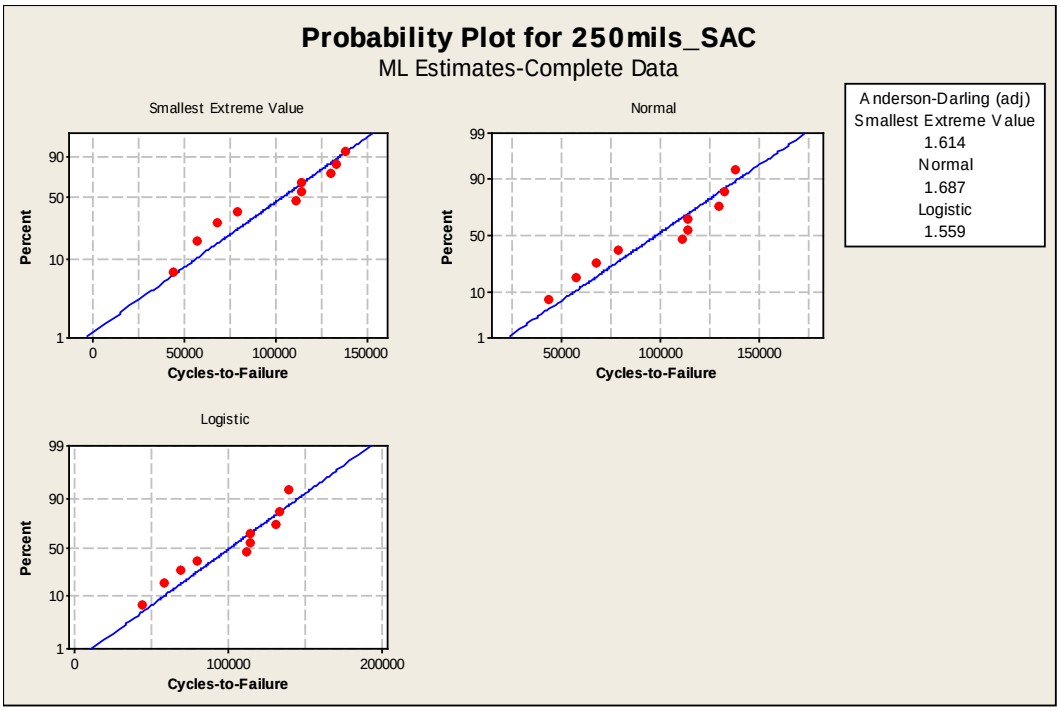
Probability Plot for 250mils_SAC
ML Estimates-Complete Data
Smallest Extreme Value
Normal
Logistic
Percent
Cycles-to-Failure
Anderson-Darling (adj)
Smallest Extreme Value
1.614
Normal
1.687
Logistic
1.559

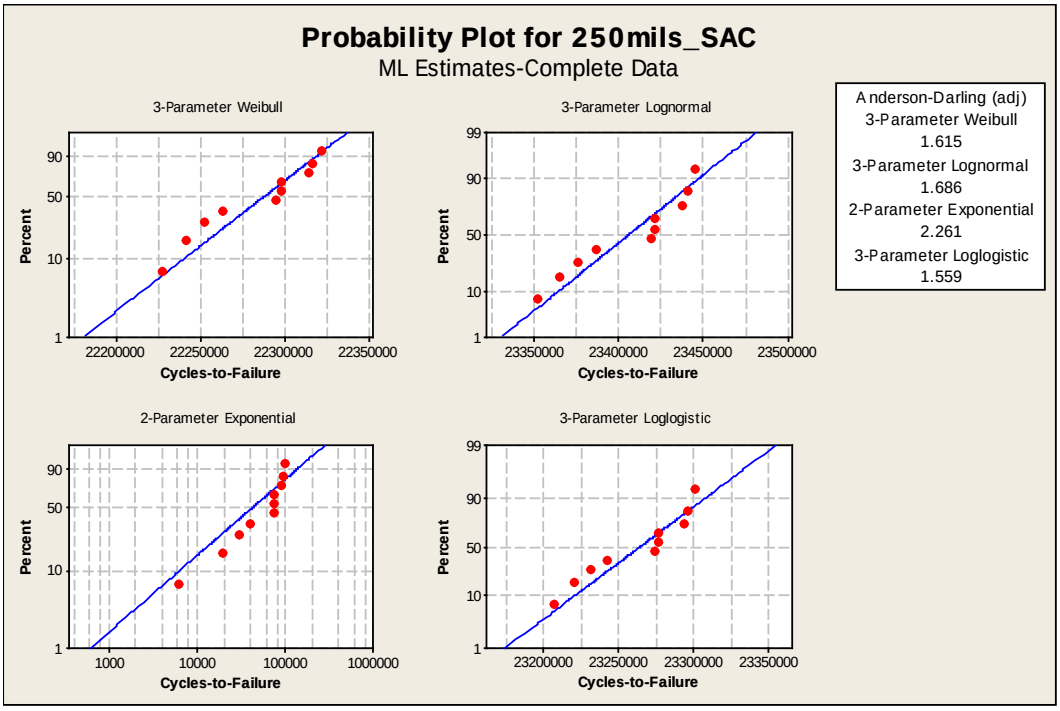
Probability Plot for 250mils_SAC
ML Estimates-Complete Data
3-Parameter Weibull
3-Parameter Lognormal
2-Parameter Exponential
3-Parameter Loglogistic
Percent
Cycles-to-Failure
Anderson-Darling (adj)
3-Parameter Weibull
1.615
3-Parameter Lognormal
1.686
2-Parameter Exponential
2.261
3-Parameter Loglogistic
1.559

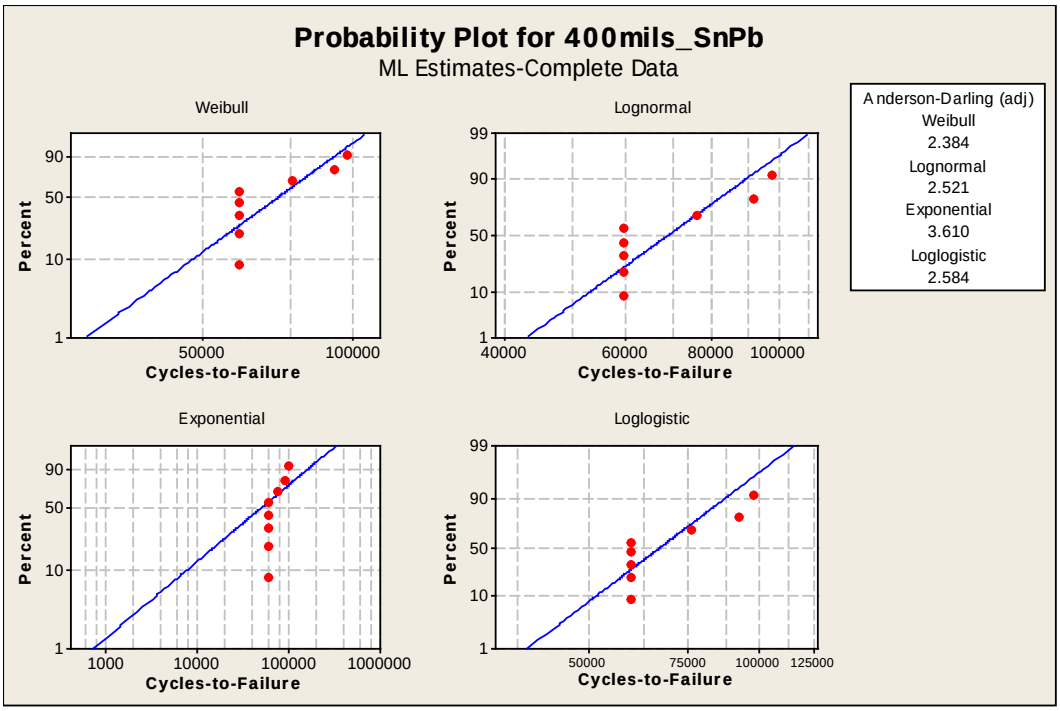
Probability Plot for 400mils_SnPb
ML Estimates-Complete Data
Weibull
Lognormal
Exponential
Loglogistic
Percent
Cycles-to-Failure
Anderson-Darling (adj)
Weibull
2.384
Lognormal
2.521
Exponential
3.610
Loglogistic
2.584

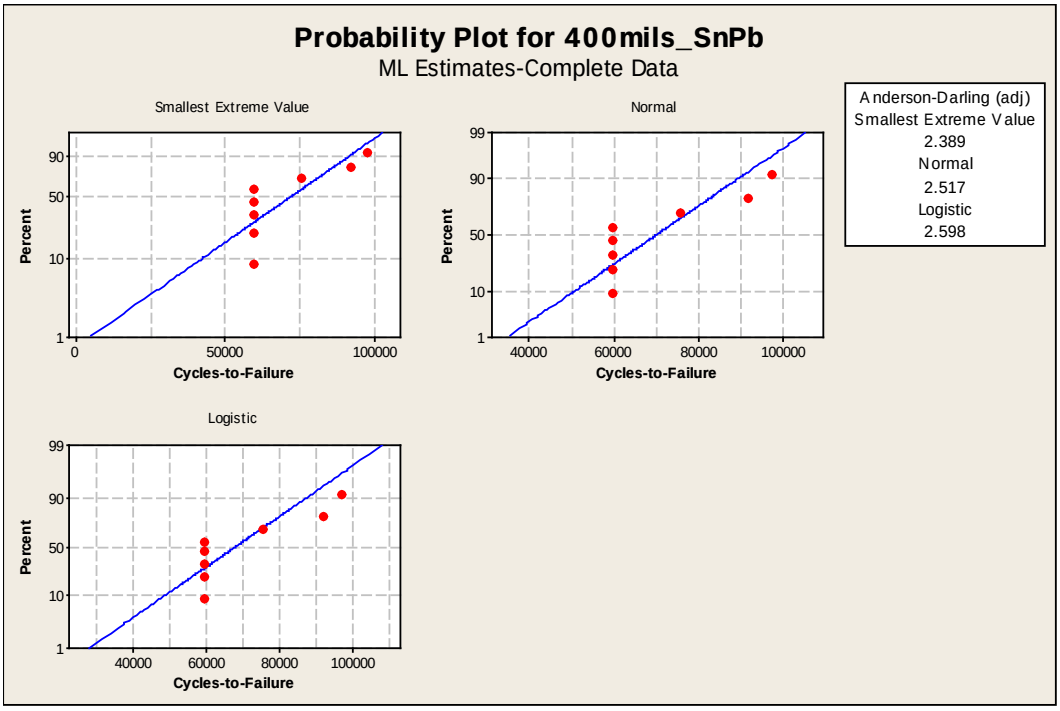
Probability Plot for 400mils_SnPb
ML Estimates-Complete Data
Smallest Extreme Value
Normal
Logistic
Percent
Cycles-to-Failure
Anderson-Darling (adj)
Smallest Extreme Value
2.389
Normal
2.517
Logistic
2.598

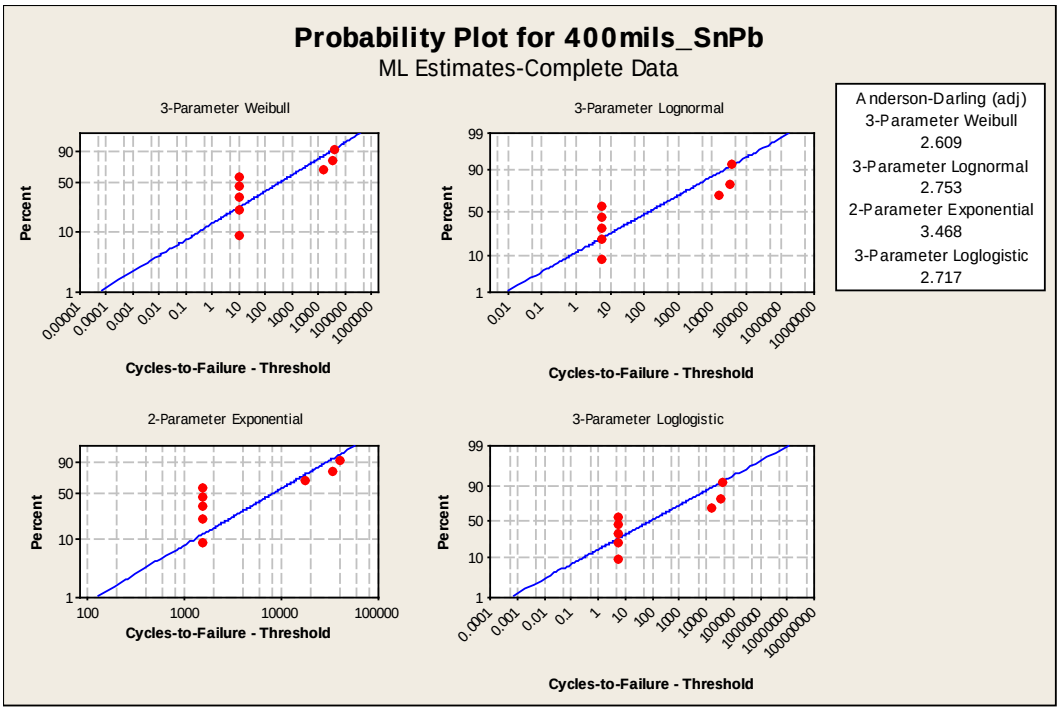
Probability Plot for 400mils_SnPb
ML Estimates-Complete Data
3-Parameter Weibull
3-Parameter Lognormal
2-Parameter Exponential
3-Parameter Loglogistic
Percent
Cycles-to-Failure - Threshold
Anderson-Darling (adj)
3-Parameter Weibull
2.609
3-Parameter Lognormal
2.753
2-Parameter Exponential
3.468
3-Parameter Loglogistic
2.717

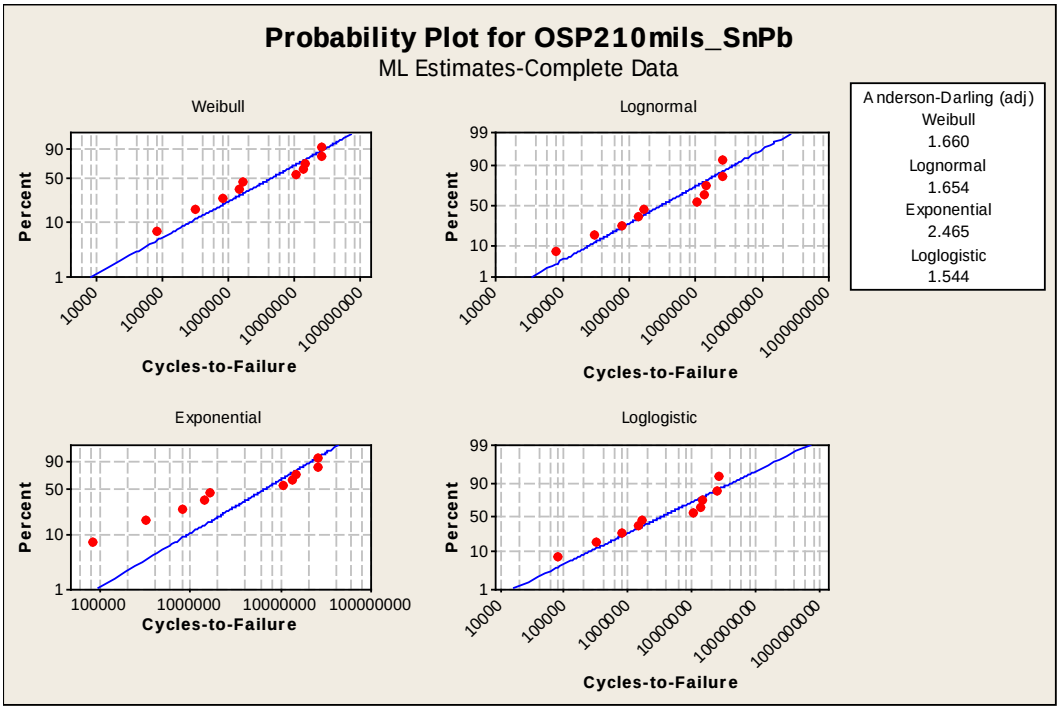
Probability Plot for OSP210mils_SnPb
ML Estimates-Complete Data
Weibull
Lognormal
Exponential
Loglogistic
Percent
Cycles-to-Failure
Anderson-Darling (adj)
Weibull
1.660
Lognormal
1.654
Exponential
2.465
Loglogistic
1.544

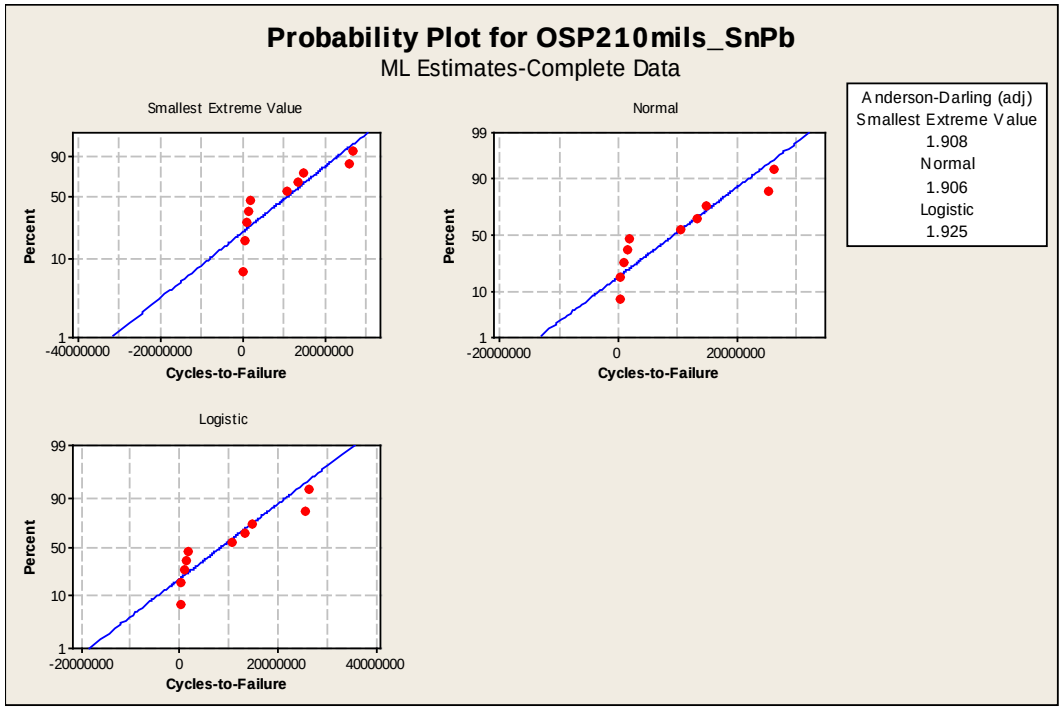
Probability Plot for OSP210mils_SnPb
ML Estimates-Complete Data
Smallest Extreme Value
Normal
Logistic
Percent
Cycles-to-Failure
Anderson-Darling (adj)
Smallest Extreme Value
1.908
Normal
1.906
Logistic
1.925

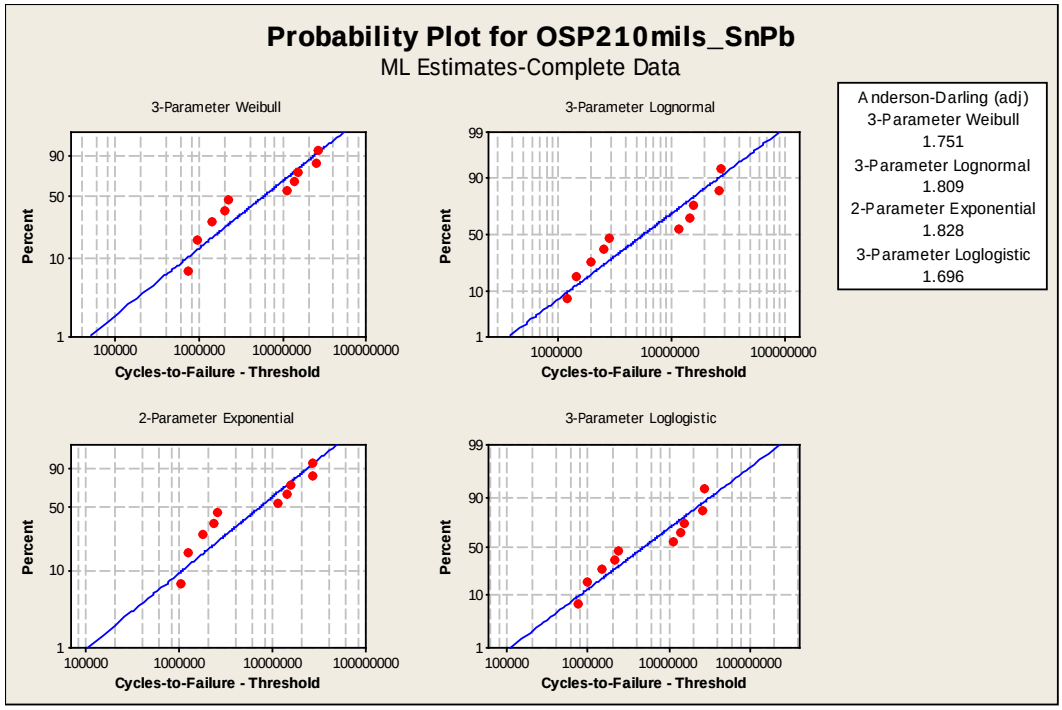
Probability Plot for OSP210mils_SnPb
ML Estimates-Complete Data
3-Parameter Weibull
3-Parameter Lognormal
2-Parameter Exponential
3-Parameter Loglogistic
Percent
Cycles-to-Failure - Threshold
Anderson-Darling (adj)
3-Parameter Weibull
1.751
3-Parameter Lognormal
1.809
2-Parameter Exponential
1.828
3-Parameter Loglogistic
1.696

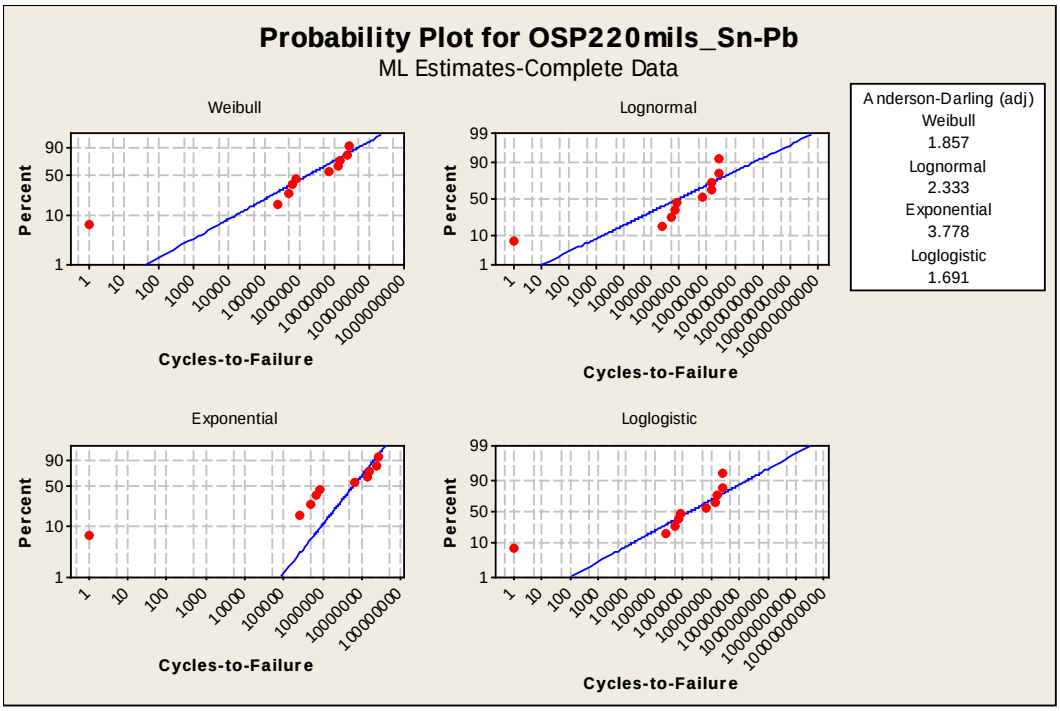
Probability Plot for OSP220mils_Sn-Pb
ML Estimates-Complete Data
Weibull
Lognormal
Exponential
Loglogistic
Percent
Cycles-to-Failure
Anderson-Darling (adj)
Weibull
1.857
Lognormal
2.333
Exponential
3.778
Loglogistic
1.691

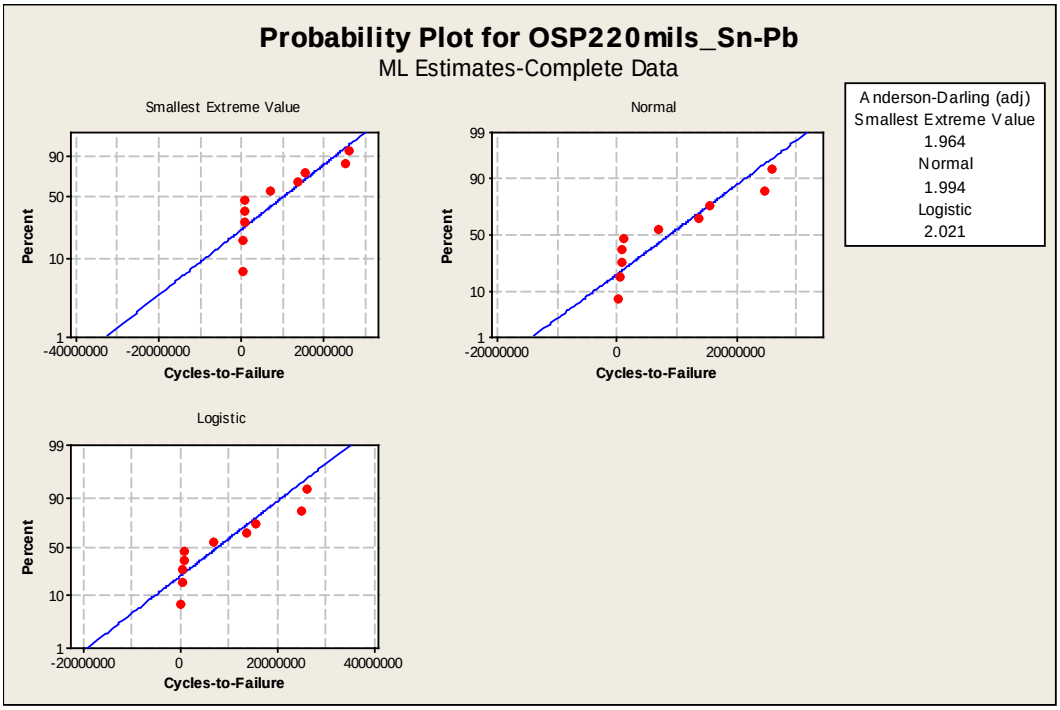
Probability Plot for OSP220mils_Sn-Pb
ML Estimates-Complete Data
Smallest Extreme Value
Normal
Logistic
Percent
Cycles-to-Failure
Anderson-Darling (adj)
Smallest Extreme Value
1.964
Normal
1.994
Logistic
2.021

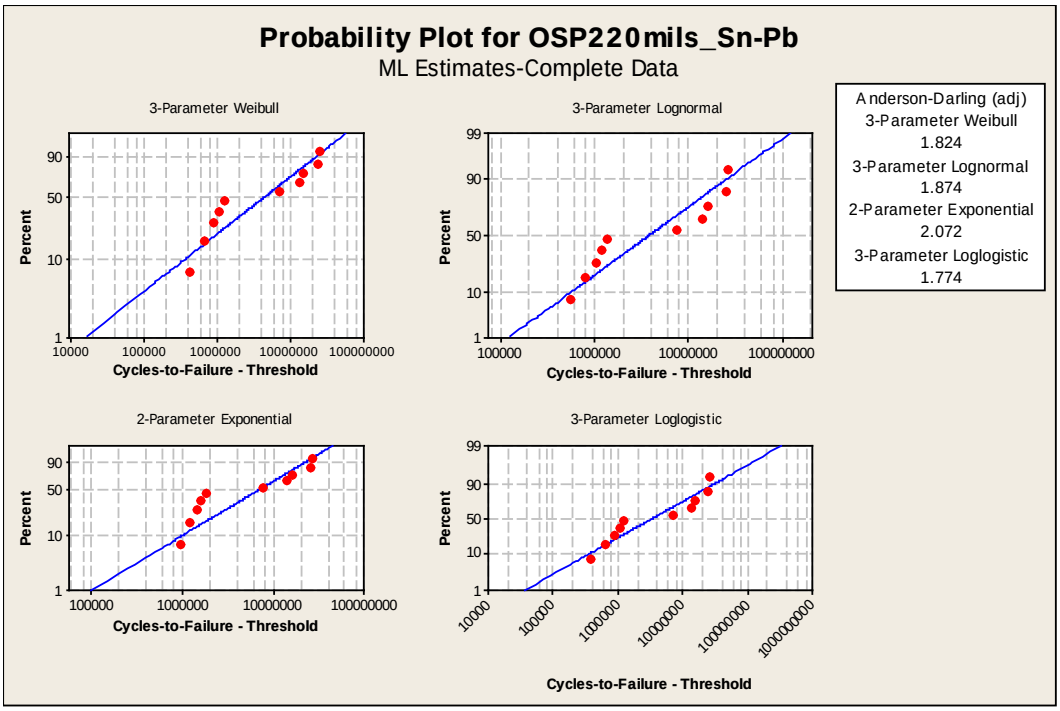
Probability Plot for OSP220mils_Sn-Pb
ML Estimates-Complete Data
3-Parameter Weibull
3-Parameter Lognormal
2-Parameter Exponential
3-Parameter Loglogistic
Percent
Cycles-to-Failure - Threshold
Anderson-Darling (adj)
3-Parameter Weibull
1.824
3-Parameter Lognormal
1.874
2-Parameter Exponential
2.072
3-Parameter Loglogistic
1.774

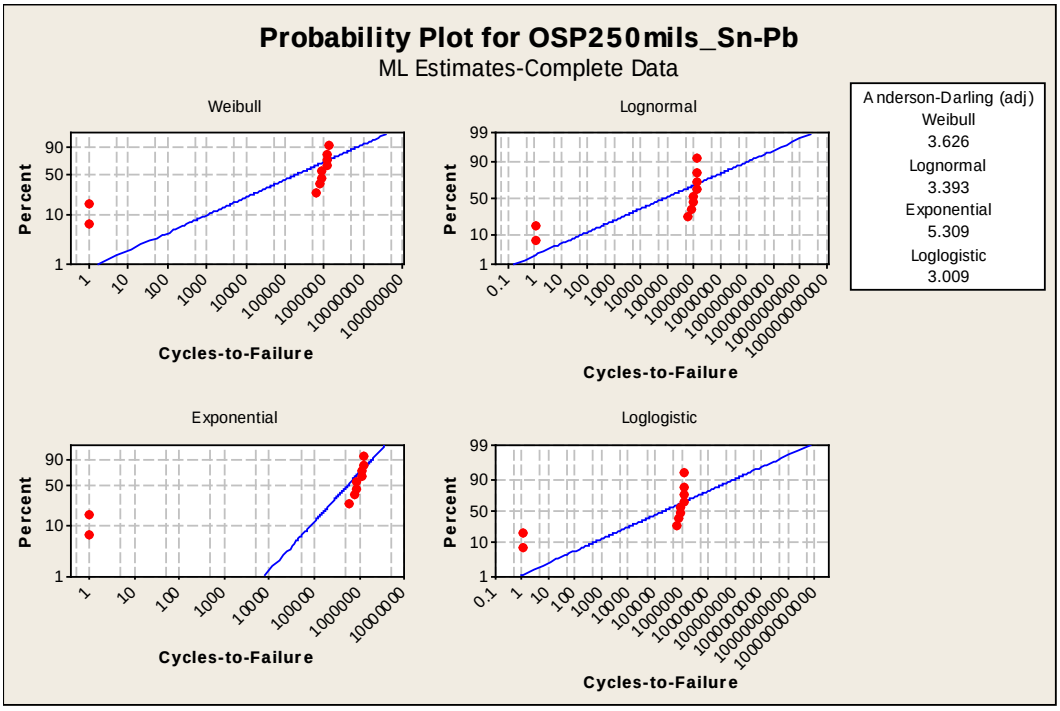
Probability Plot for OSP250mils_Sn-Pb
ML Estimates-Complete Data
Weibull
Lognormal
Exponential
Loglogistic
Percent
Cycles-to-Failure
Anderson-Darling (adj)
Weibull
3.626
Lognormal
3.393
Exponential
5.309
Loglogistic
3.009

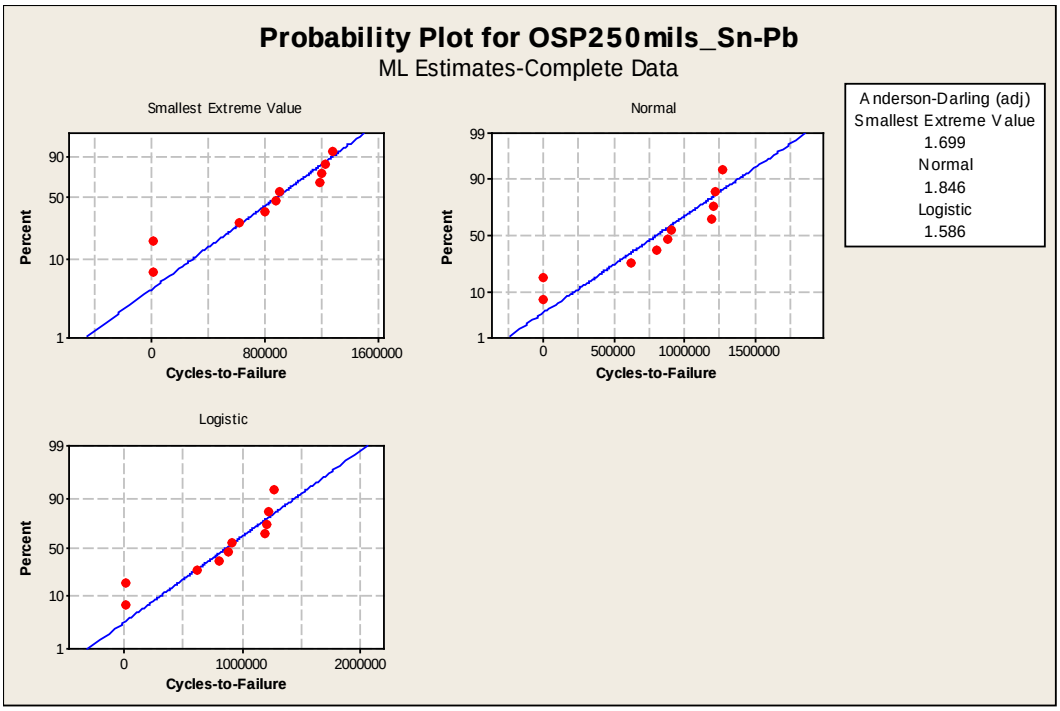
Probability Plot for OSP250mils_Sn-Pb
ML Estimates-Complete Data
Smallest Extreme Value
Normal
Logistic
Percent
Cycles-to-Failure
Anderson-Darling (adj)
Smallest Extreme Value
1.699
Normal
1.846
Logistic
1.586

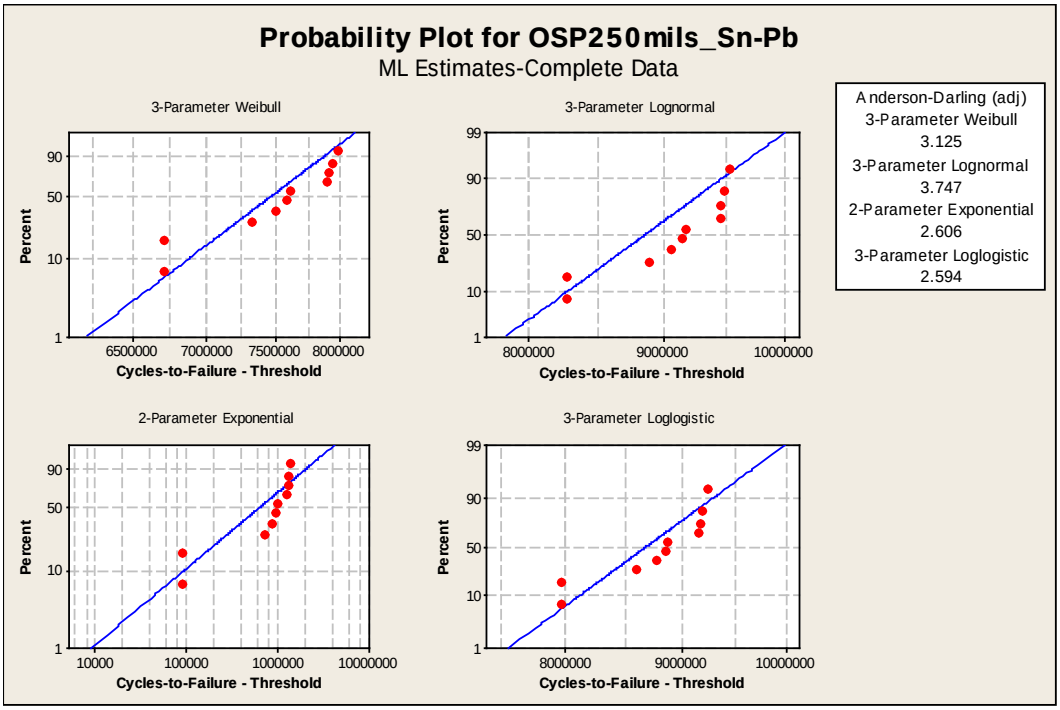
Probability Plot for OSP250mils_Sn-Pb
ML Estimates-Complete Data
3-Parameter Weibull
3-Parameter Lognormal
2-Parameter Exponential
3-Parameter Loglogistic
Percent
Cycles-to-Failure - Threshold
Anderson-Darling (adj)
3-Parameter Weibull
3.125
3-Parameter Lognormal
3.747
2-Parameter Exponential
2.606
3-Parameter Loglogistic
2.594

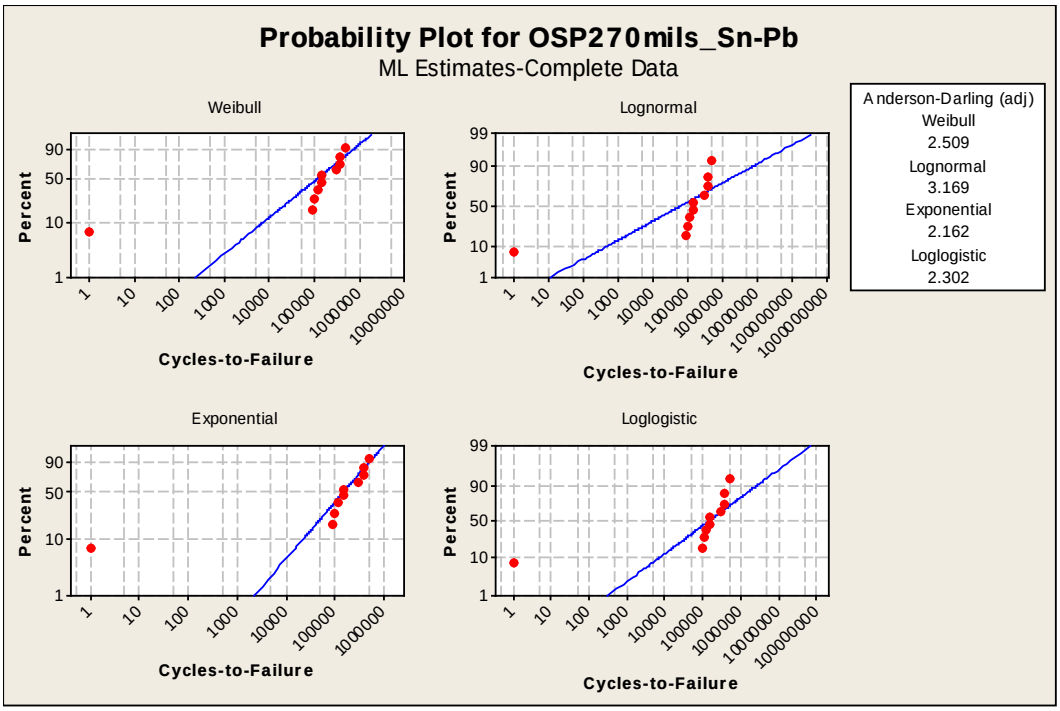
Probability Plot for OSP270mils_Sn-Pb
ML Estimates-Complete Data
Weibull
Lognormal
Exponential
Loglogistic
Percent
Cycles-to-Failure
Anderson-Darling (adj)
Weibull
2.509
Lognormal
3.169
Exponential
2.162
Loglogistic
2.302

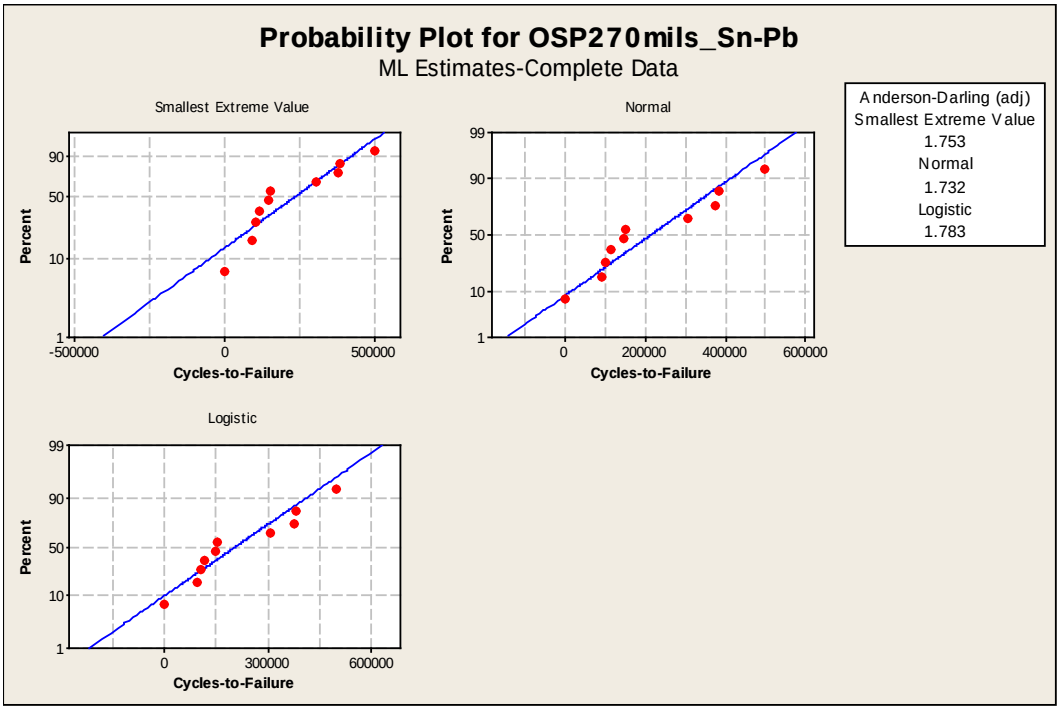
Probability Plot for OSP270mils_Sn-Pb
ML Estimates-Complete Data
Smallest Extreme Value
Normal
Logistic
Percent
Cycles-to-Failure
Anderson-Darling (adj)
Smallest Extreme Value
1.753
Normal
1.732
Logistic
1.783

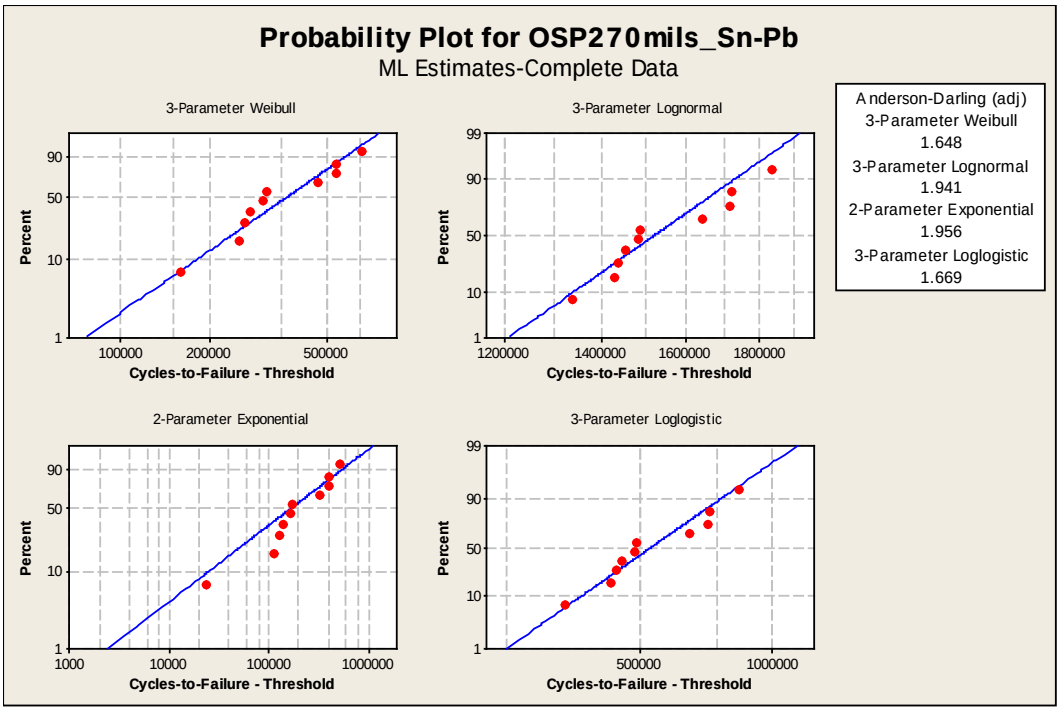
Probability Plot for OSP270mils_Sn-Pb
ML Estimates-Complete Data
3-Parameter Weibull
3-Parameter Lognormal
2-Parameter Exponential
3-Parameter Loglogistic
Percent
Cycles-to-Failure - Threshold
Anderson-Darling (adj)
3-Parameter Weibull
1.648
3-Parameter Lognormal
1.941
2-Parameter Exponential
1.956
3-Parameter Loglogistic
1.669

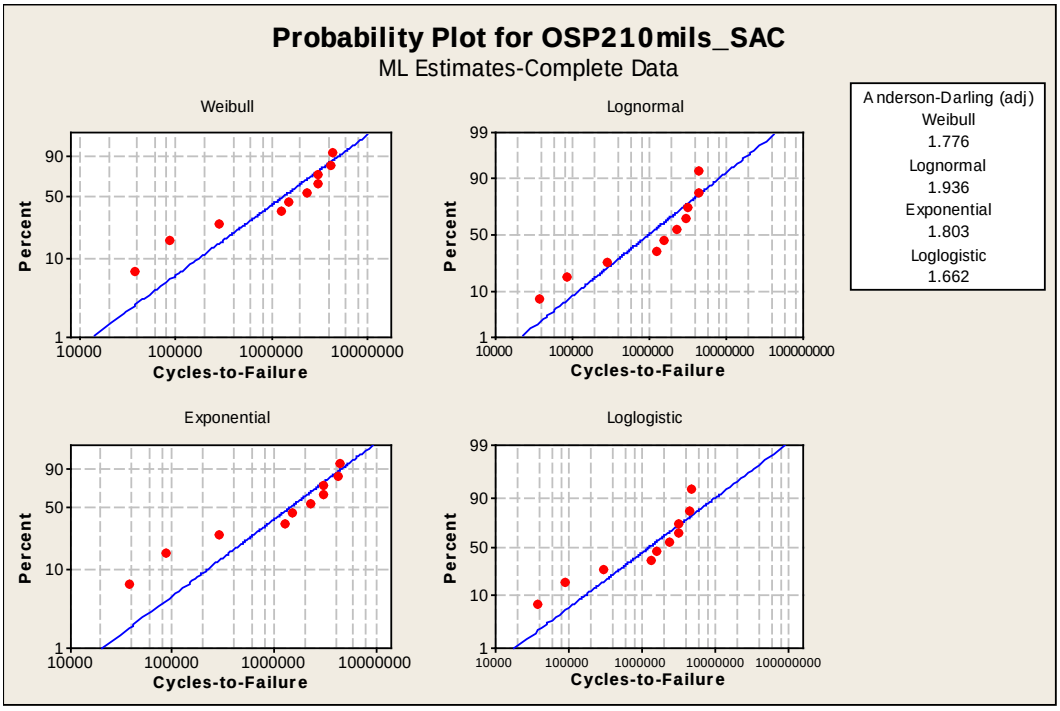
Probability Plot for OSP210mils_SAC
ML Estimates-Complete Data
Weibull
Lognormal
Exponential
Loglogistic
Percent
Cycles-to-Failure
Anderson-Darling (adj)
Weibull
1.776
Lognormal
1.936
Exponential
1.803
Loglogistic
1.662

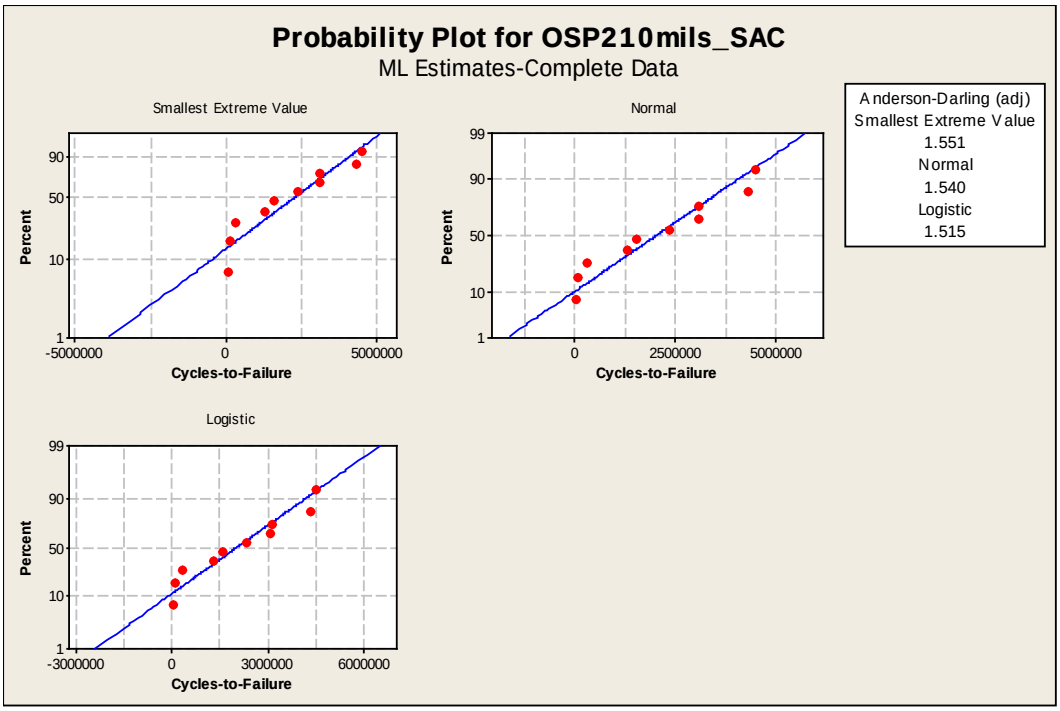
Probability Plot for OSP210mils_SAC
ML Estimates-Complete Data
Smallest Extreme Value
Normal
Logistic
Percent
Cycles-to-Failure
Anderson-Darling (adj)
Smallest Extreme Value
1.551
Normal
1.540
Logistic
1.515

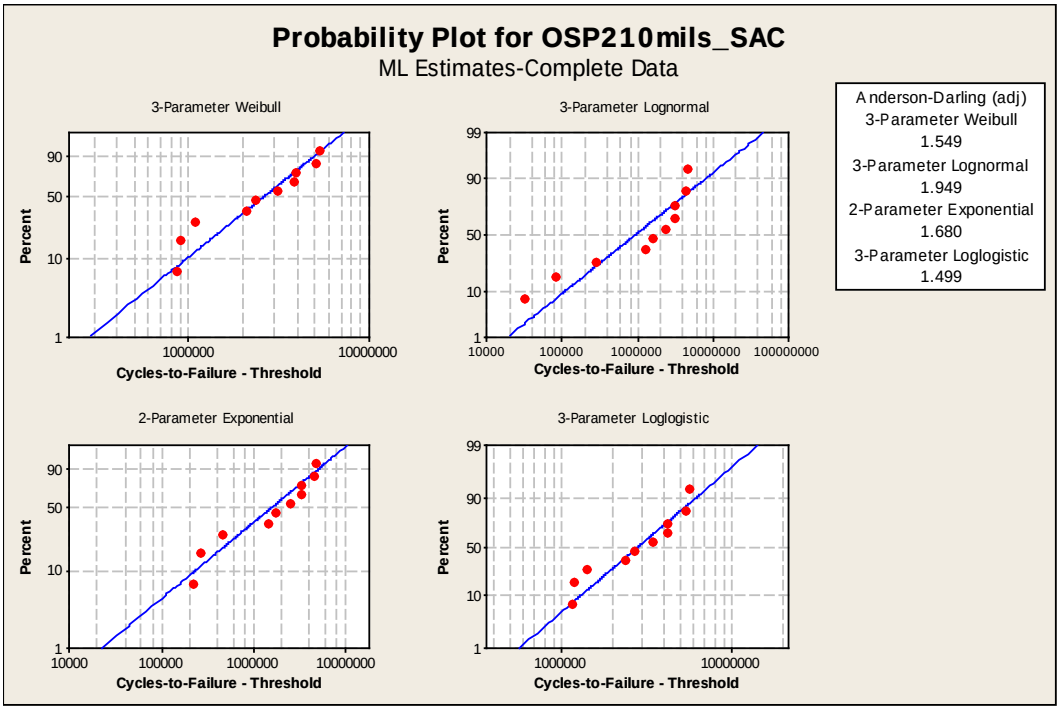
Probability Plot for OSP210mils_SAC
ML Estimates-Complete Data
3-Parameter Weibull
3-Parameter Lognormal
2-Parameter Exponential
3-Parameter Loglogistic
Percent
Cycles-to-Failure - Threshold
Anderson-Darling (adj)
3-Parameter Weibull
1.549
3-Parameter Lognormal
1.949
2-Parameter Exponential
1.680
3-Parameter Loglogistic
1.499

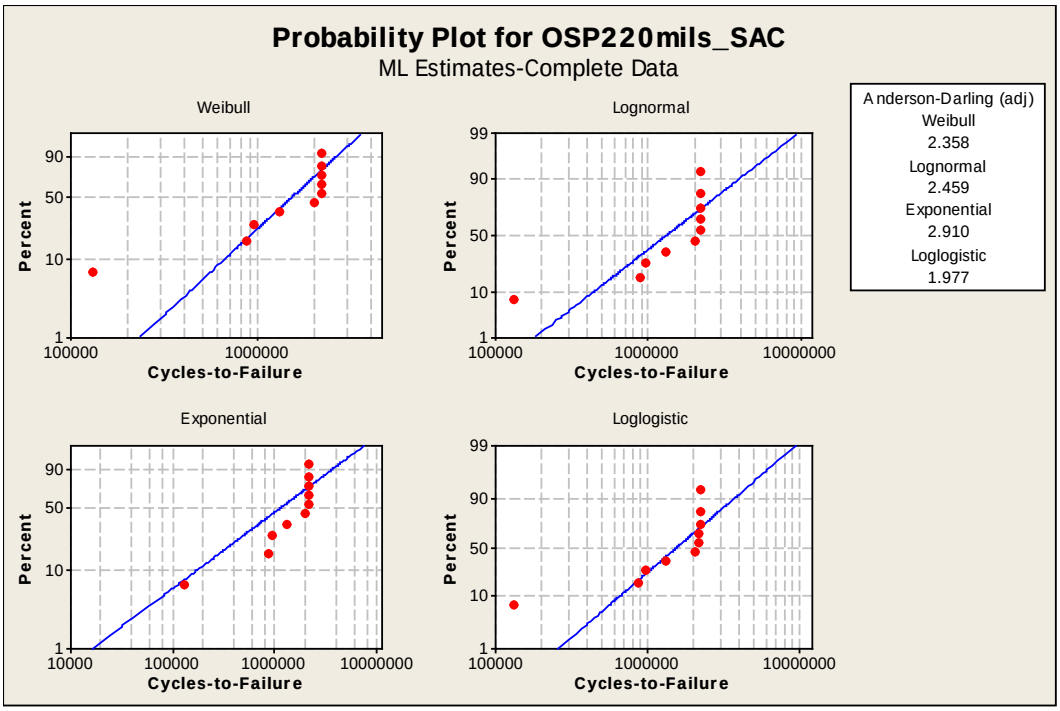
Probability Plot for OSP220mils_SAC
ML Estimates-Complete Data
Weibull
Lognormal
Exponential
Loglogistic
Percent
Cycles-to-Failure
Anderson-Darling (adj)
Weibull
2.358
Lognormal
2.459
Exponential
2.910
Loglogistic
1.977

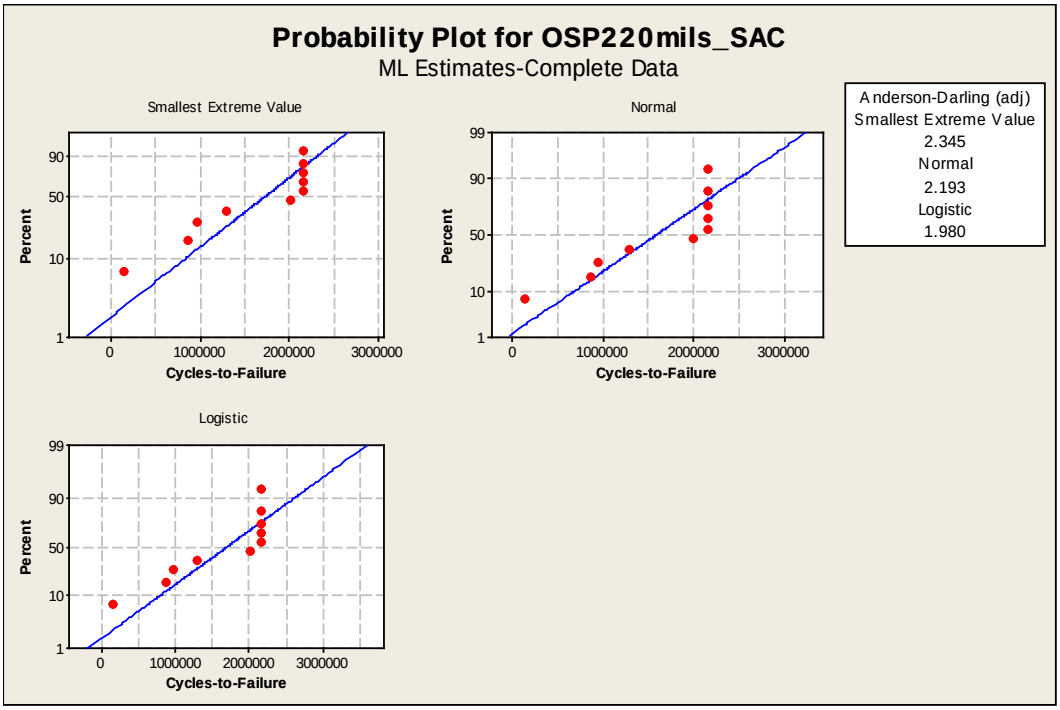
Probability Plot for OSP220mils_SAC
ML Estimates-Complete Data
Smallest Extreme Value
Normal
Logistic
Percent
Cycles-to-Failure
Anderson-Darling (adj)
Smallest Extreme Value
2.345
Normal
2.193
Logistic
1.980

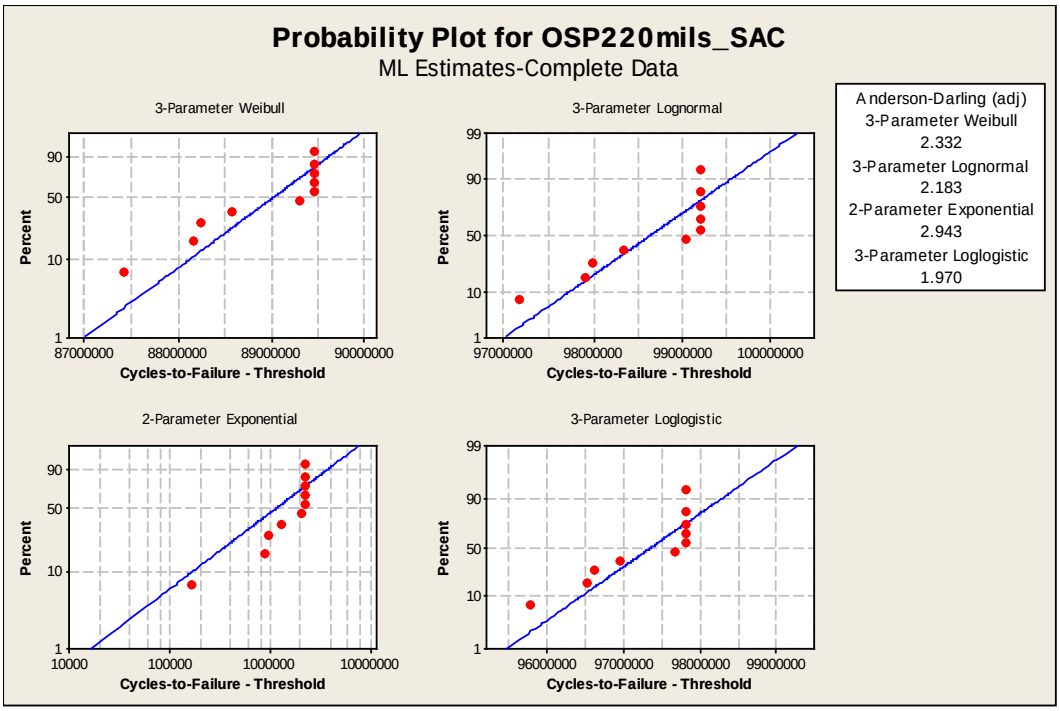
Probability Plot for OSP220mils_SAC
ML Estimates-Complete Data
3-Parameter Weibull
3-Parameter Lognormal
2-Parameter Exponential
3-Parameter Loglogistic
Percent
Cycles-to-Failure - Threshold
Anderson-Darling (adj)
3-Parameter Weibull
2.332
3-Parameter Lognormal
2.183
2-Parameter Exponential
2.943
3-Parameter Loglogistic
1.970

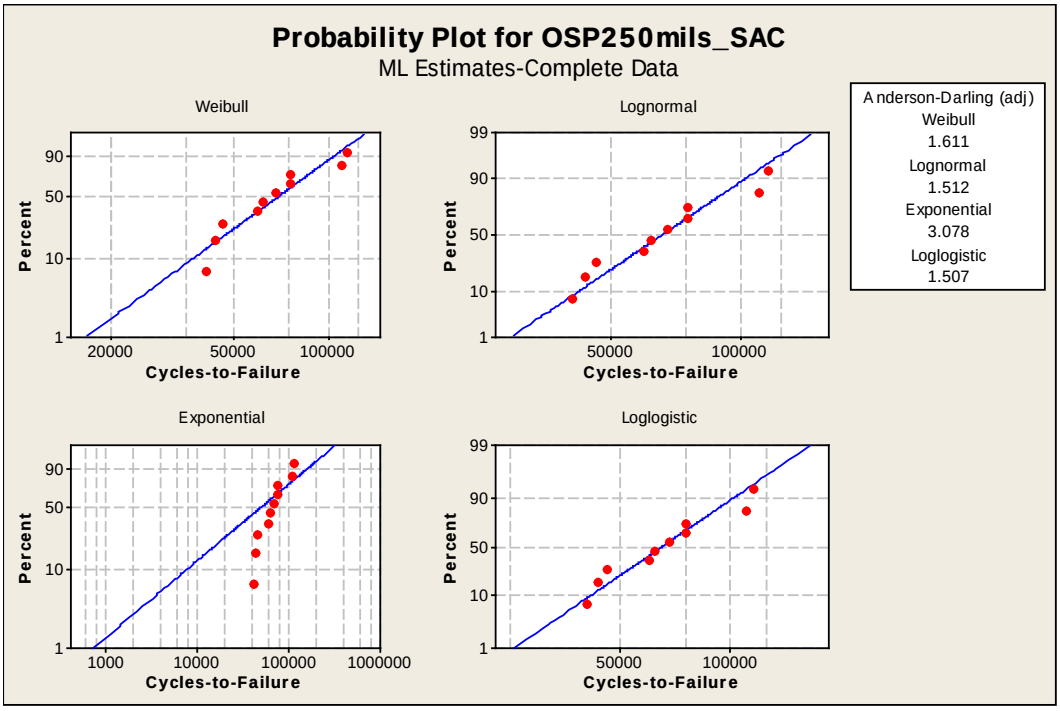
Probability Plot for OSP250mils_SAC
ML Estimates-Complete Data
Weibull
Lognormal
Exponential
Loglogistic
Percent
Cycles-to-Failure
Anderson-Darling (adj)
Weibull
1.611
Lognormal
1.512
Exponential
3.078
Loglogistic
1.507

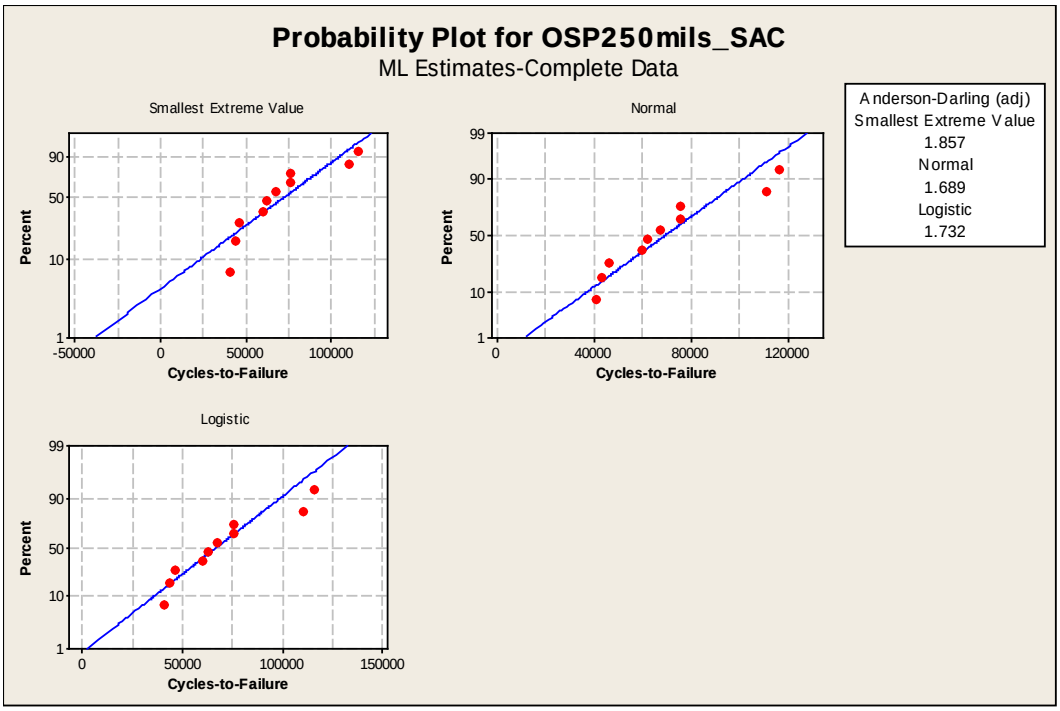
Probability Plot for OSP250mils_SAC
ML Estimates-Complete Data
Smallest Extreme Value
Normal
Logistic
Percent
Cycles-to-Failure
Anderson-Darling (adj)
Smallest Extreme Value
1.857
Normal
1.689
Logistic
1.732

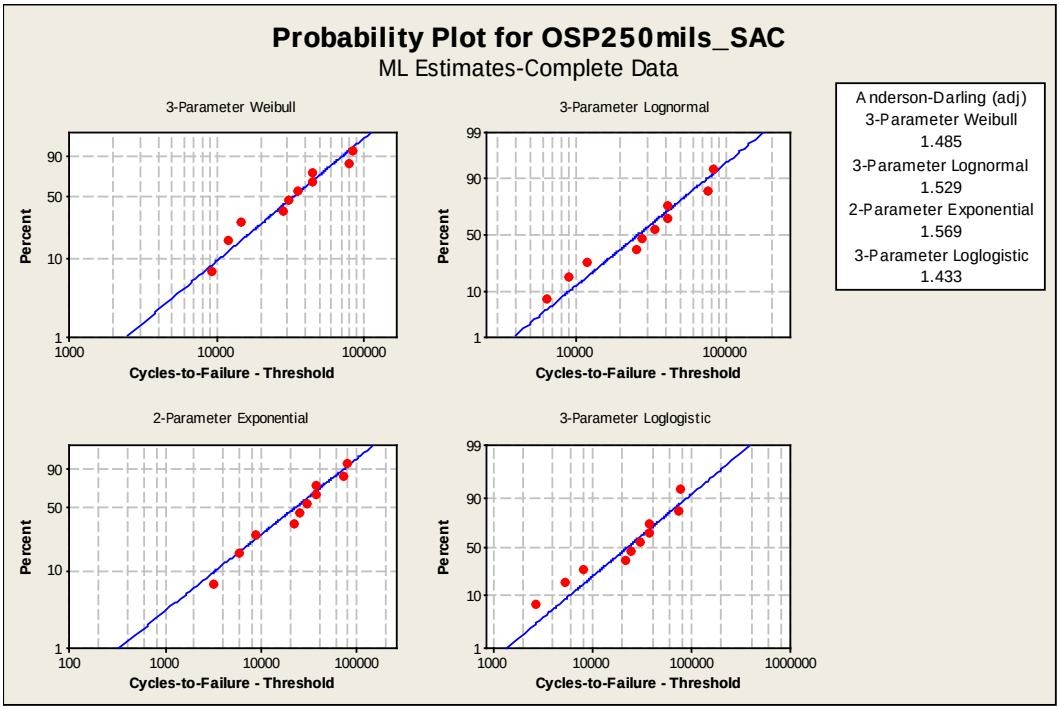
Probability Plot for OSP250mils_SAC
ML Estimates-Complete Data
3-Parameter Weibull
3-Parameter Lognormal
2-Parameter Exponential
3-Parameter Loglogistic
Percent
Cycles-to-Failure - Threshold
Anderson-Darling (adj)
3-Parameter Weibull
1.485
3-Parameter Lognormal
1.529
2-Parameter Exponential
1.569
3-Parameter Loglogistic
1.433

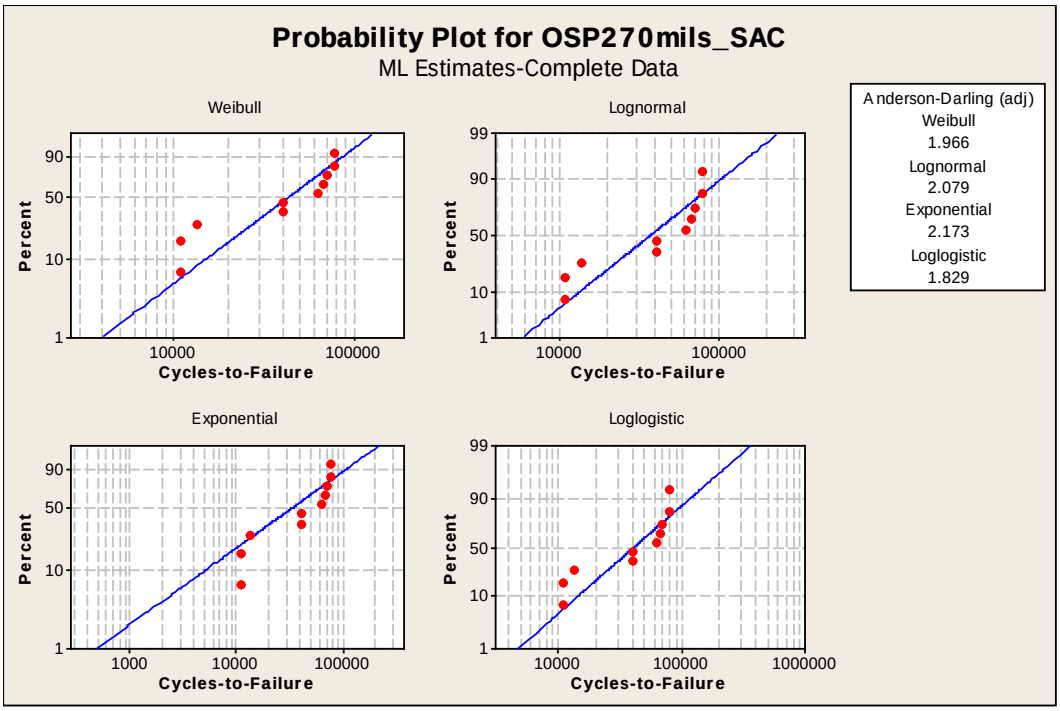
Probability Plot for OSP270mils_SAC
ML Estimates-Complete Data
Weibull
Lognormal
Exponential
Loglogistic
Percent
Cycles-to-Failure
Anderson-Darling (adj)
Weibull
1.966
Lognormal
2.079
Exponential
2.173
Loglogistic
1.829

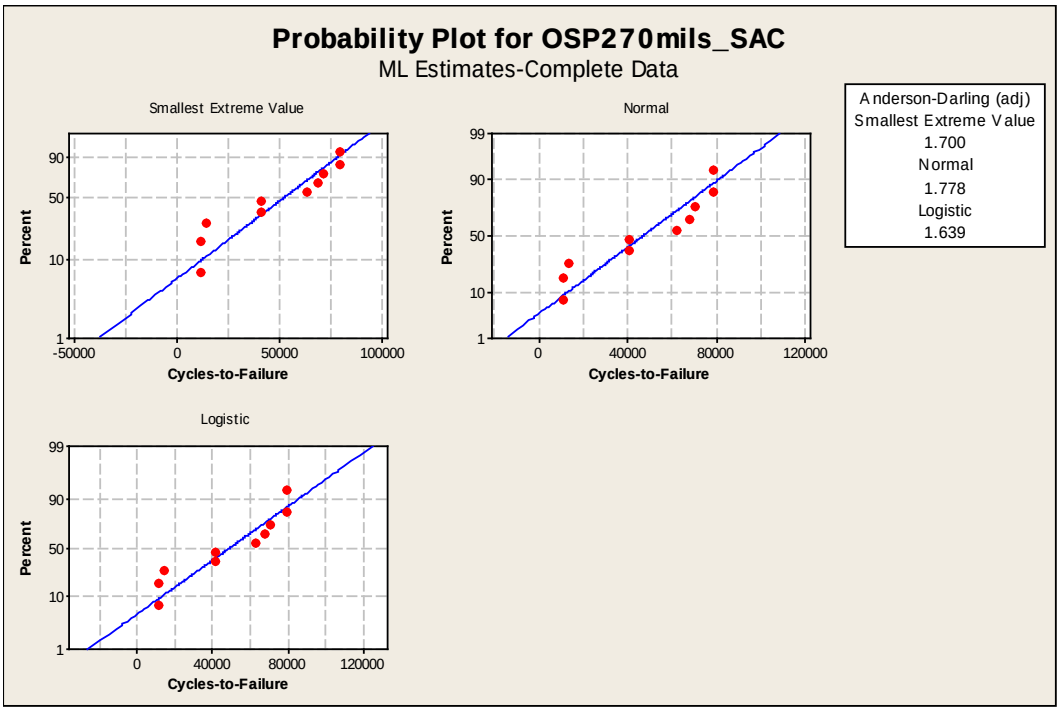
Probability Plot for OSP270mils_SAC
ML Estimates-Complete Data
Smallest Extreme Value
Normal
Logistic
Percent
Cycles-to-Failure
Anderson-Darling (adj)
Smallest Extreme Value
1.700
Normal
1.778
Logistic
1.639

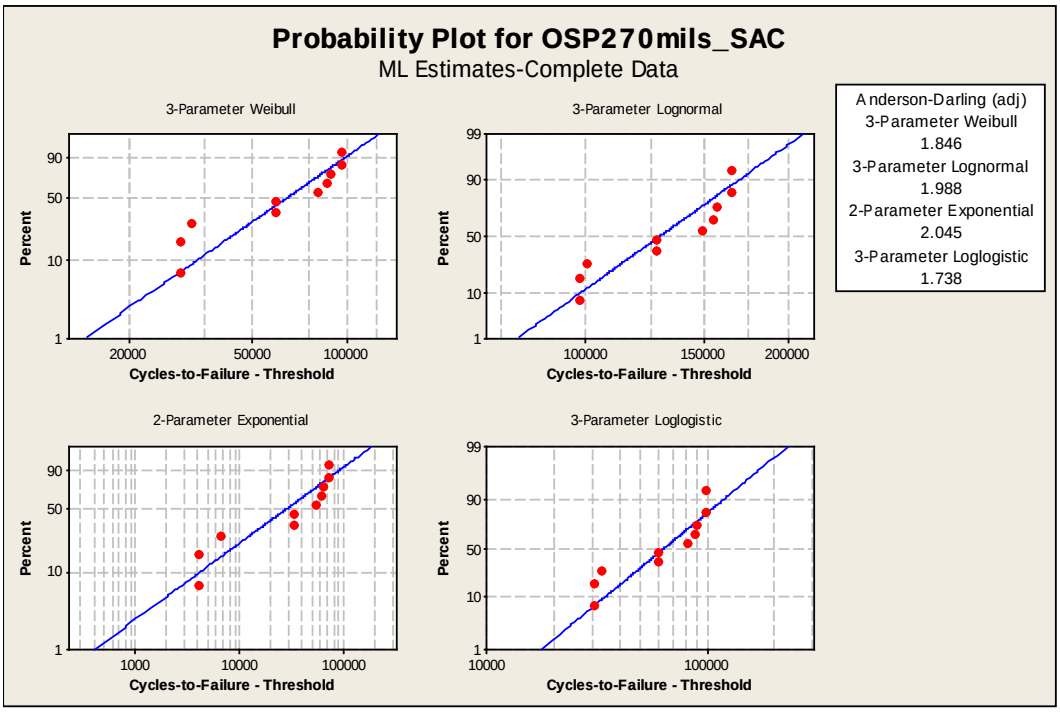
Probability Plot for OSP270mils_SAC
ML Estimates-Complete Data
3-Parameter Weibull
3-Parameter Lognormal
2-Parameter Exponential
3-Parameter Loglogistic
Percent
Cycles-to-Failure - Threshold
Anderson-Darling (adj)
3-Parameter Weibull
1.846
3-Parameter Lognormal
1.988
2-Parameter Exponential
2.045
3-Parameter Loglogistic
1.738

BIOGRAPHICAL SKETCH

Joseph (Joe) Moses Juarez, Jr. is a native Texan with parents who were born deep in the heart of Texas. The Juarez family traces its Texas roots back 200 years or 5 generations to times when Texas was Mexican, then a Republic, a Confederate State before becoming part of the U.S.A. Joe Sr. had been a U.S. Army enlisted man stationed at some time in Fort Ord in Monterey Bay California during the Korean Conflict and loved California so much that soon after Joe Jr. was born the family moved to Los Angeles in the late 1950's. Joe the eldest of three children has two younger sisters and all attended Catholic School K-12 in the 60's to mid-70s. These times are marked by a dichotomy of hope and despair; the wonders of the space race and the finality of the Vietnam War especially as the draft number approached and not having any expectation of coming home alive. Joe's dad is an electrical engineer who owned a radio and television repair shop at the time President Kennedy's moon speech struck a deep chord hearing, "We choose to go to the moon in this decade and do the other things, not because they are easy, but because they are hard." Joe wanted to learn everything about science from his mentor and dad, but also entered into the martial arts preparing for how he would survive the end. This conflict of a great interest in science or death in the jungle intensified into high school, but tempered by his love for the live performances of Jimi Hendrix, Black Sabbath, and Led Zeppelin. Joe's favorite high school teacher Mrs. Wheeler saw this conflict in her student and gave him a special assignment for their Science-fiction class to investigate what Dante's Inferno had to do with Thermodynamics. This would have a lasting effect.

The war is over, missed applying to UC Berkeley, but the University in the San Fernando Valley of Los Angeles where Joe had heard Hendrix five years earlier accepted him. Joe's mother also encouraged him to become involved in student politics. His greatest achievement as the Engineering Student Senator when on the University Foundation Board along with fellow student Senators was to have the university divest of its investments in corporations that supported apartheid. He worked at Hughes Aircraft Company in their Missiles division as a student to pay for his education and also was an officer in the Society of Hispanic Professional Engineers (SHPE). Joe was also student president of Tau Beta Pi and after attending the national convention in New York decided to attend graduate school in the east coast. Joe was a triple major in Electrical, Mechanical, and Computer Science, but his advisor Professor Raymond Landis convinced Joe that dropping the computer science major and pursuing a master's degree would be a better use of time. So Ray being the great guy that he is financed travel with Joe to MIT, Ray's alma mater for a visit to Cambridge. Joe received a B.S. in Engineering from California State University Northridge (CSUN) in 1980.

In 1983, he earned an M.S. in Mechanical Engineering from the Massachusetts Institute of Technology, with a concentration of courses in the Dynamics and Control Subdivision and materials minor. His thesis advisor was Klaus Jürgen- Bathe and Joe's thesis investigated the mathematics that unified

computer graphics and finite element methods for minimizing computational errors. His education was funded by The Aerospace Corporation under the auspices of the National Consortium for increasing the number of Graduate Engineering Minorities (GEM) Program. While at MIT, Joe met the late Professor Henry M. Paynter IV and became Paynter's perpetual graduate student publishing robotics articles applying pneumatic actuators. Joe is currently working on the collected papers of Henry Martyn Paynter IV.

Joseph M. Juarez has been a Principal Mechanical Engineer at Honeywell International Phoenix, AZ, since 1997 primarily responsible for packaging of Commercial and Military Avionics equipment. He is currently the technical lead for Lead-free solder joint reliability predictions due to high cycle fatigue. Prior to Honeywell he was a Senior Project Engineer for missile and satellite technology development at The Aerospace Corporation in El Segundo, CA for 13 years. During those years he met his lovely wife Deborah K. Moorhead, another engineer, at a conference on "Breakthrough Thinking" at USC and they now live with their son in Scottsdale, Arizona.

He has also worked as a consultant for George Group Accenture in Systems Engineering best practices and worked in a Mexican maquiladora reducing the scrap rates of permanent magnet production from 60% to 6% using Six Sigma methods, 1995-1997. His Ph.D. studies at Arizona State University Industrial Engineering are in Quality Reliability Engineering. Joe was also on the Extension faculty at UCLA teaching TQM principles 1991-1992 and a lecturer at CSUN between 1980 and 1992 in Dynamics and Control topics. He is an ASQ Senior Member and Member of ASME